



# **Mechanically-regulated microRNAs in articular cartilage**

**Paulina Zaklina Stadnik**

**A thesis submitted to Cardiff University in accordance with the  
requirements for the degree of Doctor of Philosophy  
in the School of Biosciences**

**September 2016**

Dedicated to my Uncle Karol

who was always proud of me and  
my education

## **Acknowledgements**

*I would like to firstly thank my supervisors Dr. Emma Blain and Prof. Vic Duance for their support, guidance, patience and giving me the opportunity to conduct research in their lab.*

*A big thank you to my external supervisor Prof. David Young from Newcastle University for his help and ideas.*

*I would like to say a special thank you to Prof. Darek Gorecki from Portsmouth University for guiding me back on the scientific path. Without the experience I had in his lab, I would have never thought of doing a PhD.*

*I would like to also acknowledge Dr. Jessica Tarn and Ms. Angela Marchbank for helping me with the library preparation for Next Generation Sequencing, Dr. Daniel Pass, Dr. Timothy Stone and Mr. Andrew Skelton for their bioinformatics analysis and Dr. Matt Barter for his advice concerning miR experiments.*

*I would like to mostly thank my family and my partner for believing in me all the time and encouraging me to make my dreams come true.*

*Special thanks goes to my Kuwaiti sister and my best friend Dr. Aisha Al-Sabah who was always there to help me and answer my questions throughout my PhD, and having this special power to be able to spread her positivity on other people. Thank you for your friendship and all the happy and less happy moments we went through together.*

*I would also like to thank to Dr. Cleo Bonnet for being so optimistic, energetic and life loving who did not allow anyone to have a bad day, and to Dr. Sophie Gilbert for her advice and help.*

*Thank you all for making the period of my PhD so fantastic, full of scientific experience, and many enjoyable days, it was a great pleasure to work with you.*

*Many thanks also goes to Mama and Papa Al-Sabah for their unconditional financial support which allowed me to focus on writing this PhD thesis.*

*Finally, I would like to thank to Arthritis Research UK and The President's Research Scholarship for funding this research.*

## List of abbreviations

<b>18S</b>	18S ribosomal RNA
<b>3D</b>	Three dimensional
<b>ACVR2A</b>	Activin receptor 2B
<b>ADAMTS</b>	A disintegrin and metalloprotease with thrombospondin motifs
<b>ANOVA</b>	Analysis of variance
<b>AP-1</b>	Activator protein 1
<b>APC</b>	Adenomatous Polyposis Coli
<b>APS</b>	Ammonium persulphate
<b>AT</b>	Annealing temperature
<b>ATC</b>	Anaplastic thyroid carcinoma
<b>Axin2</b>	Axis Inhibition Protein 2
<b>BBB</b>	Bead Binding Buffer
<b>BMP</b>	Bone Morphogenetic Protein
<b>bp</b>	Base pair
<b>bta</b>	Bos taurus
<b>BWB</b>	Bead Washing Buffer
<b>cDNA</b>	Complementary DNA
<b>CDS</b>	Coding sequence
<b>CHRD/CHL</b>	Chordin-like
<b>CILP-1</b>	Cartilage intermediate layer protein 1
<b>COMP</b>	Cartilage oligomeric matrix protein
<b>CPEB3</b>	Cytoplasmic Polyadenylation Element Binding Protein 3
<b>CS</b>	Chondroitin sulphate
<b>CSNK2A2</b>	Casein kinase 2 alpha 2 polypeptide
<b>Ct</b>	Threshold cycle
<b>CTNNB1</b>	Catenin Beta 1
<b>CTS</b>	Cyclic tensile strain
<b>Cy3</b>	Cyanine dye 3
<b>DAPI</b>	4',6-Diamidino-2-Phenylindole
<b>DHh</b>	Desert hedgehog
<b>DKK</b>	Dickkopf
<b>DMA</b>	Dynamic mechanical analysis
<b>DMEM</b>	Dulbecco's Modified Eagle's Medium
<b>DMM</b>	Destabilization of the medial meniscus
<b>DNA</b>	Deoxyribonucleic acid
<b>Dnpep</b>	Aspartyl aminopeptidase enzyme
<b>dNTP</b>	Deoxynucleotide
<b>dsDNA</b>	Double stranded DNA
<b>DTT</b>	Dithiothreitol
<b>DVL</b>	Dishevelled
<b>EC</b>	Endothelial cells
<b>ECM</b>	Extracellular matrix
<b>EGFR</b>	Epidermal growth factor receptor
<b>EHHADH</b>	Enoyl-CoA, hydratase/3-hydroxyacyl CoA dehydrogenase
<b>ELB</b>	Elution Buffer

<b>ER</b>	Estrogen receptor
<b>ERK1/2</b>	Extracellular signal–regulated kinase 1/2
<b>Exp-5</b>	Exportin 5
<b>FAK</b>	Focal adhesion kinase
<b>FBS</b>	Foetal Bovine Serum
<b>FDR</b>	False discovery rate
<b>Fn-f</b>	Fibronectin fragments
<b>FOS</b>	FBJ Murine Osteosarcoma Viral Oncogene Homolog
<b>FOSL</b>	FOS Like Antigen
<b>FOXM1</b>	Forkhead Box N1
<b>FPF</b>	Fragment, Prime, Finish mix
<b>FRAT2</b>	Frequently Rearranged In Advanced T-Cell Lymphomas 2
<b>FRZB</b>	Frizzled-Related Protein
<b>FZD</b>	Frizzled family receptor
<b>G-1, -2, -3</b>	Globular domains -1, -2, -3
<b>GAGs</b>	Glycosaminoglycans
<b>GAPDH</b>	Glyceraldehyde-3-phosphate dehydrogenase
<b>GDF-5</b>	Growth differentiation factor 5
<b>GPRC5A</b>	G-Protein Coupled Receptor, Family C, Group 5, Member A
<b>GSK3</b>	Glycogen Synthase Kinase 3
<b>GTP</b>	Guanosine-5'-triphosphate
<b>HA</b>	Hyaluronan
<b>HASMCs</b>	Human airway smooth muscle cells
<b>hBMSCs</b>	Human bone marrow stromal cells
<b>HDAC4</b>	Histone deacetylase 4
<b>Hh</b>	Hedgehog
<b>HIF</b>	Hypoxia-inducible factors
<b>HKGs</b>	Housekeeping genes
<b>HMGB1</b>	High mobility group box 1
<b>hMSC</b>	Human Bone Marrow Derived Mesenchymal Stem Cells
<b>HPRT1</b>	Hypoxanthine phosphoribosyltransferase 1
<b>hsa</b>	Homo sapiens
<b>HT1</b>	Hybridisation buffer
<b>IGD</b>	Interglobular domain
<b>IGF</b>	Insulin Growth Factors
<b>IGFB</b>	Insulin Like Growth Factor Binding Protein
<b>IHh</b>	Indian hedgehog
<b>Il-1</b>	Interleukin-1
<b>INHBA</b>	Inhibin Beta A
<b>IRAK1</b>	IL-1-receptor associated kinase 1
<b>ITS</b>	Insulin-Transferrin-Selenium
<b>JNK</b>	c-Jun N-terminal kinase
<b>KS</b>	Keratan sulphate
<b>LAMC2</b>	Laminin subunit gamma-2
<b>LIFR</b>	Leukemia Inhibitory Factor Receptor Alpha
<b>lncRNAs</b>	Long non-coding RNAs
<b>LP</b>	Link protein

<b>LPS</b>	Lipopolysaccharide
<b>LRRs</b>	Leucine-rich repeats
<b>MAPKs</b>	Mitogen activated protein kinases
<b>Mdm2</b>	Mouse double minute 2
<b>Mef-2</b>	Myocyte Enhancer Factor 2A
<b>MGB</b>	Minor groove binder
<b>MIQE</b>	Minimum Information for Publication of Quantitative Real-Time PCR Experiments
<b>miR</b>	microRNA
<b>MMP</b>	Metalloproteinase
<b>mmu</b>	Mus musculus
<b>mRNA</b>	Messenger RNA
<b>MSMP/PSMP</b>	Microseminoprotein
<b>MT1</b>	Membrane type 1
<b>NF-kappa B</b>	Nuclear factor kappa B
<b>NFQ</b>	Non-fluorescent quencher
<b>NGS</b>	Next Generation Sequencing
<b>NMDAR</b>	N-methyl-D-aspartate receptor
<b>NT</b>	Non-targeting
<b>NTC</b>	Non-template control
<b>OA</b>	Osteoarthritis
<b>PBP</b>	RNA Purification beads
<b>PCM</b>	Pericellular matrix
<b>PCP</b>	Planar cell polarity
<b>PGE2</b>	Prostaglandin E2
<b>PI3K</b>	Phosphoinositide 3-kinase
<b>piRNA</b>	PIWI-interacting RNA
<b>PITX2</b>	Paired Like Homeodomain 2
<b>PL</b>	Post-load
<b>PMM</b>	PCR Master Mix
<b>PPARA</b>	Peroxisome proliferator-activated receptor
<b>PPC</b>	PCR Primer Cocktail
<b>PPIA</b>	Peptidylprolyl isomerase A
<b>PRELP</b>	Proline-arginine-rich end leucine-rich repeat protein
<b>PRG4</b>	Proteoglycan 4
<b>pre-miR</b>	Precursor microRNA
<b>pri-miR</b>	Primary microRNA
<b>PSACH</b>	Pseudoachondroplasia
<b>Ptch1</b>	Patched 1
<b>qPCR</b>	Quantitative polymerase chain reaction
<b>RAI3</b>	Retinoic acid induced three
<b>RAIG1</b>	Retinoic acid induced gene 1
<b>Ran</b>	Ras-related nuclear protein
<b>RERG</b>	Ras-like and oestrogen-regulated growth inhibitor
<b>RIN</b>	RNA integrity number
<b>RISC</b>	RNA-induced silencing complex
<b>RNA</b>	Ribonucleic acid

<b>RNAi</b>	RNA interference
<b>RPL4</b>	Ribosomal protein L4
<b>rRNA</b>	Ribosomal ribonucleic acid
<b>RSB</b>	Resuspension buffer
<b>RUNX-2</b>	Runt-related transcription factor 2
<b>SD</b>	Standard deviation
<b>SDHA</b>	Succinate Dehydrogenase Complex Flavoprotein Subunit A
<b>SEM</b>	Scanning electron microscopy
<b>SFRP2</b>	Secreted Frizzled-Related Protein 2
<b>SHh</b>	Sonic hedgehog
<b>siRNA</b>	Small interfering RNA
<b>SLRPs</b>	Small non-aggregating leucine rich proteoglycans
<b>SMM</b>	Second Strand Master Mix
<b>Smo</b>	Smoothened
<b>snoRNA</b>	Small nucleolar RNA
<b>SOX9</b>	Sex determining region Y box 9
<b>SP</b>	Signal peptide
<b>SPRY4</b>	Sprouty RTK Signalling Antagonist 4
<b>ssRNA</b>	Single stranded RNA
<b>stat5b</b>	Signal transducer activated transcription 5b
<b>STL</b>	Stop Ligation Buffer
<b>SZP</b>	Superficial Zone Protein
<b>TEM</b>	Transmission electron microscopy
<b>TEMED</b>	Tetramethylethylenediamine
<b>TGF</b>	Transforming Growth Factor
<b>TGF-<math>\beta</math></b>	Transforming growth factor- $\beta$
<b>TIMP</b>	Tissue inhibitors of metalloproteinase
<b>TM</b>	Trabecular meshwork
<b>TNF</b>	Tumour Necrosis Factor
<b>TRAF6</b>	TNF-receptor associated factor 6
<b>tRFs</b>	tRNAs-derived RNA fragments
<b>tRNA</b>	Transfer RNA
<b>TSP</b>	Thrombospondin motifs
<b>U</b>	Unit
<b>U1</b>	U1 spliceosomal RNA
<b>UNG</b>	Uracil -N glycosylase
<b>UTR</b>	Untranslated region
<b>UV</b>	Ultraviolet
<b>v/v</b>	Volume per volume
<b>VEGF</b>	Vascular endothelial growth factor
<b>vs</b>	Versus
<b>w/v</b>	Weight per volume
<b>WISP-1</b>	Wnt-1 induced secreted protein-1
<b>WNTs</b>	Wingless-type MMTV integration site family members
<b>YWHAZ</b>	Tyrosine 3-Monooxygenase/Tryptophan 5-Monooxygenase Activation Protein Zeta

**Units of measurement abbreviations:**

<b>N</b>	Newton
<b>μg</b>	Microgram
<b>μl</b>	Microlitre
<b>μm</b>	Micron
<b>μM</b>	Micromolar
<b>cm</b>	Centimetre
<b>Dyn</b>	Dyne
<b>h</b>	Hour
<b>Hz</b>	Hertz
<b>kDa</b>	Kilo Dalton
<b>mg</b>	Milligram
<b>min</b>	Minute
<b>ml</b>	Millilitre
<b>mm</b>	Millimetre
<b>MPa</b>	Mega Pascal
<b>pM</b>	Picomolar
<b>rpm</b>	Revolutions per minute
<b>Sec</b>	Second
<b>V</b>	Volt

## **Abstract**

**Introduction:** *The role of microRNAs (miRs) in articular cartilage is still not well established, however many studies have reported the differential expression of a number of miRs between healthy and osteoarthritic (OA) articular cartilage. These studies have focused on the OA pathology itself without considering the impact of mechanical load, which is one of the major risk factors implicated in the loss of cartilage integrity and the onset of OA development. Previous studies have already identified a number of mechanically-regulated miRs, therefore I hypothesised that (i) physiological and non-physiological magnitudes of compressive load differentially regulate the expression of mechano-sensitive miRs, and (ii) mechanically-regulated miRs differentially expressed in response to a non-physiological magnitude of load are implicated in the regulation of mechano-sensitive matrix molecule turnover and are involved in OA development.*

**Results:** *Transcriptional assessment of selected mechanically-regulated matrix molecules demonstrated that loading regimes of 2.5MPa and 7MPa (1Hz, 15 minutes) induced homeostatic and catabolic responses at the gene level respectively, therefore they were selected to represent 'physiological' and 'non-physiological' magnitudes of loads which have the potential to induce biosynthetic and degradative protein responses if applied for prolonged periods of time. Next generation sequencing (NGS) of articular cartilage miRs libraries demonstrated that the alteration in expression of specific miRs occurs in a magnitude- and time-dependent manner. However, 24h post-load, according to the NGS data, seems to be the most appropriate to observe significant changes in miRs levels. Validation of a few miRs, important for cartilage integrity, at 24h post-load indicated up-regulation of miR-21-5p, miR-27a-5p, miR-221 and miR-222 and down-regulation of miR-483 in response to the 'non-physiological' 7MPa magnitude (1Hz, 15 minutes) whereas in explants subjected to a 'physiological' 2.5MPa magnitude (1Hz, 15 minutes) the level of these miRs remained unchanged. Identification of target genes of miR-21-5p, miR-221 and miR-222 performed by NGS of RNA extracted from primary articular chondrocytes transfected with specific miR inhibitors demonstrated a number of differentially expressed genes. qPCR validation of these potential miR target genes on RNA collected from cells transfected with functional miR-21-5p, miR-221 and miR-222 inhibitors or mimics identified TIMP-3 as a direct target of miR-21-5p, miR-221 and miR-222, whereas CPEB was targeted by miR-21-5p.*

**Conclusion:** *This current study confirms the reported mechano-regulation of miR-221 and miR-222, and furthermore demonstrates the novel mechano-regulation of miR-21-5p, miR-27a-5p and miR-483 in cartilage explants. This work is the first to identify TIMP-3 as a target of miR-21-5p and miR-221/-222, and CPEB3 as a direct target of miR-21-5p in primary chondrocytes. An association between the identified differentially-regulated miRs in response to a non-physiological magnitude of load, with those that are expressed in OA cartilage and their regulatory effect on molecules important for cartilage integrity, described in this thesis may pioneer future studies aimed at identifying cartilage biomarkers of load-induced OA and provide therapeutic potential for OA treatment.*

## List of Figures

### Chapter 1

<b>Figure 1.1.</b> Cross-sectional diagram of mature articular cartilage.....	<b>5</b>
<b>Figure 1.2.</b> Schematic diagram depicting the organization of ECM molecules in articular cartilage.....	<b>7</b>
<b>Figure 1.3.</b> Potential interactions between collagens type II, IX and XI in a cartilage collagen fibril.....	<b>10</b>
<b>Figure 1.4.</b> Schematic diagram of multi-molecular aggregate of aggrecan bound to a hyaluronan molecule and proteoglycan aggrecan monomer.....	<b>14</b>
<b>Figure 1.5.</b> Schematic diagram of domain structure of MMPs.....	<b>19</b>
<b>Figure 1.6.</b> Schematic diagram of ADAMTS-4 and ADAMTS-5 structure.....	<b>22</b>
<b>Figure 1.7.</b> Aggrecanase cleavage sites for human and bovine aggrecan core protein...	<b>22</b>
<b>Figure 1.8.</b> Representative toluidine blue stained sections of healthy and OA cartilage regions from the femoral condyle of human OA knee joint.....	<b>25</b>
<b>Figure 1.9.</b> Illustration of different types of load to which articular cartilage in the joint is exposed to and its physical and biochemical alteration in response to everyday movement.....	<b>29</b>
<b>Figure 1.10.</b> Diagram of response of articular cartilage to mechanical loading.....	<b>35</b>
<b>Figure 1.11.</b> The miR maturation canonical pathway and the working mechanism of action.....	<b>43</b>
<b>Figure 1.12.</b> Non-canonical, Drosha independent pathway of mirtron derived miR biogenesis.....	<b>46</b>
<b>Figure 1.13.</b> Non-canonical, Drosha independent pathway of miR biogenesis via the tRNA derived pathway.....	<b>47</b>
<b>Figure 1.14.</b> Types of matching seed sites in mRNA.....	<b>49</b>

## **Chapter 2**

<b>Figure 2.1.</b> Schematic diagram of explant loading using the Bose ElectroForce® 3200 rig.....	<b>66</b>
<b>Figure 2.2.</b> Sample electrophoretograms illustrating different RNA qualities.....	<b>72</b>
<b>Figure 2.3.</b> Representative amplification plot and melting curve for TIMP-3 SYBR® Green qPCR.....	<b>79</b>
<b>Figure 2.4.</b> Schematic diagram of pooled experimental RNA to create representative samples.....	<b>87</b>
<b>Figure 2.5.</b> Schematic diagram of miR Illumina Next Generation Sequencing workflow.....	<b>88</b>
<b>Figure 2.6.</b> Representative 8% polyacrylamide gel before and after library excision.....	<b>92</b>
<b>Figure 2.7.</b> Schematic diagram of pooled experimental RNA to create representative samples for Illumina® TruSeq® sequencing.....	<b>95</b>
<b>Figure 2.8.</b> Schematic diagram of the Illumina Next Generation Sequencing workflow.....	<b>96</b>
<b>Figure 2.9.</b> Schematic diagram of sample preparation, purification and fragmentation of mRNA for Next Generation Sequencing.....	<b>98</b>

## **Chapter 3**

<b>Figure 3.1.</b> RIN table (A), representative ribosomal peak plot (B) and electrophoresis gel (C) showing good quality RNA used for NGS.....	<b>115</b>
<b>Figure 3.2.</b> Analysis of reference gene stability by the comparative $\Delta C_t$ method, BestKeeper, geNorm and NormFinder.....	<b>116</b>
<b>Figure 3.3.</b> Reference gene stability output using RefFinder software.....	<b>117</b>

<b>Figure 3.4.</b> qPCR standard curves of SDHA (A) and YWHAZ (B) conducted on pooled cDNAs from samples subjected to 2.5MPa and 7MPa loading regimes (1Hz, 15 minutes) and unloaded explants.....	<b>118</b>
<b>Figure 3.5.</b> mRNA quantification of Aggrecan (A,B) and Collagen type II (C,D) in cartilage explants subjected to varying loading regimes (1Hz, 15 minutes).....	<b>121</b>
<b>Figure 3.6.</b> mRNA quantification of MMP-1 (A,B), MMP-3 (C,D), MMP-9 (E,F) and MMP-13 (G,H) in cartilage explants subjected to varying loading regimes (1Hz, 15 minutes).....	<b>122</b>
<b>Figure 3.7.</b> mRNA quantification of ADMTS-4 (A,B) and ADAMTS-5 (C,D) in cartilage explants subjected to varying loading regimes (1Hz, 15 minutes).....	<b>124</b>
<b>Figure 3.8.</b> mRNA quantification of TIMP-1 (A,B), TIMP-2 (C,D) and TIMP-3 (E,F) in cartilage explants subjected to varying loading regimes (1Hz, 15 minutes).....	<b>125</b>
<b>Figure 3.9.</b> Classification, according to protein classes provided by PANTHER annotation, of differentially expressed genes at 4h post-load in articular cartilage subjected to 2.5MPa or 7MPa load (1Hz, 15 minutes).....	<b>135</b>
<b>Figure 3.10.</b> Pie charts demonstrating the characterisation of the differentially expressed genes according to protein class in response to a 2.5MPa load analysed 4h post-load.....	<b>136</b>
<b>Figure 3.11.</b> Pie charts demonstrating the characterisation of the differentially expressed genes according to protein class in response to a 7MPa load analysed 4h post-load.....	<b>137</b>
<b>Figure 3.12.</b> Pie charts demonstrating the characterisation of the differentially expressed genes according to protein class in response to a 7MPa load analysed 4h post-load.....	<b>138</b>
<b>Figure 3.13.</b> Classification, according to protein classes provided by PANTHER annotation, of differentially expressed genes at 24h post-load in articular cartilage subjected to 2.5MPa or 7MPa load (1Hz, 15 minutes).....	<b>141</b>

**Figure 3.14.** Pie charts demonstrating the characterisation of the differentially expressed genes according to protein class in response to a 2.5MPa load analysed 24h post-load.....**142**

**Figure 3.15.** Pie charts demonstrating the characterisation of the differentially expressed genes according to protein class in response to a 7MPa load analysed 24h post-load.....**143**

**Chapter 4**

**Figure 4.1.** Relative expression levels of miR-140 (A,B), miR-221 (C,D) and miR-222 (E,F) in cartilage explants subjected to 2.5MPa or 7MPa load (1 Hz, 15 minutes) and analysed 2h (A,C,E) or 24h (B,D,F) post-load.....**164**

**Figure 4.2.** Top 50 most abundantly expressed miRs in articular cartilage at 2h post-load.....**167**

**Figure 4.3.** Top 50 most abundantly expressed miRs in articular cartilage at 6h post-load.....**168**

**Figure 4.4.** Top 50 most abundantly expressed miRs in articular cartilage at 24h post-load.....**169**

**Figure 4.5.** The base mean counts of all differentially expressed miRs when comparing expression levels between 7MPa and 2.5MPa vs unloaded or 7MPa vs 2.5MPa load.....**171**

**Figure 4.6.** Differential expression of mechanically regulated miRs in explants subjected to either a 2.5MPa (A) or 7MPa (B) load and analysed at 2h post-load.....**175**

**Figure 4.7.** Differential expression of mechanically regulated miRs in explants subjected to either a 2.5MPa (A) or 7MPa (B) load and analysed at specific periods of 6h post-load.....**176**

<b>Figure 4.8.</b> Differential expression of mechanically regulated miRs in explants subjected to either a 2.5MPa (A) or 7MPa (B) load and analysed at specific periods of 6h post-load.....	<b>177</b>
<b>Figure 4.9.</b> Validation of significant mechanically regulated mature miRs: miR-21-5p (A), miR-27a-5p (B), miR-221 (C), miR-222 (D) that were selected on the basis of NGS data.....	<b>180</b>
<b>Figure 4.10.</b> Validation of significant mechanically regulated mature miRs: miR-451 (A) miR-483-3p (B) and miR-543 (C) that were selected on the basis of NGS data.....	<b>181</b>

## ***Chapter 5***

<b>Figure 5.1.</b> Cellular uptake of siRNA over a 48h transfection period.....	<b>193</b>
<b>Figure 5.2.</b> Expression level of miR-21 in response to 48h of transfection.....	<b>196</b>
<b>Figure 5.3.</b> Expression level of miR-27a-5p in response to 48h of transfection.....	<b>197</b>
<b>Figure 5.4.</b> Expression level of miR-221 in response to 48h of transfection.....	<b>198</b>
<b>Figure 5.5.</b> Expression level of miR-222 in response to 48h of transfection.....	<b>199</b>
<b>Figure 5.6.</b> Morphology of untreated or transfected primary chondrocytes.....	<b>201</b>
<b>Figure 5.7.</b> Representative images of Live/Dead® assay to monitor cell viability in chondrocytes.....	<b>202-204</b>
<b>Figure 5.8.</b> Calculation of cell viability (A) and death (B) expressed as a % as assessed by Live/Dead® assay.....	<b>206</b>
<b>Figure 5.9.</b> Scatterplots of Qiagen Wnt signalling PCR array data comparing the transcriptional profile of Wnt-related genes between untreated and cells transfected with non-targeting inhibitor.....	<b>209</b>

<b>Figure 5.10.</b> Scatterplots of Qiagen Wnt signalling PCR array data comparing the transcriptional profile of genes between transfected cells with miR-21-5p inhibitor and non-targeting miR inhibitor.....	<b>210</b>
<b>Figure 5.11.</b> Scatterplots of Qiagen Wnt signalling PCR array data comparing the transcriptional profile of genes between transfected cells with miR-221 inhibitor and non-targeting miR inhibitor.....	<b>211</b>
<b>Figure 5.12.</b> Scatterplots of Qiagen Wnt signalling PCR array data comparing the transcriptional profile of genes between transfected cells with miR-222 inhibitor and non-targeting miR inhibitor.....	<b>212</b>
<b>Figure 5.13.</b> Validation of MMP-7 as a putative target gene of miR-21-5p.....	<b>214</b>
<b>Figure 5.14.</b> Validation of Wnt3A as a putative target gene of miR-221/-222.....	<b>215</b>
<b>Figure 5.15.</b> Validation of CPEB3 - a putative target gene of miR-21-5p.....	<b>228</b>
<b>Figure 5.16.</b> Validation of SPRY4 - a putative target gene of miR-21-5p.....	<b>229</b>
<b>Figure 5.17.</b> Validation of MMP-13 - a putative target gene of miR-21-5p.....	<b>230</b>
<b>Figure 5.18.</b> Validation of TIMP-3 - a putative target gene of miR-21-5p.....	<b>231</b>
<b>Figure 5.19.</b> Validation of SPRY4 – a putative target gene of miR-221 and miR-222.....	<b>235</b>
<b>Figure 5.20.</b> Validation of Runx2 – a putative target gene of miR-221 and -222.....	<b>236</b>
<b>Figure 5.21.</b> Validation of CPEB3 - putative target gene of miR-221 and -222.....	<b>237</b>
<b>Figure 5.22.</b> Validation of LIFR – a putative target gene of miR-221 and -222.....	<b>238</b>
<b>Figure 5.23.</b> Validation of TIMP-3 – a putative target gene of miR-221 and -222.....	<b>239</b>
<b>Figure 5.24.</b> Validation of HDAC4 - a putative target gene of miR-221 and -222.....	<b>240</b>
<b>Figure 5.25.</b> Validation of MMP-13 – a putative target gene of miR-221 and -222.....	<b>241</b>

## List of Tables

### *Chapter 1*

<b>Table 1.1.</b> Members of the human matrix metalloproteinase family.....	<b>20</b>
<b>Table 1.2.</b> Up-regulated miRs in OA cartilage.....	<b>54</b>
<b>Table 1.3.</b> OA-stage dependent miR expression.....	<b>57</b>
<b>Table 1.4.</b> Down-regulated miRs in OA cartilage.....	<b>59</b>

### *Chapter 2*

<b>Table 2.1.</b> Stem-looped reverse transcription primer sequences used in the amplification of mature miRs using TaqMan® MicroRNA assays.....	<b>74</b>
<b>Table 2.2.</b> Quantitative PCR primer sequences for reference genes, annealing temperature (AT°) and product size.....	<b>75</b>
<b>Table 2.3.</b> Quantitative PCR primer sequences for target genes of interest, annealing temperature (AT°) and product size.....	<b>76-77</b>
<b>Table 2.4.</b> Components for a single SYBR® Green qPCR reaction.....	<b>80</b>
<b>Table 2.5.</b> SYBR® Green qPCR cycling conditions to amplify genes of interest.....	<b>80</b>
<b>Table 2.6.</b> TaqMan® Gene expression assays used in the quantification of genes of interest.....	<b>81</b>
<b>Table 2.7.</b> Components for a single TaqMan® miR qPCR reaction.....	<b>82</b>
<b>Table 2.8.</b> Components for a single TaqMan® gene expression qPCR reaction.....	<b>83</b>
<b>Table 2.9.</b> TaqMan qPCR cycling conditions to amplify miRs or genes of interest.....	<b>83</b>
<b>Table 2.10.</b> Function of tested reference genes.....	<b>85</b>
<b>Table 2.11.</b> PCR cycling conditions utilised to amplify miR libraries.....	<b>89</b>

<b>Table 2.12.</b> Reagents used in the preparation of an 8% polyacrylamide gel.....	<b>90</b>
<b>Table 2.13.</b> PCR cycling conditions to amplify the libraries for Next Generation Sequencing.....	<b>102</b>
<b>Table 2.14.</b> Absolute qPCR cycling conditions to normalise the final concentration of prepared libraries.....	<b>104</b>

### ***Chapter 3***

<b>Table 3.1.</b> Top 50 genes from microarray analysis with highest relative expression in response to physiological (2.5MPa) and non-physiological (7MPa) magnitude of load at 4h post-load.....	<b>130</b>
<b>Table 3.2.</b> Top 50 genes from microarray analysis with highest relative expression in response to physiological (2.5MPa) and non-physiological (7MPa) magnitude of load at 24h post-load.....	<b>131</b>

### ***Chapter 4***

<b>Table 4.1.</b> Mechanically regulated miRs identified in explants subjected to compressive load (2.5MPa or 7MPa, 1Hz, 15 minutes) compared to unloaded explants, and processed 2, 6 or 24h post-load.....	<b>170</b>
--	------------

### ***Chapter 5***

<b>Table 5.1.</b> Top 5 most highly elevated genes in response to miR-21-5p knock-down.....	<b>218</b>
<b>Table 5.2.</b> Top 5 most highly reduced genes in response to miR-21-5p knock-down.....	<b>218</b>

<b>Table 5.3.</b> Top 5 most highly elevated genes in response to miR-221 knock-down.....	<b>219</b>
<b>Table 5.4.</b> Top 5 most highly reduced genes in response to miR-221 knock-down.....	<b>219</b>
<b>Table 5.5.</b> Top 5 most highly elevated genes in response to miR-222 knock-down.....	<b>220</b>
<b>Table 5.6.</b> Top 5 most highly reduced genes in response to miR-222 knock-down.....	<b>220</b>
<b>Table 5.7.</b> Up-regulated genes ( $\geq 1.5$ -fold) in cells transfected with miR-21-5p inhibitor compared to expression in the non-targeting inhibitor control, as identified using NGS.....	<b>222</b>
<b>Table 5.8.</b> Up-regulated genes ( $\geq 1.5$ -fold) in cells transfected with miR-221 inhibitor compared to expression in the non-targeting inhibitor control, as identified using NGS.....	<b>223</b>
<b>Table 5.9.</b> Up-regulated genes ( $\geq 1.5$ -fold) in cells transfected with miR-222 inhibitor compared to expression in the non-targeting inhibitor control, as identified using NGS.....	<b>224</b>
<b>Table 5.10.</b> List of putative target genes of miR-21-5p based on NGS data and computational target gene prediction using TargetScan.....	<b>226</b>
<b>Table 5.11.</b> List of putative target genes of miR-221 and miR-222 based on NGS data and computational target gene prediction using TargetScan.....	<b>232</b>

## Table of contents

Chapter 1 .....	1
1.1. Articular cartilage .....	2
1.1.2. Structure of articular cartilage .....	2
1.1.2.1. Superficial zone .....	2
1.1.2.2. Mid zone .....	3
1.1.2.3. Deep zone .....	3
1.1.2.4. Calcified zone.....	4
1.1.3. Composition of articular cartilage.....	6
1.1.3.1. Tissue fluid .....	6
1.1.3.2. Structural macromolecules .....	8
1.1.3.3. Collagens.....	8
1.1.3.4. Proteoglycans .....	11
1.1.3.4.1. Non-aggregating proteoglycans.....	11
1.1.3.4.2. Aggrecan .....	12
1.1.3.5. Hyaluronan .....	15
1.1.3.6. Non-collagenous proteins and glycoproteins.....	15
1.1.4. Tissue homeostasis.....	17
1.1.4.1. Matrix metalloproteinases .....	18
1.1.4.2. Aggrecanases .....	21
1.1.4.3. Tissue inhibitors of metalloproteinases .....	23
1.2. Osteoarthritis .....	24
1.2.1. OA cartilage turnover .....	26
1.3. Mechanical load .....	27
1.3.1. <i>In vivo</i> studies .....	31
1.3.2. <i>In vitro</i> studies .....	32

1.3.2.1. Effect of static compression on ECM homeostasis .....	32
1.3.2.2. Effect of dynamic compression on ECM homeostasis .....	33
1.3.2.3. Effect of loading frequency on ECM homeostasis in articular cartilage explants .....	33
1.3.2.4. Effect of loading amplitude on ECM homeostasis in articular cartilage explants .....	33
1.3.2.5. Effect of the duration of loading on ECM homeostasis in articular cartilage explants .....	34
1.4. Mechano-transduction.....	35
1.4.1. Chondrocyte mechano-sensors/receptors .....	36
1.4.2. Intracellular signalling cascades activated by mechanical forces .....	37
1.4.2.1. Hedgehog (Hh) signalling pathway.....	37
1.4.2.2. Mitogen activated protein kinases (MAPKs) .....	38
1.4.2.3. Nuclear factor kappa B (NF-kappa B) pathway .....	39
1.5. RNA interference (RNAi) .....	40
1.5.1. microRNA.....	41
1.5.1.1. Canonical pathway of miR maturation.....	41
1.5.1.2. Non-canonical pathway of miR biogenesis .....	44
1.5.1.3. miR activity and its target sites .....	48
1.5.1.4. Nomenclature of miR .....	50
1.5.1.5. Importance of miR in articular cartilage.....	50
1.5.1.6. miR in OA cartilage .....	52
1.5.1.6.1. Up-regulated miRs in OA cartilage.....	52
1.5.1.6.2. OA-stage dependent differential expression of miRs.....	55
1.5.1.6.3. Down-regulated miRs in OA cartilage.....	58
1.5.1.7. Mechanically-regulated miRs .....	60

1.5.1.8. Mechanically–regulated miRs in chondrocytes.....	61
1.6. PhD hypothesis.....	63
1.7. PhD objectives.....	63
Chapter 2 .....	64
2.1. Cartilage explants.....	65
2.1.1. Preparation of articular cartilage explants .....	65
2.1.2. Application of mechanical load to articular cartilage explants.....	65
2. 2. Primary articular chondrocytes.....	67
2.2.1. Isolation of primary articular chondrocytes.....	67
2.2.2. Transfection of primary articular chondrocytes .....	67
2.2.2.1. Measurement of cell viability/death.....	68
2.2.2.2. Analysis of transfection efficiency using immunofluorescence microscopy	69
2.3. RNA extraction .....	69
2.3.1. RNA extraction from articular cartilage explants for mRNA analysis .....	69
2.3.2. RNA extraction from articular cartilage explants for miR analysis .....	70
2.3.3. Total RNA extraction from chondrocytes for both mRNA and miR analysis .....	71
2.3.4. Evaluation of RNA quality and yield - Bioanalyzer analysis .....	71
2.4. cDNA synthesis.....	73
2.4.1. Reverse transcription of mRNA template .....	73
2.4.2. Reverse transcription of miR template .....	73
2.5. Quantitative Polymerase Chain Reaction (qPCR) .....	74
2.5.1. Primers .....	74
2.5.2. SYBR® Green qPCR .....	78
2.5.3. Probes.....	81
2.5.4. TaqMan®PCR.....	81

2.6. Selection of suitable reference genes for quantitative PCR .....	84
2.7. Global gene analysis using Affymetrix mRNA arrays .....	86
2.7.1. Bioinformatic analysis of Affymetrix mRNA arrays .....	86
2.8. Next Generation Sequencing of miRs .....	87
2.8.1. Preparation of pooled samples .....	87
2.8.2. miR library preparation .....	88
2.8.2.1. Amplification of miR libraries .....	89
2.8.2.2. Purification of cDNA .....	90
2.8.2.3. Confirmation and size selection of amplified miRs .....	90
2.8.2.4. Elution and purification of miRs from 8% polyacrylamide gel .....	93
2.8.2.9. Purification and concentration of miR libraries .....	93
2.8.3. Bioinformatic analysis of miR Next Generation Sequencing .....	93
2.9. Next Generation Sequencing of chondrocytes transfected with miR inhibitors.....	94
2.9.1. Preparation of pooled samples .....	94
2.9.2. mRNA library preparation .....	96
2.9.2.1. Sample preparation, purification and fragmentation of mRNA.....	97
2.9.2.2. First strand cDNA synthesis .....	98
2.9.2.3. Second strand cDNA synthesis .....	99
2.9.2.4. Adenylation of 3'ends.....	100
2.9.2.5. Ligation of adapters.....	100
2.9.2.6. DNA fragment enrichment .....	101
2.9.2.7. Library validation and normalisation.....	102
2.9.2.8. Quality control .....	102
2.9.2.9. Quantity control .....	103
2.9.2.10. Normalisation and pooling of libraries.....	103
2.9.2.11. Denaturation and dilution of libraries.....	104

2.9.3. Bioinformatic analysis of mRNA Next Generation Sequencing .....	105
2.10. RT <sup>2</sup> Profiler PCR array system.....	105
2.10.1. cDNA synthesis .....	105
2.10.2. WNT RT <sup>2</sup> Profiler PCR Array .....	106
2.11. Statistical analysis .....	107
Chapter 3 .....	108
3.1. Background .....	109
3.2. Results .....	112
3.2.1. Analysis of RNA quality.....	112
3.2.2. Investigation of appropriate reference genes for assessing cartilage chondrocyte mechano-responsiveness .....	112
3.2.3. Optimisation of loading regimes.....	119
3.2.4. Characterisation of physiological and non-physiological loading regimes on the basis of ECM mRNA expression levels. ....	119
3.2.5. Global overview of differentially expressed genes in explants subjected to loads of 2.5MPa and 7MPa and analysed 4h and 24h post-load .....	127
3.2.5. Classification of differentially expressed genes in explants subjected to 2.5MPa and 7MPa loading regimes into protein classes .....	132
3. 3. Discussion.....	144
3.3.1. Identification and validation of appropriate reference genes that are unaffected by mechanical load.....	145
3.3.2. Characterisation of physiological and non-physiological magnitudes of load that induce transcriptional differences in chondrocyte response .....	147
3.3.3. Global overview of genes that are sensitive to compressive mechanical load	151
3.3.4. Protein classes of differentially expressed genes in response to 2.5MPa and 7MPa loading regimes at 4h and 24h after loading.....	157

3.3.5. Summary: .....	159
Chapter 4 .....	160
4.1. Background .....	161
4.2. Results .....	163
4.2.1. Differential expression of miR-140, -221 and -222 at 24h post-load (7MPa only) .....	163
4.2.2. Identification of mechano-regulated miRs and time post-load required for differential expression of mechano-sensitive miRs .....	165
4.2.2.1. Most abundant miRs in articular cartilage subjected to load .....	166
4.2.3. Validation of putative mechanically regulated miRs in articular cartilage .....	178
4.3. Discussion.....	182
4.3.1. Preliminary examination of mechano-sensitive miRs.....	183
4.3.2. Which miRs are the most abundant in articular cartilage? .....	183
4.3.3. Identification of mechanically regulated miRs in articular cartilage .....	184
4.3.4. Summary: .....	187
Chapter 5 .....	188
5.1. Background .....	189
5.2. Results .....	192
5.2.1. Evaluation of cellular uptake of siRNA.....	192
5.2.2. Transfection efficiency of miR inhibitors/mimics .....	194
5.2.3. Impact of transfection on cell morphology and viability .....	200
5.2.4. Differential expression of Wnt signalling components in response to inhibition of miR-21-5p, miR-221 and miR-222.....	207

5.2.5. Quantitative PCR validation of miR-21-5p, miR-221 and miR-222 target genes identified from the PCR arrays .....	213
5.2.6. Identification of miR-21-5p, miR-221 and miR-222 target genes using Next Generation Sequencing.....	216
5.2.7. Quantitative PCR validation of target genes of miR-21-5p, -221 and -222 identified from the NGS .....	225
5.3. Discussion.....	242
5.3.1. Transfection, toxicity and quantification of manipulated miRs.....	243
5.3.2. Differential expression of Wnt signalling components in response to inhibition of miR-21-5p, miR-221 and miR-222.....	244
5.3.3. qPCR validation of miR-21-5p, miR-221 and miR-222 target genes identified using Next Generation Sequencing.....	246
5.3.4. Summary: .....	253
<b>Chapter 6</b> .....	<b>254</b>
6.1. Importance of miRs in articular cartilage homeostasis .....	255
6.2. SDHA and YWHAZ are the most appropriate reference genes in mechanically loaded cartilage explants .....	258
6.3. Identification of physiological and non-physiological magnitudes of cyclic compressive load .....	258
6.3.1. Time dependent transcriptional response of mechano-sensitive genes.....	260
6.4. 24h time point is the most appropriate to observe differentially expressed miRs .....	263
6.5. Differential regulation of cartilage miRs in response to cyclic compressive load..	265
6.6. Functional analysis of mechano-sensitive miRs in transfected primary chondrocytes.....	267
6.7. Mechano-regulation of miR-21-5p and its potential role in OA pathogenesis .....	269

6.8. Is miR-221/-222 sensitivity to non-physiological magnitudes of load involved in controlling turnover of cartilage molecules?.....	271
6.9. Differential regulation of miR-21-5p, miR-221 and miR-222 in loaded cartilage explants does not inhibit expression of their direct target TIMP-3.....	272
6.10. Future directions .....	273
6.11. Conclusion .....	277
Bibliography.....	278
Appendices .....	304
Appendix 1.....	305
Publications.....	308

# Chapter 1

## Introduction

## **1.1. Articular cartilage**

Healthy joints undergo normal, pain free movement because the ends of long bones are covered by articular cartilage; due to its composition and structure, articular cartilage is viscoelastic and dissipates mechanical forces enabling painless, low-friction movement of synovial joints (Buckwalter et al., 2005).

### **1.1.2. Structure of articular cartilage**

Articular cartilage is an avascular and aneural thin tissue (Buckwalter et al., 2005), in which the organisation and structure of the cells (chondrocytes) and extracellular matrix (ECM) confers its functional properties. The thickness of cartilage between different species differ; it has been reported that the average thickness of human knee cartilage is 2.2 - 2.5mm, whereas the animal equivalents range from 0.3mm for rabbit, 0.4 - 0.5mm for sheep, 0.6 - 1.3mm for dog, 0.7 - 1.5mm for goat and 1.5 - 2mm for horse (Frisbie et al., 2006). The mature articular cartilage is divided into four zones: superficial, middle, deep and calcified cartilage (Figure 1.1) (Pearle et al., 2005, Bhosale and Richardson, 2008).

#### **1.1.2.1. Superficial zone**

The lamina splendens was first observed by MacConaill et al. using phase contrast microscopy (MacConaill, 1951), and its existence confirmed using transmission electron microscopy (TEM) (Ghadially, 1983) and scanning electron microscopy (SEM) (Clark, 1985). Lamina splendens - the outermost layer of the superficial zone is acellular (Teshima et al., 1995) and collagen types I, II and III in this layer are arranged in fine fibrils which are often observed in bundles (Fujioka et al., 2013); this differs to their organisation in the deep zone where the fibrils are thicker and rarely aggregated into bundles (Duance, 1983). The other important difference is the presence of a high concentration of type I collagen in the lamina splendens, which is absent in the deeper zone of mature mammalian cartilage (Duance, 1983). The lamina splendens also comprises lubricin (alternatively known as Superficial Zone Protein (SZP) or proteoglycan 4 (PRG4)) which is synthesised by the superficial zone chondrocytes and secreted to the

surface (Klein et al., 2003). Lubricin, together with hyaluronan serve a primary function in joint boundary lubrication (Jones et al., 2007). It provides low friction by repelling one cartilage surface from another based on strong repulsive charges (Waller et al., 2013, Jay and Waller, 2014).

The superficial zone is the thinnest zone of articular cartilage and is made from fine, tightly packed, collagen fibrils oriented parallel to the surface (mainly types II and IX collagen) (Pearle et al., 2005, Wardale and Duance, 1993). It consists of a layer of flattened chondrocytes oriented parallel to the surface (Buckwalter et al., 2005). This zone is characterised by a high concentration of water and collagen fibrils and a low concentration of proteoglycans with respect to the deeper zone (Buckwalter et al., 2005). The collagen orientation resists tensile/shear forces imposed on cartilage by everyday joint movement (Bhosale and Richardson, 2008). Apart from the mechanical properties of packed collagen fibrils, they also act as a filter for molecules and control the movement of macromolecules in and out of cartilage (Buckwalter et al., 2005).

#### **1.1.2.2. Mid zone**

The mid zone is several times thicker than the superficial zone and represents 40 – 60% of the total cartilage volume in humans (Buckwalter et al., 2005). The spheroidal shaped, randomly organised chondrocytes have more synthetic organelles (Golgi membranes and endoplasmic reticulum) than cells in the zone above, therefore in comparison to the superficial zone, the ECM contains more proteoglycan and thicker collagen fibrils (Buckwalter et al., 2005); these collagen fibrils are arranged into arcade-like structures and are referred to as Benninghoff arcades (Benninghoff, 1925, Eyre, 2002). The matrix composition of the mid zone provides cartilage with the first line of resistance against compressive load (Buckwalter et al., 2005).

#### **1.1.2.3. Deep zone**

The spherical chondrocytes are arranged in columns parallel to the collagen fibrils and perpendicular to the joint surface (Buckwalter et al., 2005); these deep zone cells synthesise the highest concentration of collagen and proteoglycans compared to cells in the other zones. The deep zone contains the largest diameter collagen fibrils, the highest

concentration of proteoglycans and the lowest content of water (Buckwalter et al., 2005). Due to the perpendicular arrangement of collagen fibrils to the joint surface and the swelling pressure derived from the high proteoglycan content, the deep zone provides the greatest resistance to compressive forces (Roughley, 2006).

#### **1.1.2.4. Calcified zone**

In mature animals the tidemark is a visible border between the uncalcified and calcified cartilage that is characterised by a low cell density, a calcified matrix and a very low metabolic activity (Buckwalter et al., 2005). Most of the cells in this zone have a hypertrophic phenotype and synthesise type X collagen (Poole et al., 2001). The calcified zone, intermediate in stiffness between the uncalcified cartilage and subchondral bone, reduces high stress forces at the cartilage/bone interface. The calcified zone plays an integral role in the attachment of the articular cartilage to the subchondral bone by fastening the collagen fibrils present in the deep zone to the underlying subchondral bone.

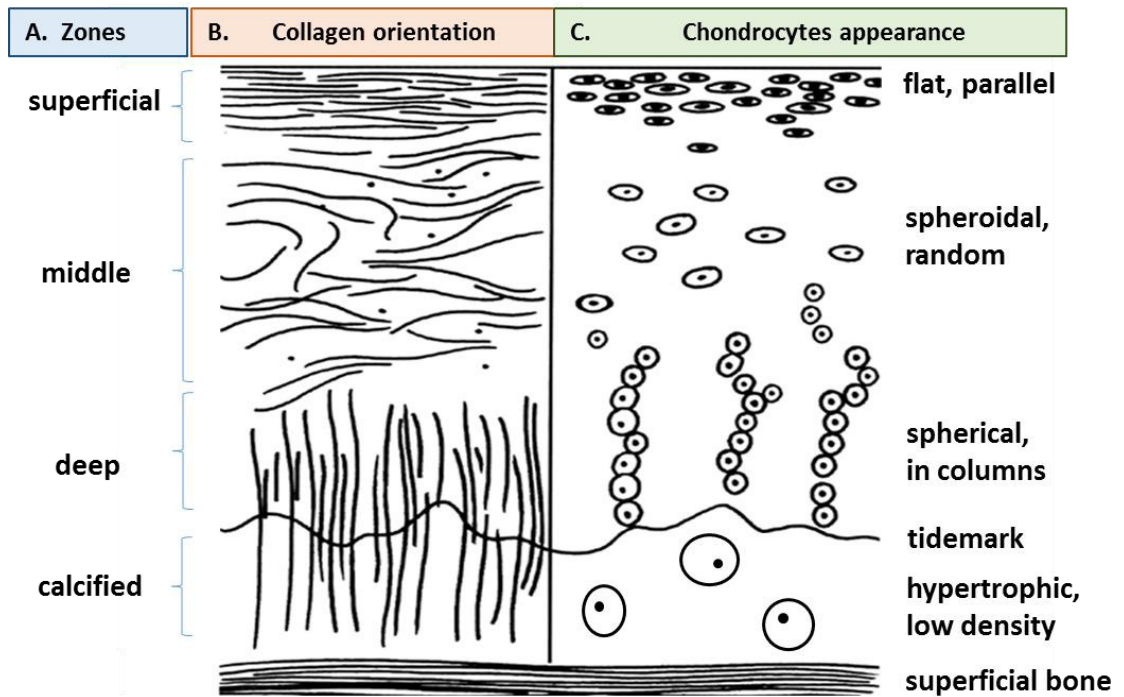


**Figure 1.1.** Cross-sectional diagram of mature articular cartilage. Organisation of zones **(A)**, collagen framework **(B)** and chondrocytes **(C)** in articular cartilage. Adapted from (Browne and Branch, 2000).

### **1.1.3. Composition of articular cartilage**

Articular cartilage is composed of a specialised extracellular matrix (ECM) of collagens (mainly collagen type II), proteoglycans and non-collagenous proteins (Figure 1.2) (Goldring and Marcu, 2009). Chondrocytes form approximately 1% of the total volume of human articular cartilage, and are responsible for synthesising and maintaining the matrix infrastructure (Buckwalter et al., 2005). The cartilage ECM is responsible for the tensile strength and compressive resistance of the tissue to mechanical load (Goldring and Marcu, 2012) and it consists of two components: tissue fluid and macromolecules that form a framework that gives the tissue its form and structure (Buckwalter et al., 2005).

#### **1.1.3.1. Tissue fluid**

The fluid phase is the most abundant component of articular cartilage and is composed of water and dissolved gases, metabolites and inorganic ions such as sodium, calcium and potassium, to balance the negatively charged proteoglycans. The water phase contributes up to 80% of the wet weight of articular cartilage and its volume can change depending on the cartilage zone, age and pathological stage of osteoarthritis (Bhosale and Richardson, 2008). The volume, concentration and movement of water in articular cartilage depend on interactions with structural macromolecules, mainly with hyaluronan/proteoglycans. Due to the negative charge of glycosaminoglycans they control the fluid's behaviour and electrolyte concentration (Buckwalter et al., 2005). The solid phase of cartilage tissue has a low permeability which causes a pressurisation of water in the tissue and plays a large role in load transmission in cartilage (Buckwalter et al., 2005). Both the low permeability of the solid phase and the high pressure of the fluid phase contribute to the stiffness and viscoelastic properties of articular cartilage and allows it to withstand a high load, i.e. many times that of body weight (Buckwalter et al., 2005).

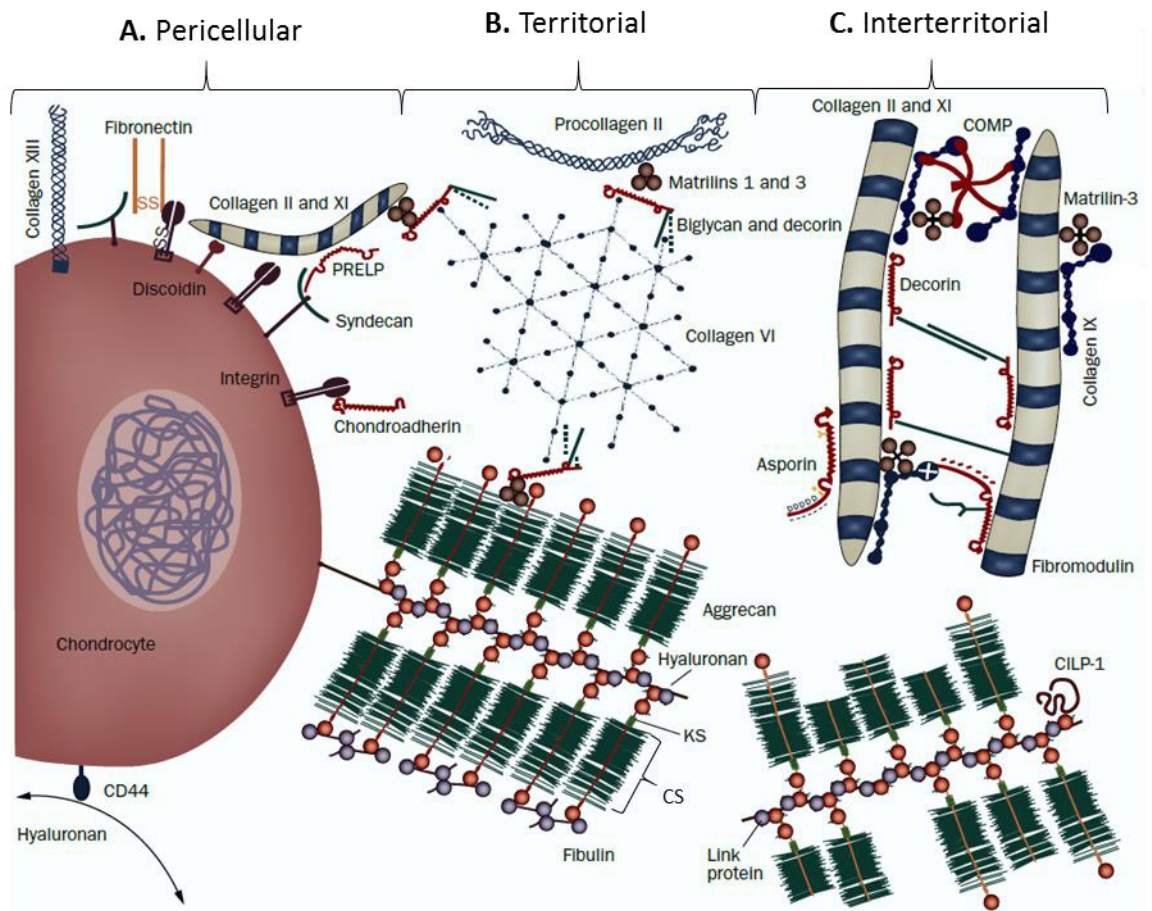


**Figure 1.2.** Schematic diagram depicting the organization of ECM molecules in articular cartilage. Due to the distance from the cells, the matrix can be divided into three zones: pericellular: which is the closest zone to the chondrocyte where ECM components interact with cell surface/cell receptors **(A)**, territorial matrix: which is the second zone in order from the cell **(B)** and the inter-territorial zone: which lies furthest in distance from the cell **(C)**. Key: CD44 - CD44 molecule, CILP-1 - cartilage intermediate layer protein 1, COMP - cartilage oligomeric matrix protein, CS - chondroitin sulphate, KS - keratan sulphate; PRELP - proline-arginine-rich end leucine-rich repeat protein. Adapted from (Heinegård and Saxne, 2011).

### **1.1.3.2. Structural macromolecules**

The solid component of articular cartilage is mainly composed of collagen type II fibrils and aggregating proteoglycans (Pearle et al., 2005). Other components of cartilage such as lipids, phospholipids, non-collagenous proteins and other types of collagen are also present, but in a minor proportion (Pearle et al., 2005, Buckwalter et al., 2005).

### **1.1.3.3. Collagens**

All collagen molecules contain three parallel polypeptide strands coiled around each other forming a triple helix (Ramshaw et al., 1998). Each polypeptide chain consists of repeating peptide triplets of Glycine-X-Y. Although X and Y can be any amino acid proline (Pro) and hydroxyproline (Hyp) are dominant in these positions (Ramshaw et al., 1998, Shoulders and Raines, 2009) The Gly-Pro-Hyp triplet contributes to the maximal stability of the collagen triple-helix (Ramshaw et al., 1998, Shoulders and Raines, 2009).

Collagen type II which constitutes 90-95 % of the collagen in the cartilage ECM forms the principal framework with proteoglycans; other types of collagen such as collagen VI, IX, X and XI (Buckwalter et al., 2005) and collagen types I and III identified in the superficial zone (Eyre, 2002, Fujioka et al., 2013, Wardale and Duance, 1993) are also present in articular cartilage. The type II collagen molecule lines up end to end and side to side to create microfibrils which are covalently cross-linked to each other to form collagen fibrils in association with collagens IX and XI (Figure 1.3) providing strength and stability to the articular cartilage (Eyre, 2002, Buckwalter et al., 2005).

Collagen type VI creates important aggregates in the ECM surrounding the chondrocytes termed the pericellular matrix (PCM); this helps the cells to attach to the ECM (Buckwalter et al., 2005, Gordon and Hahn, 2010, Poole et al., 1988).

Type X collagen is produced only by hypertrophic chondrocytes in the calcified zone of cartilage (Reichenberger et al., 1991); it is localised within the pericellular environment suggesting that it acts as a structural support for hypertrophic chondrocytes and plays a role in cartilage mineralisation and endochondral ossification (Gelse et al., 2003, Reichenberger et al., 1991).

Collagen type IX is cross-linked to the surface of collagen type II fibrils and has an ability to create bridges between adjacent collagen fibrils which increases network mechanical integrity (Eyre, 2002). Type XI collagen nucleates collagen type II fibrils promoting stabilisation of the fibrillar type II collagen network (Buckwalter et al., 2005).

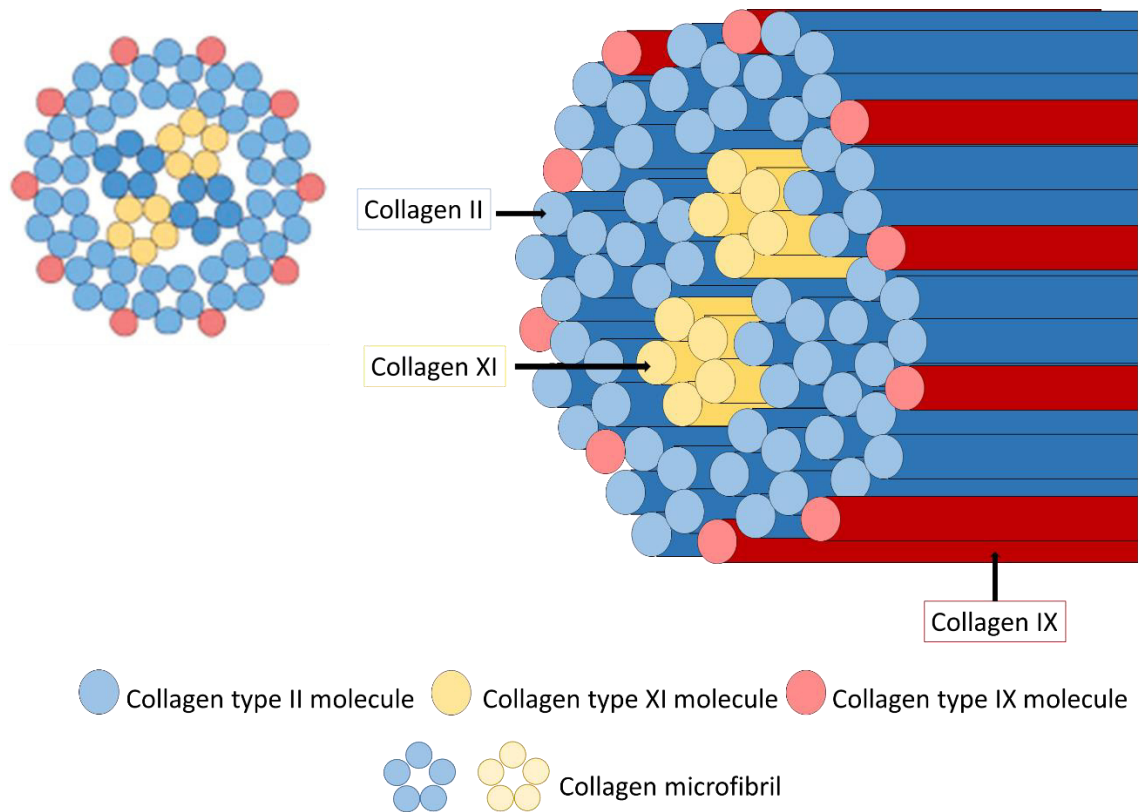


**Figure 1.3.** Potential interactions between collagens type II, IX and XI in a cartilage collagen fibril. Collagen IX is covalently linked to the surface of thin cartilage collagen fibrils which are constructed from two collagen II microfibrils and two collagen XI microfibrils at the core of the fibril, surrounded by ten microfibrils comprising five collagen type II molecules (Holmes and Kadler, 2006, Kadler et al., 2008). Adapted from (Kadler et al., 2008).

#### **1.1.3.4. Proteoglycans**

Heavily glycosylated proteins that occur in the cartilage ECM belong to the proteoglycan family and comprise 10 - 20% wet weight of cartilage (Buckwalter et al., 2005). The proteoglycans consist of a protein core to which at least one glycosaminoglycan (GAG) chain is covalently attached (Kiani et al., 2002). GAGs protrude from the protein core and remain separated from each other because of their negative charge which repel each other and other negatively charged molecules, but attract cations (Buckwalter et al., 2005). In articular cartilage, two major classes of proteoglycans have been found: small non-aggregating leucine rich proteoglycans (SLRPs): e.g. decorin, biglycan and fibromodulin, and large aggregating proteoglycan monomers, namely aggrecan (Buckwalter et al., 2005).

##### **1.1.3.4.1. Non-aggregating proteoglycans**

The small leucine-rich proteoglycans (SLRPs) are biologically active components of the ECM proteoglycans consisting of one or more GAG chains attached to a protein core that is made up of leucine-rich repeats (LRRs) bordered by cysteine-clusters (Douglas et al., 2006, Iozzo, 1998, Heinegård, 2009). Members of SLRPs are classified based on the amount of LRRs and positioning of cysteine-clusters in the protein core, and the type of GAG covalently attached (Roughley, 2006). SLRPs that are present in articular cartilage can be divided into two distinct classes: class I – decorin and biglycan that possess one or two GAG chains, respectively, consisting either chondroitin or dermatan sulphate, and class II – fibromodulin that carries several GAG chains (keratan sulphate) (Hedbom and Heinegård, 1993).

SLRPs regulate collagen network organisation by connection through their protein core/ GAG chains to collagen which contribute to cartilage integrity and function (Dellett et al., 2012). Decorin and biglycan interact with collagen type VI microfibrils through their core protein and facilitate interactions with other ECM components, for example with matrilin-1 (Heinegård, 2009) which provides further cross-linking to aggrecan or alternatively collagen type II fibrils (Wiberg et al., 2003). Recently, evidence of a strong interaction of biglycan with collagen type II fibrils was reported (Douglas et al., 2006,

Vynios et al., 2001); this suggests that biglycan, similar to decorin and fibromodulin, has the capacity to decorate collagen type II fibrils (Buckwalter et al., 2005, Hedbom and Heinegård, 1993) and may have a role in organising and stabilising the type II collagen framework (Figure 1.2). Moreover, studies have shown the ability of SLRPs to regulate some signalling pathways through binding to their ligands, receptors or members of the pathway (Dellett et al., 2012). Decorin, biglycan and fibromodulin bind transforming growth factor- $\beta$  (TGF- $\beta$ ) sequestering its activity (Hildebrand et al., 1994), and therefore may influence the activity of the TGF- $\beta$  signalling pathway which is important in the regulation of articular chondrocyte metabolism (Swingler et al., 2012). Decorin and biglycan are also associated with Wnt-1 induced secreted protein-1 (WISP-1) (Desnoyers et al., 2001), known to be up-regulated in OA cartilage, and a component of the canonical Wnt signalling pathway regulating both MMPs and aggrecanases expression (Blom et al., 2009). Decorin through its protein core is also able to bind and activate the insulin-like growth factor 1 (IGF-1) receptor (Schönherr et al., 2005), which is particularly important in cartilage homeostasis as IGF-1 is a vital anabolic stimulus activating proteoglycan synthesis in articular cartilage (Verschure et al., 1996).

#### **1.1.3.4.2. Aggrecan**

In articular cartilage, aggrecan is found in multi-molecular aggregates, comprised of numerous monomers bound to a hyaluronan molecule (HA) (Figure 1.4) and this structure is stabilised by link protein (Kiani et al., 2002). The aggrecan core protein consists of three globular domains: G1 and G2, at the N-terminus, and G3 at the C-terminus (Aspberg, 2012, Roughley, 2006). The G1 and G2 domains are separated by a short interglobular domain (IGD). The G2 and G3 domains are separated by a long GAG-attachment region, which is subdivided into a keratan sulphate (KS) domain and two chondroitin sulphate (CS) domains (CS1 and CS2) (Aspberg, 2012, Roughley, 2006). The aggrecan monomers are non-covalently bound to HA via the G1 domain and the presence of link protein that stabilises this interaction (Figure 1.4) (Aspberg, 2012, Roughley, 2006). The very large multi-molecular aggregates of HA - aggrecan are trapped within the collagen framework of cartilage (Bhosale and Richardson, 2008). Due to their fixed negative charges that attract positive ions they have an ability to draw

water into the tissue causing the cartilage swelling pressure which is crucial to the biomechanical properties of cartilage, as it provides the tissue with the ability to resist compressive load (Huang and Wu, 2008). The biomechanical capability of articular tissue is described in more detail in Section 1.3.

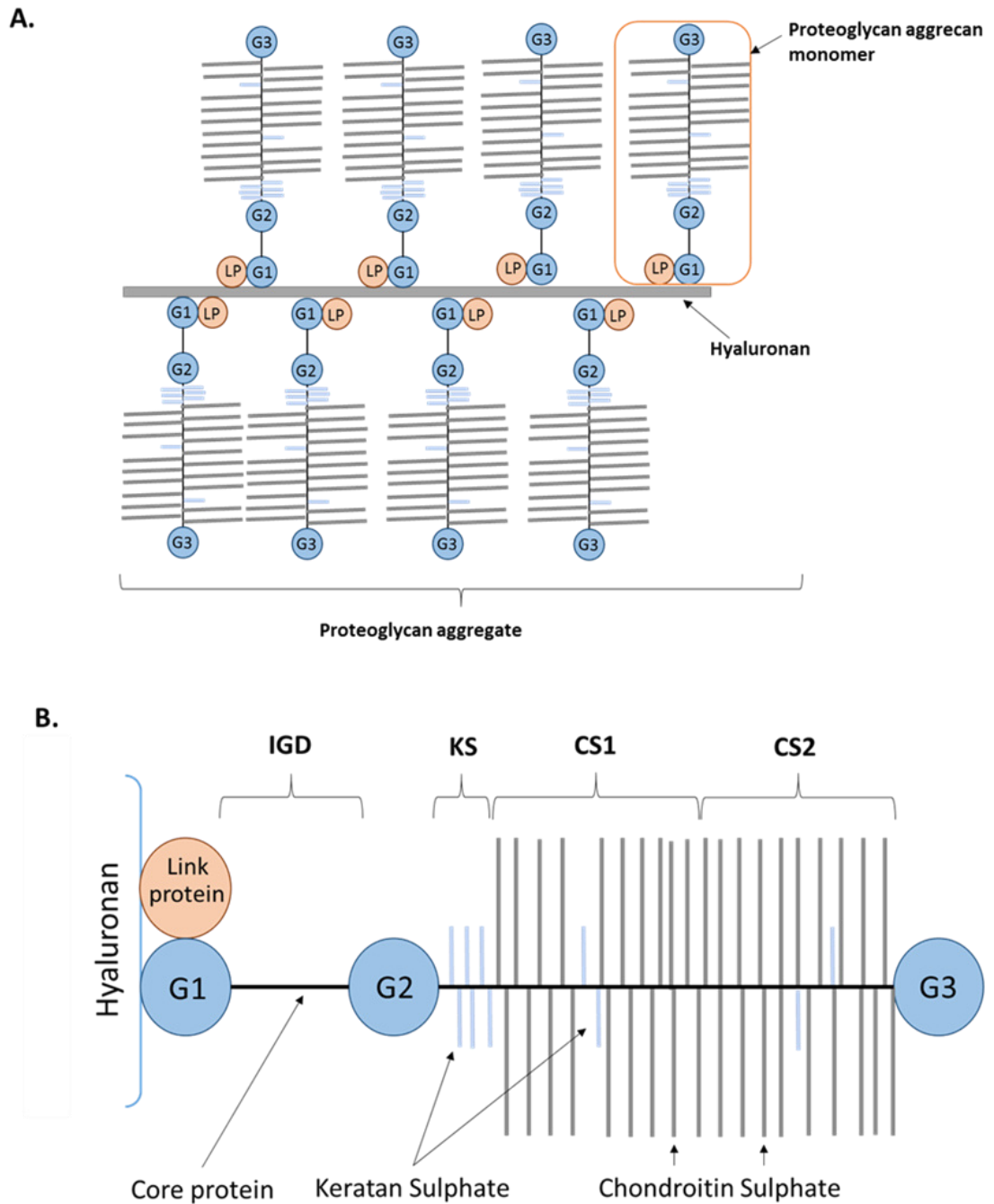


**Figure 1.4.** Schematic diagram of multi-molecular aggregate of aggrecan bound to a hyaluronan molecule **(A)** and proteoglycan aggrecan monomer **(B)**. G1, G2, G3 - globular domains, IGD - interglobular domain, KS - keratan sulphate domain, CS1, CS2 - chondroitin sulphate domains. Adapted from (Huang and Wu, 2008, Pearle et al., 2005).

### **1.1.3.5. Hyaluronan**

Hyaluronic acid (HA) is a non-sulphated glycosaminoglycan synthesised in the cellular membrane directly to the ECM (Roughley, 2006). It has a very high affinity to water binding therefore it plays a crucial role in water movement and homeostasis. In a water rich environment it creates a gel-like solution and together with the collagen type II – aggrecan network it provides tissue viscoelasticity which is very important in cartilage protection and functionality (Fraser et al., 1997). HA occurs freely or in association with matrix or cell surface proteins in the intercellular matrix. It is involved in creating aggrecan aggregates which are located between collagen fibrils and which attract water into cartilage via osmosis. Moreover, the proteoglycan-collagen type II network stabilises the intercellular matrix structure; due to the association with the major cellular HA receptor CD44 localised in the plasma membrane it anchors chondrocytes into the intercellular matrix (Fraser et al., 1997, Laurent and Fraser, 1992).

Intra-articular injection with medium (800kDa) and high (2000-3000kDa) molecular mass HA are used to treat osteoarthritis (OA) of the knee; recent studies have reported that HA, apart from symptom modifying effects such as relief of joint pain, also represses the expression of catabolic molecules in OA cartilage (Yatabe et al., 2009). Binding of HA2700 with CD44 in IL-1 stimulated human OA chondrocytes inhibited mRNA and protein levels of ADAMTS-4 (Yatabe et al., 2009), whereas HA800 binding to CD44 had a protective role via MMP-1, -3 and -13 inhibition in both healthy and IL-1 treated human OA chondrocytes (Julovi et al., 2004).

### **1.1.3.6. Non-collagenous proteins and glycoproteins**

The ECM of cartilage contains numerous additional matrix glycoproteins. To that class of protein belong for example: link protein, cartilage oligomeric matrix protein (COMP), matrilins and structural proteins e.g. fibronectin (Roughley, 2001). It is thought that their main role is to help organise and maintain the macromolecular structure of the cartilage ECM (Buckwalter et al., 2005).

Link proteins are involved in creating aggrecan aggregates through conformational alterations in the G1 domain of the aggrecan monomer which allows binding to HA (Roughley, 2006).

COMP, also called thrombospondin-5 (TSP-5), interacts with many ECM proteins e.g. collagen, matrilins, fibronectin and aggrecan, and one of its main functions is in ECM assembly (Acharya et al., 2014). COMP promotes collagen type II fibrillogenesis in cartilage as its five domains interact with five collagen type II molecules bringing them closer to each other to create a microfibril (Heinegård, 2009). The association of COMP with collagen type IX that is located on the collagen type II fibril surface suggests a role for COMP as a “bridging molecule” involved in fibril network stabilisation (Acharya et al., 2014).

The matrilins are also considered as one of the most important molecules affecting matrix assembly. Of the four members of the matrilin family, matrilin-1 and matrilin-3 are the most abundant in cartilage; they are often referred to as “bridging molecules” as they connect indirectly other matrix molecules e.g. COMP and collagen type X (Klatt et al., 2011). Matrilin-1 is the only matrilin that has been reported to associate with aggrecan (Paulsson and Heinegård, 1979). In turn, matrilin-1, -3, and -4 were localised in a complex with decorin and biglycan bound to collagen type VI (Klatt et al., 2011); this complex could further bind to aggrecan or collagen type II fibrils either directly or via collagen type IX (Klatt et al., 2011).

Specific mutations in the COMP gene lead to pseudoachondroplasia (PSACH) and multiple epiphyseal dysplasia (MED), diseases which can also manifest due to mutations in matrilin-3 or collagen type IX genes (Briggs et al., 2015). Both of these diseases are defined by limb dwarfism with normal skull size and are characterised by joint pain, stiffness and early OA development (Briggs et al., 2015). Interestingly, COMP mutations (d469del, D511Y and G427E) in PSACH chondrocytes showed impaired secretion of collagen type IX and matrilin-3, whereas the expression levels of collagen type II and aggrecan did not change (Hecht et al., 2005). They also reported destabilisation of intercellular matrix structure in PSACH cartilage indicating the importance of COMP,

matrilin-3 and collagen IX in maintaining cartilage structure and integrity (Hecht et al., 2005).

Fibronectin is a molecule responsible for cell adhesion to the intercellular matrix (Acharya et al., 2014). One end of a fibronectin molecule can interact with the cell surface directly or through receptors e.g. integrins, whereas the other end binds to matrix molecules such as COMP (Acharya et al., 2014), collagen and sulphated proteoglycans (Perkins et al., 1979, Martin and Buckwalter, 1998). The abundance of fibronectin in human OA cartilage is elevated approximately 10-fold in comparison to healthy tissue (Brown and Jones, 1990). Although, the functional implication of fibronectin in OA degradation is unknown (Roughley, 2001), the fibronectin fragments are able to promote aggrecan degradation at the well-characterised aggrecanase cleavage sites (Homandberg et al., 1997). Therefore it is believed that fibronectin fragments present in arthritic cartilage induce expression of inflammatory cytokines, e.g. IL-1 that stimulates elevated production of aggrecanases (Homandberg et al., 1997, Roughley, 2006).

#### **1.1.4. Tissue homeostasis**

Chondrocytes are responsible for maintaining tissue homeostasis e.g. composition and organisation of the ECM. In healthy tissue they respond to their environment to maintain the balance between anabolic and catabolic activity, thereby regulating the synthesis and degradation processes of cartilage components (Goldring and Marcu, 2009). They maintain healthy cartilage by controlling the optimal amount of ECM molecules, mainly collagen type II and aggrecan. Cartilage degradation is mediated by proteolytic enzymes, such as matrix metalloproteinases and aggrecanases: a disintegrin and metalloprotease with thrombospondin motifs (ADAMTS -4 and -5) that degrade the main components in cartilage, collagen and proteoglycans respectively (Barter et al., 2012).

#### **1.1.4.1. Matrix metalloproteinases**

Matrix metalloproteinases (MMPs) belong to a family of zinc containing endopeptidases and are responsible for tissue turnover and ECM degradation, where substrates include collagen, gelatin, matrix glycoproteins and proteoglycans (Verma and Hansch, 2007). Most MMPs have a very low activity in normal, healthy tissue. Their expression and activity is regulated by specific factors e.g. inflammatory cytokines, hormones, growth factors, mechanical load, cell-cell and cell-ECM interactions, but their activity is strictly controlled by tissue inhibitors of metalloproteinases (TIMPs) (Nagase et al., 2006, Verma and Hansch, 2007). Thus, the balance between MMPs and TIMPs is crucial to ECM homeostasis (Nagase et al., 2006). MMPs are synthesised as pro-enzymes and require activation by other proteolytic enzymes (Verma and Hansch, 2007). MMPs are composed of 5 homologous domains: **1.** Signal peptide which is required for the secretion of MMPs into the ECM (Bonnans et al., 2014). **2.** Pro-peptide domain to maintain the enzyme in an inactive form. This domain contains a cysteine residue which binds the  $Zn^{2+}$  site in the catalytic domain to keep the enzyme in a latent form **3.** Catalytic domain that is required for proteolytic activity. The activation of MMP enzyme is conducted by disruption of the cysteine residue -  $Zn^{2+}$  association. This process is called a “cysteine switch” and it replaces cysteine with water in connection with  $Zn^{2+}$ . **4.** Hinge region which links the catalytic and hemopexin domain, **5.** Hemopexin domain which is responsible for interactions with substrates and confers enzyme specificity (Murphy et al., 2002, Snoek-van Beurden and Von den Hoff, 2005) (Figure 1.5). Some MMPs have additional domains, such as transmembrane or cytoplasmic domains (Snoek-van Beurden and Von den Hoff, 2005). Based on the domain arrangement, substrate specificity and sequence similarity, MMPs have been divided into six subfamilies (Table 1.1).

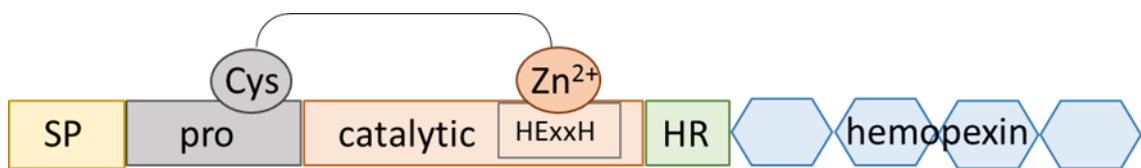


**Figure 1.5.** Schematic diagram of domain structure of MMPs. Key: SP - signal peptide, pro - pro-peptide domain, Cys – cysteine residue, Zn<sup>2+</sup> - zinc ion, HExxH - Zn<sup>2+</sup> binding motif, HR - hinge region. Adapted from (Gong et al., 2014).

**Table 1.1.** Members of the human matrix metalloproteinase family (Snoek-van Beurden and Von den Hoff, 2005). Key: ✓ - MMPs involved in cartilage matrix degradation in OA (Troeberg and Nagase, 2012).

Subgroup	MMP	Name	Substrate
1. Collagenases	✓ MMP-1	Collagenase-1	Col I, II, III, VII, VIII, X, gelatin
	✓ MMP-8	Collagenase-2	Col I, II, III, VII, VIII, X, aggrecan, gelatin
	✓ MMP-13	Collagenase-3	Col I, II, III, IV, IX, X, XIV, gelatin
2. Gelatinases	✓ MMP-2	Gelatinase A	Gelatin, Col I, II, III, IV, VII, X
	✓ MMP-9	Gelatinase B	Gelatin, Col IV, V
3. Stromelysins	✓ MMP-3	Stromelysin-1	Col II, IV, IX, X, XI, gelatin
	MMP-10	Stromelysin-2	Col IV, laminin, fibronectin, elastin
	MMP-11	Stromelysin-3	Col IV, fibronectin, laminin, aggrecan
4. Matrilysins	✓ MMP-7	Matrilysin-1	Fibronectin, laminin, Col IV, gelatin
	MMP-26	Matrilysin-2	Fibrinogen, fibronectin, gelatin
5. MT-MMP	✓ MMP-14	MT1-MMP	Gelatin, fibronectin, laminin
	MMP-15	MT2-MMP	Gelatin, fibronectin, laminin
	MMP-16	MT3-MMP	Gelatin, fibronectin, laminin
	MMP-17	MT4-MMP	Fibrinogen, fibrin
	MMP-24	MT5-MMP	Gelatin, fibronectin, laminin
	MMP-25	MT6-MMP	Gelatin
6. Others	MMP-12	Macrophage metalloelastase	Elastin, fibronectin, Col IV
	MMP-19		Aggrecan, elastin, fibrillin, Col IV, gelatin
	MMP-20	Enamelysin	Aggrecan
	MMP-21	XMMP	Aggrecan
	MMP-23		Gelatin, casein, fibronectin
	MMP-27	CMMP	Unknown
	✓ MMP-28	Epilysin	Unknown

MMPs are categorized according to the organization of their peptide domains, their substrate specificity, and their sequence similarity (8,12,17,22–24,85–87). MMP, matrix metalloproteinase; MT-MMP, membrane-type matrix metalloproteinase.

#### 1.1.4.2. Aggrecanases

The principal aggrecanases present in articular cartilage are aggrecanase-1 and aggrecanase-2 called ADAMTS-4 and ADAMTS-5, respectively (Caterson et al., 2000). Both of these are multi-domain metalloproteinases which consist of a signal sequence, pro-domain, catalytic domain, disintegrin-like domain, spacer domain, thrombospondin motifs (TSP) and sub-motifs which help to regulate enzyme activity and substrate specificity (Huang and Wu, 2008). ADAMTS-4 and ADAMTS-5 are the shortest members of the ADAMTS family because they have only one or two TSP motifs, respectively (Figure 1.6) (Nagase et al., 2006). They are synthesised as zymogens and before they are secreted into the ECM, furin cleaves the furin recognition sequence localised in the pro-domains of ADAMTS-4 and -5 resulting in their activation (Verma and Hansch, 2007). The ancillary domains of both ADAMTSs have a crucial role in directing these enzymes to the cell surface, ECM and their substrates, whereas the cysteine rich domain and spacer domain are essential for these enzymes interaction with the GAGs on aggrecan (Verma and Hansch, 2007).

ADAMTS-4 and ADAMTS-5 are involved in controlling aggrecan turnover in the cartilage ECM (Caterson et al., 2000, Caterson et al., 1999). The critical site of cleavage by ADAMTS-4 and -5 occurs within the aggrecan IGD domain, between G1 and G2 (Figure 1.7); this releases the negatively charged GAG containing domain from the aggregate that is critical in maintaining the high osmotic pressure, hence hydration state of the tissue essential to resist compressive mechanical loads. The presence of GAGs (occurring after cleavage of the Glu<sup>373</sup>-Ala<sup>374</sup> in IGD domain) in the synovial fluid of patients with OA indicates that this cleavage site mediates aggrecan degradation and can drive pathology in articular cartilage (Huang and Wu, 2008). However, the Glu<sup>373</sup>-Ala<sup>374</sup> bond is not the only cleavage site of these enzymes (Huang and Wu, 2008). ADAMTS-4 and -5 also cleave aggrecan at four other sites that are located between the G2 and G3 domain (Figure 1.7) (Nagase and Kashiwagi, 2003, Huang and Wu, 2008, Caterson et al., 2000).

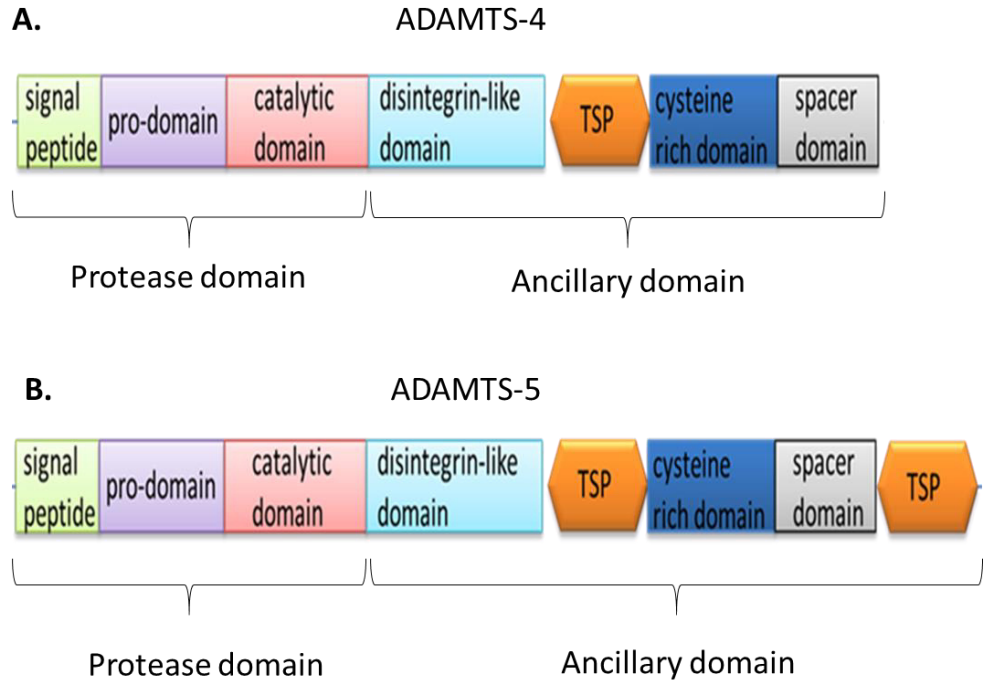


**Figure 1.6.** Schematic diagram of ADAMTS-4 **(A)** and ADAMTS-5 **(B)** structure. The protease domain is responsible for the enzyme's transformation from a zymogen into its active form and hence its enzymatic activity. The ancillary domain affects the enzymatic specificity of these ADAMTSs (Verma and Hansch, 2007). Key: TSP - thrombospondin type I domain. Adapted from (Verma and Hansch, 2007).

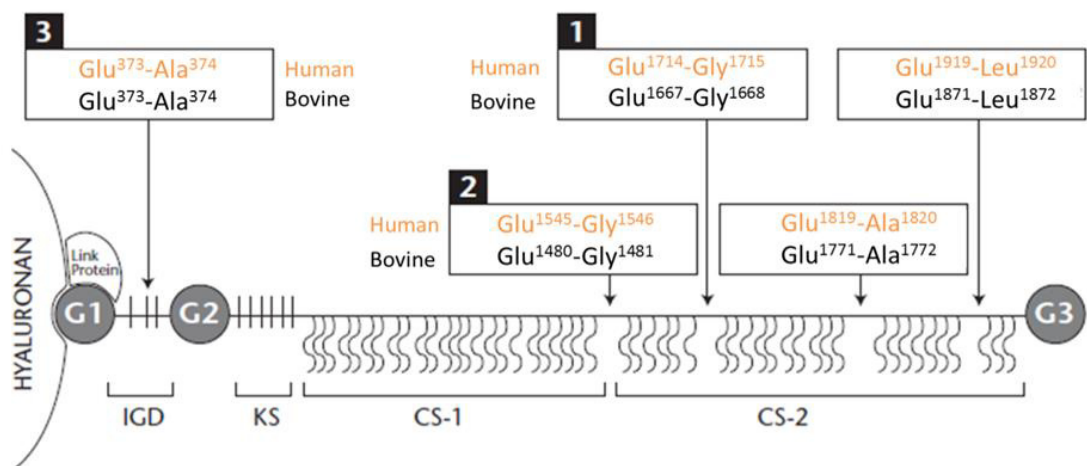


**Figure 1.7.** Aggrecanase cleavage sites for human (orange) and bovine (black) aggrecan core protein. Numbers above the boxes indicate the preferred order of enzymatic cleavage. Modified image from (Huang and Wu, 2008).

#### **1.1.4.3. Tissue inhibitors of metalloproteinases**

The activity of metalloproteinases can be controlled and regulated by endogenous inhibitors (Lipka and Boratynski, 2008). Tissue inhibitor of metalloproteinases (TIMPs) is the main group of regulators and comprise four inhibitors including TIMP-1, TIMP-2, TIMP-3 and TIMP-4 (Snoek-van Beurden and Von den Hoff, 2005). TIMPs comprise 2 subdomains: N-terminal and C-terminal. The N-terminal subdomain binds to the catalytic site of MMPs and inhibits their activity through removing water bound to the  $Zn^{2+}$  in the catalytic domain and displacing it with cysteine residues belonging to the N-terminal domain of TIMP (Brew and Nagase, 2010). TIMPs inhibit all MMPs tested to date, however the efficiency of inhibition varies with each TIMP. Interestingly, TIMP-3 is bound to GAGs and is considered to be a better inhibitor of aggrecanases (ADAMTS-4 and -5) than MMPs (Visse and Nagase, 2003, Lipka and Boratynski, 2008).

## **1.2. Osteoarthritis**

In healthy cartilage, anabolic and catabolic activities of chondrocytes are balanced; however, there are several factors which can disturb this homeostasis and limit the ability of the cells to maintain tissue homeostasis, thereby contributing to the development and progression of articular cartilage degeneration e.g. osteoarthritis (OA). Several risk factors that contribute to the development of OA include ageing, abnormal mechanical stress, joint injury, obesity, inflammation and genetic predisposition. OA is characterised by progressive loss of articular cartilage and bone remodelling inducing osteophyte formation (Lorenz and Richter, 2006). The typical feature of OA is tissue degradation which results in a progressive loss of the structure and function of articular cartilage. The progressive loss of cartilage can be divided into three stages (Figure 1.8). As a first step in OA, the surface loses its smoothness and some changes to the cartilage surface are noticeable, and aggrecan levels decrease (Lorenz and Richter, 2006). There is a higher concentration of water in the ECM, tissue permeability increases resulting in a significantly lower hydrostatic pressure. Decreased hydrostatic pressure in the ECM causes a reduction in the compressive stiffness of the tissue (Pearle et al., 2005). The next stage, that can last several years, is the further loss of proteoglycans and the formation of chondrocyte clusters surrounded by newly synthesised matrix molecules which are produced to attempt to repair the damage. However, chondrocytes are not able to adequately renew the tissue, therefore the third and last stage of OA is the complete loss of cartilage tissue (Lorenz and Richter, 2006).

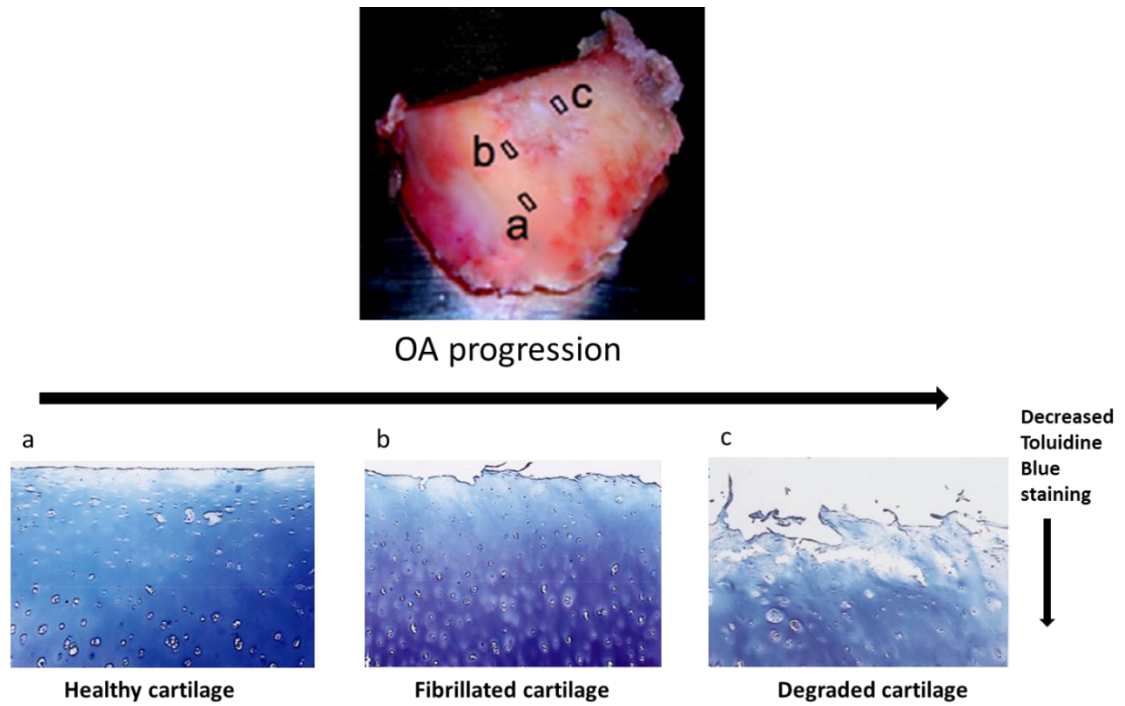


**Figure 1.8.** Representative toluidine blue stained sections of healthy and OA cartilage regions from the femoral condyle of human OA knee joint. Healthy area with smooth articular cartilage surface **(a)**. Section from an early stage of OA (fibrillated area) showing dense staining for proteoglycans in the mid zone, where chondrocytes remain active **(b)**. Section from the late stage of OA showing a degraded articular cartilage surface, loss of proteoglycan staining and chondrocyte clusters **(c)** (Venkatesan et al., 2012).

### 1.2.1. OA cartilage turnover

OA results from an imbalance of anabolic and catabolic activities with increased expression and activation of proteolytic enzymes such as the MMPs and ADAMTSs that degrade the main components in cartilage: collagen and proteoglycans respectively (Goldring and Marcu 2009a). Collagenase-1, -2, -3 (MMP-1, -8, -13), stromelysin-1 (MMP-3) and membrane type I (MT1) MMP (MMP-14) are all involved in collagen degradation in OA (Goldring and Marcu, 2009). MMP-3 activates pro-collagenases (pro-MMP- 1, -13) and pro-gelatinases (pro-MMP-9, -2) (Ramos-DeSimone et al., 1999, Johnson et al., 2011); MMP-14 synthesised by chondrocytes activates pro-MMP-13 which in turn activates pro-MMP-9 (Goldring and Marcu, 2009). Some MMPs such as MMP-3, -7, -8 and -14 have an ability to degrade proteoglycans, but ADAMTS-4 and-5 are thought to be the principal aggrecan degrading enzymes (Goldring and Marcu, 2009). Some studies have shown that abnormal mechanical load, inflammatory cytokines, genetic and epigenetic alterations (e.g. microRNAs (miRs)) can increase expression and activity of catabolic enzymes, affecting chondrocyte viability and ECM breakdown (Barter et al., 2012, Blain et al., 2001, Goldring and Marcu, 2012, Thomas et al., 2011). All MMPs, but also ADAMTS-4 and -5, that are involved in cartilage turnover/degradation are regulated by the specific endogenous protein inhibitors TIMPs in a 1:1 stoichiometry (Visse and Nagase, 2003), therefore disruption of this balance may lead to OA development. TIMP-1, -2, -3 and -4 inhibit the activity of all MMPs, but with different affinities for different MMPs (Murphy, 2011); TIMP-1 interacts the most effectively with MMP-1, -3, -7 and -9, whereas TIMP-2 presents a preference for inhibition of MMP-2, however TIMP-2 can also act as an activator of pro-MMP-2 (Brew and Nagase, 2010, Murphy, 2011, Bourbonliou and Stetler-Stevenson, 2010). TIMP-3, apart from its preference to inhibit MMP-2 and -9, also represses ADAMTS-4 and -5 (Brew and Nagase, 2010, Murphy, 2011, Bourbonliou and Stetler-Stevenson, 2010). In turn, TIMP-4 preferentially inhibits MMP-14 (Brew and Nagase, 2010, Murphy, 2011, Bourbonliou and Stetler-Stevenson, 2010). TIMP-1 and TIMP-4 are also capable of binding to pro-MMP-9 and pro-MMP-2 respectively and prevent their activation, whereas TIMP-3 plays an inhibitor role by association with both of these inactive forms of MMPs (Bourboulia and Stetler-Stevenson, 2010).

### 1.3. Mechanical load

Mechanical load is one of the most important factors that affects cartilage structure and function through chondrocyte stimulation (Buckwalter et al., 2005). At the joint level articular cartilage is mostly exposed to compressive load; however, there are also other mechanical stimuli such as tension and shear that occur in cartilage as a result of everyday movement which affects the cellular response and induces deformation, fluid flow, hydrostatic pressure, osmotic pressure, ion concentration changes and pH alteration in tissue (Figure 1.9) (Lee et al., 2005a).

Cartilage has unique viscoelastic properties that enable its deformation when the joint is exposed to mechanical load and reduces the magnitude of compression applied to the bone (Buckwalter et al., 2005). The biomechanical properties of the cartilage is facilitated by one of the most abundant components of the ECM which are the proteoglycans (Buschmann et al., 1995). According to the principle of the Donnan effect, negatively charged GAGs, to maintain cartilage electro-neutrality, attract positively charged ions (mainly  $\text{Ca}^{2+}$  and  $\text{Na}^{+}$ ) (Prydz, 2015). This process results in electro-neutrality but also in a large difference in the ionic concentration between the cartilage matrix and surrounding tissues. The increased cation concentration in the cartilage ECM creates an internal osmotic pressure in the tissue, also referred to as the Donnan osmotic pressure (Wilson et al., 2005). The higher concentration of ions within the cartilage ECM compared to the outside of the tissue is followed by water influx, ECM swelling and expansion resisted by the collagen fibril network, therefore collagen is subjected to a “pre-stress” even if the external load is not applied (Lai et al., 1991). When the cartilage is exposed to mechanical compression, the water is expelled from the cartilage increasing the osmotic pressure and limiting the degree of compression; but when the load is removed, water molecules are re-imbibed into the tissue and restore the structure of cartilage to what it was before the load (Buckwalter et al., 2005, Buschmann et al., 1995). Moderate mechanical load is essential to maintain cartilage homeostasis as it induces chondrocytes to balance the synthesis of molecules that are involved in anabolic/catabolic cell processes. Abnormal joint loading which is characterised by either over-load or insufficient load has been reported to disrupt the

homeostatic production of molecules by chondrocytes and cause cartilage degeneration which contributes to OA development.

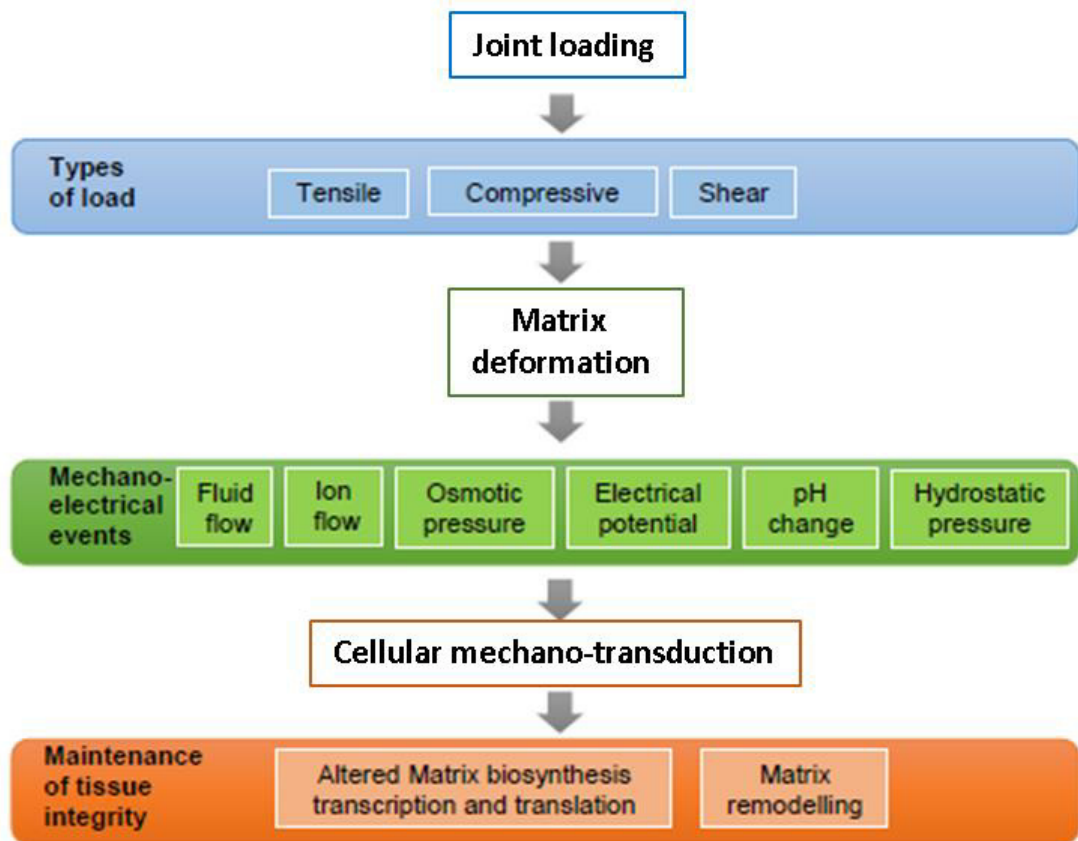


**Figure 1.9.** Illustration of different types of load to which articular cartilage in the joint is exposed to and the accompanying physical and biochemical alterations in response to everyday movement. Adapted from (Al-Sabah, 2014, PhD thesis).

Many studies have been performed to investigate the effect of mechanical forces on articular cartilage homeostasis. *In vitro* studies have been conducted to observe the chondrocyte's response to biomechanical signals without any interaction with other surrounding joint tissues e.g. bone, synovium. For this kind of experiment, either a cell culture system (monolayer or 3D) or articular cartilage explants have been utilised. Also, *in vivo* studies have been performed to determine the effect of load on the whole joint. *In vitro* studies have demonstrated that chondrocytes are mechano-responsive to compressive, shear and tensile loads (Das et al., 2008, Huang et al., 2007, Urban, 1994, Ramage et al., 2009, Blain, 2007, Thomas et al., 2011). *In vivo* studies have shown that moderate mechanical loading like walking and jogging is necessary to maintain healthy cartilage, while over- or insufficiently loaded articular cartilage can activate catabolic enzymes and promote cartilage degradation (Bader et al., 2011).

Chondrocyte activity is stimulated by mechanical and biochemical signals that can induce a wide range of metabolic responses in articular cartilage (Buckwalter et al., 2005, Griffin and Guilak, 2005). Depending on the type of loading, mechanical load may have both degenerative and biosynthetic roles in cartilage metabolism and homeostasis. Normal mechanical load, such as walking and moderate exercise stimulates chondrocytes to produce collagen and aggrecan enabling the maintenance of normal cartilage integrity. Abnormal, non-physiological loading, such as insufficient or over load may lead to loss of proteoglycans, destruction of the collagen network and inhibition of matrix protein synthesis which can drive the development of OA. Different joints and different types of physical activities are associated with different mechanical forces (Ramage et al., 2009). Articular cartilage is mainly loaded in compression; however, chondrocytes also perceive hydrostatic pressure generated by shear and tensile strain (Blain, 2007, Lee et al., 2005c). Changes in amplitude, frequency and duration of loading have significant effects on cell activity and ECM synthesis, and also affects the production of molecules leading to cartilage breakdown (Urban, 1994).

### 1.3.1. *In vivo* studies

Abnormal joint loading such as immobilisation has been reported to affect collagen-proteoglycan network components of articular cartilage decreasing its biomechanical properties and increasing the risk of pathology.

Early *in vivo* sheep studies performed by Caterson et al. reported the necessity of mechanical load to maintain cartilage homeostasis (Caterson and Lowther, 1978). A 4-week immobilisation period of one of the sheep forelegs resulted in a decrease in cartilage proteoglycan molecular weight in the non-weight bearing ankle joint; in contrast, the articular cartilage of the loaded joint in the contralateral leg presented a significant increase in proteoglycan molecular weight (Caterson and Lowther, 1978).

Palmoski et al. further confirmed the importance of mechanical load on cartilage homeostasis (Palmoski et al., 1979, Palmoski and Brandt, 1981). Immobilisation of adult canine joints by casting the limb led to decreased proteoglycan synthesis in cartilage as soon as 6 days after immobilisation, whereas after 3 weeks alterations in proteoglycan aggregation were observed (aggregates of proteoglycans were smaller); 2 weeks of reloading of these joints immobilised for 6 weeks restored proteoglycan aggregates to their normal size (Palmoski et al., 1979). Furthermore, it was found that knee joint cartilage unloaded for 6 weeks was characterised by increased water content and reduced tissue thickness (Palmoski and Brandt, 1981).

In turn, a study performed on young dogs where the hind limb was immobilised for 11 weeks demonstrated no effect on proteoglycan synthesis but a decreased concentration of GAGs in the uncalcified (mainly superficial) zones of knee articular cartilage (Kiviranta et al., 1987, Haapala et al., 1999, Jortikka et al., 1997). Interestingly, the cartilage of the contralateral leg presented a 25-35% increase in GAG concentration (Kiviranta et al., 1987). The collagen fibril network did not show a significant alteration in response to joint immobilisation, however there was a reduction of collagen cross-links resulting in decreased stiffness of cartilage (Haapala et al., 1999).

In the human hip joint, light and moderate activities such as walking have been estimated to apply pressures in the range of 0.1 - 4MPa (Ramage et al., 2009, Urban, 1994). Under more strenuous activities such as jumping the peak stress of load may

reach 20MPa, whereas the contact pressure of body weight during standing i.e. static compression has been measured as 1MPa (Ramage et al., 2009, Urban, 1994).

*In vivo* studies conducted on hamsters and rodents have shown that moderate load bearing exercise maintains cartilage homeostasis (Bader et al., 2011). In the study of Otterness et al., housed hamsters that had undergone 3 months daily wheel running exercise (6-12 km per day) had smooth, healthy cartilage, whereas the cartilage of hamsters that had 3 months of sedentary activity was fibrillated. This study also demonstrated a lower content and synthesis of proteoglycans in the group of inactive hamsters (Otterness et al., 1998).

Histological assessment of the knee joints of Wistar rats which ran excessively i.e. 30 km in the wheel within six weeks, demonstrated a moderate severity of OA; transcriptional analysis showed increased expression of MMP-3 compared to non-exercising animals (Pap et al., 1998).

### **1.3.2. *In vitro* studies**

*In vitro* studies on the effect of mechanical forces on chondrocytes have been conducted either on chondrocyte cultures (monolayer or 3D) or cartilage tissue explants, and both have demonstrated the influence of loading regimes on the synthesis of ECM components (Fitzgerald et al., 2008). Static compression inhibits synthesis of proteoglycans and proteins whereas dynamic compression (depending on frequency, amplitude and loading time) can be either degenerative or biosynthetic (Urban, 1994, Grodzinsky et al., 2000).

#### **1.3.2.1. Effect of static compression on ECM homeostasis**

Static compression is characterised by fluid loss and compaction of the solid matrix (Kim et al., 1994), and its degenerative activity is magnitude-dependent (Sah et al., 1989). Water efflux and compressed negatively charged components of the ECM attract in positively charged ions (including H<sup>+</sup>, Na<sup>+</sup>, K<sup>+</sup>) causing a reduction in pH (Kim et al., 1994). It is thought that these physicochemical changes inhibit proteoglycan synthesis (Sah et al., 1989).

### **1.3.2.2. Effect of dynamic compression on ECM homeostasis**

It has been shown that dynamic compression can stimulate matrix synthesis, however, different amplitudes, frequency and time of load may have a significant impact on the chondrocytes' response (Sah et al., 1989).

### **1.3.2.3. Effect of loading frequency on ECM homeostasis in articular cartilage explants**

The frequency of compressive loading indicates how often the tissue is subjected to deformation within 1 second. Several studies have investigated how high (0.1-1Hz) and low (<0.001Hz) loading frequencies, in which deformation phenomena and fluid flow behave differently, affect ECM homeostasis (Sah et al., 1989, Kim et al., 1994). Both groups showed that low amplitude strain at the range 0.63 – 10.4% and high frequency resulted in proteoglycan synthesis, whereas at low frequency there was either a reduction in proteoglycan production or no biosynthetic response (Sah et al., 1989, Kim et al., 1994). The explanation of these results may be that fluid flow has a significant impact on the chondrocyte's response due to alterations in the matrix environment i.e. pH (Wong et al., 1999). At low frequency, the deformation period is longer than at high frequency and there is a consistent fluid flow between cycles, whereas at the minimum period of deformation at high frequency there is very little fluid flow (Sah et al., 1989, Kim et al., 1994). Wong et al. also showed that compressive load at a rate  $\geq 0.1$ Hz increased protein synthesis, mainly COMP and fibronectin (Wong et al., 1999).

### **1.3.2.4. Effect of loading amplitude on ECM homeostasis in articular cartilage explants**

One of the key regulators of cartilage biosynthetic activity is the magnitude of load. Normal load (0.1 - 5MPa) applied to cartilage explants increased proteoglycan and protein synthesis (Arokoski et al., 2000). Patwari et al. showed that injurious cyclic compression ( $\geq 50\%$  strain,  $\sim 23$ MPa) activated a catabolic response in chondrocytes as characterised by up-regulation of MMP-3 and loss of proteoglycans (Patwari et al., 2003).

### **1.3.2.5. Effect of the duration of loading on ECM homeostasis in articular cartilage explants**

The duration of loading, similar to the magnitude and frequency, has an impact on chondrocyte biosynthesis (Arokoski et al., 2000). Parkkinen et al. showed that 1.5h of load (5MPa, 0.5Hz) induced proteoglycan synthesis (Parkkinen et al., 1993). Király et al. demonstrated that 1 - 20h of load (0.5Hz, 4.1MPa) activated a different response in chondrocytes and the ECM depending on the duration of applied load. Both a 1 and 20h loading period altered the collagen structure with thickening of the superficial zone up to 41.4% after 20h (Király et al., 1998). The thickness of the mid zone was increased by 22% at 1h and 43.4% after 20h of loading, however there was a reduction in thickness in the deep zone (Király et al., 1998). Proteoglycan synthesis was increased up to 8.8% after 4h of load, whereas 8h of load decreased chondrocyte biosynthetic activity and 20h totally inhibited proteoglycan synthesis (Király et al., 1998).

## 1.4. Mechano-transduction

The main function of articular cartilage is to dissipate mechanical loads, therefore to maintain ECM homeostasis and cartilage integrity, chondrocytes react to alterations within the ECM brought about by mechanical loads (Ramage et al., 2009). The process by which cells control their activity and behaviour in response to biomechanical signals is referred to as mechano-transduction or mechano-chemical signalling (Figure 1.10).

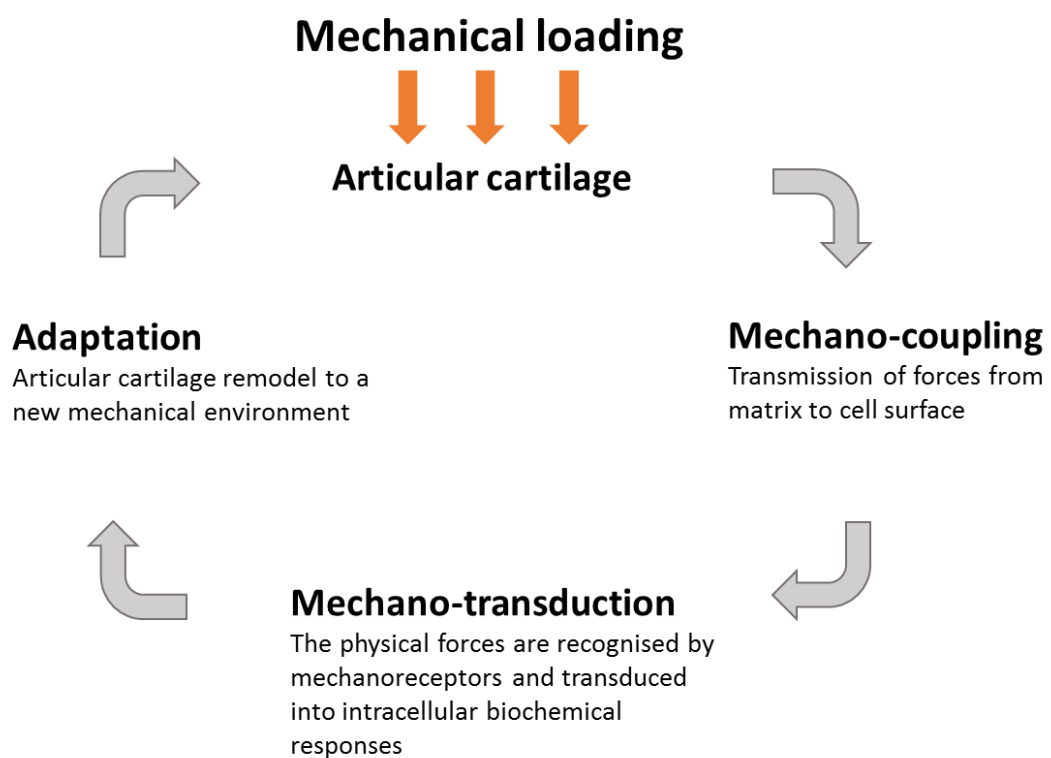


**Figure 1.10.** Diagram of response of articular cartilage to mechanical loading (Adapted from Bader et al. 2011).

### 1.4.1. Chondrocyte mechano-sensors/receptors

The mechano-signalling process is initiated by stimulation of mechano-receptors such as ion channels or integrin receptors located on the cell membrane, induced by biochemical changes occurring in response to ECM deformation generated by mechanical stimuli (Leong et al., 2011, Ramage et al., 2009).

**Primary cilia:** Primary cilia, a microtubule-based structure extending from the cell surface and protruding into the ECM, is a key mechanical sensor involved in mechano-chemical signalling in cartilage (Irianto et al., 2014, Salter and Lee, 2010b). The location of the chondrocyte primary cilium is ideal to sense mechanical stimuli deformation, as the primary cilia is structurally associated with collagen fibrils and can mechanically bend in response to ECM deformity (Wann et al., 2012). Moreover, the primary cilium contains several mechano-receptors present at the cell membrane e.g. integrins and ion channels allowing them to transduce mechanical signals from the ECM and induce biochemical and cellular responses (Salter and Lee, 2010b). It was reported that the primary cilia is involved in increased synthesis of proteoglycans through  $\text{Ca}^{2+}$  dependent signalling pathways mediated by ATP release in 3D chondrocytes/agarose constructs subjected to a cyclic compressive load (15% compression, 1Hz, 24h) (Wann et al., 2012). A previous study also reported that mechanical load reversibly affects the length of the primary cilium showing decreased length in chondrocytes embedded into 3D agarose constructs subjected to a long term compressive load (0-15% compression, 1Hz, 48h); whereas shorter periods of the same loading regimes (0.5, 6 and 24h) did not affect the length of the primary cilia (McGlashan et al., 2010).

**Ion channels:** Mechanical stimulation induces changes in ion flux across the stretch activated ion channels (SACs) localised on the plasma membrane which are directly activated by mechanical stress causing membrane tension and lipid bilayer distortion (Ramage et al., 2009). One of the first signalling responses to mechanical load is activation of  $\text{Ca}^{2+}$  channels which allow the influx of  $\text{Ca}^{2+}$  into the chondrocyte and leads to initiation of intracellular  $\text{Ca}^{2+}$  dependent signalling pathways (Guilak et al., 1999, Wann et al., 2012).

**Integrins:** Another major chondrocyte mechanoreceptor is the  $\alpha 5\beta 1$  integrin (Salter et al., 1992, Wright et al., 1997). Integrins are a family of heterodimeric transmembrane receptors consisting of  $\alpha$  and  $\beta$  subunits that determine the ligand specificity of the receptor (Ramage et al., 2009). Chondrocytes express several members of the integrin family including  $\alpha 1\beta 1$ ,  $\alpha 10\beta 1$ ,  $\alpha v\beta 5$  in addition to  $\alpha 5\beta 1$  (Loeser, 2002). The transmembrane location of integrins allows transduction of mechanical signals from the ECM converting them into biochemical responses within the cells (Salter and Lee 2010). While the extracellular domain is exposed to bind ligands such as collagen or fibronectin, the intracellular tail interacts with cytoplasmic molecules to transduce the external signal into a cellular response (Ramage et al., 2009). Integrins when bound to a ligand in the ECM form a focal adhesion complex at the cell surface to transmit the mechanical signal intracellularly. Focal adhesion kinase (FAK) is an intracellular tyrosine kinase that has been reported to play an important role in integrin-mediated signal transduction (Guan, 1997). An inactive FAK molecule binds to a  $\beta 1$  integrin subunit resulting in FAK auto-phosphorylation, creating binding sites for the Src family proteins which further amplify FAK phosphorylation at specific tyrosine residues to maximise its activity (Guan, 1997). The FAK-Src complex activates, via phosphorylation, other signal transduction adaptor proteins e.g. paxillin which can modulate the architecture of the actin cytoskeleton via a connection with vinculin (Guan, 1997, Ramage et al., 2009) binding directly to actin filaments (F-actin) (Golji and Mofrad, 2013).

#### **1.4.2. Intracellular signalling cascades activated by mechanical forces**

Biomechanical stimulation of the chondrocyte mechano-receptors also induces activation of downstream signalling cascades which regulate gene expression and cell function (Salter and Lee, 2010b).

##### **1.4.2.1. Hedgehog (Hh) signalling pathway**

Hh signalling pathway is implicated in chondrogenesis, chondrocyte proliferation and differentiation in growth plates during development (Mariani et al., 2014). Recent studies reported that the Hedgehog (Hh) signalling pathway is initiated in primary cilia (Muhammad et al., 2012). Mammals have three homologues of Hh: Desert (DHH), Indian

(Ihh), and Sonic (Shh) genes which are necessary to activate this pathway (Pathi et al., 2001). In the absence of Hh ligands, transmembrane protein Patched 1 (Ptch1) inhibits the movement of a signal transducer Smoothed (Smo) to the primary cilium which prevents activation of the signalling pathway (Evangelista et al., 2006, Rohatgi et al., 2007). In the presence of Hh protein which associates with the Ptch1 receptor, the inhibitory effect on Smo is relieved, therefore Smo enters the primary cilium where it relocates to the cell membrane and is activated by phosphorylation (Humke et al., 2010). The Smo protein indirectly activates Gli transcription factors which are translocated into the nucleus to induce expression of Hh signalling target genes e.g. Ptch1, Gli1 (Humke et al., 2010, Rohatgi et al., 2007). Hh signalling has been reported to be abnormally induced in OA cartilage where it promotes cartilage degradation triggering expression of catabolic enzymes such as MMP-13 and ADAMTS-5 (Thompson et al., 2014); furthermore, inhibition of Hh signalling in OA chondrocytes reduced the severity of the disease (Lin et al., 2009). An *in vivo* study also reported up-regulation of Hh signalling and OA biomarkers (MMP-13, ADAMTS-5, collagen type X and Runx2) in cartilage of primary cilia knock-out mice (Chang et al., 2012). Thompson et al. reported that 1h of cyclic tensile strain (CTS; 10%, 0.33Hz) induces the Hh signalling pathway concomitant with expression of ADAMTS-5 in healthy bovine adult chondrocytes (Thompson et al., 2014); whereas, increasing the amount of strain applied to the cells (20%, 0.33Hz) did not activate Hh signalling and ADAMTS-5 suggesting that this pathway is mechano-sensitive but the response is dependent on the magnitude of load applied (Thompson et al., 2014).

#### **1.4.2.2. Mitogen activated protein kinases (MAPKs)**

In chondrocytes, the MAPKs play an important role in response to inflammatory cytokines (Salter and Lee, 2010b). ERK1/2, p38 and JNK are the central components of the MAPK family. The phosphorylation and activation of MAPKs transmit the signal down the cascade and activates many downstream genes such as transcription factors, cytoskeletal proteins and other protein kinases (Fitzgerald et al., 2008). MAP kinases regulate multiple cellular activities, for example: gene expression, mitosis, differentiation and cell apoptosis (Salter and Lee, 2010b). Different mechanical stimuli

can activate different MAPKs and through this mechanism differential cellular responses may occur (Fitzgerald et al., 2008). The activation of extracellular-regulated kinase (ERK1/2) can be induced in response to static compression (~50% compression, 2h or 24h) and dynamic shear stress (3% shear strain at 0.1Hz, 0.5, 2, 6 or 24h) applied to cartilage explants (Fitzgerald et al., 2008). This ERK1/2 response to mechanical stimuli may have a degradative effect on cartilage homeostasis, as ERK1/2 is believed to be a major regulator of pro-inflammatory cytokines IL-1 $\beta$ , IL-6, IL-12, IL-23 and TNF- $\alpha$  (Mariani et al., 2014). p38, another component regulating expression of downstream genes of the MAPK signalling pathway, has been reported to be activated in articular cartilage in response to dynamic compression (0.1MPa, 0.5Hz, 24h), resulting in synthesis of nitric oxide (NO) and prostaglandin E2 (PGE<sub>2</sub>) (Ruiz-de-Luzuriaga et al., 2003). Both of these molecules play an important role in cartilage integrity as they inhibit expression of collagen type II and proteoglycans, and induces chondrocyte apoptosis (Amin and Abramson, 1998, Attur et al., 2008). Studies on monolayer chondrocyte cultures have shown that the integrin-dependant Jun N-terminal kinase (JNK) pathway is involved in up-regulation of proteoglycan synthesis following cyclic mechanical stimulation (pressurization) (26.7kPa, 0.33Hz, 30 min, 1, 2 or 3h) (Zhou et al., 2007), indicating its role in regulating load-induced cartilage homeostasis. Phosphorylation of ERK, JNK and p38 leads to activation of MAPK signalling cascades that induce the expression of many transcription factors involved in regulation of many genes of catabolic molecules, e.g. AP-1 (c-Fos/c-Jun), RUNX-2, HIF-2 $\alpha$  in articular cartilage (Mariani et al., 2014).

#### **1.4.2.3. Nuclear factor kappa B (NF-kappa B) pathway**

The transcription factor NF- $\kappa$ B is directly regulated by mechanical stimulation (Agarwal et al., 2004, Akanji et al., 2010, Salter and Lee, 2010b) and can up-regulate MMPs, IL-1, PGE<sub>2</sub> and NO levels (Novack, 2011). The mechanical stimuli appears to affect NF- $\kappa$ B activity in a magnitude dependent manner in articular cartilage (Salter and Lee, 2010b). Physiological biomechanical stimuli (6% elongation, 0.05Hz, 15 – 90 minutes) blocked the nuclear translocation of NF- $\kappa$ B in monolayer cultures of rabbit articular chondrocytes stimulated with IL-1 $\beta$  (Agarwal et al., 2004). Moreover, in chondrocytes

treated simultaneously with load and IL-1 $\beta$  NF- $\kappa$ B synthesis was significantly reduced when compared to chondrocytes treated with IL-1 $\beta$  only (Agarwal et al., 2004). In contrast, abnormal mechanical load (15% elongation, 0.05Hz, 15 – 90 minutes) elevated NF- $\kappa$ B synthesis and induced the rapid translocation of NF- $\kappa$ B subunits p65 and p50 into the nucleus in a similar manner to IL-1 $\beta$  treatment (Agarwal et al., 2004). 3D bovine chondrocyte/agarose constructs treated with IL-1 $\beta$  and subjected to mechanical compression (15% compression, 1Hz, 60 minutes) demonstrated partial translocation of the p65 NF- $\kappa$ B subunit when compared to unloaded cells (Akanji et al., 2010).

### **1.5. RNA interference (RNAi)**

To date, there are several studies showing that mechanical force has an impact on cellular responses through RNA interference expression levels (Qin et al., 2010, Luna et al., 2011b, Liu et al., 2014, Dunn et al., 2009, Guan et al., 2011). RNAi, a biological process based on sequence specific post-transcriptional gene silencing by single stranded RNA (ssRNA) results in messenger RNA (mRNA) degradation or inhibition of mRNA translation. The key players in RNA silencing are small RNAs such as: small interfering RNA (siRNA), small nucleolar RNA (snoRNA), tRNA-derived RNA fragments/small RNA (tRFs/tsRNA), PIWI-interacting RNA (piRNA) and microRNAs (miRs) (Gomes et al., 2013). There is also an increasing number of reports describing the vital function of long, non-coding RNAs (lncRNAs) in many cellular processes. Liu et al. demonstrated that lncRNAs differ in expression between healthy and OA cartilage, showing that lncRNAs related to cartilage injury promote ECM degradation in OA (Liu et al., 2014). The aim of this study is to identify mechano-sensitive miRs in articular cartilage, therefore I will focus on these small RNA molecules only from here on in.

### **1.5.1. microRNA**

miRs are very small (20 – 23bp), cytoplasmic RNAs that control post-transcriptional regulation of one third of all genes (Miyaki and Asahara 2012). As miRs are involved in many fundamental cellular processes, they play extremely important roles in the regulation of the proper functioning of organisms. Any dysregulation of miRs may contribute to the development of various diseases such as cardiovascular disease, cancer, arthritis, etc. The expression pattern of most miRs depends very often on the tissue, the developmental stage where they exist and the cellular environment in which they are expressed (Miyaki and Asahara, 2012, Dunn et al., 2009). The function of some miRs is driven by certain stress factors, for example ageing, inflammation and mechanical stress which are also known to contribute to OA development (Miyaki and Asahara, 2012).

#### **1.5.1.1. Canonical pathway of miR maturation**

miR is functional only as a mature, single stranded RNA binding to the RNA-induced silencing complex (RISC). It is generated as a long pri-miR and then processed by the enzymes Drosha and Dicer into the short, single stranded ribonucleotide form. The mature miR is then incorporated into the RISC complex and can bind target mRNA (Miyaki et al., 2010). The metabolic pathway of miR maturation begins in the nucleus and finishes in the cell cytoplasm (Figure 1.11).

- 1.** miRs are transcribed by RNA polymerase II in the nucleus and the first step of miR maturation starts from the moment of transcript inception of the pri-miR.
- 2.** The next stage also occurs in the cell nucleus and involves removal of approximately 70 - 90 nucleotides folding into an imperfect stem-loop structure from a long pri-miR transcript. The result is a hairpin-like molecule called precursor miR (pre-miR) which has two overhanging nucleotides at the 3' end and phosphate residues at the 5'end (Cowland et al., 2007, Filipowicz et al., 2005, Mendell, 2005, Pillai, 2005). This process involves a microprocessor complex, consisting of the RNase III enzyme Drosha, and the double-stranded-RNA-binding protein, Pasha/DGCR8 (Han et al., 2004).

- 3.** The next step is the binding of the pre-miR molecule with the karyopherin exportin 5 (Exp-5) and Ran-GTP complex which is then exported from the nucleus into the cytoplasm. Ran (ras-related nuclear protein) is a small GTP binding protein belonging to the RAS family that is essential for the translocation of RNA and proteins through the nuclear pore complex (Filipowicz et al., 2005, Gregory and Shiekhattar, 2005, Han et al., 2004, Pillai, 2005).
- 4.** The cytoplasmic miR biogenesis stage is initiated by Dicer, which has a high affinity for double-stranded RNA molecules having two over-hanging nucleotides at the 3' end.
- 5.** Dicer, as with Drosha, belongs to the Ribonuclease class III family (RNase III) characterised by a 2-nucleotide 3' overhang in its products; it cuts the double stranded RNA at about 22 nucleotides from the binding site.
- 6.** The product of Dicer is an approximate 22 nucleotide miR-miR\* duplex with a shorter 5' end and about 2 nucleotides longer at the 3' end (Araldi and Schipani, 2010, Dunn et al., 2009, Fernandes-Silva et al., 2012, Stefani and Slack, 2008).
- 7.** It has been reported that only one strand is integrated into the RISC complex and acts as a functional miR. RISC is a ribonucleoprotein complex containing members of the Argonaute (Ago) family of proteins which have endonuclease activity directed against target mRNA strands that are complementary to their bound miR fragment. Ago is also responsible for selection of the guide strand (incorporated strand) and destruction of the passenger strand (\*) of the miR-miR duplex. The RISC complex binds to the miR-miR (\*) duplex to select the guide strand (Schwarz et al., 2003).
- 8.** The guide strand is selected by Ago on the basis of the stability of the 5' end. The strand characterised by lower thermodynamic energy (has a lower stability base pairing of the 2–4 nucleotides at the 5' end, which indicates lower complementarity to the 3'UTR end of the second strand) is incorporated into the RISC complex, making the miR available to regulate gene expression (Fernandes-Silva et al., 2012, Dunn et al., 2009, Miyaki et al., 2010, Pillai, 2005). There is an increasing number of studies reporting that the passenger strand of several miRs may also be incorporated into the RISC complex and play functional roles in post-transcriptional gene regulation (Yang and Lai, 2011). Step 9 and 10 will be described in more details in Section 1.5.1.3.

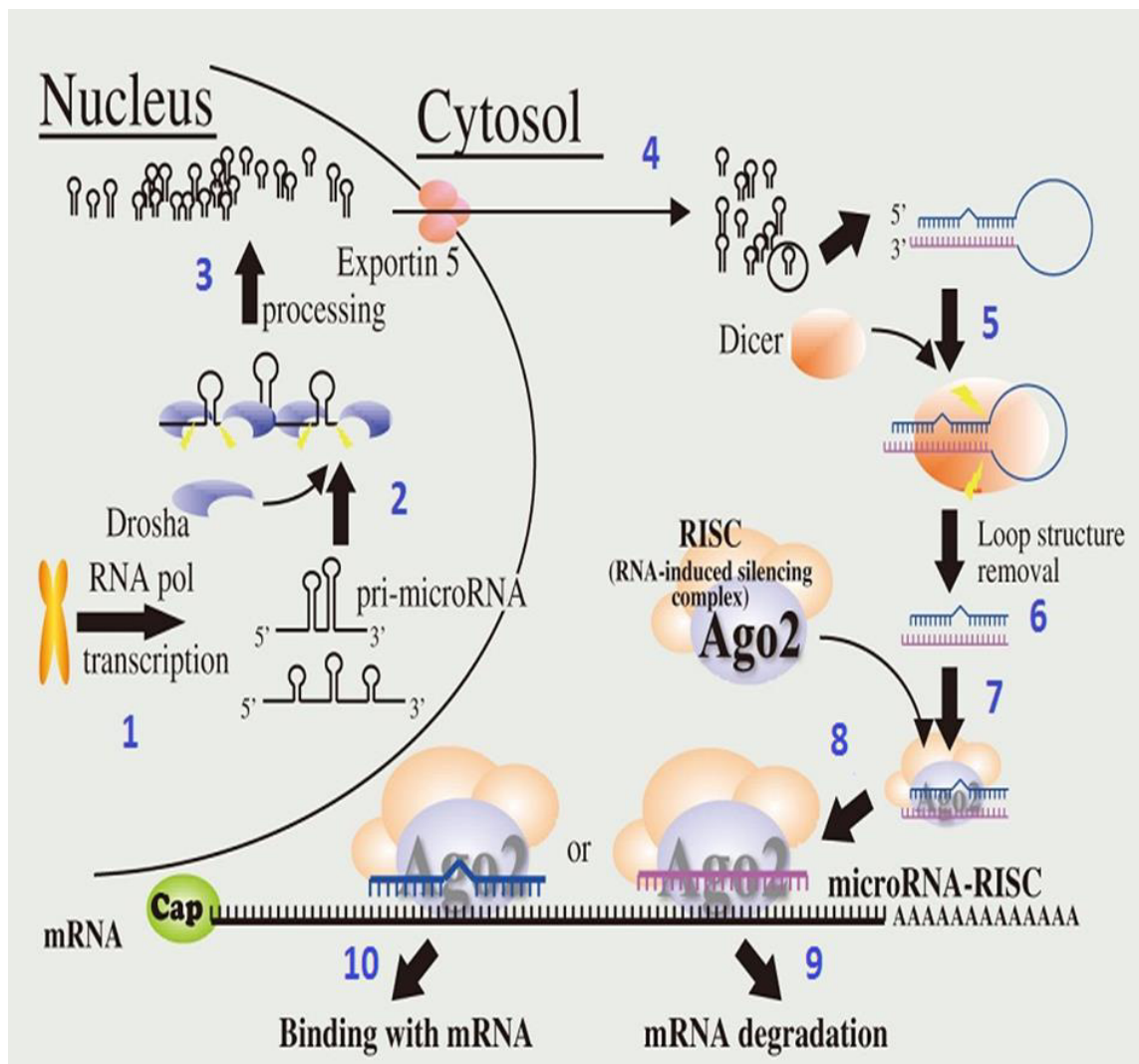


**Figure 1.11.** The miR maturation canonical pathway and the working mechanism of action. The maturation of a miR is mediated by Drosha and Dicer enzymes. It starts in the nucleus of the cell and ends in its cytoplasm, with a mature miR incorporated into the RISC and available for post-transcriptional regulation (Fernandes-Silva et al., 2012). The activity of a miR depends on matching to its target mRNA. If the complementarity of miR and mRNA is perfect, the 3'UTR of the mRNA is cleaved by Ago2 which has a slicer activity; if it is not a perfect match, then the translation of mRNA is inhibited (Tong and Nemunaitis, 2008).

Adapted from (<http://www.wako-chem.co.jp/english/labchem/article/microRNA.htm>).

### 1.5.1.2. Non-canonical pathway of miR biogenesis

One of the most frequently occurring mechanisms for non-canonical miR biogenesis is a splicing-mediated and Drosha independent “mirtron pathway” (Figure 1.12) (Berezikov et al., 2007, Ladewig et al., 2012). Introns with hairpin potential are cut out from protein coded genes by spliceosomes (Ladewig et al., 2012, Westholm and Lai, 2011). The initial spliced introns appear in a branched form with the 3' end ligated to the 5' end of the intron and can form either conventional mirtrons where both ends of the pre-miR is defined by the spliceosome or 5' and 3' tailed mirtrons which must be processed by nucleases to trim additional nucleotides prior to eventual processing by Dicer (Figure 1.12i) (Westholm and Lai, 2011). To form the pre-miR, the “loop form” is cleaved by lariat debranching enzyme (Figure 1.12ii) and then the pre-miR hairpin is further processed as a pre-miR in a canonical manner (Ladewig et al., 2012, Okamura et al., 2007, Westholm and Lai, 2011). In terms of tailed mirtrons, they require additional nucleotide trimming (Figure 1.12iii) prior to binding to Exportin-5. It has been found that the 3' mirtron tail is trimmed by an exosome (RNA 3'->5' exonucleases complex) (Ladewig et al., 2012, Westholm and Lai, 2011). So far, nucleases that remove the 5' tail have not been identified, however it is believed that the major RNA 5'->3' exonucleases (XRN1/2) in eukaryotes do the trimming (Westholm and Lai, 2011).

Other sources of a Drosha independent pathway of miR biogenesis are tRNA-derived RNA such as short tRFs that on the basis of their generation are grouped into: type I (Dicer dependent), and type II (Dicer independent) (Raina and Ibba, 2014, Haussecker et al., 2010). 3'U tRFs that belong to the Dicer independent group are mainly produced in the nucleus by the action of the tRNaseZ during tRNA maturation and exported to the cytoplasm (Raina and Ibba, 2014). 5' tRFs, 3'CCA tRFs belong to the first group and they are generated in the cytoplasm from mature tRNA through the Dicer activity that cleaves tRNA in the D and T loop producing 5' tRFs and 3'CCA tRFs respectively (Figure 1.13A) (Raina and Ibba, 2014). When immature tRNA leaves the nucleus, RNaseP and tRNaseZ localised in the cytoplasm may process pre-tRNA and generate 5' leader-exon tRFs and 3'U tRFs. 5' tRFs, 3'CCA tRFs and 3'U tRFs bind to Ago proteins (preferentially Ago 1, 3 and 4 over 2) and form a functional RISC complex that can regulate the expression of a target mRNA (Kumar et al., 2014).

Another Drosha independent source of pre-miR is the small nucleolar RNA (snoRNA) derived pathway (Miyoshi et al., 2010). Some snoRNAs, whose secondary structure is characterised by at least two stem-loops linked by a hinge may be a source of miR-like molecules (Ender et al., 2008). Only a minor proportion of snoRNAs, involved in modifying the function of other noncoding RNAs in the nucleus, are exported to the cytoplasm, where Dicer along with other nucleases cleaves it into small RNAs that are loaded into the RISC complex (Figure 1.13B), (Brameier et al., 2011, Ender et al., 2008, Scott et al., 2009).

**mirtron derived pathway**

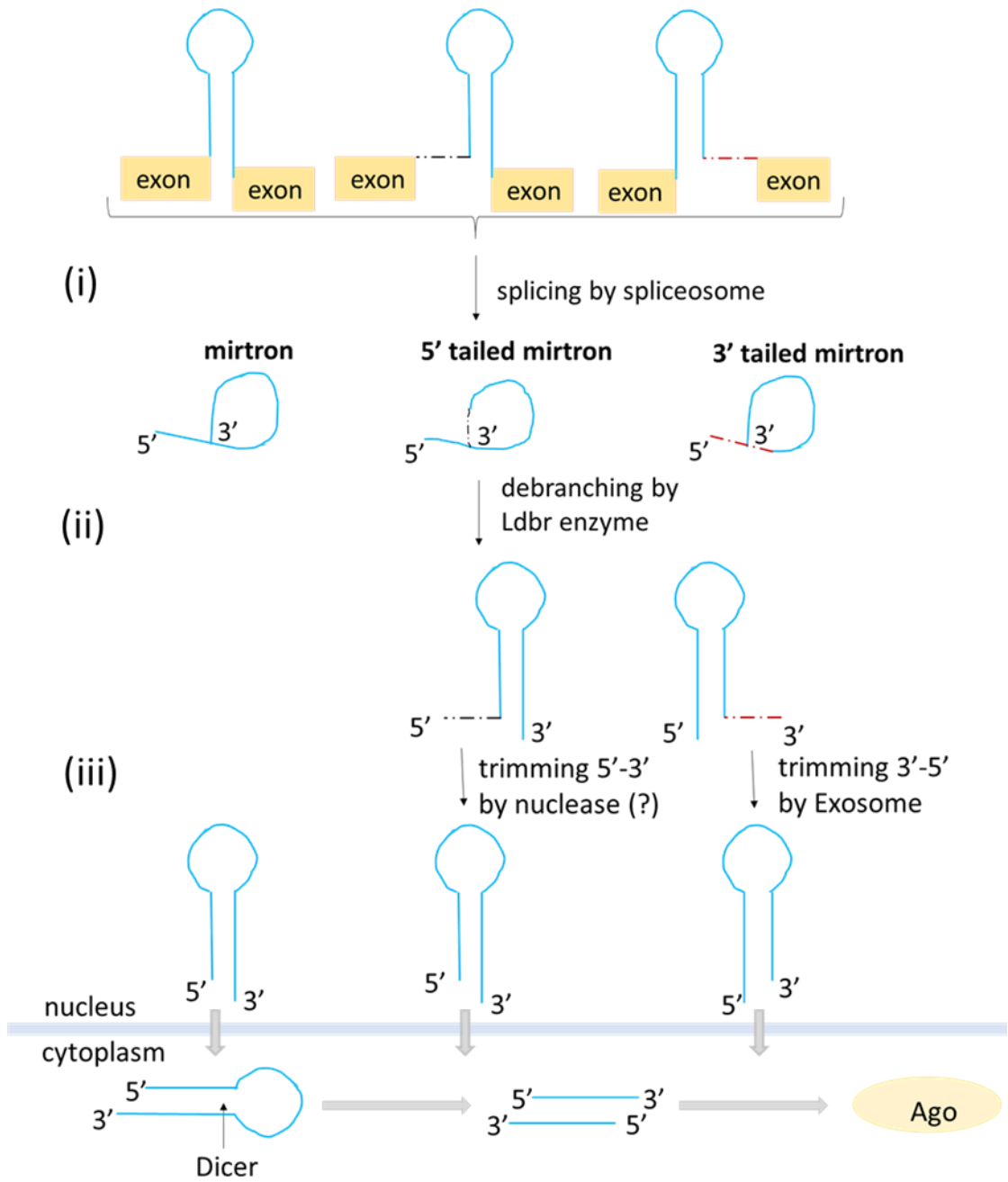
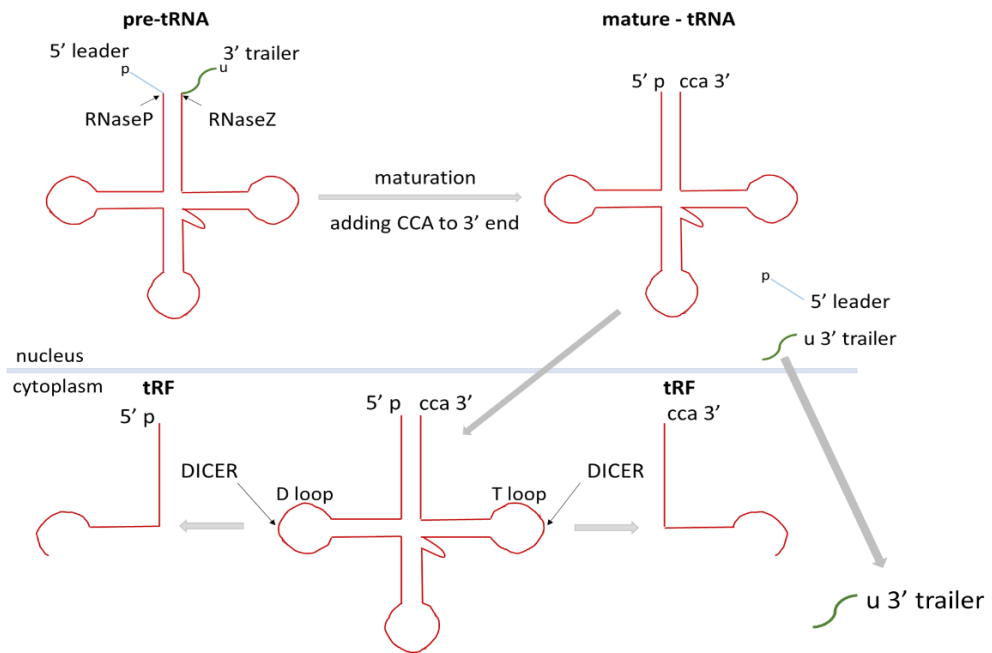


**Figure 1.12.** Non-canonical, Drosha independent pathway of mirtron derived miR biogenesis. Short introns with hairpin potential are spliced **(i)** and debranched into pre-miR **(ii)**; tailed mirtrons are additionally trimmed **(iii)**. Debranched mirtrons are processed further in canonical miR biogenesis.

**A. tRNA derived RNA pathway**



**B. snoRNA derived pathway**

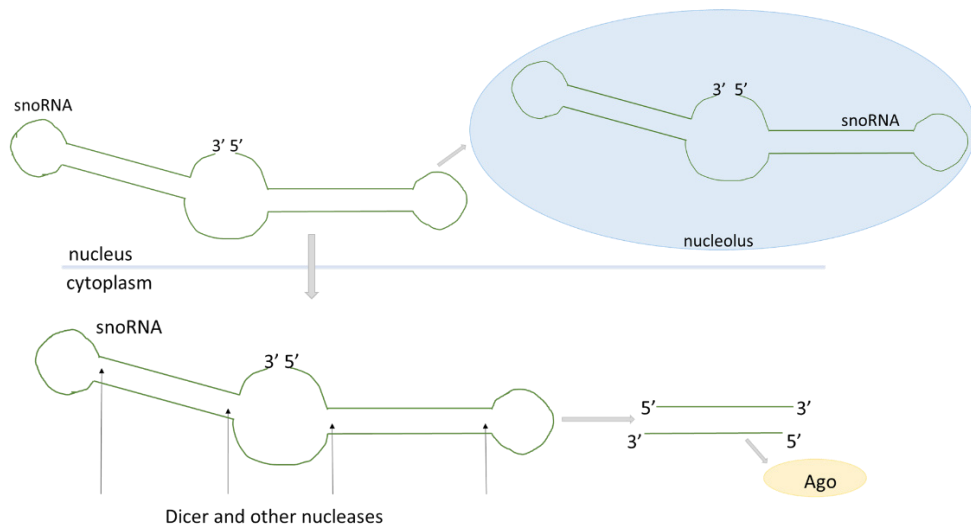


**Figure 1.13.** Non-canonical, Drosha independent pathway of miR biogenesis via the tRNA derived pathway: mature tRNA transported to the cytoplasm can be cleaved by Dicer in the T and D loop of tRNA giving the single stranded tRFs that are bound to the Ago protein. Dicer independent 3'U tRF formed by RNaseZ activity can also be transported to the cytoplasm and act as a miR after binding the Ago protein **(A)**. snoRNA derived pathway: some snoRNAs transported to the cytoplasm are cleaved by Dicer creating a pre-miR that is incorporated into Ago and acts as a miR **(B)**.

### 1.5.1.3. miR activity and its target sites

Regulation of gene expression by miRs may occur in two ways, either by mRNA destabilisation which is permanent (Figure 1.11:9) or inhibition of translation which has been reported to be reversible (Figure 1.11:10). It has been shown that application of different stress conditions i.e. amino acid starvation or oxidative stress to human hepatoma Huh7 cells led to the release of catalase-1 (CAT-1) from miR-122 inhibition (Bhattacharyya et al., 2006). The manner of this control depends on the complementarity between the miR and the target mRNA (Marin et al., 2013). The target mRNA has at least one region which is totally complementary to the “seed region” of the miR, that is responsible for binding to mRNA targets (Mitra and Bandyopadhyay, 2011), and is located between the 2<sup>nd</sup> and 7<sup>th</sup> nucleotide at the 5’ end of the miR (Saito and Sætrom, 2010, Bartel, 2009). These corresponding regions in the mRNA are called “seed sites” and according to their sizes and seed region which they are complementary to, they are divided into 4 seed matching sites (Mitra and Bandyopadhyay, 2011): 6mer that is 6 nucleotides long (starts at the 2<sup>nd</sup> miR nucleotide and finishes at the 7<sup>th</sup>) (Figure 1.14A), 7merA1 that is 7 nucleotides long (starts at the 1<sup>st</sup> nucleotide and finishes at the 7<sup>th</sup> and has to have adenosine across from the first nucleotide in the miR) (Figure 1.14B), 7mer-m8 that is also 7 nucleotides long (starts at the 2<sup>nd</sup> nucleotide and finishes at the 8<sup>th</sup>) (Figure 1.14C) and 8mer that is 8 nucleotides long (starts at the 1<sup>st</sup> nucleotide and finishes at the 8<sup>th</sup>) (Figure 1.14D) (Friedman et al., 2009, Bartel, 2009, Mitra and Bandyopadhyay, 2011). When the entire miR is completely complementary to the mRNA, the mRNA is degraded by the endonuclease Ago2; however, when the miR is not perfectly matched to the mRNA, protein production is inhibited by repression of translation (Reynard and Loughlin, 2012). Most functional miR target sites are located in the 3’UTR of the target mRNA, but some studies have demonstrated that seed sites also occur in the coding sequence (CDS) and 5’UTR of the target mRNA (Hausser et al., 2013, Fang and Rajewsky, 2011, Lee et al., 2009). The 3’ UTR is thought to be more accessible for the miR/RISC complex than the other two sites (Fang and Rajewsky, 2011, Hausser et al., 2013).



#### **1.5.1.4. Nomenclature of miR**

miRBase ([www.mirbase.org](http://www.mirbase.org)) is an online database including the nomenclature, sequences and predicted targets of mature miRs. **bta-mir-146** refers to a bos taurus "bta" precursor "mir" 146. The bta-mir-146 has two mature "miR" products: **bta-miR-146-5p** and **bta-miR-146-3p**, which means that they arise from the 5' or 3' precursor respectively. Several papers have shown that the passenger strand derived from the 3' precursor (miR\*) can be functional, therefore the miR/miR\* has been changed to -5p/-3p indicating that both forms of miR-146 may control gene expression. miRs which are closely related and differ in one or two nucleotides have a lettered suffix to their "name", for example **bta-miR-146a-5p**, **bta-miR-146b-5p** meaning that they are expressed from bta-mir-146a and bta-mir-146b respectively. Mature miRs which have the same sequence and target genes, but have been generated from different genes are given additional numerical suffixes e.g. **has-miR-1-1** and **has-miR-1-2**, whose genomic loci are on chromosome 20 and 18 respectively (Griffiths-Jones et al., 2006).

#### **1.5.1.5. Importance of miR in articular cartilage**

In 2003 Bernstein et al. demonstrated that complete deletion of the enzyme Dicer, essential for miR maturation, caused lethal effects on mice embryos indicating a crucial role for miRs in embryonic development (Bernstein et al., 2003). However, one of the first indications that miRs may be involved in chondrogenesis was shown by Wienholds et al. (2005). They demonstrated by *in situ* hybridization that most of the highly conserved vertebrate miRs in zebrafish embryos are expressed in a tissue specific manner, and furthermore that miR-140 is expressed only in cartilaginous tissue (Wienholds et al., 2005). This expression pattern of miR-140 has been confirmed in mouse embryos by Tuddenham et al. who also identified that miR-140 targets histone deacetylase 4 (HDAC4) which inhibits Runx2, a transcription factor that controls chondrocyte hypertrophy and osteoblast differentiation (Tuddenham et al., 2006). Kobayashi et al. also demonstrated that miRs play a crucial role in chondrocyte proliferation and differentiation. Although the Dicer-null mice (Dicer -/-) were viable, they showed greatly decreased chondrocyte proliferation and faster hypertrophy leading to growth defects and premature death in these mice (Kobayashi et al., 2008).

The importance of miR-140 in skeletal development has been reported by Miyaki et al. and Nakamura et al. Independent *in vivo* studies demonstrated that miR-140 knock-out mice exhibited short statures and craniofacial deformities (Miyaki et al., 2010, Nakamura et al., 2011). The effect of dwarfism in mice lacking miR-140 expression was attributed to premature chondrocyte differentiation and a reduction in proliferating chondrocytes which led to shortening of the bones (Miyaki et al., 2010, Nakamura et al., 2011). It is believed that one of the reasons for reduced chondrocyte proliferation might have been increased expression of the aspartyl aminopeptidase enzyme (Dnpep) in miR-140 knock-out chondrocytes (Nakamura et al., 2011). Dnpep is a miR-140 target which reduces BMP/Smad signalling, however its antagonistic mechanism towards the BMP pathway is still unclear (Nakamura et al., 2011). It is known that loss of BMP/Smad signalling causes decreased proliferation and increased chondrocyte apoptosis (Retting et al., 2009).

miR-140 is not the only miR involved in cartilage development and more miRs have been identified as regulators of chondrocyte differentiation and ECM biosynthesis. Dai et al. reported that miR-101 is involved in IL-1 $\beta$ -induced aggrecan and collagen type II suppression by targeting the transcription factor Sox9, essential for cartilage formation and production of ECM molecules (Dai et al., 2012). Decreased expression of miR-145 that also controls expression of Sox9, was observed in TGF- $\beta$ -induced chondrogenic differentiation of murine mesenchymal stem cells (Yang et al., 2011). Moreover, Martinez-Sanchez et al. reported that over-expression of miR-145 in human chondrocytes differentially altered expression of Sox9-inducible downstream genes. Decreased levels of collagen type II and aggrecan were observed, in addition to reductions in miR-140 and -675 expression, whereas expression of hypertrophic markers were elevated e.g. Runx2 and MMP-13, that is regulated by Runx2 (Martinez-Sanchez et al., 2012). Similar to miR-140, mechano-sensitive miR-365 also targets HDAC4 and can regulate chondrocyte differentiation (Guan et al., 2011). Collagen type II was also reported to be negatively regulated by miR29-a/b in murine mesenchymal stem cells (Yan et al., 2011) and positively regulated by miR-675 in human articular chondrocytes (Dudek et al., 2010).

### **1.5.1.6. miR in OA cartilage**

Due to the important role of the aforementioned miRs in cartilage homeostasis, all of them are likely to influence cartilage degradation, however in this subsection I will only discuss miRs that have been reported in the literature as being differentially expressed in OA cartilage. Iliopoulos et al. found that 16 miRs from 365 tested were differentially expressed in human OA cartilage when compared to healthy samples (Iliopoulos et al., 2008). In turn, Jones et al. identified 17 miRs out of 157 presenting at least a 4-fold change in expression level between human OA and healthy cartilage (Jones et al., 2009). Based on the direction of significant changes of miR levels altered in OA cartilage compared to healthy tissue, miRs were grouped into three classes: up-regulated (Table 1.2), OA stage-dependent (Table 1.3) and down-regulated (Table 1.4).

#### **1.5.1.6.1. Up-regulated miRs in OA cartilage**

The analysis of biological function of miR-9 and -98 demonstrated a repressive impact of miR-9 on MMP-13 transcription, and also an inhibitory effect of miR-9 and -98 on IL-1 $\beta$ -induced tumour necrosis factor alpha (TNF $\alpha$ ) synthesis indicating a protective role in OA (Jones et al., 2009).

The examination of miR-21 demonstrated that this miR directly regulates expression of growth differentiation factor 5 (GDF-5) in OA cartilage (Zhang et al., 2014b). GDF-5 has been shown to be involved in chondrocyte proliferation in later stages of skeletal development (Francis-West et al., 1999) suggesting its positive role in cartilage regeneration.

Functional analysis of miR-22 demonstrated elevated expression of IL-1 $\beta$  (a cytokine involved in OA pathogenesis) and MMP-13, and decreased expression of aggrecan through direct targeting of peroxisome proliferator-activated receptor (PPARA) and bone morphogenetic protein 7 (BMP7) (Iliopoulos et al., 2008).

A recent study showed that the miR-29 family is regulated by several molecules important for maintaining cartilage homeostasis including Sox9, TGF- $\beta$ 1 (inhibits miR-29 expression) and IL-1 (elevates miR-29 expression). miR-29 has also been reported to be

up-regulated at the onset of OA (using the DMM model) and in end-stage human OA cartilage (Le et al., 2016). A functional analysis of this miR family was assessed by using luciferase reporters with specific genes measuring the activity of those involved in cartilage degradation: SMAD, NF $\kappa$ B and canonical Wnt signalling pathways induced respectively by TGF- $\beta$ 1, IL-1 $\beta$  or Wnt3a. The results indicated involvement of the miR-29 family in the negative regulation of these pathways, and more specifically the negative regulation of ADAMTS-4, MMP3 and Axin2 that are respectively TGF- $\beta$ 1, IL-1 and Wnt-inducible genes (Le et al., 2016). Furthermore, the same group reported that the miR-29 family directly targets the following Wnt signalling pathway genes: casein kinase 2 alpha 2 polypeptide (CSNK2A2), Dishevelled 3 (DVL3), Frequently Rearranged In Advanced T-Cell Lymphomas 2 (FRAT2), Frizzled family receptor 3 (FZD3) and Frizzled family receptor 5 (FZD5) (Le et al., 2016). Functional analysis demonstrated the involvement of this miR family in the negative regulation of SMAD, NF $\kappa$ B and canonical Wnt signalling pathways indicating critical roles in cartilage homeostasis (Le et al., 2016).

miR-455-3p has also been reported to be elevated in OA cartilage (Swingler et al., 2012). This miR is induced by the growth factor TGF $\beta$  and via the direct targeting of Smad2, activin receptor 2B (ACVR2A) and chordin-like 1 (CHRDL1) it regulates the TGF $\beta$ /Smad2/3 dependent signalling pathway (Swingler et al., 2012); this pathway is involved in ECM synthesis and degradation therefore its repression is known to lead to OA-like changes (van der Kraan et al., 2012).

**Table 1.2.** Up-regulated miRs identified in OA cartilage, along with their putative direct and indirect targets.

<b>miR</b>	<b>Direct targets</b>	<b>Indirect targets</b>	<b>References</b>
<b>miR-9</b> Human	Human: MMP-13, TNF $\alpha$		(Jones et al., 2009)
<b>miR-21</b> Human	Human: GDF-5		(Zhang et al., 2014b)
<b>miR-22</b> Human	Human: PPARA, BMP7	Human: IL-1 $\beta$ , MMP-13 (p.c.)	(Iliopoulos et al., 2008)
<b>miR-98</b> Human	Human: IL-1 $\beta$ (human)		(Jones et al., 2009)
<b>miR-29</b> Human, mouse	Human: FZD-3/-5, DVL3, FRAT2, CSNK2A2	Human: ADAMTS-4, MMP-3, Axin2	(Le et al., 2016)
<b>miR-455</b> Human	Human, mouse: SMAD2, ACVR2A, CHRD1		(Swingler et al., 2012)

Key: p.c. - positive correlation

#### **1.5.1.6.2. OA-stage dependent differential expression of miRs**

The level of miR146a is much higher in low-grade OA cartilage and decreases with the extent of cartilage degradation, leading to the belief that cartilage degradation might progress due to loss of miR-146 (Yamasaki et al., 2009). Therefore, the experiment reporting decreased expression of miR-146 in OA human chondrocytes seems to be performed on late stage disease tissue, however it was not specified. miR-146 directly suppresses the expression of the IL-1-receptor associated kinase 1 (IRAK1) and TNF-receptor associated factor 6 (TRAF6), which are induced by inflammatory cytokines and are necessary to activate catabolic factors such as MMPs and ADAMTSs (Taganov et al., 2006, Li et al., 2011c). Moreover, miR-146a was also reported to stimulate cartilage degradation by targeting Smad4, which is an important regulator in the anabolic TGF $\beta$  pathway, and by indirect up-regulation of vascular endothelial growth factor (VEGF) that activates angiogenesis. Up-regulation of miR-146a results in down-regulation of Smad4 and a higher expression of VEGF (Li et al., 2012, Jin et al., 2014). Interestingly, Li et al. reported that miR-146a is an anti-catabolic miR by showing its inhibitory effect on MMP-13 and ADAMTS-5, and anabolic effect on aggrecan and collagen type II in human chondrocytes treated with IL-1 (Li et al., 2011c).

The most studied cartilage miR-140 was also reported as involved in cartilage pathogenesis, however the data from the literature is conflicting. Decreased levels of miR-140 were detected in cartilage collected from OA patients and was found to target IGFBP-5 expression, hence influencing cartilage integrity (Tardif et al., 2009). This finding was confirmed by Miyaki et al. who showed reduced expression of miR-140 in OA chondrocytes compared to healthy control (Miyaki et al., 2010, Miyaki et al., 2009), and furthermore, that ADAMTS-5 is a direct target of miR-140 (Miyaki et al., 2010). However, Swingler et al. reported an elevation of miR-140 in human OA cartilage (Swingler et al., 2012). This group has confirmed HDAC4, a corepressor of Runx-2 and Mef-2, as a direct target of miR-140 (Tuddenham et al., 2006). It is thought that the contradictory findings regarding the expression of miR-140 in OA may depend on the stage of the disease analysed (Le et al., 2013). To date, the regulatory mechanism of miR-140 expression in cartilage is still unclear. Nakamura et al. demonstrated that miR-140 is regulated by SOX9 in zebrafish and mammalian chondrocytes (Nakamura et al.,

2012). Contradictory information exists in terms of IL-1 $\beta$  influence on miR-140 expression. Liang et al. demonstrated that miR-140 is up-regulated after treating human chondrocytes with 10 ng/ml IL-1 $\beta$  (Liang et al., 2012), whereas Miyaki et al. showed that 5 ng/ml of IL-1 $\beta$  suppresses miR-140 expression in human chondrocytes (Miyaki et al., 2009).

**Table 1.3.** OA-stage dependent miR expression, along with their putative direct and indirect targets.

miR	Direct targets	Indirect targets
<p><b>miR-140</b></p> <p> Human (Miyaki et al., 2009, Tardif et al., 2009)</p> <p> Human (Swingler et al., 2012)</p>	<p>Human: <b>IGFBP-5</b> (Tardif et al., 2009)</p> <p>Human and mouse: <b>ADAMTS-5</b> (Miyaki et al., 2010, Miyaki et al., 2009),</p> <p>Mouse: <b>HDAC4</b> (Tuddenham et al., 2006)</p>	
<p><b>miR-146a</b></p> <p>  Human (Yamasaki et al., 2009)</p> <p> Human (Jones et al., 2009)</p>	<p>Human: <b>ADAMTS-5, MMP-13</b> (Li et al., 2011c), <b>IRAK1, TRAF6</b> (Li et al., 2011c, Taganov et al., 2006), <b>TNF<math>\alpha</math></b> (Jones et al., 2009)</p> <p>Human and rat: <b>SMAD4</b> (Jin et al., 2014, Li et al., 2012)</p>	<p>Human and rat: <b>VEGF</b> (p.c) (Jin et al., 2014, Li et al., 2012)</p> <p>Human: <b>Aggrecan, collagen type II</b> (p.c.) (Li et al., 2011c)</p>

Key: p.c. - positive correlation

### **1.5.1.6.3. Down-regulated miRs in OA cartilage**

miRs that are decreased in expression in OA cartilage include miR-27a (Tardif et al., 2009), miR-27b (Akhtar et al., 2010), miR-125b (Matsukawa et al., 2013), miR-142-3p (Wang et al., 2016a) and miR-222 (Song et al., 2015).

miR-27a and miR-27b have been reported to be downregulated in human OA cartilage and negatively correlate, either indirectly or directly respectively, with MMP-13 expression in IL-1-stimulated human OA chondrocytes (Akhtar et al., 2010, Tardif et al., 2009); in addition, miR-27a has also been demonstrated to act in a secondary manner by inhibiting IGFBP-5 (Tardif et al., 2009).

miR-125b downregulation has also been identified in human OA chondrocytes, where it has been shown to repress ADAMTS-4 expression in IL-1 $\beta$  stimulated OA chondrocytes by 72% and 62% respectively at the transcriptional and protein levels (Matsukawa et al., 2013).

In turn, miR-142-3p found to be reduced in expression in murine OA cartilage, confers regulatory effects on cell apoptosis, NF $\kappa$ B and the synthesis of cytokines e.g. IL-1, IL-6 and TNF- $\alpha$  in response to stimulation with the pro-inflammatory agent lipopolysaccharide (LPS) (Wang et al., 2016a). Furthermore, miR-142-3p directly targets an inflammatory OA mediator: high mobility group box 1 (HMGB1) (Wang et al., 2016a). HMGB1 in synergy with IL-1 $\alpha$ , IL-1 $\beta$  and LPS, amplifies the inflammatory response by increasing expression of cytokines such as TNF $\alpha$ , IL-6 and IL-8, whereas a HMGB1-IL-1 $\beta$  complex enhances MMP-3 production in synovial fibroblasts collected from rheumatoid arthritis (RA) and OA patients (Wähämaa et al., 2011).

Mechanically-regulated miR-222 has also been reported to be down-regulated in OA chondrocytes in which it regulates expression of MMP-13 through direct targeting of HDAC4 (Song et al., 2015).

**Table 1.4.** Down-regulated miRs identified in OA cartilage, along with their putative direct and indirect targets.

<b>miR</b>	<b>Direct targets</b>	<b>Indirect targets</b>	<b>References</b>
<b>miR-27a</b> Human		Human: <b>MMP-13</b> , <b>IGFBP-5</b> (n.c.)	(Tardif et al., 2009)
<b>miR-27b</b> Human	Human: <b>MMP-13</b>		(Akhtar et al., 2010)
<b>miR-125b</b> Human	Human: <b>ADAMTS-4</b>		(Matsukawa et al., 2013)
<b>miR-142-3p</b> Mouse	Mouse: <b>HMGB1</b>		(Wang et al., 2016a)
<b>miR-222</b> Human	Human: <b>HDAC4</b>	Human: <b>MMP-13</b> (n.c.)	(Song et al., 2015)

Key: n.c. - negative correlation

### 1.5.1.7. Mechanically-regulated miRs

miR expression has become very important in the understanding of biological processes, therefore it is not surprising that, to date, many studies have been performed to identify mechano-sensitive miRs.

Experiments performed on endothelial cells (EC) demonstrated that laminar fluid flow (12 dyn/cm<sup>2</sup>, 12h) up-regulates miR-19a which inhibits EC proliferation (Qin et al., 2010). In contrast, oscillatory shear stress ( $\pm 5$  dyn/cm<sup>2</sup>, 1Hz, 24h) increases the level of miR-663 expression and at the same time activates the inflammatory response of EC which may lead to the development of atherosclerosis (Ni et al., 2011).

Variations in the levels of miR in response to mechanical load were also documented in the trabecular meshwork (TM) of the eye. Cyclic mechanical stress (20% tensile strain, 1Hz, 3h) up-regulated miR-24 that targets and inhibits the subtilisin-like proprotein convertase family furin which activates the latent form of transforming growth factor beta 1 (TGF- $\beta$ 1) (Luna et al., 2011b); to date, pathophysiological mechanisms involved in changes in TM and dysregulation of normal levels of aqueous outflow in glaucoma are not yet understood (Liton et al., 2005). It is presumed that the active form of TGF- $\beta$ 1 can significantly change the morphology of the TM such that aqueous humour is less able to evacuate from the eye increasing intraocular pressure (Luna et al., 2011a).

Alterations in miR expression have also been observed in cultured rat cardiac myocytes that were subjected to mechanical stretch (20% tensile strain, 1Hz, 4h), with both TGF- $\beta$ 1 and miR-208a over-expressed in mechanically stimulated myocytes (Wang et al., 2013a). miR-208a was also up-regulated after exogenous addition of TGF- $\beta$ 1 (Wang et al., 2013a). TGF- $\beta$ 1 plays an important role in hypertrophic remodelling and modulates matrix metabolism in the pressure over-loaded heart (Dobaczewski et al., 2011). Wang et al. suggest that miR-208a regulation is mediated by TGF- $\beta$ 1 and plays a role in stretch-induced cardiac hypertrophy (Wang et al., 2013a).

Mohamed et al. showed that mechanical stretch (12% tensile strain, 1Hz, 1h) applied to a primary cell line of human airway smooth muscle cells (HASMCs) up-regulated miR-16, miR-26a and miR-140 and induced airway smooth muscle hypertrophy (Mohamed et al.,

2010). HASMC hypertrophy plays a role in airway remodelling which is a characteristic feature in people with severe asthma (Bentley et al., 2009, Mohamed et al., 2010). miR-26a was shown to induce HASMC hypertrophy by direct inhibition of glycogen synthase kinase-3 $\beta$  (GSK-3 $\beta$ ) that controls cell growth (Haque et al., 2010, Bentley et al., 2009, Mohamed et al., 2010).

*In vivo* studies on tendon fibroblasts demonstrated an elevation of miR-378 and down-regulation of miR-100 in the Achilles tendons of rats running for 30 minutes at a constant speed of 12m/minute with progressively increased treadmill elevation every 10 minutes: 0°, 5° and 10° (Mendias et al., 2012). The role of these miRs are unknown in tendon fibroblasts, but in cervical cell lines the down-regulation of miR-100 is partially responsible for increased cell proliferation (Mendias et al., 2012, Li et al., 2011a), whereas up-regulation of miR-378 in U87 and MT-1 cell lines also promotes cell proliferation, enhances cell survival, tumour growth and angiogenesis (Lee et al., 2007). Interestingly, miR-140 which is involved in cartilage development and homeostasis was significantly decreased in mechanically stimulated tendons (Mendias et al., 2012).

#### **1.5.1.8. Mechanically-regulated miRs in chondrocytes**

One of the best known mechano-responsive miRs in chondrocytes is miR-365 that was shown to be up-regulated in a 3D model of primary chondrocytes subjected to cyclic load with regimes of 5% deformation (1 Hz, 15 min/h for 24 and 48h) (Guan et al., 2011) and 10% deformation (1 Hz, 15 min/h for 24h) (Yang et al., 2016a); this was mediated via NF $\kappa$ B signalling (Yang et al., 2016a). miR-365 was found to stimulate chondrocyte differentiation and catabolic activity via direct targeting of HDAC4 (Guan et al., 2011, Yang et al., 2016a); moreover, it has been reported that this miR is IL-1 $\beta$  responsive and its increased expression in OA cartilage correlates with decreased HDAC4 (Yang et al., 2016a). It is well known that HDAC4 regulates chondrocyte hypertrophy and bone formation by repressing the expression and activity of the transcription factor Runx2 which is necessary for pre-terminal chondrocyte differentiation and endochondral ossification (Guan et al., 2011). Additionally, a recent study reported the significant repression of HDAC4 in cartilage from both primary OA and traumatic OA patients associated with elevation of Runx2 and Runx2-regulated molecules e.g. MMP-13 and

type X collagen (Cao et al., 2014). Over-expression/inhibition of miR-365 results in elevated/reduced expression of Runx2, MMP-13 and type X collagen in primary human chondrocytes confirming that miR-365 promotes chondrocyte hypertrophy (Yang et al., 2016a).

Guan et al. showed that miR-146a, which is elevated in the early stages and decreased in the late stages of OA, was also up-regulated in a 3D model of primary chicken chondrocytes subjected to mechanical load (either 5% or 10% elongation, 1Hz, 15 min/h for 24h) (Guan et al., 2014). miR-146a has been reported to be significantly increased in human chondrocytes subjected to a static load (10MPa, 60 minutes) (Jin et al., 2014) corroborating these findings (Guan et al., 2014).

miR-221 and miR-222 are also examples of mechanical stress induced miRs that are up-regulated with increased weight bearing (Dunn et al., 2009). Their expression level is elevated in the weight-bearing anterior medial condyle bovine stifle joint compared with the non-weight-bearing posterior medial region (Mendell, 2005, Dunn et al., 2009). The precise roles of these miRs are unknown, but on the basis of other studies it is thought that miR-221 is involved in the chondrogenic differentiation of mesenchymal cells (Kim et al., 2010), whereas miR-222 plays a role in chondrocyte proliferation (Goldring and Marcu 2012b). miR-221 has been shown to regulate chondrogenesis by inhibition of Mdm2 expression, with down-regulation of Mdm2 preventing Slug protein degradation, necessary for inhibition of chondroprogenitor proliferation (Lolli et al., 2014, Kim et al., 2010). Studies performed on glioma cells demonstrated that miR-222 regulates the WNT/ $\beta$ -catenin signalling pathway which is also implicated in OA pathogenesis (Li et al., 2013, Corr, 2008). miR-222 can regulate the expression of  $\beta$ -catenin and other downstream genes of the Wnt/ $\beta$ -catenin pathway by inhibition of its direct target DKK2 which is a known Wnt antagonist (Li et al., 2013).

## 1.6. PhD hypothesis

Recent studies have shown that mechanical load affects the expression of miRs in chondrocytes; there is also evidence that the expression of several miRs differ between healthy and OA cartilage. Clearly, abnormal mechanical load is a primary risk factor for OA and taken together with these recent studies I hypothesise that:

- **Mechano-sensitive miRs in articular cartilage are involved in controlling genes that play key roles in cartilage homeostasis and OA development and progression.**

## 1.7. PhD objectives

1. To establish *in vitro* regimes representing “physiological” and “non-physiological” magnitudes of load that induce early transcriptional responses of molecules involved in cartilage homeostasis (and has the potential to induce biosynthetic/degradative changes at the protein level if applied for suitably prolonged periods of time)
2. To establish which miRs, expressed by chondrocytes, are sensitive to mechanical force in response to loads characterised in objective 1
3. To determine the target genes of mechano-sensitive miRs identified in objective 2

# Chapter 2

## Materials and methods

All reagents were obtained from Sigma (Poole, UK) unless otherwise stated. Molecular biology analyses were conducted using reagents, plastic ware and filter tips which were RNase and DNase free.

## **2.1. Cartilage explants**

### **2.1.1. Preparation of articular cartilage explants**

Full-depth articular cartilage explants were collected from the *metacarpophalangeal* joints of immature bovine calves (F. Drury and Sons abattoir, Swindon, UK) within 6h of slaughter using 5 mm diameter biopsy punches (Selles Medical, Hull, UK). Explants were washed four times for 20 minutes each with the first three washes in Hank's balanced salt solution (HBSS) (Invitrogen, Paisley, UK) containing 400U/ml penicillin and 400µg/ml streptomycin (Invitrogen, Paisley, UK) and the fourth wash, prior to explant culturing, was conducted in HBSS containing 100U/ml penicillin and 100µg/ml streptomycin.

The culture media used in experiments comprised Dulbecco's Modified Eagle's Medium-F12 with GlutaMAX™-I (DMEM/F12 – GlutaMAX™) (Invitrogen, Paisley, UK) supplemented with 100U/ml penicillin, 100µg/ml streptomycin, 1x Insulin-Transferrin-Selenium (ITS) (Invitrogen, Paisley, UK) and 50µg/ml ascorbate-2-phosphate. ITS was used to avoid the presence of any growth factors which occur in Foetal Bovine Serum (FBS) and to prevent chondrocyte dedifferentiation (Kisiday et al., 2005); addition of ascorbate-2-phosphate was used to promote collagen synthesis (Murad et al., 1981). The tissue explants were maintained in culture medium in a 5% (v/v) CO<sub>2</sub> incubator at 37°C for three days prior to loading.

### **2.1.2. Application of mechanical load to articular cartilage explants**

Cartilage tissue explants were cyclically loaded using the Bose ElectroForce® 3200 rig (TA Instruments, Minnesota, USA) (Figure 2.1), controlled through WinTest dynamic mechanical analysis (DMA) software (TA Instruments, ElectroForce® Systems Group, Minnesota, USA). Explants were placed into a small 70 mm diameter glass Petri dish (Fisher Scientific, Loughborough, UK) containing culture media (described in 2.1.1)

which was placed on the ElectroForce® 3200 stage. The platen was lowered until it made contact with the tissue and the baseline force, prior to loading, was set at 0.1 Newton (N) to keep the explant in position.

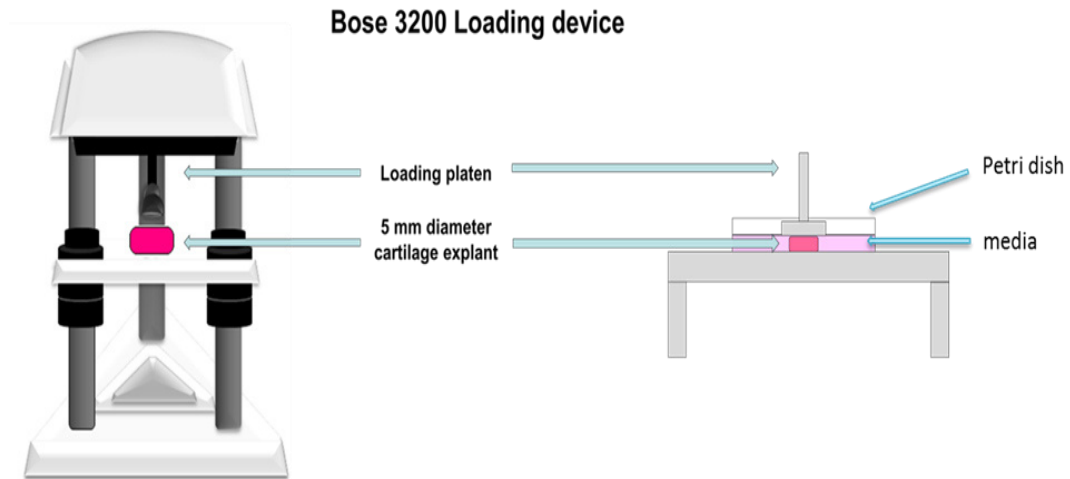


**Figure 2.1.** Schematic diagram of explant loading using the Bose ElectroForce® 3200 rig.

To establish loading regimes that induce early cartilage ECM responses at the gene level, potentially indicative of anabolic (or homeostatic) or catabolic molecule responses, three different loading regimes were utilised (2.5MPa, 5MPa or 7MPa). Selection of these loading magnitudes was made based on previous studies. In the literature  $\leq 5$ MPa load is generally accepted as physiological load (Fehrenbacher et al., 2003, Grodzinsky et al., 2000), while peak loads above 5MPa are considered as degradative (Fehrenbacher et al., 2003); unloaded explants were used as controls. Loading was conducted at a set frequency of 1Hz which has previously been demonstrated to resemble a fast walking speed (Bader et al., 2011). Furthermore, explants were only loaded for 15 minutes to enable investigation of early transcriptional changes in the cartilage in response to load and then cultured in a CO<sub>2</sub> incubator (37°C, 5% (v/v) CO<sub>2</sub>, 95% humidity). Explants were maintained for 24h post-cessation of load to assess their response to the loading regimes and also to investigate appropriate selection of reference genes.

## **2.2. Primary articular chondrocytes**

### **2.2.1. Isolation of primary articular chondrocytes**

Slivers of full-depth articular cartilage were removed from bovine *metacarpophalangeal* joints using a sterile scalpel and washed as previously described (Section 2.1.1). Cartilage tissue was incubated, with gentle agitation, at 37°C, 5% (v/v) CO<sub>2</sub> for 50 minutes in 0.1% (w/v) pronase (Roche, West Sussex, UK) dissolved in DMEM/F12 – GlutaMAX™ (Invitrogen, Paisley, UK) containing 5% (v/v) foetal calf serum (Invitrogen, Paisley, UK) and 100µg/ml penicillin and 100U/ml streptomycin. Pronase was removed and tissue subsequently incubated overnight at 37°C, 5% (v/v) CO<sub>2</sub> with gentle agitation in 0.04% (w/v) collagenase type II isolated from *Clostridium histolyticum* (Invitrogen, Paisley, UK) dissolved in the same media as for pronase. The digestion mixture was filtered through a 40µm cell strainer (Fisher Scientific, Loughborough, UK) and the cells pelleted by centrifugation at 246g for 5 minutes. The cell pellet was re-suspended in fresh media (described in Section 2.1.1) except for exclusion of the antibiotics. A cell count was performed using a haemocytometer (Sussex, UK).

### **2.2.2. Transfection of primary articular chondrocytes**

Isolated chondrocytes were seeded onto 6-well culture plates (VWR, Lutterworth, UK) at a density of  $4.4 \times 10^5 / \text{cm}^2$  ( $4 \times 10^6$  cells/well) in penicillin/streptomycin free DMEM/F12–GlutaMAX™ (Invitrogen, Paisley, UK) or plated onto 8-well chamber slides (Thermo Fisher Scientific, Hempstead, UK) at a density of  $7.14 \times 10^4 / \text{cm}^2$  ( $5 \times 10^5$  cells/well) supplemented with 1x ITS and 50µg/ml ascorbate-2-phosphate. Cells were incubated at 37°C, 5% (v/v) CO<sub>2</sub> for 24h prior to transfection.

Chondrocytes were transfected with miR oligonucleotides (inhibitors or mimics) using DharmaFECT1™ lipid reagent (Dharmacon, UK). To assess transfection levels, Cy3™- anti-miR™ negative control #1 (Thermo Fisher Scientific, St. Leon-Rot, Germany) was transfected into the cells. mirVana® miR inhibitors (Applied Biosystems, Paisley, UK) or miScript miR Mimic (Qiagen, West Sussex, UK) were used to manipulate the level of examined miRs, whereas mirVana™ miR Inhibitor Negative Control #1 (Applied Biosystems, Paisley, UK) and AllStars negative control siRNA (Qiagen, West Sussex, UK)

were used as transfection controls. Mock (DharmaFECT1™ only) and untreated cells presented additional controls. Cells were incubated in transfection reagents with 50nM final concentration of siRNA at 37°C, 5% (v/v) CO<sub>2</sub> for 48h. Transfections were performed according to the manufacturer's protocol and volumes described in this subsection are representative of a single well in a 6-well plate. 10µl (20µM stock) siRNA and 8µl DharmaFECT1™ were diluted respectively in 90µl and 92µl DMEM/F12–GlutaMAX™ and left for 5 minutes at room temperature. They were then combined, mixed and left at room temperature for 20 minutes to form the lipid-siRNA complex. The complex was subsequently added to 3.8ml penicillin/streptomycin free DMEM/F12–GlutaMAX™ supplemented with 1x ITS and 50µg/ml ascorbate-2-phosphate. After removing culture media from the plated cells, the total volume (4ml) of transfection mix was transferred onto the cells in the well.

#### **2.2.2.1. Measurement of cell viability/death**

Viability of transfected cells was assessed by a Live/Dead® Assay according to the manufacturer's protocol (Invitrogen, Paisley, UK). The kit contains 2 dyes, green calcein AM which is converted into fluorescent calcein by enzymes in live cells, and red ethidium homodimer-1 that diffuses into dead cells through their damaged membrane and produces a bright red fluorescence in dead cells after binding to nucleic acids. Transfected and untreated cells cultured on plastic Nunc Lab-Tek Chamber Slides were treated with 0.1µM calcein AM and 0.2µM ethidium homodimer-1 (diluted in culture media at 37°C) for 20 minutes in the dark, washed briefly in 37°C 1% PBS (VWR, Lutterworth, UK) and imaged with a Zeiss LSM 800 laser confocal microscope using ZEN lite software (Carl Zeiss, Cambridge, UK). A 20x objective lens was used to image live (green) and dead (red) cells using appropriate filters for FITC and Alexa Fluor® 594 with excitation/emission wavelengths of ~490/525nm and ~590/617nm, respectively. Three individual regions from each chamber in two repeats were visualised giving in total n = 6 images per condition. A count of green and red labelled cells was performed using Image J (<http://imagej.en.softonic.com>) and the percentage of cell viability/death per treatment was assessed as a mean from six individual data sets.

#### **2.2.2.2. Analysis of transfection efficiency using immunofluorescence microscopy**

The Bx61 upright fluorescence microscope controlled by MicroSuite™ Software (Olympus, Essex, UK) was used to assess the siRNA uptake by transfected cells. The chamber slides were mounted with VECTASHIELD® containing DAPI (Vector Laboratories Ltd, Peterborough, UK) and covered with coverslips. The level of transfection was examined using 20x and 40x oil immersion objective lens to image chondrocytes with excitation/emission wavelength settings for Alexa Fluor® 594 (red) at ~590/617nm and DAPI (blue) at ~358/461nm.

### **2.3. RNA extraction**

#### **2.3.1. RNA extraction from articular cartilage explants for mRNA analysis**

Total RNA was extracted from articular cartilage explants using 500µl Trizol® reagent (Invitrogen, Paisley, UK). Snap frozen cartilage tissue was powdered in 250µl Trizol® (Invitrogen, Paisley, UK) at 2,000rpm for 90 seconds using liquid nitrogen cooled chambers in a Mikro-Dismembrator (Braun Biotech, Melsungen, Germany). An additional volume of 250µl Trizol® was added to powdered tissue, pipetted up and down several times to ensure complete mixture of the Trizol® with the tissue and transferred to 1.5ml RNase free tubes (Alpha Laboratories, Eastleigh, UK). After 5 minutes incubation at room temperature, 150µl chloroform was added to the Trizol® extract to denature proteins and solubilise them in the organic phase. After a further 10 minutes incubation at room temperature, the samples were subjected to centrifugation (12,500g, 15 minutes, 4°C) and the upper aqueous phase containing RNA was transferred to a new tube; 300µl of 100% (v/v) ethanol was added and mixed by inversion at room temperature. RNA was then purified using Qiagen RNeasy mini kits following the manufacturer's protocols (Qiagen, West Sussex, UK). All centrifugation steps were conducted at room temperature. The aqueous phase-ethanol mix was applied to the RNeasy spin columns and centrifuged at 15,100g for 15 minutes. The flow-through was discarded and the columns were washed twice with 300µl RW1 buffer, with centrifugation at 12,200g for 45 seconds after each wash. After the second wash, spin

columns were washed with 500µl of RPE buffer and centrifuged at 12,200g for 45 seconds. The flow-through was discarded and the columns were centrifuged at 21,700g for 2 minutes to eliminate any residual wash buffer. To elute RNA residing in the columns, 30µl of water was added to the spin columns placed in new collection tubes, and after 1 minute incubation the spin columns were centrifuged at 15,100g for 45 seconds. RNA was transferred into sterile tubes and submitted for Bioanalyzer analysis (Agilent Technologies, Wokingham, UK); remaining RNA was stored at -80°C.

### **2.3.2. RNA extraction from articular cartilage explants for miR analysis**

Total RNA was extracted from articular cartilage explants using 500µl Trizol® reagent. Snap frozen cartilage tissue was powdered in 250µl Trizol® as previously described (Section 2.3.1). An additional 750µl volume of Trizol® was added to the powdered tissue, pipetted up and down 30 times to ensure complete mixing of the Trizol® and tissue, and transferred to 1.5ml RNase free tubes. After 5 minutes incubation at room temperature, 200µl chloroform was added to the Trizol®-tissue homogenate and samples were vortexed for 15 seconds. Following 10 minutes incubation (5 minutes at room temperature and 5 minutes on ice) samples were centrifuged at 13,800g (4°C, 10 minutes). The aqueous phase was transferred to new RNase free tubes followed by precipitation of RNA with 100% (v/v) ethanol (1.25 volumes per aqueous phase volume) at room temperature. Total RNA was then purified using a mirVana™ miR Isolation Kit (Ambion, Paisley, UK) following the manufacturer's protocol. All centrifugation steps were carried out at room temperature. The lysate/ethanol mix was transferred to the spin column and centrifuged at 10,000g for 15 seconds. The flow-through was removed and the spin columns were then washed with 700µl wash solution 1 and then briefly centrifuged at 10,000g. The flow-through was again discarded and the spin columns were washed twice with 500µl of wash solution 2/3 buffer followed by centrifugation at 10,000g for 15 seconds after each wash. The supernatant was removed and the spin columns were centrifuged at 10,000g for 2 minutes to remove residual ethanol. Finally, to elute RNA residing in the columns, 40µl of pre-heated (95°C) elution buffer was added to the spin columns placed in new collection tubes; after 1 minute incubation, the spin columns were centrifuged at 10,000g for 1 minute. Eluted RNA was applied to the filter

cartridge and centrifuged at 46,800g for 1 minute. In a final volume of 40µl, RNA was treated with 4µl 10x DNase buffer and 1µl DNase (2U/µl, Ambion, Paisley, UK) for 30 minutes at 37°C to remove genomic DNA. 4µl of inactivating reagent (Ambion, Paisley, UK), was then added to inhibit the DNase activity (2 minutes, room temperature). After a brief spin at 14,500g (1.5 minutes, 4°C), RNA was transferred to sterile tubes and RNA purity and yield determined using the Bioanalyser (Agilent Technologies, Wokingham, UK). RNA was stored at -80°C.

### **2.3.3. Total RNA extraction from chondrocytes for both mRNA and miR analysis**

Total RNA was extracted from primary chondrocytes by applying 1ml Trizol® reagent to each well containing cells, and contents pipetted up and down several times to increase the efficiency of Trizol® activity. The Trizol®- cell homogenate was transferred into 1.5ml RNase free tubes and processed as previously described (Sections 2. 3. 1 and 2. 3. 2 for mRNA and miR respectively).

### **2.3.4. Evaluation of RNA quality and yield - Bioanalyzer analysis**

The Agilent 2100 Bioanalyzer and associated RNA 6000 Nano kit (Agilent Technologies, Wokingham, UK) was used to assess the quality and concentration of purified RNA by producing an RNA integrity number (RIN); the RIN is a measurement designed to establish the integrity of total RNA by determining the ratio of 18S and 28S ribosomal subunits. The RIN software algorithm classifies the total RNA based on a numeric system from 1 to 10, with 1 being totally degraded and 10 being the most intact (Figure 2.2) (Mueller et al., 2004). The analysis of RIN was performed by Central Biotechnology Services (School of Medicine, Cardiff University) on 1.5µl of total RNA.

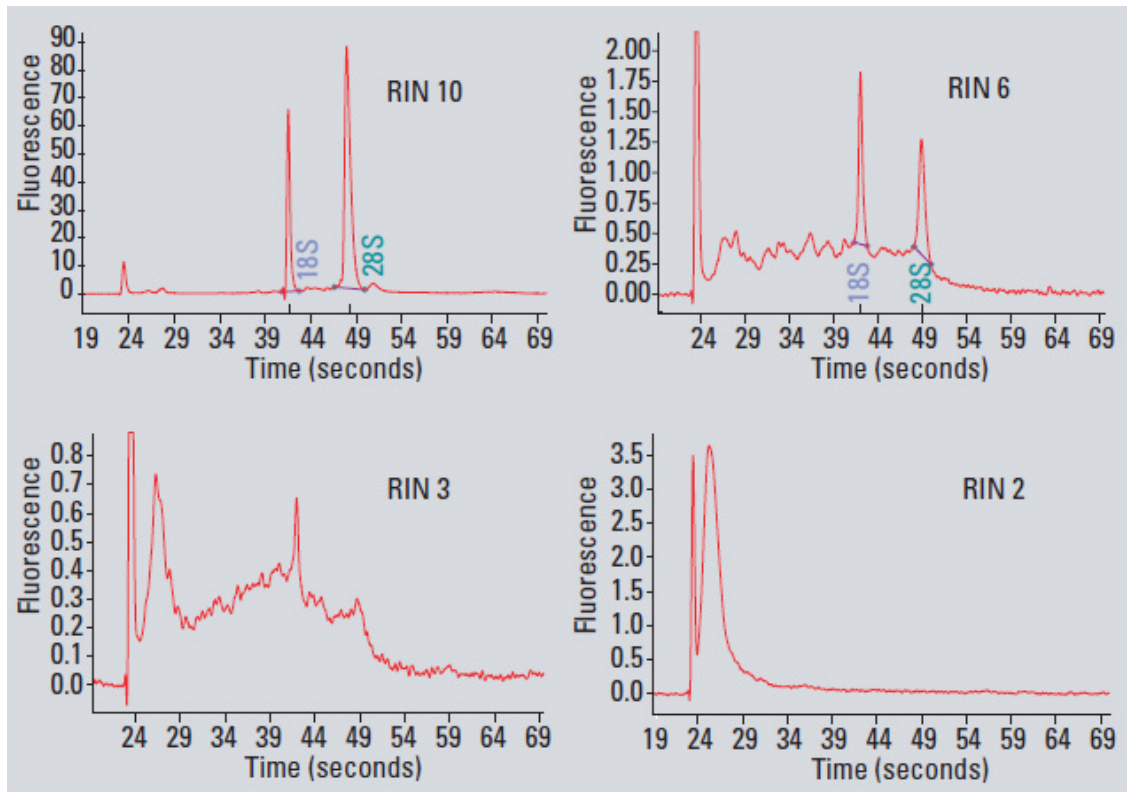


**Figure 2.2.** Sample electrophoretograms illustrating different RNA qualities as described by the RNA Integrity Number (RIN). Samples range from intact (RIN 10) to degraded (RIN 2) (Mueller et al., 2004).

## **2.4. cDNA synthesis**

### **2.4.1. Reverse transcription of mRNA template**

First strand complementary deoxyribonucleic acid (cDNA) was generated using Superscript™ III reverse transcriptase according to the manufacturer's protocol (Invitrogen, Paisley, UK). 1µl random primers (500µg/ml, Promega, Southampton, UK), 1µl dNTPs (10mM, Promega, Southampton, UK), 300ng RNA and sterile water were added together to give a total volume of 13µl, and incubated at 65°C for 5 minutes. After adding 4µl 5×first-strand buffer (250mM Tris-HCl, pH 8.3, 375mM KCl, 15mM MgCl<sub>2</sub>), 1µl dithiothreitol (0.1M DTT) and 1µl Recombinant RNase Inhibitor (40U/µl, Promega, Southampton, UK), 1µl Superscript III reverse transcriptase (200U/µl, Invitrogen, Paisley, UK) was added and incubated at the following temperatures: 25°C for 5 minutes, 50°C for 60 minutes in a Prime Techne thermocycler (Bibby Scientific Limited, Staffordshire, UK). The reaction was terminated by heating the samples at 70°C for 15 minutes.

### **2.4.2. Reverse transcription of miR template**

cDNA of mature miRs was generated separately from total RNA (purified by mirVana™ miR Isolation Kit, Section 2.3.2) using the TaqMan® MicroRNA Reverse Transcription Kit (Applied Biosystems, Paisley, UK) and stem-looped RT primers, specific to individual miRs, from TaqMan® MicroRNA Assays (Applied Biosystems, Paisley, UK) as indicated (Table 2.1). miR was synthesised in a 15µl reaction following the manufacturer's protocol: 1.5µl 10x reverse transcription buffer, 0.15µl dNTPs (100mM), 0.19µl RNase inhibitor (20U/µl), 1µl MultiScribe™ Reverse Transcriptase (50U/µl) and 4.16µl sterile water were added together to give a total volume of 7µl of Master Mix. Master Mix was then added to 5µl RNA (5ng), mixed and centrifuged (16,200g, 5 seconds at room temperature). 3µl 5x reverse transcription primers were then added to the Master Mix/RNA. Samples were incubated at 16°C for 30 minutes, 42°C for 30 minutes and the reaction was terminated by heating the samples at 85°C for 5 minutes. Reactions were carried out using a Prime Techne thermocycler (Bibby Scientific Limited, Staffordshire, UK).

**Table 2.1.** Stem-looped reverse transcription primer sequences used in the amplification of mature miRs using TaqMan® MicroRNA assays.

Assay ID	Assay name	miRBase ID	Mature miR sequence 5'-3'
005982_mat	bta-miR-21	bta-miR-21-5p	UAGCUUAUCAGACUGAUGUUGACU
002445	hsa-miR-27a*	bta-miR-27a-5p	AGGGCUUAGCUGCUUGUGAGCA
001188	mmu-miR-140*	bta-miR-140	UACCACAGGGUAGAACCACGGA
001134	mmu-miR-221	bta-miR-221	AGCUACAUUGUCUGCUGGGUUU
002276	hsa-miR-222	bta-miR-221	AGCUACAUCUGGCUACUGGGU
001105	hsa-miR-451	bta-miR-451	AAACCGUUACCAUJACUGAGUUU
002339	hsa-miR-483-3p	bta-miR-483	UCACUCCUCUCCUCCCGUCUU
002376	hsa-miR-543	bta-miR-543	AAACAUUCGCGGUGCACUUCUU

## 2.5. Quantitative Polymerase Chain Reaction (qPCR)

mRNA quantification of genes of interest in experimental samples were measured by qPCR with either Brilliant III Ultra-Fast SYBR® Green QPCR Master Mix (Agilent Genomics, Berkshire, UK) or TaqMan® Fast Advanced Master Mix (Applied Biosystems, Paisley, UK).

### 2.5.1. Primers

Bovine-specific primer sequences (Tables 2.2 - 2.3) were either adapted from the literature or designed using Primer-Blast software with the following criteria: [i] to span exon-exon boundaries and [ii] to generate an amplicon within the range of 70-250bp. Designed primers were checked through the NCBI BLAST database to eliminate the possibility of binding to unintended targets. Primers (Eurofins Genomics, Ebersberg, Germany) were optimised by polymerase chain reaction (PCR). Primer efficiencies were examined by generating standard curves of individual genes, created from a series of

five 10-fold dilutions of pooled cDNA from untreated (controls) and treated (loaded/transfected) samples. Efficiencies in the range of 95-110% indicated that the examined genes were appropriate for cross-comparing with other genes of interest.

**Table 2.2.** Quantitative PCR primer sequences for reference genes, annealing temperature (AT°) and product size.

Primers	Sequences 5'-3'	Annealing temperature (AT°)	Amplicon length (bp)
<b>SDHA-F</b> <b>SDHA-R</b>	GATGTGGGATCTAGGAAAAGGCCTG ACATGGCTGCCAGCCCTACAGA	60	104
<b>YWHAZ-F</b> <b>YWHAZ-R</b>	CTGAGGTTGCAGCTGGTGATGACA AGCAGGCTTTCTCAGGGGAGTTCA	60	180
<b>PPIA-F</b> <b>PPIA-R</b>	GGTGGTGACTTCACACGCCATAATG CTTGCCATCCAACCACTCAGTCTTG	60	186
<b>RPL4-F</b> <b>RPL4-R</b>	TTTGAAACTTGCTCCTGGTGGTCAC TCGGAGTGCTCTTTGGATTTCTGG	60	199
<b>HPRT-F</b> <b>HPRT-R</b>	TAATTATGGACAGGACCGAACGGCT TTGATGTAATCCAACAGGTCGGCA	60	127
<b>GAPDH-F</b> <b>GAPDH-R</b>	TTGTCTCCTGCGACTTCAACAGCG CACCACCCTGTTGCTGTAGCCAAAT	60	133
<b>β-actin-F</b> <b>β-actin-R</b>	CATCGCGGACAGGATGCAGAAA CCTGCTTGCTGATCCACATCTGCT	60	157
<b>18S-F</b> <b>18S-R</b>	GCAATTATTCCCATGAAACG GGCCTCACTAAACCATCCAA	60	123

Primer sequences for 18S were taken from (Frye et al., 2005), whereas the other primer sequences were obtained from (Anstaett et al., 2010).

**Table 2.3.** Quantitative PCR primer sequences for target genes of interest, annealing temperature (AT°) and product size.

Primers	Sequences 5'-3'	Annealing temperature (AT°)	Amplicon length (bp)	References
<b>MMP1-F</b> <b>MMP1-R</b>	CAAATGCTGGAGGTATGATGA AATTCCGGGAAAGTCTTCTG	60	82	(Shieh and Athanasiou, 2007)
<b>MMP3-F</b> <b>MMP3-R</b>	TGGAGATGCTCACTTTGATGATG GAGACCCGTACAGGAAGTGAATG	60	221	(Li et al., 2011b)
<b>MMP7-F</b> <b>MMP7-R</b>	GGAGCGAAGCAATCCCACTGACG GGGTCCCCATGAGCTCTTCTTGC	60	91	
<b>MMP9-F</b> <b>MMP9-R</b>	TAGCACGCACGACATCTTTC GAAGGTCACGTAGCCACAT	60	121	(Blain et al., 2010)
<b>MMP-13-F</b> <b>MMP-13-R</b>	CCCTTGATGCCATAACCAAGT GCCCAAATTTTCTGCCTCT	60	201	(Blain et al., 2010)
<b>ADAMTS4-F</b> <b>ADAMTS4-R</b>	CTCCATGACAACCTCGAAGCA CTAGGAGACAGTGCCCGAAG	60	169	(Blain et al., 2010)
<b>ADAMTS5-F</b> <b>ADAMTS5-R</b>	CTCCCATGACGATTCCAAGT TACCGTGACCATCATCCAGA	60	155	(Blain et al., 2010)
<b>Collagen2-F</b> <b>Collagen2-R</b>	AACGGTGGCTTCCACTTC GCAGGAAGGTCATCT GGA	60	69	(Darling and Athanasiou, 2005)
<b>Aggrecan-F</b> <b>Aggrecan-R</b>	GCTACCCTGACCCTTCATC AAGCTTTCTGGGATGTCCAC	60	76	(Darling and Athanasiou, 2005)
<b>TIMP-1-F</b> <b>TIMP-1-R</b>	CTGCGGATACTTCCACAGGT ATGGATGAGCAGGGAAACAC	60	75	(Li et al., 2011b)
<b>TIMP-2-F</b> <b>TIMP-2-R</b>	ATAGTGATCAGGGCCAAAGCAGTC TGTCCCAGGGCACGATGAAGTC	60	277	(Milner et al., 2006)
<b>TIMP-3-F</b> <b>TIMP-3-R</b>	GACATCGTGATCCGAGCCAA TGGGGCATCTTGGTGAATCC	60	119	(Al-Sabah, 2014, PhD thesis, Cardiff University)
<b>HDAC4-F</b> <b>HDAC4-R</b>	AACAAGGAGAAGGGCAAAGAG CGTCCTTCCCGTACCAGTAGC	60	150	

<b>Runx2-F</b>	CATGGTGGAGATCATCGCTG	60	172	
<b>Runx2-R</b>	CGCCATGACAGTAACCACAG			
<b>SPRY4-F</b>	GATAGCGGCGTCCGATCC	60	94	
<b>SPRY4-R</b>	AGGCTTCTAGGGGCCTTTGAG			
<b>Wnt3A-F</b>	GGGGCTGGCAGAGTGTCCT	60	72	
<b>Wnt3A-R</b>	GGCGCAGAGGATGGGCTGTG			

### 2.5.2. SYBR® Green qPCR

SYBR® Green qPCR requires a fluorescent dye which specifically binds to double-stranded DNA in the PCR reaction. SYBR® Green I binding to the newly synthesised double-stranded DNA generates a fluorescent signal that is proportional to the amount of amplified DNA. The point at which the fluorescence signal is significantly higher than the background is referred to as the threshold cycle ( $C_t$ ). The  $C_t$  value for individual amplification is the number of cycles at which the amplification plot crosses the baseline set (threshold) (Figure 2.3A). The  $C_t$  values were used to establish the relative quantification for all genes analysed. As SYBR® green I binds all double stranded DNA, the dissociation curve was performed at the end of the qPCR to confirm that only the product of interest was amplified as indicated by a single fluorescent peak on the melting curve (Figure 2.3B). To work out relative changes in target gene expression the  $2^{-\Delta\Delta CT}$  method (Livak and Schmittgen, 2001) was used; relative quantification is presented as fold change in a gene of interest in experimental samples in comparison to unloaded/negative control samples. The fold change was normalised to the geometric mean of two reference genes in combination that were identified as being unaffected by the experimental conditions under investigation. qPCR reactions were performed with the Mx3000P®QPCR System and MxPro QPCR software (Stratagene, Cambridge, UK) using Brilliant III Ultra-Fast SYBR® Green QPCR Master Mix (Agilent Technologies, Wokingham, UK) on RNase/DNase-free 96 well plates (Agilent Technologies, Wokingham, UK). cDNA was amplified in a total reaction volume of 20µl (Table 2.4). The plate contents were collected by centrifugation for 1 minute and amplification performed using the conditions shown in Table 2.5. An annealing step was carried out at 60°C unless indicated otherwise (Table 2.2 and Table 2.3).

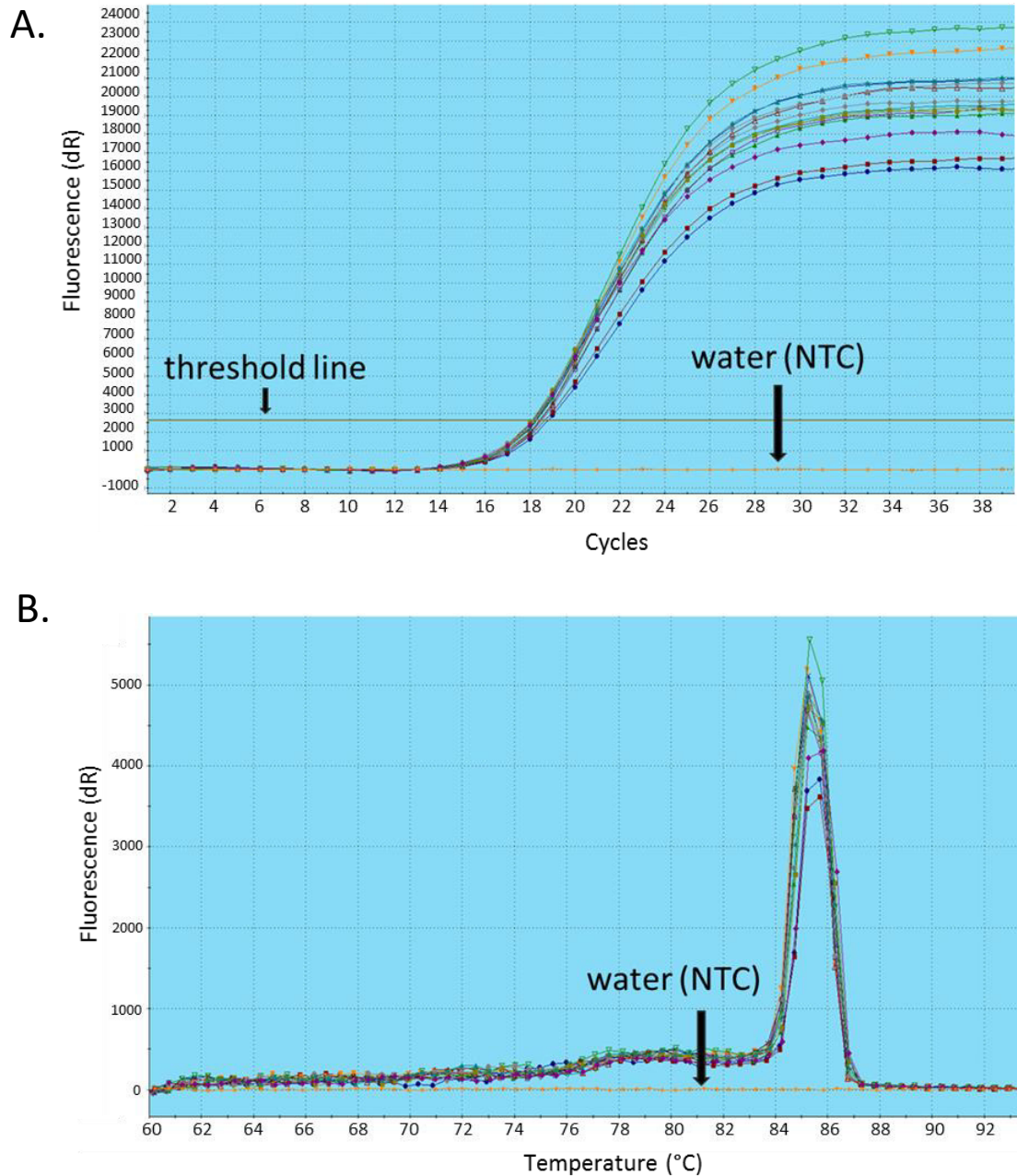


**Figure 2.3.** Representative amplification plot and melting curve for TIMP-3 SYBR® Green qPCR. Amplification plot showing cycle numbers at which fluorescent signal from the gene of interest was significantly elevated against the background and crossed the threshold ( $C_t$  values) **(A)**. Melting curve generated from amplicons subjected to dissociation analysis showing a single peak indicative that only a single product was amplified in the qPCR reaction **(B)**. The orange line shows no amplification and represents a no template control.

**Table 2.4.** Components for a single SYBR® Green qPCR reaction.

Component	Volume
2x SYBR® Green QPCR Master Mix buffer	10µl
primers (forward and reverse) (10µM stock)	0.4µl
cDNA / water (non-template control)	1µl
water	8.6µl
<b>Total</b>	<b>20µl</b>

**Table 2.5.** SYBR® Green qPCR cycling conditions to amplify genes of interest.

Cycle step	Temperature (°C)	Time	Cycles
<b>Initial Denaturation</b>	95	3 minutes	1
<b>Denaturation</b>	95	15 seconds	40
<b>Annealing/Extension</b>	60	20 seconds	
<b>Dissociation</b>	95	1 minutes	1
	60	30 seconds	
	95	30 seconds	

### 2.5.3. Probes

Quantification of expression levels of target genes of interest were measured using bovine-specific TaqMan<sup>®</sup> probes (Applied Biosystems, Paisley, UK) as described (Table 2.1 and Table 2.6).

**Table 2.6.** TaqMan<sup>®</sup> Gene expression assays used in the quantification of genes of interest.

Gene	Assay ID	Assay name	Amplicon length
CPEB3	Bt02655331_m1	CPEB3 TaqMan <sup>®</sup> Gene Expression	71
LIFR	Bt02626849_m1	LIFR TaqMan <sup>®</sup> Gene Expression	121

### 2.5.4. TaqMan<sup>®</sup>PCR

TaqMan<sup>®</sup> qPCR relies upon the use of fluorescently labelled oligonucleotides complementary to the region of target gene which produces a fluorescent signal upon amplification of cDNA. Each TaqMan<sup>®</sup> MGB (minor groove binder) probe contains: (i) reporter fluorescent dye (FAM<sup>™</sup> dye) at the 5' end (ii) a non-fluorescent quencher (NFQ) attached to the 3' end to block the activity of fluorescent dye and (iii) a minor groove binder (MGB) at the 3' end that allows an extremely stable duplex to form with single stranded target DNA. The probe is designed to bind the gene of interest and resides between the forward and reverse primers. During strand elongation, the DNA polymerase cleaves the hybridized target gene probe, separating the fluorescent reporter from the quencher, hence promoting a fluorescent signal. Despite differences in the chemistry between SYBR<sup>®</sup> Green and TaqMan<sup>®</sup> qPCR, the concept and principles

of the data analysis are identical. Quantification of the relative expression levels of target genes amplified using probe qPCR was performed as described for SYBR® Green (Section 2.5.2).

TaqMan® qPCR was conducted using the same system, software and 96-well plates as for SYBR® Green qPCR (Section 2.5.2); however, TaqMan® Fast Advanced Master Mix (AmpliTaq® Fast DNA Polymerase, Uracil-N glycosylase (UNG), dNTPs with dUTP, ROX™ dye (passive reference), optimised buffer components; Applied Biosystems, Paisley, UK) were utilised instead. Following the manufacturer’s protocol, miR expression was analysed in a reaction of 10µl (Table 2.7), whilst mRNA expression of target genes was assessed in a 20µl reaction (Table 2.8), with qPCR performed under specific cycling conditions (Table 2.9).

**Table 2.7.** Components for a single TaqMan® miR qPCR reaction.

Component	Volume
TaqMan® Fast Advanced Master Mix (2x)	5µl
TaqMan® Gene Expression Assay (20x)	0.5µl
reverse transcribed miR/water	1µl
water	3.5µl
<b>Total</b>	<b>10µl</b>

**Table 2.8.** Components for a single TaqMan® gene expression qPCR reaction.

Component	Volume
TaqMan® Fast Advanced Master Mix (2x)	10µl
TaqMan® Gene Expression Assay (20x)	1µl
cDNA/water	2µl
water	7µl
<b>Total</b>	<b>20µl</b>

**Table 2.9.** TaqMan qPCR cycling conditions to amplify miRs or genes of interest.

Cycle step	Temperature (°C)	Time	Cycles
<b>UNG incubation (to avoid DNA contamination)</b>	50	2 minutes	1
<b>Polymerase activation</b>	95	20 seconds	1
<b>Denaturation</b>	95	3 seconds	40
<b>Annealing/Extension</b>	60	30 seconds	

## **2.6. Selection of suitable reference genes for quantitative PCR**

To optimise the most appropriate reference genes for the experimental system in use i.e. mechanical load, transfection with miR inhibitor or mimic, a panel of reference genes was analysed: SDHA, YWHAZ, PPIA, RPL4, HPRT, GAPDH,  $\beta$ -actin, (Anstaett et al., 2010) and 18S (Frye et al., 2005) (Table 2.10). Selection of the most stable combination of reference genes for normalisation of experimental samples was performed using RefFinder software (<http://fulxie.0fees.us/>). RefFinder integrates the most popular softwares designed for assessment of reference gene stability on the basis of gene  $C_t$  values: geNorm (Vandesompele et al., 2002), BestKeeper (Pfaffl et al., 2004), Normfinder (Andersen et al., 2004) and the comparative delta- $C_t$  method (Silver et al., 2006). Each of these computational programmes contains individual algorithms to evaluate the most appropriate reference gene. Based on the data from each individual software, RefFinder assigns a value to each tested gene and then calculates the geometric mean of their values to rank the genes according to their stability (from most to least stable).

**Table 2.10.** Function of tested reference genes.

Gene	Function	Reference
<b>β-actin</b> (β-actin)	Cytoskeletal structural molecule	(Gunning et al., 2015)
<b>GAPDH</b> (glyceraldehyde-3-phosphate dehydrogenase)	An enzyme involved in glycolysis and gluconeogenesis	(Glare et al., 2002)
<b>HPRT1</b> (hypoxanthine phosphoribosyltransferase 1)	An enzyme involved in biosynthesis of purine nucleotides via the salvage pathway (from intermediates of degraded RNA and DNA)	(Torres and Puig, 2007)
<b>PPIA</b> (peptidylprolyl isomerase A (cyclophilin A))	A molecule with isomerase activity which assists in protein folding	(Thali et al., 1994)
<b>RPL4</b> (ribosomal protein L4)	It is a component of large ribosomal subunit involved in forming the protein exit tunnel	(O'Connor et al., 2004)
<b>SDHA</b> (Succinate Dehydrogenase Complex Flavoprotein Subunit A)	A flavoprotein-containing subunit of SDH complex which is bound to the inner membrane of the mitochondria and participates in oxidative phosphorylation.	(Lee et al., 2016)
<b>YWHAZ</b> (Tyrosine 3-Monooxygenase/Tryptophan 5-Monooxygenase Activation Protein Zeta)	Molecule belonging to 14-3-3 protein family which modulate signal transduction by binding phospho-serine containing proteins and is therefore implicated in a wide array of cellular activities such as cell signalling, division, apoptosis and cytoskeletal organization.	(Kuboki et al., 2012, Mackintosh, 2004, Yang et al., 2016b)
<b>18S</b> (18S ribosomal RNA)	Ribosome subunit	(Doudna and Rath, 2002)

## **2. 7. Global gene analysis using Affymetrix mRNA arrays**

Analysis of the entire bovine genome was performed using the Bovine GeneChip® Gene 1.0 ST array containing 26,773 genes to identify mechanically-regulated transcripts. Explants were subjected to either a 2.5MPa or 7MPa load (1Hz, 15 min) or left unloaded, and RNA processed 4h or 24h post-cessation of load; arrays were conducted on two independent sets of samples (n = 6, N = 2) (Central Biotechnology Services, School of Medicine, Cardiff University). RNA quality was assessed using the Bioanalyzer (Section 2.3.4) with all selected samples containing a RNA integrity number (RIN) of >8. RNA (100ng) was biotinylated using Genechip® WT Plus Reagent kit and subsequently hybridized to the Genechip® Bovine 1.0 ST arrays. Genechip® poly A RNA control kit was used to ensure equivalent preparation and labelling efficiencies. Hybridized RNA was detected using the Genechip® Hybridization, wash and stain kit. Arrays were washed and stained in conjunction with Genechip® Fluidics station 450, and arrays scanned using the GeneChip® Scanner 3000 7G.

### **2.7.1. Bioinformatic analysis of Affymetrix mRNA arrays**

The mRNA arrays were analysed by Dr Timothy Stone (Central Biotechnology Services Bioinformatician, Cardiff, UK) in the R Statistical programming environment using the “oligo” (Carvalho and Irizarry, 2010) and “limma” (Ritchie et al., 2015) packages that are available on Bioconductor (<https://www.bioconductor.org/>). The arrays were normalised via RMA normalisation (Irizarry et al., 2003). The quality of the arrays was assessed via principal component analysis to determine if there were any sample arrays that contained significant global outliers in terms of gene expression. Statistical testing for differential expression was performed by testing P-values using Benjamini-Hochberg (Benjamini and Hochberg, 1995) and adjusted p-values at a threshold of 5% were used to determine statistical significance.

## 2.8. Next Generation Sequencing of miRs

Identification of mechanically-regulated miRs in articular cartilage was performed using Next Generation Sequencing (NGS). Explants were subjected to either a 2.5MPa or 7MPa load (1Hz, 15 minutes) or left unloaded, and RNA processed 2, 6 or 24h post-cessation of load.

### 2.8.1. Preparation of pooled samples

RNA samples (n = 6) from each loading regime and duration post-load (Figure 2.4A) were pooled respectively to create representative samples containing >3.5µg of RNA per sample (Figure 2.4B). For every combination of load and period post-load, 3 independent repeat experiments were performed providing 3 independent samples of pooled RNA per regime (Figure 2.4C).

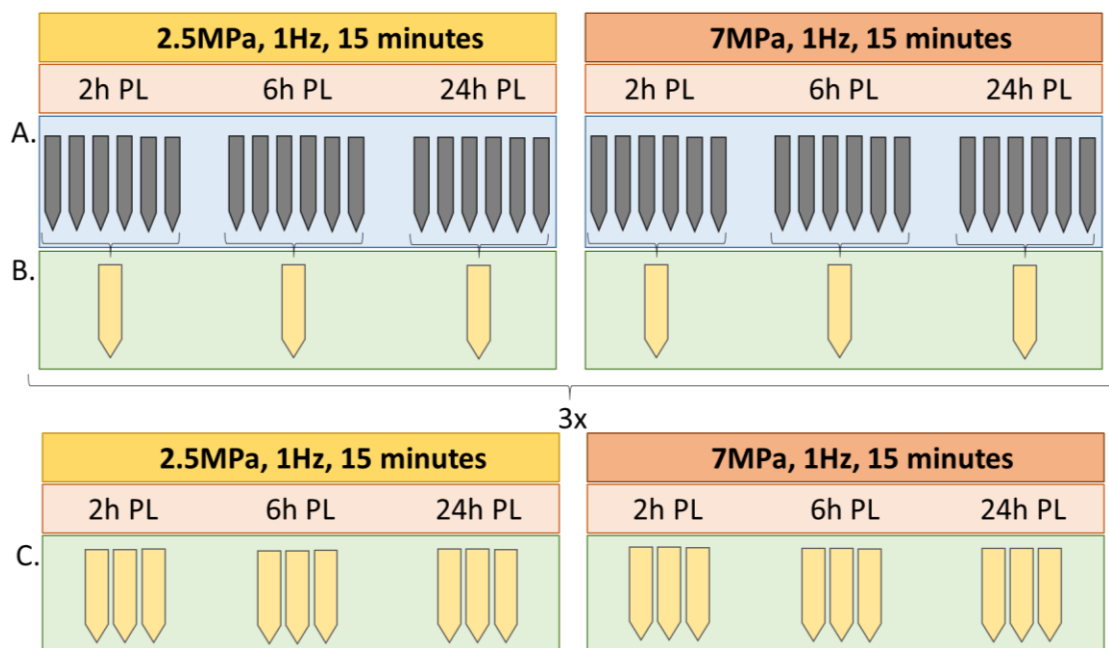


**Figure 2.4.** Schematic diagram of pooled experimental RNA to create representative samples. 6 independent samples from each period post load (**A**) were pooled to provide a single sample (**B**). Each experiment was performed 3 times which resulted in 3 representative independent repeats (**C**) of each combination of loading regime and period post-cessation of load. Key: MPa - megapascal, Hz - hertz, PL - post-load, h - hours.

### 2.8.2. miR library preparation

The purity and yield of total RNA was assessed using the Bioanalyzer (Section 2.3.4), and RNA integrity number (RIN) of all RNA samples was  $\geq 8$ . Library preparation for all samples was conducted on 6  $\mu$ l of total RNA containing 450ng of RNA. The library preparation workflow consisted of the following 9 steps: **1.** Ligation of 3' adaptor, **2.** Primer hybridisation, **3.** Ligation of 5' adaptor, **4.** Reverse transcription, **5.** PCR, **6.** Electrophoresis and recovery of library band, **7.** Elution of library from gel, **8.** Next Generation Sequencing, and **9.** Data analysis (Figure 2.5). To prepare miR libraries, NEBNext® Small RNA Library Prep Set for Illumina® (Multiplex Compatible: BioLabs, Hitchin, UK) components were used.

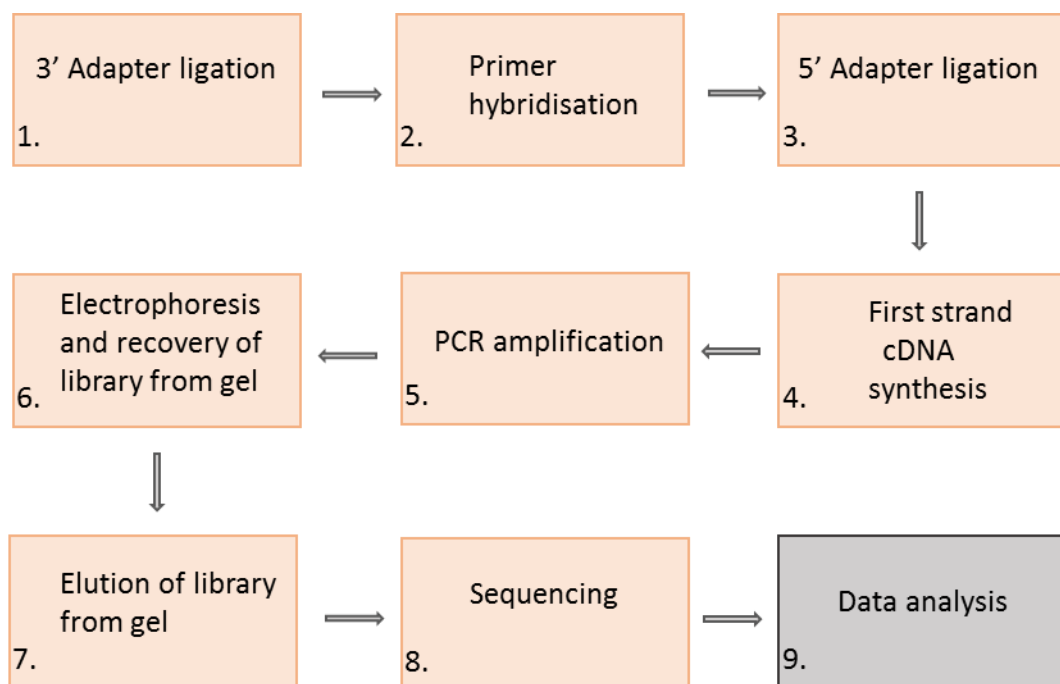


**Figure 2.5.** Schematic diagram of miR Illumina Next Generation Sequencing workflow. Adapted from (Borodina et al., 2011).

### 2.8.2.1. Amplification of miR libraries

Amplification of miR libraries was performed according to the manufacturer's protocol (BioLabs, Hitchin, UK). The 3' adaptor ligation was conducted in a 20µl total volume. 1µl 3' SR Adaptor for Illumina was added to 450ng RNA and incubated in a thermal cycler at 70°C for 2 minutes. 10µl 3' Ligation Reaction Buffer (2x) and 3µl 3' Ligation Enzyme Mix were added to the tubes on ice and incubated at 25°C for 1h. To prevent formation of 3' Adaptor - 5' Adaptor, the primer hybridisation step was performed to transform the single stranded DNA adaptor into double-stranded DNA molecules. This step was conducted by adding 1µl SR RT primer for Illumina and 4.5µl water. Samples were heated at 75°C for 5 minutes and then transferred to 37°C for 15 minutes, followed by 15 minutes at 25°C. 5' SR Adaptor was ligated by mixing 1µl 5' SR Adaptor for Illumina (denatured at 70°C for 2minutes), 1µl 5' Ligation Reaction Buffer (10x) and 5' Ligation Enzyme Mix, and heating at 25°C for 1h. Reverse transcription of miRs was then performed by adding 8µl First Strand Synthesis Reaction Buffer (5x), 1µl Murine RNase Inhibitor and 1µl ProtoScript II Reverse Transcriptase (200,000U/ml) to 30µl of adaptor ligated RNA and incubation at 50°C for 1h. PCR amplification was conducted immediately after cDNA synthesis. 50µl LongAmp® Taq 2x Master Mix, 2.5µl SR Primers for Illumina, 2.5µl bar coded primers (10µM) and 5µl water were mixed with 40µl reverse transcription reaction. PCR reaction was performed using the MJ Research PTC-200 thermal cycler (Hertfordshire, UK) under the following conditions (Table 2.11).

**Table 2.11.** PCR cycling conditions utilised to amplify miR libraries.

Cycle Step	Temperature (°C)	Time	Cycles
Initial denaturation	94	30 seconds	1
Denaturation	94	15 seconds	15
Annealing	62	30 seconds	
Extension	70	15 seconds	
Final Extension	70	5 minutes	1
Hold	4	∞	

### 2.8.2.2. Purification of cDNA

To remove primers, nucleotides, polymerases and salts from the PCR product, 100µl PCR amplified cDNA was purified using a QIAquick PCR Purification Kit (Qiagen, West Sussex, UK) following the manufacturer's protocol. All centrifugation steps were carried out at 18,000g at room temperature. PB Buffer was added to the PCR sample in a ratio of 1:5 and then transferred to QIAquick spin columns placed in collection tubes, followed by centrifugation for 60 seconds. The flow-through was discarded and the columns washed with 750µl PE Buffer and centrifuged twice for 2 minutes with removal of flow-through in between; the second spin was conducted with lids of the spin columns opened. QIAquick columns were transferred to clean 1.5ml tubes and 30µl Buffer EB (10mM Tris-HCl, pH 8.5) was added. The QIAquick columns were incubated at room temperature for 1 minute before being centrifuged for 1 minute to elute the DNA.

### 2.8.2.3. Confirmation and size selection of amplified miRs

To select miR libraries, purified cDNA samples were run on 8% polyacrylamide gels (Table 2.12).

**Table 2.12.** Reagents used in the preparation of an 8% polyacrylamide gel.

Reagents	8% polyacrylamide gel
40% 19:1 bis/acrylamide	3 ml
5x TBE buffer	1.5 ml
10% (w/v) ammonium persulphate (APS)	300 µl
Tetramethylethylenediamine (TEMED)	15 µl
dH <sub>2</sub> O	10.185ml
<b>Total</b>	<b>15 ml</b>

Samples were mixed with 1µl 6x Bromophenol Blue Dye (BioLabs, Hitchin, UK) and loaded into the wells of the gel (one sample per gel) next to 5µl diluted (1:2) DNA ladder (final concentration 125ng; BioLabs, Hitchin, UK). Electrophoresis using 0.5x TBE as running buffer was carried out at 120V until the dye was at the bottom of the gel. The gel was stained in 5ml 0.5% TBE with 5µl SYBR® Gold Nucleic Acid Gel Stain (10,000x) (Invitrogen, Paisley, UK) for 5 minutes. The SYBR® gold stained libraries were then visualised using an UV transilluminator (Figure 2.6A) and bands in the appropriate region of the gel were excised using a sterile scalpel blade (Figure 2.6B). miR libraries were located at the level of ~140bp.

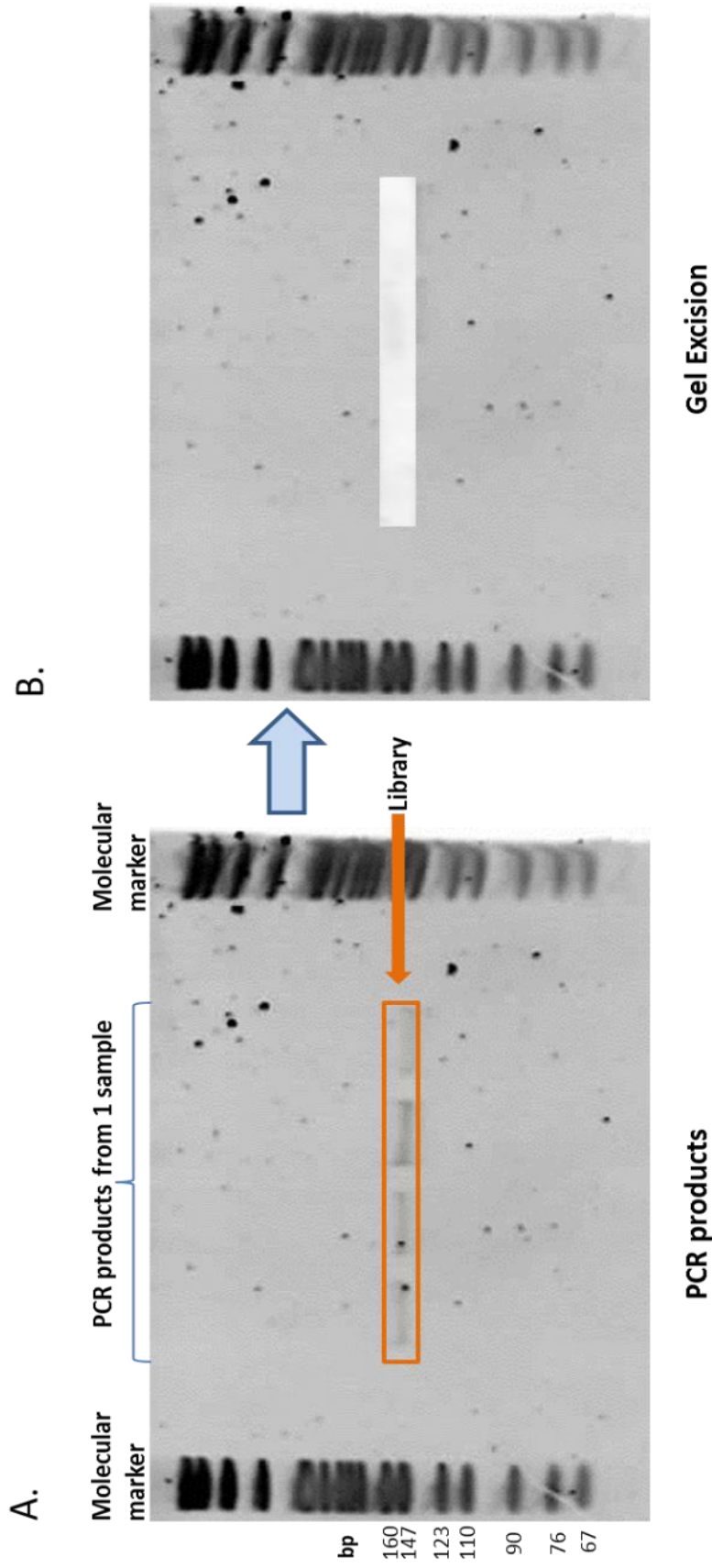


**Figure 2.6.** Representative 8% polyacrylamide gel before and after library excision. After gel visualisation the ~140bp miR library bands were observed below the 147bp marker **(A)**. The library bands were excised using a sterile scalpel and placed into 1.5ml tubes; the remaining gel was re-visualised to ensure correct band removal **(B)**.

#### **2.8.2.4. Elution and purification of miRs from 8% polyacrylamide gel**

Gel bands were transferred into microtube gel breaker tubes (made by puncturing the bottom of a sterile, nuclease-free, 1.5ml microcentrifuge tube 5 times with a 21-gauge needle); the punctured tubes were located in 2ml collection tubes and centrifuged at 13,000g for 5 minutes at room temperature. 250µl of 1x DNA Gel Elution Buffer (NEB Next® Small RNA Library Prep Set for Illumina® (Multiplex Compatible) kit) was added to the collection tubes containing the excised gel and the tubes were shaken at room temperature for 4h. The eluates with the remaining gels were then transferred to the top of the Corning Costar® Spin-X® Columns (0.45µm); to remove the gel debris, the columns were centrifuged at 13,000g for 5 minutes until all the eluate moved to the bottom of the collecting tube.

#### **2.8.2.9. Purification and concentration of miR libraries**

2µl of glycogen (GlycoBlue™; Invitrogen, Paisley, UK), 40µl of 3M sodium acetate (pH 5.2) and 975µl of pre-chilled (-25°C) 100% (v/v) ethanol were added to the eluted miRs, and briefly vortexed and centrifuged prior to incubation at -80°C for 30 minutes to precipitate the miRs. The samples were then centrifuged at 13,000g for 30 minutes at 4°C and the resulting DNA pellet was washed with 80% (v/v) ethanol. After further centrifugation (14,500g, 30 minutes, 4°C) the supernatant was removed and the pellet left to air dry. The pellet containing the miR library was treated with 12µl TE buffer to resuspend the cDNA. miR libraries (a library from a single sample contains an individual barcode for later identification) was measured and then the libraries were pooled and sent for NGS to The Genome Analysis Centre™ (Norwich, UK) to be sequenced on a HiSeq™ Sequencing System.

#### **2.8.3. Bioinformatic analysis of miR Next Generation Sequencing**

The data obtained from the miR deep sequencing was analysed by bioinformatician Mr. Andrew Skelton (Newcastle University Medical School). Initially, raw FASTQ files were run through FastQC to assess the quality of the data, and confirm the presence of a known 3' adapter, as the 5' adapters had already been removed (Andrews, 2010). Cutadapt was used to trim the FASTQ files (Martin, 2011), and discard any reads less

than 17 bases in length. Trimmed FASTQ files were aligned against known bos taurus miR sequences from miRBase. Quantification was determined by counting aligned reads against a reference, using a combination of RSamTools (Morgan, 2011) and ShortRead (Morgan et al., 2009) bioconductor packages. Differential expression was assessed using DESeq2 (Love et al., 2014). Global experimental variance was analysed using principal component analysis to assess for outlier samples. Statistical significance from differential expression tests was determined by retaining miRs that had an adjusted p value < 0.05 (Benjamini and Hochberg, 1995).

## **2.9. Next Generation Sequencing of chondrocytes transfected with miR inhibitors**

Next Generation Sequencing (NGS) was performed on primary chondrocytes transfected with specific miR inhibitors to identify putative target mRNAs; cells were transfected with miR-21-5p, miR-221 or miR-222 inhibitors, a non-targeting control or untransfected cells for 48 h prior to analysis.

### **2.9.1. Preparation of pooled samples**

RNA samples (n = 3) from each condition (Figure 2.7A) were pooled respectively to create representative samples containing >2µg of RNA per sample (Figure 2.7B). Transfection was conducted on 3 independent repeat experiments for miR-21-5p, miR-221 and miR-222 inhibitor and untransfected cells (n = 3, N = 3), but mirVana™ miR Inhibitor Negative Control #1 (Applied Biosystems, Paisley, UK) was included in 2 repeats only (n = 3, N = 2) (Figure 2.7C).

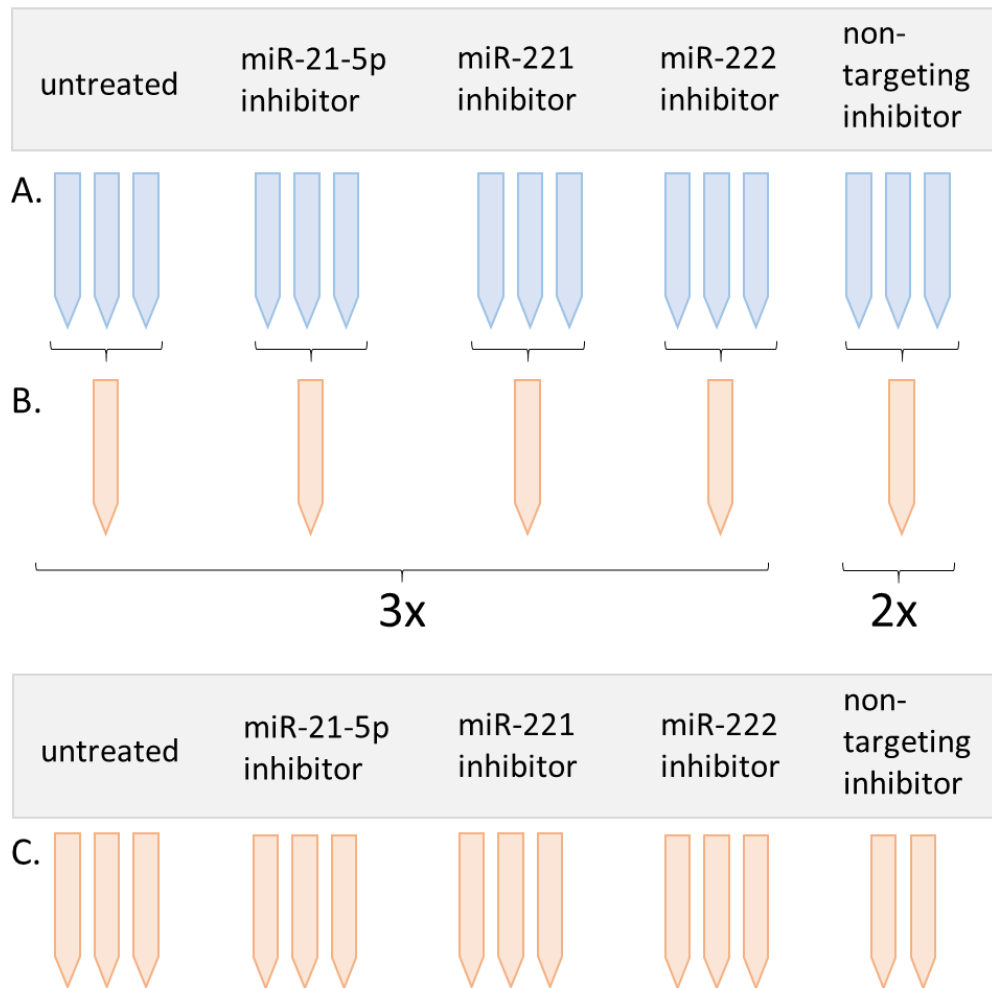


**Figure 2.7.** Schematic diagram of pooled experimental RNA to create representative samples for Illumina® TruSeq® sequencing. 3 independent samples from each treatment **(A)** were pooled into one **(B)**. Each experiment was performed on 3 independent cell preparations for miR-21-5p, miR-221 and miR-222 inhibitor and untransfected cells ( $n = 3$ ,  $N = 3$ ), however for the non-targeting miR inhibitor (MirVana™ miR Inhibitor Negative Control #1) this was performed on 2 independent cell preparations only ( $n = 3$ ,  $N = 2$ ) **(C)**.

### 2.9.2. mRNA library preparation

The purity and yield of total RNA was assessed using the Bioanalyzer (Section 2.3.4) and Qubit® 3.0 fluorometer using Qubit® RNA BR Assay Kit (Invitrogen, Paisley, UK). RNA integrity number (RIN) of all RNA samples was  $\geq 9$ . The library preparation was conducted according to the Illumina® TruSeq® Stranded mRNA Sample Preparation LS protocol (Illumina, Cambridge, UK) (Figure 2.8).

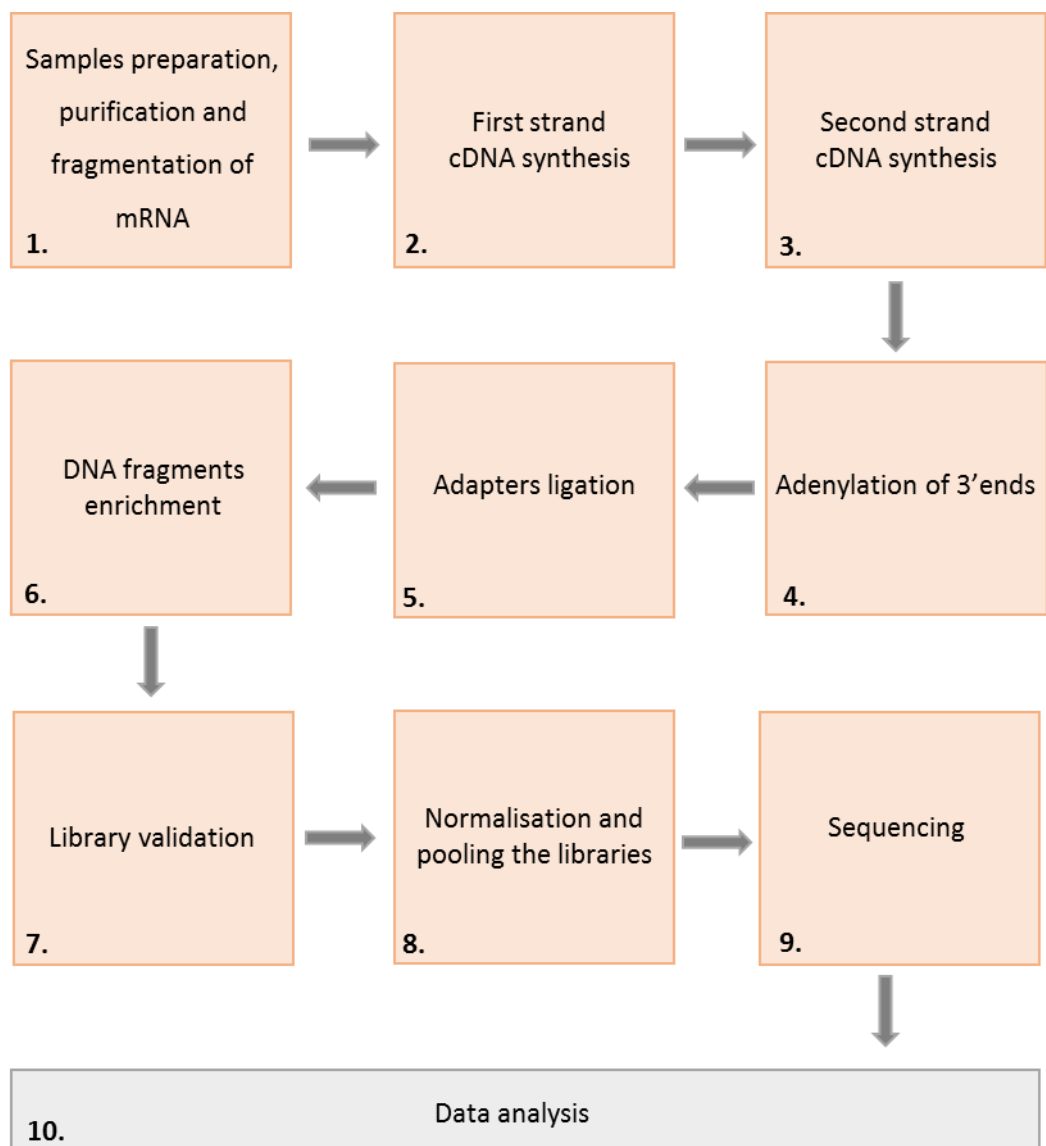


**Figure 2.8.** Schematic diagram of the Illumina Next Generation Sequencing workflow. Adapted from (Borodina et al., 2011).

### **2.9.2.1. Sample preparation, purification and fragmentation of mRNA**

This step aims to purify the poly(A) containing mRNA using poly-T oligo attached magnetic beads. This process contains two rounds of purification. RNA is chemically fragmented and prepared for cDNA synthesis in the final elution (Figure 2.9).

Library preparation for all samples was conducted on 50µl of total RNA containing 1µg of RNA. Isolation of poly(A) mRNAs was performed by adding 50µl of RNA Purification Beads (RPB) (Illumina, Cambridge, UK) to the RNA. Samples were incubated at 65°C for 5 minutes to denature the RNA and subsequently incubated at room temperature for 5 minutes to facilitate binding of the poly(A) mRNA to the beads. To separate the poly(A) mRNA bound to the beads from the remaining solution, the samples were placed on a magnetic stand at room temperature for 5 minutes followed by discarding the supernatant without disturbing the beads. To remove unbound RNA, the beads were washed by gently pipetting up and down with 200µl of Bead Washing Buffer (BWB). After 5 minutes incubation on a magnetic stand at room temperature, the supernatant containing most of the ribosomal and non-messenger RNA was removed from each sample. To elute the mRNA from the beads, 50µl of Elution Buffer (ELB) was added gently to the beads and then incubated at 80°C for 2 minutes. This step released both the mRNA and the rRNA that had bound non-specifically to the beads, therefore a second round of purification was performed. To rebind mRNA to the beads and decrease the amount of non-specific rRNA binding, 50µl of Bead Binding Buffer was added to each sample; samples were pipetted up and down and incubated at room temperature for 5 minutes, followed by 5 minutes on the magnetic stand. Next, all of the supernatant was removed and the beads were washed by adding BWB and pipetting up and down. After 5 minutes incubation on the magnetic stand at room temperature, the supernatant containing contaminants that did not rebind to the beads was discarded. Samples were removed from the magnetic stand and 19.5µl of Fragment, Prime, Finish Mix was added to each sample; this reagent contains random hexamers for reverse transcription priming and acts as a reaction buffer for the 1<sup>st</sup> strand cDNA synthesis. Samples were incubated at 94°C for 8 minutes to elute, fragment and prime the RNA.

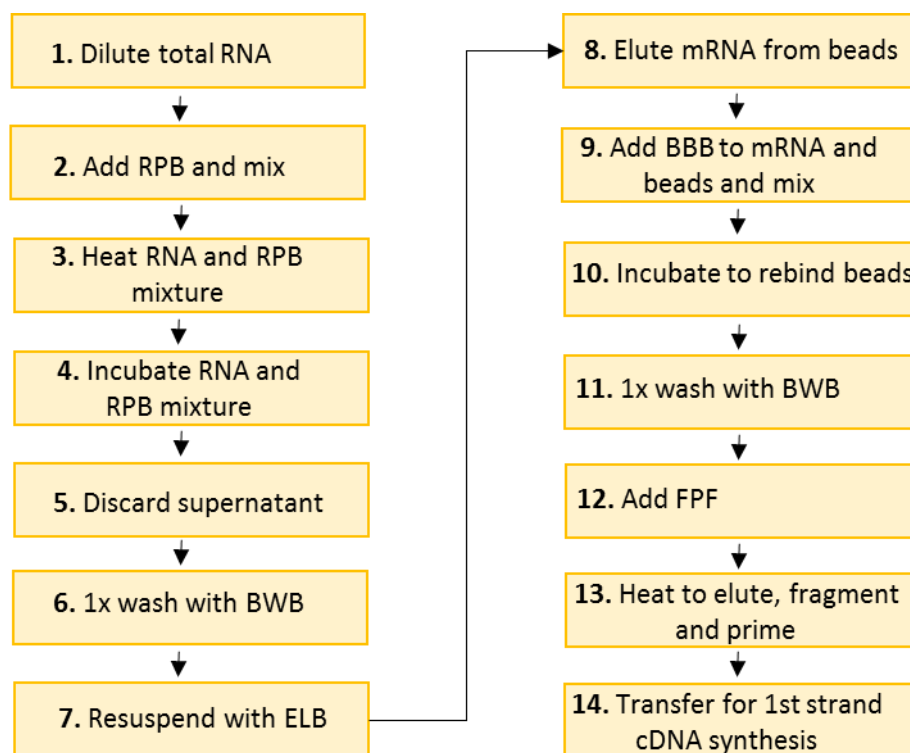


**Figure 2.9.** Schematic diagram of sample preparation, purification and fragmentation of mRNA for Next Generation Sequencing (TruSeq Stranded mRNA Sample Preparation Guide); Key: RPB - RNA Purification beads, BWB - Bead Washing Buffer, ELB - Elution Buffer and BBB - Bead Binding Buffer, FPF - Fragment, Prime, Finish mix. Adapted from TruSeq Stranded mRNA Sample Preparation Guide.

### 2.9.2.2. First strand cDNA synthesis

Cleaved RNA fragments were reverse transcribed into first strand cDNA using Super Script II reverse transcriptase (200U/ $\mu$ l, Invitrogen, Paisley, UK). To avoid DNA-dependent synthesis, Actinomycin D which inhibits DNA transcription and does not affect RNA-dependant synthesis was added to the First Strand Synthesis Act D mix (FSA).

After the elute, fragment and prime step (step 13, Figure 2.9, Section 2.9.2.1), samples were placed onto the magnetic stand at room temperature for 5 minutes; 17 $\mu$ l of supernatant from each tube was transferred into the new tube whilst on the magnetic

stand. Following this, 8µl of the FSA and Super Script II mix, in a ratio of 9:1 was added to each sample and mixed gently. The samples were placed in a thermal cycler and heated at 25°C for 10 minutes, 42°C for 15 minutes, followed by 15 minutes at 70°C. In the next three steps in-line DNA controls such as: End Repair Control, A-Tailing Control and Ligation Control were used to assess the enzymatic efficiency of the following reagents: Second Strand Marking Master Mix, A-Tailing Mix and Ligation Mix, respectively. Each in-line control contains a fragment of dsDNA and was designed to determine whether the enzymes present in the aforementioned mixes were active. The results of the activity of examined enzymes is estimated based on the presence of sequences of the specific DNA controls in the final sequencing data; if the sequence of in-line DNA control is present, it indicates that the enzyme worked perfectly, however if the sequence of in-line control is absent, it suggests that the step failed.

### **2.9.2.3. Second strand cDNA synthesis**

The purpose of this reaction is to remove the RNA template and replace it with the second cDNA strand. Second strand cDNA was synthesised by using Second Strand Master Mix (SMM) containing polymerase I, RNase H and a nucleotide mixture in which dTTP is replaced by dUTP. The incorporation of dUTP into the second strand inhibits its amplification as polymerase, used in this reaction, is not able to incorporate beyond this nucleotide. 5µl of End Repair Control (diluted in Resuspension Buffer at a ratio of 1:50) was added to each sample, followed by the addition of 20µl of Second Strand Marking Master Mix. The mix was pipetted up and down and then placed into the thermal cycler, and incubated at 16°C for 1h. 90µl of AMPure XP beads (BioLabs, Hitchin, UK) was added to each sample by pipetting up and down for 5 minutes at room temperature. After 15 minutes incubation at room temperature, the sample was transferred onto the magnetic stand for 5 minutes at room temperature, and then 135µl of supernatant was discarded without disturbing the beads. The beads were washed twice with 200µl of 80% (v/v) ethanol, with complete removal of the supernatant at each step. The second supernatant was removed and the beads left to air dry for 15 minutes. 17.5µl of Resuspension Buffer was added to each sample, pipetted up and down, incubated for 2

minutes and left for 5 minutes on the magnetic stand at room temperature. 15µl supernatant containing ds cDNA was transferred to new 0.2ml PCR tubes.

#### **2.9.2.4. Adenylation of 3'ends**

To avoid ligation of two blunt fragments of ds cDNA during the adaptor binding reaction, a single 'A' nucleotide was added to the 3' ends of the DNA. This strategy provided the correct ligation between the adenylated 3'ends of the ds cDNA and increased the efficiency of the reaction as the adapters are 'T' tailed. 2.5µl of A-Tailing Control (diluted in Resuspension Buffer in a ratio of 1:100) was added to each sample followed by 12.5µl A-Tailing Mix. After pipetting up and down, the samples were incubated for 30 minutes at 37°C followed by 5 minutes at 70°C and a hold at 4°C.

#### **2.9.2.5. Ligation of adapters**

NGS permits the sequencing of multiple libraries on a single lane, however this is reliant on the pooling of libraries. Thus, the purpose of this step was to barcode the DNA libraries with their individual indexed adapters that would allow libraries to be distinguished during bioinformatics analysis. Ligation of barcoded adapters was conducted immediately after adenylation of the 3'ends.

2.5µl of Ligation Control (diluted in Resuspension Buffer in a ratio of 1:100) was added to each sample followed by 2.5µl Ligation Mix. After adding 2.5µl of RNA Adapter Index to each library the samples were incubated at 30°C for 10 minutes. To inactivate the ligation, 5µl of Stop Ligation Buffer (STL) was added to each tube and pipetted up and down to mix. Based on the AMPure XP Beads capability to bind amplicons greater than 100bp, 42µl of AMPure XP Beads were added to each sample and pipetted gently up and down to select the libraries and remove all unbound adapters and adapter dimers. After 15 minutes incubation at room temperature, the samples were transferred onto the magnetic stand for 5 minutes and then 79.5µl supernatant was removed. With the samples left on the magnetic stand, the beads were washed twice with 200µl of 80% (v/v) ethanol, with complete removal of the supernatant at each step.

The second supernatant was removed and the beads left to air dry for 15 minutes. 17.5µl of Resuspension Buffer was added to each sample, pipetted up and down, incubated for 2 minutes and subsequently incubated for 5 minutes on the magnetic stand at room temperature. 50µl supernatant containing the libraries was transferred to new 0.2ml PCR tubes and the entire cleaning process was repeated one more time. The second ds cDNA clean-up was performed using 50µl of AMPure XP Beads, followed by removal of 95µl of supernatant. After the second wash with 80% (v/v) ethanol and corresponding air-dry, 22.5µl of Resuspension Buffer was added to each library and pipetted up and down until the beads were fully resuspended. After 2 minutes incubation at room temperature, the samples were placed on the magnetic stand and when the liquid was clear 20µl of supernatant containing the cDNA was transferred into new 0.2ml PCR tubes.

#### **2.9.2.6. DNA fragment enrichment**

The purpose of this library amplification step was to (i) amplify first strand cDNA only, (ii) enrich properly ligated DNA fragments (with adapters on both ends), (iii) increase the amount of libraries for NGS and library quantification, and (iv) add a sequence of nucleotides (primers) to the template strands that allows them to hybridize with oligonucleotides attached to the surface of the flow cell.

5µl of PCR Primer Cocktail (PPC) and 25µl of PCR Master Mix (PMM) was added to each sample. Amplification was conducted under the following conditions (Table 2.13). To purify the PCR product, 50µl of AMPure XP Beads was pipetted gently with each PCR amplified library, incubated for 15 minutes at room temperature and separated from the supernatant on the magnetic stand. 95µl of supernatant was removed and the beads were washed twice with 200µl of 80% (v/v) ethanol as previously described (Section 2.9.2.5). Air-dried beads were pipetted with 32.5µl of Resuspension Buffer and incubated for 2 minutes at room temperature. The samples were placed on the magnetic stands and 30µl of supernatant containing amplified libraries was transferred to new PCR tubes.

**Table 2.13.** PCR cycling conditions to amplify the libraries for Next Generation Sequencing.

Cycle Step	Temperature (°C)	Time	Cycles
Initial denaturation	98	30 seconds	1
Denaturation	98	10 seconds	15
Annealing	60	30 seconds	
Extension	72	30 seconds	
Final Extension	72	5 minutes	1
Hold	4	∞	

#### 2.9.2.7. Library validation and normalisation

Accurate quantitation of DNA libraries is a key step in achieving reliable and good quality results from NGS as it informs on (i) ensuring the correct balance between all libraries pooled/loaded on the flow cell sample and (ii) amplifying the correct amount of clusters, as both over-clustering and under-clustering reduces the yield of data (Bronner et al., 2014).

#### 2.9.2.8. Quality control

Library sizes were determined using the 2200 TapeStation (Agilent Technology Wokingham, UK) following the manufacturer's protocol. Firstly, Load D1000ScreenTape and loading tips were placed into the 2200 TapeStation. 3µl of D1000 Sample Buffer was mixed with 1µl of each library and 1µl of D1000 Ladder. Samples were vortexed using an IKA vortex and adaptor at 2000rpm for 1 minute, and samples collected using a short centrifugation step. Samples were loaded into the 2200 TapeStation and read using the Agilent 2200 TapeStation software.

### **2.9.2.9. Quantity control**

Libraries were quantified twice using: (i) a Qubit 3.0 fluorometer and Qubit® dsDNA BR Assay Kit (Invitrogen, Paisley, UK) to assess library concentration, and (ii) qPCR according to the KAPA Library Quantification Kits® platforms (Kapa Biosystems, London, UK) after assessing the quality of prepared libraries to check whether the library dilutions made on the basis of Qubit 3.0 results were comparable.

### **2.9.2.10. Normalisation and pooling of libraries**

Based on the Qubit 3.0 results, all cDNA libraries were diluted in 10 mM Tris-HCl, pH 8.0 (25°C) + 0.05% Tween® 20 to normalise them to a final cDNA concentration of 4nM. To confirm that the performed dilution provided around 4nM DNA in all libraries, absolute qPCR was performed. Reactions were conducted using the same system, software and 96-well plates as described previously (Section 2.5.2), but with KAPA Library Quantification Kits® (2x KAPA SYBR® FAST qPCR Master Mix, 10x Primer Premix, 50x ROX Low). As the library amount must be in the range of the six standard concentrations provided in the kit (20 - 0.0002pM), the 4nM libraries were used to make 1:10,000 dilutions. During the qPCR process, the cDNA was amplified in a 10.2µl reaction containing 6µl 2x KAPA SYBR® FAST qPCR Master Mix with 10x Primer Premix, 0.2µl 50x ROX Low and 4µl of either libraries or standards or water (non-template control - NTCs). The plate was centrifuged for 1 minute to collect the contents and remove air bubbles. Standards, library dilutions and NTCs were assayed in triplicate, and amplification performed under the cycling conditions described (Table 2.14). Upon confirmation of similar library concentrations (~4nM), 5µl of each library (n = 14) was pooled in a new 0.2ml PCR tubes.

**Table 2.14.** Absolute qPCR cycling conditions to normalise the final concentration of prepared libraries.

Cycle step	Temperature (°C)	Time	Cycles
Initial Denaturation	95	5 minutes	1
Denaturation	95	30 seconds	35
Annealing/Extension	60	45 seconds	
Dissociation	95	1 minutes	1
	60	30 seconds	
	95	30 seconds	

#### 2.9.2.11. Denaturation and dilution of libraries

To allow efficient hybridisation of cDNA strands to primers attached to the surface of the flow cell, the pooled libraries were denatured. 5µl 0.2M sodium hydroxide was added to 5µl of 4nM pooled libraries, mixed, centrifuged at 280g for 1 minute and then incubated for 5 minutes at room temperature to denature the libraries into single strands. To entirely neutralise sodium hydroxide after the incubation period, 5µl of 200mM Tris-HCl (pH7) was added to the sample, mixed and centrifuged at 280g for 1 minute. As the recommended loading library concentration is 1.8pM, the denatured libraries were firstly diluted to 20pM by adding 985µl pre-chilled hybridisation buffer (HT1). Next, 1.3ml of a 1.8pM library was prepared by mixing 117µl of a 20pM denatured library solution with 1,183µl pre-chilled HT1.

The low-concentration spike-in (1%) of Illumina PhiX Control was used to provide a sequencing control. 10nM PhiX stock was diluted with 15µl resuspension buffer (RSB) to give the PhiX Control at 4nM. The control was denatured and diluted as described for the libraries. Next, 1.2µl (denatured and diluted) PhiX Control (20pM) was combined

with 1299 $\mu$ l of the (denatured and diluted) libraries (1.8pM) followed by loading onto the NextSeq<sup>®</sup>500/550 High Output Flow Cell Cartridge v2 and sequenced in NextSeq<sup>™</sup>500.

### **2.9.3. Bioinformatic analysis of mRNA Next Generation Sequencing**

The dataset of RNA-Seq was analysed by bioinformatician Dr Daniel Pass (School of Biosciences, Cardiff University, Cardiff, UK). The reads were de-multiplexed and aligned to a reference bovine genome (UMD3.1) using TopHat, a splice junction aware mapper (Kim et al., 2013). HTSeq-count was utilised to quantify mapped reads to gene models (Anders et al., 2014) and EdgeR was used to statistically interrogate the data (Robinson et al., 2010). Identification of possible sample outliers in global gene expression patterns across samples was performed using principal component analysis. Statistical testing for differential expression was performed on count normalised reads using a Fischer's exact test. Benjamini-Hochberg corrected p-values at a threshold of  $p < 0.05$  were used to imply statistical significance (Benjamini and Hochberg, 1995).

## **2.10. RT<sup>2</sup> Profiler PCR array system**

RT<sup>2</sup> Profiler PCR array (Qiagen, West Sussex, UK) is a customised bovine specific PCR array developed by Dr A. Al-Sabah. The 96-well qPCR plate array includes 84 WNT related genes and 12 wells containing a combination of (i) reference genes, (ii) positive controls and (iii) reverse transcription controls. The arrays were utilised to identify direct targets of down-regulated miRs in primary chondrocytes transfected with specific miR inhibitors; cells were transfected with miR-21-5p, miR-221 or miR-222 inhibitors, a non-targeting control or untransfected cells for 48h prior to analysis.

### **2.10.1. cDNA synthesis**

cDNA was synthesised using a RT<sup>2</sup> First Strand Kit (Qiagen, West Sussex, UK) as it contains additional RNA samples that are used as a reverse transcription positive control for the array. Total, non-DNase treated RNA extracted from primary chondrocytes

(Section 2.3.3) was pooled to generate a representative sample for: untreated, transfected with mirVana™ miR Inhibitor Negative Control #1 or transfected with mirVana™ miR-21-5p, miR-221 or miR-222 inhibitors. 200ng of RNA from each sample (n = 3) was taken to create a pooled sample for each condition. The reverse transcription was conducted according to the manufacturer's protocol (Qiagen, West Sussex, UK). First 2µl of genomic DNA elimination buffer (GE buffer) was added to 500ng of pooled RNA and RNase-free water was added to make a 10µl total volume. The reaction was incubated in the Prime Techne Thermocycler for 5 minutes at 42°C followed by 1 minute on ice. The reverse transcription mix containing 4µl of 5× BC3 buffer, 1µl of Control P2 buffer, 2µl RE3 Reverse Transcriptase Mix and 3µl of RNase-free water was added to each sample, pipetted up and down and then incubated at 42°C for 15 minutes. The reaction was terminated by heating the samples at 95°C for 5 minutes followed by addition of 91µl of RNase-free water.

#### **2.10.2. WNT RT<sup>2</sup> Profiler PCR Array**

A bovine-specific WNT RT<sup>2</sup> Profiler PCR Array was used for evaluation of the expression of Wnt related genes (see Appendix 1-3 for gene list). The qPCR mix of 1350µl 2× RT<sup>2</sup> SYBR® Green Mastermix (Qiagen, West Sussex, UK), 102µl of cDNA and 1248µl RNase-free water was prepared and mixed in a loading reservoir. 25µl qPCR mix was transferred into each well of the WNT RT<sup>2</sup> Profiler PCR Array. SYBR® Green qPCR was conducted using a LightCycler® 96 System with LightCycler® 96 SW 1.1 software (Roche, West Sussex, UK). The amplification reaction was performed under the following conditions: 1 cycle of 10 minutes at 95°C , 40 cycles of 15 seconds at 95°C and 1 minute at 60°C.

Analysis of the expression levels of target genes was performed using the RT<sup>2</sup> Profiler PCR Array Data Analysis software (Qiagen, West Sussex, UK) which normalised the Wnt related genes to three automatically chosen reference genes identified by the software.

## **2.11. Statistical analysis**

qPCR data are presented as mean  $\pm$  SD after normalisation to identified reference genes for explants (SDHA and YWHAZ) or for cells (HPRT and YWHAZ) and further normalised to the untreated controls. Data were analysed using the Anderson-Darling test to confirm the normality of the data and differences in variances tested using the Bartlett's test (Minitab 16; <http://onthehub.com/>). Data that was not normal or equal was subject to log or rank transformation (Minitab 16). One or two way analysis of variance (ANOVA) (Minitab 16), as indicated in the text, was performed to determine the significance of mechanical load, manipulation of miR expression levels or mechanical load and time post-load on gene expression, respectively. Results were considered statistically significant at  $p < 0.05$ . Data which was  $\pm$  two standard deviations from the mean were considered outliers and removed from the data set.

# Chapter 3

Characterisation of physiological and non-physiological magnitudes of loading regimes

### 3.1. Background

Normal load, also termed “physiological” promotes a fine balance in the expression of cartilage molecules helping to maintain cartilage function and integrity. When cartilage is subjected to abnormal, also called “non-physiological” or “injurious” load, the stability of the ECM is disrupted and catabolic processes predominate in the tissue which can promote cartilage degeneration (Grodzinsky et al., 2000, Lee et al., 2005a). It has been well-established that biomechanical factors play a crucial role in the healthy development and homeostasis of articular cartilage (Lee et al. 2005). Articular cartilage is subjected to a wide range of mechanical stimuli which depending on the type, magnitude, frequency and duration of the applied load may stimulate a degenerative or biosynthetic response in chondrocytes (Grodzinsky et al., 2000, Hodge et al., 1986). To date, several *in vitro* studies have explored the influence of load on cartilage, but these focused on the effect of long term mechanical load (from hours (h) to days) (Fitzgerald et al., 2008, Kiraly et al., 1998, Kurz et al., 2001, Palmoski and Brandt, 1984). Fitzgerald et al. demonstrated that transcription of ECM proteins such as aggrecan and type II collagen was increased up to 30-100% by long term (24h) dynamic compression (3-5%, 0.1Hz) (Fitzgerald et al., 2008). In contrast, Kurz et al. showed that compressive injurious load (12-23MPa, [~50% compression], 0.1Hz) applied for 12h resulted in significant decreases in total protein synthesis (Kurz et al., 2001).

These and other studies demonstrate the influence of mechanical stimulation on articular cartilage, and show how important it is for maintaining ECM homeostasis. Furthermore, it demonstrates how different factors e.g. amplitude, duration and frequency of applied load influence the tissues’ biological response.

The aim of the work described in this experimental chapter was to identify loading regimes that initiate the early signalling events that induce responses suggesting physiological and non-physiological magnitudes of load. To date, there is no published data investigating short durations of dynamic compressive load on articular cartilage and its influence on early responses in chondrocytes; therefore, it was necessary to optimise short-term loading regimes that induce early transcriptional effects in chondrocytes. For the purpose of optimising the loading regimes, expression of

mechano-responsive genes which are responsible for maintaining ECM homeostasis were studied. The studied genes belong to the following groups: ECM structural molecules (aggrecan, collagen type II), MMPs (MMP-1, -3, -9, -13), ADAMTSs (ADAMTS-4, -5) and TIMPs (TIMP-1, -2, -3).

Quantitative PCR (qPCR) is a sensitive method to assess transcriptional changes in experimental samples, therefore the selection of stable internal reference genes used for normalisation is crucial. Unfortunately, it is a common issue that reference genes, also referred to as housekeeping genes (HKGs), are chosen mainly on the basis of data from earlier publications. However, it must be taken into consideration that the stability of the HKGs expression obtained and presented in previous studies which were performed under certain experimental parameters is relevant only to that study (Kozera and Rapacz, 2013).

Most published studies analysing mechano-responsive genes in chondrocytes have used 18S ribosomal RNA, ACTB ( $\beta$ -actin) or glyceraldehyde-3-phosphate dehydrogenase (GAPDH) as reference genes without consideration of their sensitivity to mechanical stress. Surprisingly, a study conducted by Lee et al. analysing the stability of 18S rRNA,  $\beta$ -actin,  $\beta$ -glucuronidase,  $\beta$ -2 microglobulin and GAPDH in articular chondrocytes subjected to mechano-stimulation clearly showed that these genes (excluding 18S) are mechano-sensitive (Lee et al., 2005b), therefore should not be utilised as reference genes in qPCR in mechanobiology experiments.

Knowledge and methodologies have developed hugely over the years giving us for example softwares such as BestKeeper (Pfaffl et al., 2004), geNorm (Vandesompele et al., 2002) and NormFinder (Andersen et al., 2004) that determine the most stable gene(s) relative to experimental conditions. To use suitable reference genes in this study, it was necessary to identify genes in which the mRNA level remained unaffected by mechanical load.

**Summary of the aims of this experimental chapter:**

- **To identify reference genes with the most stable expression in both loaded and unloaded cartilage explants**
- **To identify physiological and non-physiological loading regimes that induce early transcriptional events in chondrocytes**
- **To identify more globally genes that are sensitive to load**

## **3.2. Results**

### **3.2.1. Analysis of RNA quality**

Confirmation that total RNA extracted from the experimental samples (loaded and unloaded) was of good quality and sufficient yield for downstream analysis was performed using the Agilent 2100 bioanalyzer. A Ribosomal Integrity Number (RIN) is obtained for each sample (0 degraded – 10 excellent) and as can be observed, all samples had RIN scores of >8 (Figure 3.1A). Ribosomal peak plots and gel electrophoresis of the RNA samples also indicated the presence of 18S and 28S rRNA with no sign of degradation (Figure 3.1B,C).

Total RNA from these loaded and unloaded explants was used to investigate the most appropriate reference genes for mRNA analysis to characterise the loading regimes; unloaded explants were used as a control.

### **3.2.2. Investigation of appropriate reference genes for assessing cartilage chondrocyte mechano-responsiveness**

One of the criteria of the MIQE guidelines (Minimum Information for Publication of Quantitative Real-Time PCR Experiments) that eliminates the usage of unstable reference genes for mRNA normalisation affecting the fold change of target genes giving false results is to use not less than three experimentally validated reference genes for each tissue/cell type or experimental condition, unless there are special circumstances (Bustin et al., 2009, Bustin et al., 2010). To identify the most stable reference genes expressed in articular cartilage subjected to different compressive loading regimes (2.5MPa, 5MPa and 7MPa, 1Hz, 15 minutes), eight bovine reference genes from previous study were selected for validation (Anstaett et al., 2010). Stability of reference genes was assessed using commonly used computational programmes: Bestkeeper (Pfaffl et al., 2004), geNorm (Vandesompele et al., 2002), NormFinder (Andersen et al., 2004) and the comparative  $\Delta C_t$  method (Silver et al., 2006), and the data integrated using RefFinder software (<http://www.leonxie.com/referencegene.php>). Each individual programme uses its own algorithm to compare and rank reference genes in terms of their stability.

The comparative  $\Delta C_t$  method compares  $C_t$  values of a single putative reference gene across experimental samples and determines the standard deviation of all samples and then compares this value with other potential reference genes. The lower the standard deviation the more stable the gene expression is across the experimental parameters e.g. compressive load. Large variation was presented by GAPDH and HPRT questioning the suitability of these as reference genes, whereas SDHA, PPIA, RPL4,  $\beta$ -actin, 18S and YWHAZ were consistent in unloaded tissue and those subjected to load (Figure 3.2A).

BestKeeper assesses the stability of putative reference genes in two ways. Firstly, the standard deviation of the geometric mean of the  $C_t$  values for an individual gene is calculated to exclude unstable genes from the panel of potential internal controls ( $SD > 1.5$ ). Secondly, a pairwise comparison of individual genes is performed to the BestKeeper index, which is a geometric mean of all putative reference genes to assess whether there is a correlation (Pearson correlation) of a single gene to the index. The stronger the correlation between the pair of genes the more likely it is that they are not responsive to the studied experimental conditions (Pfaffl et al., 2004). BestKeeper, similar to the comparative  $\Delta C_t$  method indicated HPRT and GAPDH as the least stable putative internal controls. The remainder of the tested genes were similarly stable, however the best stability was presented by SDHA and 18S (Figure 3.2B).

geNorm determines reference gene stability (M) which is an average pairwise variation between a single putative reference gene and the other remaining group of reference genes included in the same study. The geNorm cut off value is  $M = 1.5$  suggesting that genes with  $M > 1.5$  should not be used as internal control genes (Vandesompele et al., 2002). SDHA and YWHAZ were considered as the most stable genes from the panel of tested genes while GAPDH and HPRT were selected as the worst option for normalisation of gene expression to these reference genes (Figure 3.2C).

NormFinder software is unique as it takes into consideration experimental parameters. It determines stability of control genes based on the variation in their expression within one specific group of samples and across differently stressed experimental groups (Andersen et al., 2004). GAPDH and HPRT presented the lowest stability, whereas RPL4, SDHA and PPIA were noticeably the most stable (Figure 3.2D).

Based on the rankings obtained from each of the aforementioned softwares, RefFinder assigns an appropriate value to each gene and calculates their geometric mean to provide the final ranking of putative internal reference genes (from most to least stable) (Liang et al., 2014). RefFinder analysis showed SDHA as the most stable whereas RPL4 and YWHAZ were equally next in line of stable gene expression. In comparison, GAPDH and HPRT turned out to be the least stable reference genes amongst the eight tested (Figure 3.3).

The MIQE guidelines allows the use of less than three reference genes if there is a reasonable explanation, therefore SDHA and YWHAZ have been selected as appropriate internal controls excluding RPL4 as it showed the same stability as YWHAZ. After selecting the best combination of internal reference genes, standard curves for these genes were generated using 10-fold dilutions of pooled cDNA from loaded and unloaded samples to determine PCR efficiency. Representative standard curves of SDHA and YWHAZ indicated efficiencies of 104% and 101.3% respectively which are within the acceptable range of 95-115% (Figure 3.4). On the basis of these results, SDHA and YWHAZ were used as reference genes for the study due to their suitability for normalisation of gene expression in both loaded and unloaded articular cartilage using the parameters tested.

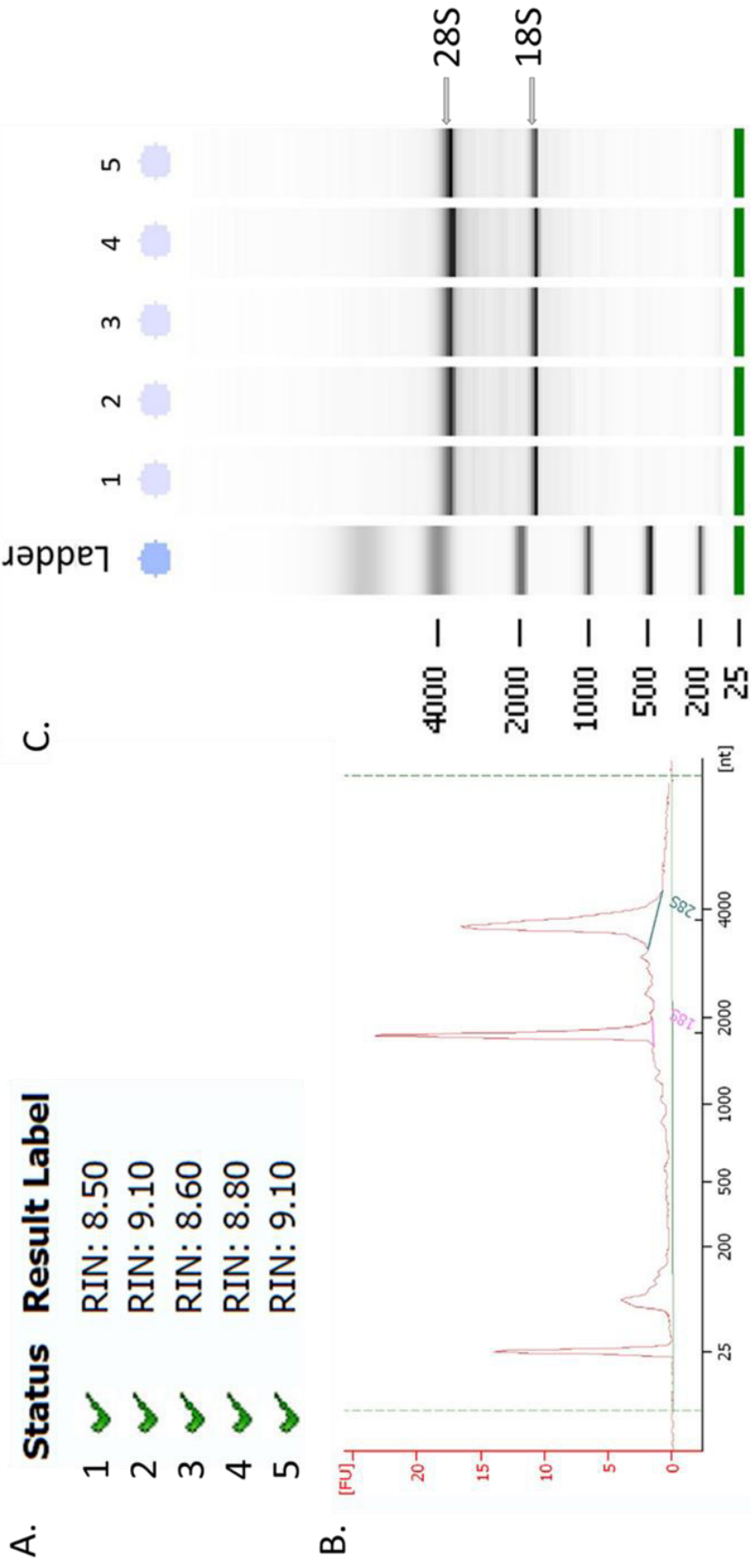


**Figure 3.1.** RIN table (A), representative ribosomal peak plot (B) and electrophoresis gel (C) shows good quality RNA used in the conducted experiments.

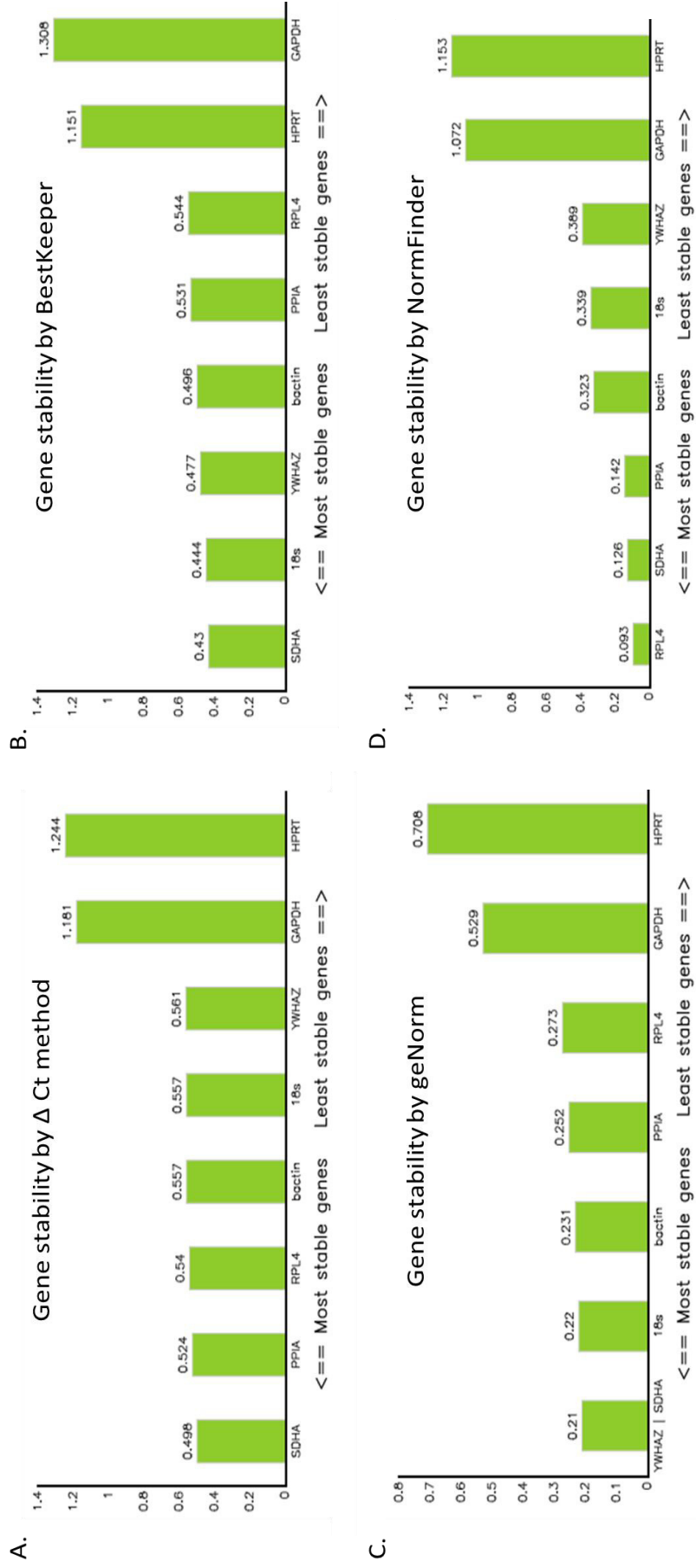


**Figure 3.2.** Analysis of reference gene stability by the comparative  $\Delta C_t$  method, BestKeeper, geNorm and NormFinder. The comparative  $\Delta C_t$  method (**A**), BestKeeper (**B**), geNorm (**C**) and NormFinder (**D**) assessed the stability of commonly used reference genes (18S,  $\beta$ actin, GAPDH, HPRT, PPIA, RPL4, SDHA, YWHAZ) in articular cartilage subjected to the following loading regimes: 2.5MPa (1Hz, 15 minutes, n = 6) and 7MPa (1Hz, 15 minutes, n = 6) or remained unloaded (n = 6).

Method	Ranking Order (Better--Good--Average)							
	1	2	3	4	5	6	7	8
Delta CT	SDHA	PPIA	RPL4	bactin	18s	YWHAZ	GAPDH	HPRT
BestKeeper	SDHA	18s	YWHAZ	bactin	PPIA	RPL4	HPRT	GAPDH
Normfinder	RPL4	SDHA	PPIA	bactin	18s	YWHAZ	GAPDH	HPRT
Genorm	YWHAZ   SDHA		18s	bactin	PPIA	RPL4	GAPDH	HPRT
<b>Recommended comprehensive ranking</b>	<b>SDHA</b>	<b>YWHAZ</b>	<b>RPL4</b>	<b>18s</b>	<b>PPIA</b>	<b>bactin</b>	<b>GAPDH</b>	<b>HPRT</b>

Genes Geomean of ranking values

SDHA 1.19  
 YWHAZ 3.22  
 RPL4 3.22  
 18s 3.50  
 PPIA 3.50  
 bactin 4.00  
 GAPDH 7.24  
 HPRT 7.74

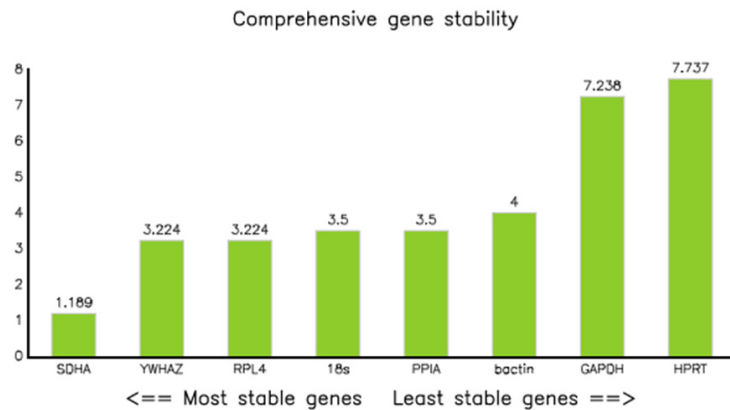
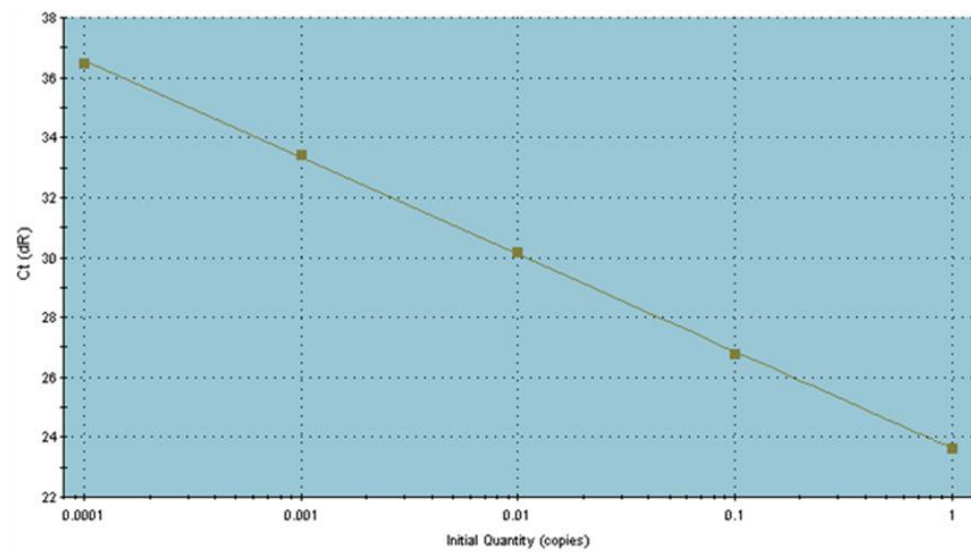


**Figure 3.3.** Reference gene stability output using RefFinder software. RefFinder software using data output from the comparative  $\Delta C_t$  method, BestKeeper, NormFinder and geNorm ranked the commonly used reference genes (18S,  $\beta$ actin, GAPDH, HPRT, PPIA, RPL4, SDHA, YWHAZ) from most to least stable. RefFinder software analysis indicated that SDHA is the most stable housekeeping gene in experimental cartilage explants (unloaded, 2.5MPa and 7MPa).

**A. SDHA – efficiency 104 %**



**B. YWHAZ – efficiency 101.3 %**

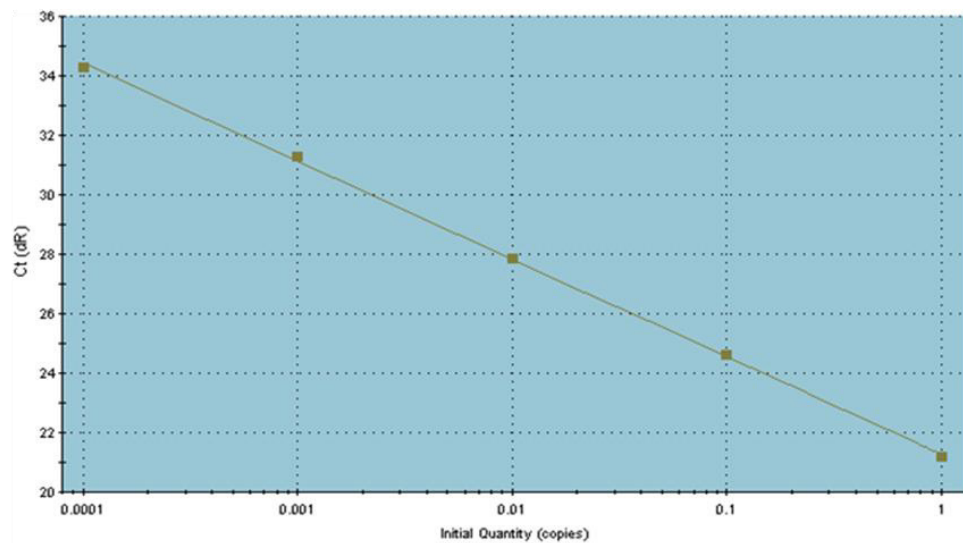


**Figure 3.4.** qPCR standard curves of SDHA **(A)** and YWHAZ **(B)** conducted on pooled cDNAs from samples subjected to 2.5MPa and 7MPa loading regimes (1Hz, 15 minutes) and unloaded explants. Data represents 3 independent experiments (n = 18 explants/experiment). qPCR efficiencies of the selected reference genes were verified to be within the acceptable range of 95-115%.

### 3.2.3. Optimisation of loading regimes

To establish loading magnitudes which either activated mainly an anabolic/turnover response or induced mainly expression of catabolic molecules, a preliminary study was conducted using three different loading regimes: 2.5MPa, 5MPa and 7MPa each at 1Hz for 15 minutes and mRNA levels assessed 24h post-load. These loads and frequency parameters were chosen on the basis of publications in which loading magnitudes between 0.1 - 5MPa were considered as normal and above 5MPa as abnormal (Arokoski et al., 2000, Hodge et al., 1986), and the frequency 1Hz which is considered as the frequency of fast walking (Bader et al., 2011).

### 3.2.4. Characterisation of physiological and non-physiological loading regimes on the basis of ECM mRNA expression levels.

Explants subjected to the various loading regimes of 2.5MPa, 5MPa or 7MPa demonstrated differing transcriptional profiles representing catabolic and anabolic molecule responses. Expression of genes in explants subjected to a 7MPa load could not be compared directly to the transcriptional level of these genes in samples treated with lower loading regimes, as the loading was performed on different days which relied on the use of different unloaded controls.

- **ECM genes:** Neither aggrecan nor collagen type II mRNA levels were significantly altered by any of the loading regimes tested (Figure 3.5A-D).
- **MMP genes:** Neither 2.5MPa nor 7MPa loading regimes changed the expression of MMP1 (Figure 3.6A,C), but surprisingly a 5MPa load induced a significant increase in MMP1 mRNA levels (6.4-fold:  $p=0.001$ ; Figure 3.6A). MMP-3 was significantly up-regulated in explants subjected to 5MPa (2.5-fold:  $p=0.01$ ; Figure 3.6C) and 7MPa (6.8-fold:  $p<0.001$ ; Figure 3.6D) load, whereas no statistically significant response was observed in explants subjected to a 2.5MPa load (Figure 3.6C). Significant up-regulation of MMP-3 transcripts was also observed between the 2.5MPa and 5MPa loaded explants (4.4-fold:  $p<0.001$ ; Figure 3.6C) with a noticeable trend of increasing expression with increasing load

(Figure 3.6C,D). In contrast, MMP-9 and MMP-13 mRNA levels were significantly down-regulated at 2.5MPa (6.25-fold:  $p=0.001$ ; Figure 3.6E and 5.5-fold:  $p<0.001$ ; Figure 3.6G, respectively) and 5MPa (6.9-fold:  $p<0.001$ ; Figure 3.6E and 5.5-fold:  $p<0.001$ ; Figure 3.6G, respectively). However, decreases observed at 7MPa were not statistically significant (Figure 3.6F,H).

- **ADAMTS genes:** Mechano-regulation of ADAMTS-4 mRNA levels was observed with significant increases in all explants correlating with increasing application of load i.e. 2.5MPa (2.2-fold:  $p=0.002$ ; Figure 3.7A), 5MPa (5.1-fold:  $p<0.001$ ; Figure 3.7A) and 7MPa (6-fold:  $p<0.001$ ; Figure 3.7B). A load-dependent increase in ADAMTS-4 levels between 2.5MPa and 5MPa (2.4-fold:  $p=0.002$ ; Figure 3.7A) was also observed. Interestingly, ADAMTS-5 transcription was significantly increased only by the 7MPa load (5.5-fold:  $p<0.001$ ; Figure 3.7D).
- **TIMP genes:** Both TIMP-1 and TIMP-3 transcription were significantly elevated in all explants subjected to 2.5MPa, 5MPa and 7MPa (Figure 3.8A,B,E,F). TIMP-1 mRNA was up-regulated in explants subjected to 2.5MPa (1.6-fold:  $p=0.008$ ; Figure 3.8A), 5MPa (2.6-fold:  $p<0.001$ ; Figure 3.8A) and 7MPa (3.6-fold:  $p<0.001$ ; Figure 3.8B). A significant increase was also observed between the 2.5MPa and 5MPa (1.6-fold,  $p=0.006$ ; Figure 3.8A). In terms of TIMP-3, each loading regime activated TIMP-3 transcription in a magnitude-dependent manner: 2.5MPa (1.8-fold:  $p=0.016$ ; Figure 3.8E), 5MPa (6-fold:  $p<0.001$ ; Figure 3.8E) and 7MPa (10.2-fold:  $p<0.001$ ; Figure 3.8F) load. In contrast to TIMP-1 and -3, transcript levels of TIMP-2 were significantly decreased in response to all applied loading regimes. The level of TIMP-2 reduction was similar in all loaded explants: 2.5MPa (2.04-fold:  $p<0.001$ ; Figure 3.8C), 5MPa (2.36-fold:  $p<0.001$ ; Figure 3.8C) and 7MPa (2.27-fold:  $p<0.001$ ; Figure 3.8D).

Based on these preliminary findings, a load of 2.5MPa (1Hz, 15 minutes) to represent a physiological magnitude and 7MPa (1Hz, 15 minutes) to represent a non-physiological magnitude were selected.

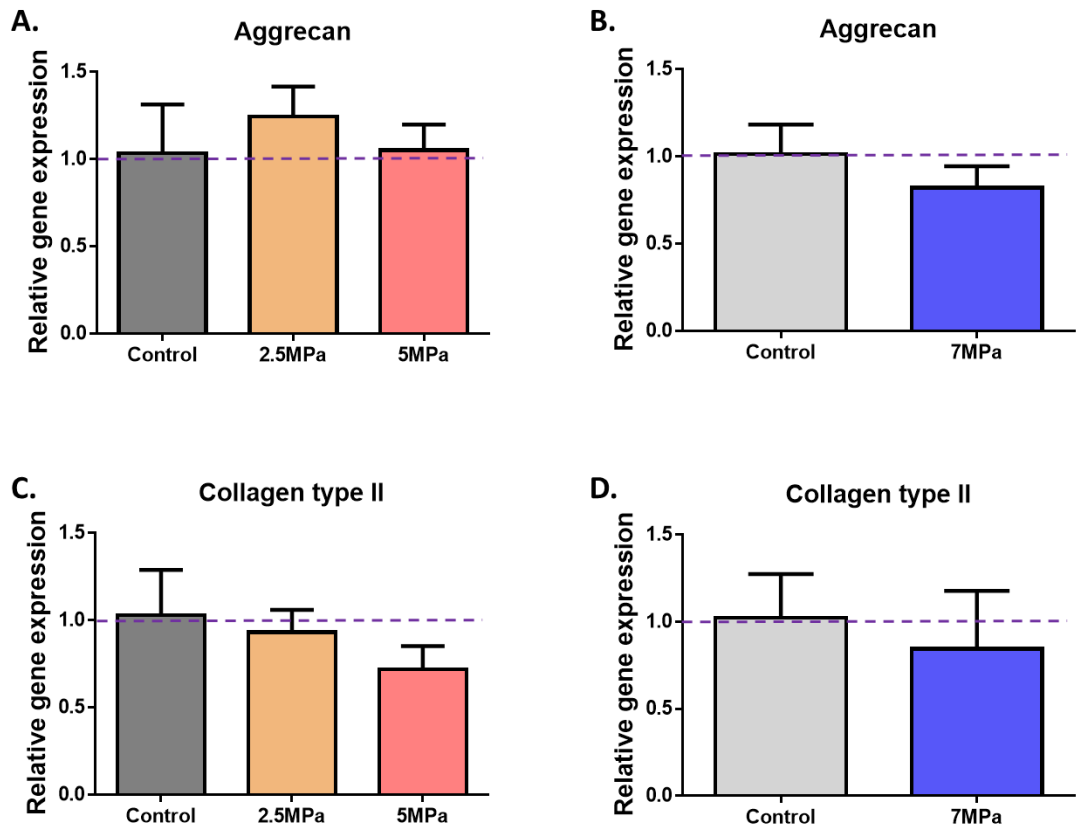


**Figure 3.5.** mRNA quantification of Aggrecan (**A,B**) and Collagen type II (**C,D**) in cartilage explants subjected to varying loading regimes (1Hz, 15 minutes); unloaded explants served as controls. Gene expression was analysed in the cartilage explants 24h post-load using qPCR with Sybr™ green technology and mRNA levels normalised to the geometric mean of reference genes (SDHA, YWHAZ) and relative to the unloaded control. Data are presented as mean  $\pm$  SD ( $n = 6$ ) and is representative of three independent experiments. Two graphs of the same gene e.g. A and B show data of independently performed loading experiments for 2.5MPa, 5MPa and for 7MPa; the presence of statistically significant differences between the controls for 2.5MPa, 5MPa and controls for 7MPa does not allow cross-comparison of data from all loading regimes. Statistical analysis was performed using a 1-way ANOVA with Tukey's post-hoc test. Key: control - unloaded, 2.5MPa, 5MPa, 7MPa (loaded).

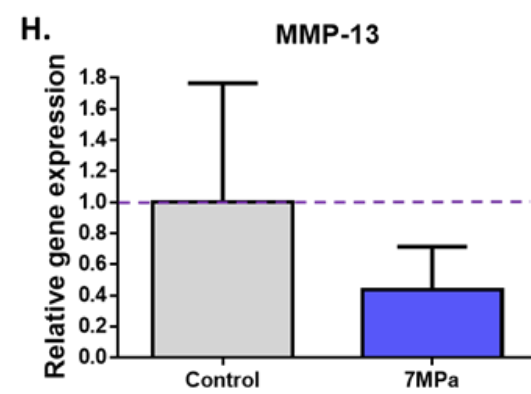
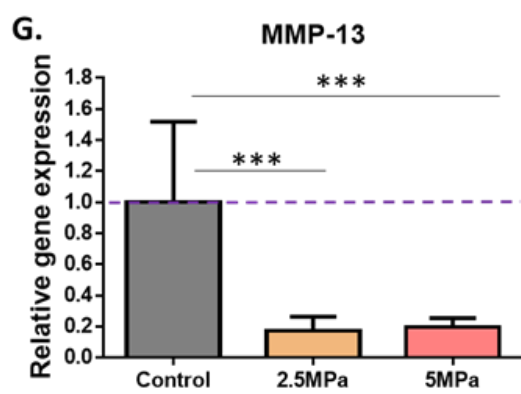
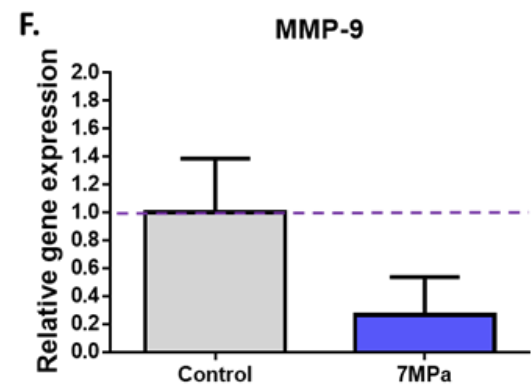
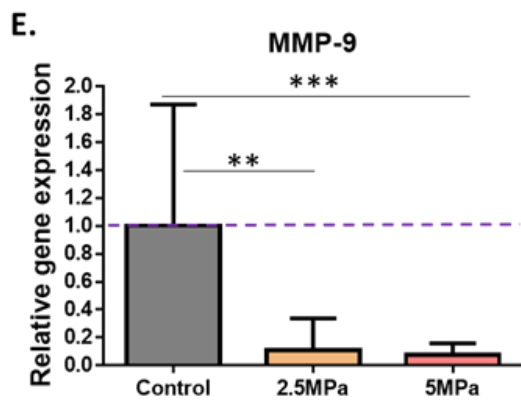
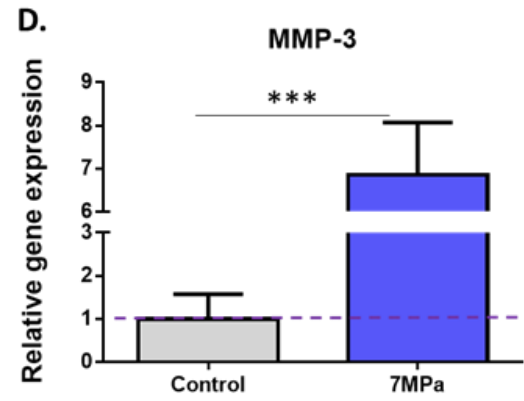
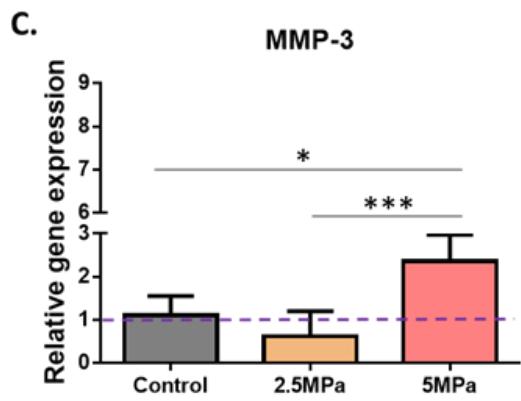
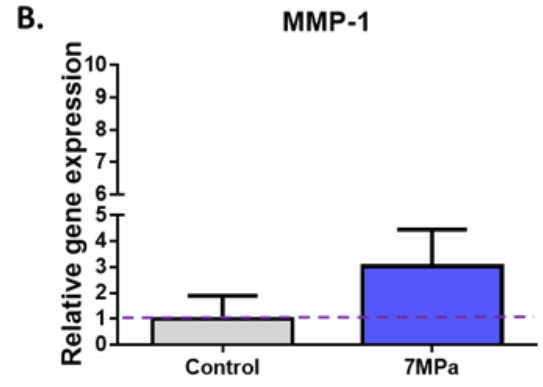
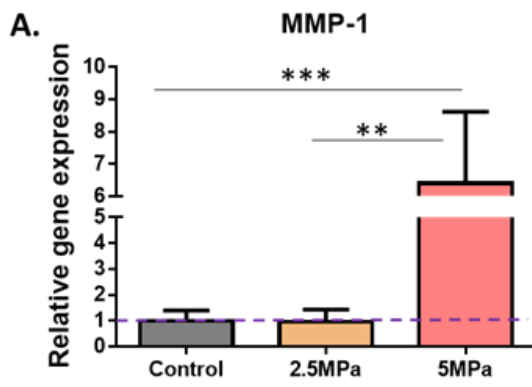


**Figure 3.6.** mRNA quantification of MMP-1 (A,B), MMP-3 (C,D), MMP-9 (E,F) and MMP-13 (G,H) in cartilage explants subjected to varying loading regimes (1Hz, 15 minutes); unloaded explants served as controls. Gene expression was analysed in the cartilage explants 24h post-load using qPCR with Sybr™ green technology and mRNA levels normalised to the geometric mean of reference genes (SDHA, YWHAZ) and relative to the unloaded control. Data are presented as mean ± SD (n = 6) and is representative of three independent experiments. Two graphs of the same gene e.g. A and B show data of independently performed loading experiments for 2.5MPa, 5MPa and for 7MPa; presence of significant differences between the controls for 2.5MPa, 5MPa and controls for 7MPa does not allow cross-comparison of data from all loading regimes. Statistical analysis was performed using a 1-way ANOVA with Tukey's post-hoc test. Key: control-unloaded, 2.5MPa, 5MPa, 7MPa (loaded) [\* p<0.05, \*\* p<0.01, \*\*\* p<0.001].

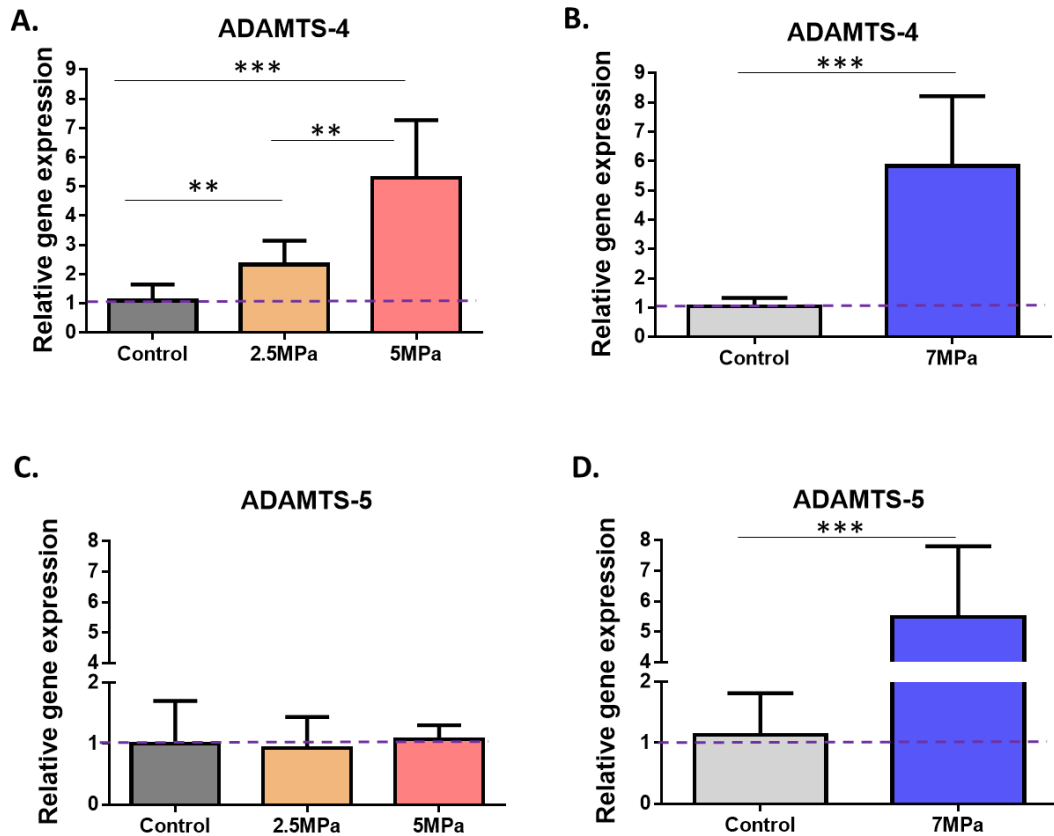


**Figure 3.7.** mRNA quantification of ADAMTS-4 (A,B) and ADAMTS-5 (C,D) in cartilage explants subjected to varying loading regimes (1Hz, 15 minutes); unloaded explants served as controls. Gene expression was analysed in the cartilage explants 24h post-load using qPCR with Sybr™ green technology and mRNA levels normalised to the geometric mean of reference genes (SDHA, YWHAZ) and relative to the unloaded control. Data are presented as mean  $\pm$  SD (n = 6) and is representative of three independent experiments. Two graphs of the same gene e.g. A and B show data of independently performed loading experiments for 2.5MPa, 5MPa and for 7MPa; presence of significant differences between the controls for 2.5MPa, 5MPa and controls for 7MPa does not allow cross-comparison of data from all loading regimes. Statistical analysis was performed using a 1-way ANOVA with Tukey's post-hoc test. Key: control - unloaded, 2.5MPa, 5MPa, 7MPa (loaded) [**\*\*** p<0.01, **\*\*\*** p<0.001].

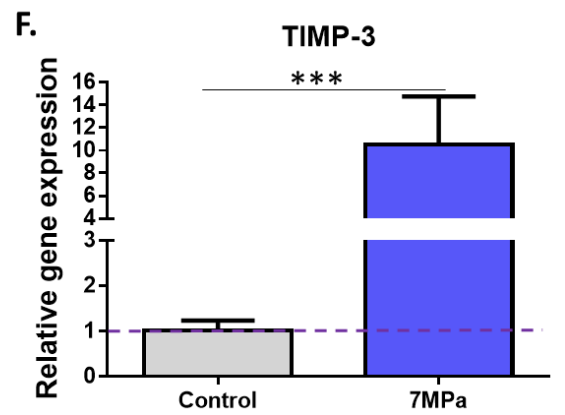
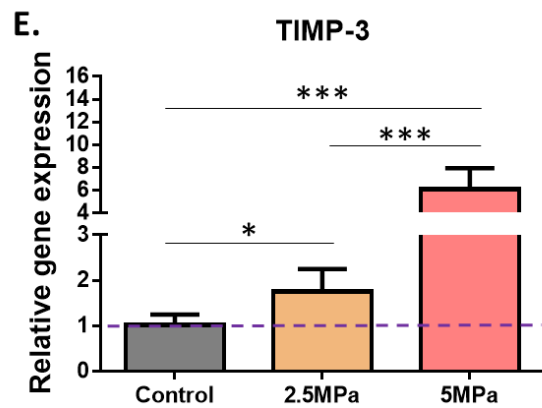
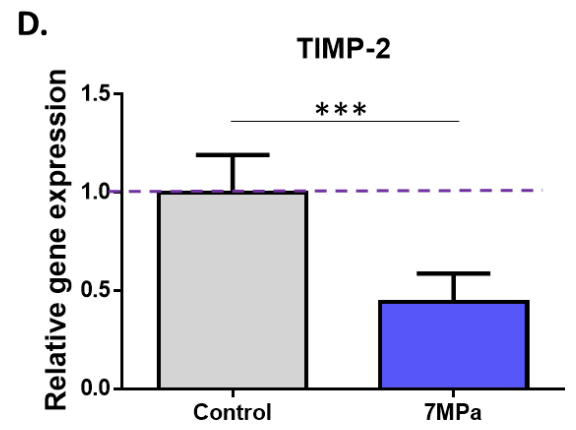
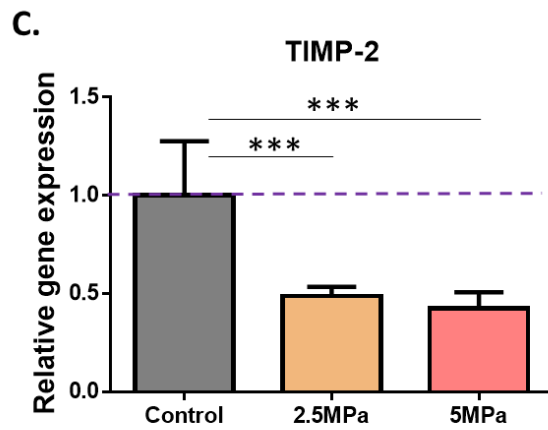
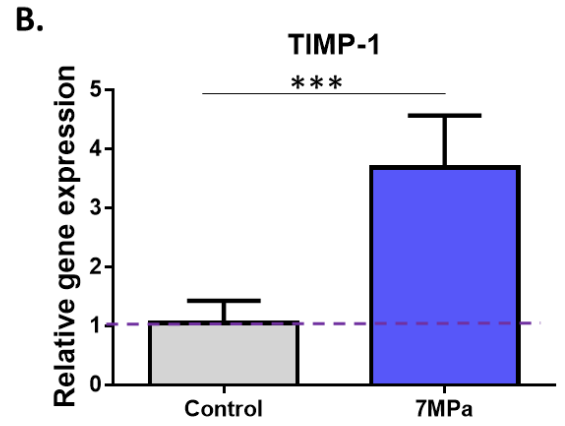
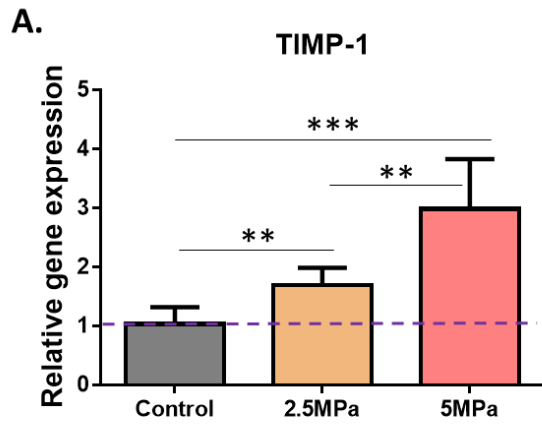


**Figure 3.8.** mRNA quantification of TIMP-1 (A,B), TIMP-2 (C,D) and TIMP-3 (E,F) in cartilage explants subjected to varying loading regimes (1Hz, 15 minutes); unloaded explants served as controls. Gene expression was analysed in the cartilage explants 24h post-load using qPCR with Sybr™ green technology and mRNA levels normalised to the geometric mean of reference genes (SDHA, YWHAZ) and relative to the unloaded control. Data are presented as mean  $\pm$  SD (n = 6) and is representative of three independent experiments. Two graphs of the same gene e.g. A and B show data of independently performed loading experiments for 2.5MPa, 5MPa and for 7MPa; presence of significant differences between the controls for 2.5MPa, 5MPa and controls for 7MPa does not allow cross-comparison of data from all loading regimes. Statistical analysis was performed using a 1-way ANOVA with Tukey's post hoc test. Key: control - unloaded, 2.5MPa, 5MPa, 7MPa (loaded) [\* p<0.05, \*\* p<0.01, \*\*\* p<0.001].

### **3.2.5. Global overview of differentially expressed genes in explants subjected to loads of 2.5MPa and 7MPa and analysed 4h and 24h post-load**

Physiological (2.5MPa) and non-physiological (7MPa) loading magnitudes, based on the differential expression of selected anabolic and catabolic molecules in explants subjected to mechanical load (section 3.2.4) were established on explants processed at 24h post-load cessation. Having established these two specific loading regimes, the next step was to analyse global changes in gene expression in unloaded tissue versus cartilage subjected to loads of 2.5MPa or 7MPa (1Hz, 15 minute); explants were then either processed at 4h (material generated by Dr A. Al-Sabah) or 24h post-cessation of load using GeneChip® Bovine 1.0 ST arrays.

The 4h post-load presented 778 differentially expressed genes in explants loaded with 2.5MPa in which 47.18% were down-regulated and 52.83% were up-regulated, whereas a 7MPa load induced the down-regulation of 57.74% and elevated 45.26% out of 2,848 significantly altered genes (Table 3.1A,B). The comparison between loads showed 76 differentially altered molecules (2.63% down-regulated and 97.37% up-regulated) (Table 3.1C). A 24h post-cessation analysis of relative gene expression in explants subjected to 2.5MPa and 7MPa loading regimes compared to unloaded tissue presented respectively 91 (39.36% decreased and 60.64% elevated) and 1,995 (40.09% reduced and 53.91% elevated) mechanically-regulated molecules (Table 3.2A,B). In turn, only 8 genes were differentially expressed when comparing the 7MPa and 2.5MPa loads showing evenly 50% of down- and up-regulated genes (Table 3.2C).

Among the mechano-sensitive genes expressed after 4h in explants subjected to 2.5MPa and 7MPa loads, there were some genes that showed differential transcription also at 24h post-load in tissue subjected to the same loading regimes. To these genes belong for example up-regulated components of the transcription factor AP-1, such as: FOS Like Antigen 1(FOSL-1) (4h: 2.5MPa (6.94-fold: FDR=0.001), 7MPa (16.50-fold: FDR>0.001), 24h: 2.5MPa (3.13-fold: FDR=0.045), 7MPa 8.92-fold: FDR>0.001) and JunB Proto-Oncogene (JUNB) (4h: 2.5MPa (4.11-fold: FDR>0.001), 7MPa (5.81-fold: FDR>0.001), 24h: 2.5MPa (2.15-fold: FDR=0.012), 7MPa (2.61-fold: FDR>0.001)). FBJ Murine Osteosarcoma Viral Oncogene Homolog (FOS) also presented elevated

expression in both time points (4h: 2.5MPa (4.03-fold: FDR>0.001), 7MPa (8.25-fold: FDR>0.001), 24h: 7MPa (1.96-fold: FDR=0.005)), however 2.5MPa at 24h post-load did not show an alteration in FOS transcription. Similar to FOS, transcription of the cartilage catabolic molecule ADAMTS-1, which degrades cartilage proteoglycans (Kuno et al., 2000), was also up-regulated at both time points (4h: 2.5MPa (7.72-fold: FDR>0.001), 7MPa (22.13-fold: FDR>0.001), 24h: 7MPa (2.81-fold: FDR=0.011)); however, 2.5MPa at 24h did not indicate transcriptional changes.

There were also a number of genes that demonstrated altered mRNA level at 4h post-load but did not show statistically significant changes by 24h. To these genes belong for example another elevated AP-1 component, such as: BJ Murine Osteosarcoma Viral Oncogene Homolog B (FOSB) (2.5MPa (8.88-fold: FDR>0.001), 7MPa (40.31-fold: FDR>0.001)) (Table 3.1A,B).

A number of genes showed altered expression at 24h only and additionally some of them represented a load-dependent nature, as they were altered at the high load (7MPa) only. To these genes belong for example decreased pro-collagenase, such as ADAM Metallopeptidase With Thrombospondin Type 1 Motif 2 (ADAMTS-2) (7MPa: 1.75-fold: FDR=0.047) involved in cartilage remodelling by biosynthetic processing of fibrillar procollagens (Alper et al., 2015).

A 2.5MPa (1Hz, 15 minutes) loading regime analysed 4h post-load demonstrated that the most elevated gene was Inhibin Beta A (INHBA) (13.97-fold: FDR>0.001) which is known to be up-regulated in OA cartilage (Bateman et al., 2013, Snelling et al., 2014). The most reduced transcription under this condition was Enoyl-CoA, hydratase/3-hydroxyacyl CoA dehydrogenase (EHHADH) (3.8-fold: FDR>0.001) which is part of the classical peroxisomal fatty acid  $\beta$ -oxidation pathway and was also observed to be down-regulated in skeletal muscle in response to mechanical overload (Chaillou et al., 2013) (Table 3.1A).

In explants subjected to a 7MPa (1Hz, 15 minutes) load and processed at 4h post-load, the 50 most differentially expressed genes showed only increased levels of mRNA (Table 3.1B). The strongest response (40.31-fold: FDR>0.001) was observed for the mechano-sensitive transcription factor FBJ osteosarcoma oncogene B (FosB).

Comparison of expression of mechano-regulated genes between low (2.5MPa) and high (7MPa) loading regimes demonstrated a dose dependency of load on the tissue's transcriptional response. The most induced transcription was in the expression of FosB (4.54-fold: FDR=0.002) in cartilage stimulated with a 7MPa load compared to 2.5MPa load. The most decreased gene in 7MPa loaded explants compared to 2.5MPa load was miR-2366 (2.42-fold: FDR=0.046) whose biological role is still unknown (Table 3.1C).

The top 50 significant mechanically-regulated molecules at 24h post-cessation of each load are listed (Table 3.2). Laminin subunit gamma-2 (LAMC2) reported to be mechano-sensitive (Wehland et al., 2015) showed the highest elevation in a load-dependent manner: 2.5MPa (7.07-fold: FDR=0.032) and 7MPa (19.27-fold: FDR=0.001). Although, very little is known about microseminoprotein (MSMP/PSMP) which is the most reduced (4.17-fold: FDR=0.033) in response to a physiological (2.5MPa) loading magnitude, it is believed to be involved in Akt phosphorylation and caspase activation in PC3 cells (prostate cancer cell line) (Pidgeon et al., 2002). Chordin-like BMP inhibitor (CHRD/L2/CHL2), which is mainly expressed in chondrocytes of developing cartilage (Nakayama et al., 2004) was significantly reduced (11.49-fold: FDR>0.001) in explants subjected to non-physiological (7MPa) magnitude.

Interestingly, the most differentially regulated genes in the 7MPa loaded explants when compared to 2.5MPa load did not overlap with these identified from comparing the respective loaded explants to unloaded tissue. So far, nothing has been published in terms of the role of G-Protein Coupled Receptor, Family C, Group 5, Member A (GPC5A) in cartilage, which was the most increased gene in explants subjected to 7MPa load in comparison 2.5MPa load (3.40-fold: FDR=0.039). The gene with the most decreased expression (2.51-fold: FDR=0.039) in explants subjected to non-physiological compared to physiological magnitude of load was ras-like and estrogen-regulated growth inhibitor (RERG) involved in inhibition of breast cancer cell proliferation (Finlin et al., 2001).

**Table 3.1.** Top 50 genes from microarray analysis with highest relative expression in response to physiological (2.5MPa) and non-physiological (7MPa) magnitudes of load at 4h post-load. Relative gene expression in explants subjected to 2.5MPa (A) or 7MPa (B) when unloaded explants were used as a control, and 7MPa compared with 2.5MPa load (C).

A. 2.5MPa vs unloaded		B. 7MPa vs unloaded		C. 7MPa vs 2.5MPa	
Gene	Fold change	Gene	Fold Change	Gene	Fold change
INHBA	13.97	FOSB	40.31	FOSB	4.54
PTGS2	10.29	ADAMTS1	22.13	MIR20A	3.93
FOSB	8.88	PTGS2	21.58	MAP3K8	3.31
CDA	8.04	INHBA	20.24	TAGLN	3.06
ADAMTS1	7.72	GPRC5A	18.18	GPRC5A	2.92
NFATC2	7.61	SERPINB2	18.11	LOC100337074	2.89
SERPINB2	7.48	ARAP2	17.43	ARC	2.83
ARAP2	7.22	FOSL1	16.50	LOC100140997	2.79
CLDN4	7.16	CDA	15.70	TRIB1	2.78
FOSL1	6.94	CLDN4	15.21	DUSP5	2.75
GPRC5A	6.22	TRIB1	15.18	MIR19A	2.74
SNCAIP	6.11	MIR2471	11.70	SERPINB1	2.70
RGS16	5.66	RGS16	11.35	EPHA2	2.68
TNFRSF11B	5.62	TNFRSF11B	10.84	MIR2460	2.66
TRIB1	5.46	SNCAIP	10.30	MIR544A	2.65
LAMC2	4.83	NFATC2	10.17	MIR125B-1	2.61
PHLDA1	4.73	RASSF8	9.99	MIR380	2.53
KRT14	4.60	LAMC2	9.80	MIR329A	2.52
RASSF8	4.51	DUSP5	9.75	LRR8B	2.44
CCK	4.47	MMP3	8.94	DUSP10	2.44
MIR2471	4.23	PHLDA1	8.92	MIR377	2.43
JUNB	4.11	MIR222	8.28	MIR2366	2.42
FOS	4.03	FOS	8.25	SERPINB2	2.42
MIR222	3.92	SGK1	8.21	NRAP	2.41
SERPINE1	3.81	MIR221	7.39	ITGA2	2.31
ULBP11	3.80	NABP1	7.25	DUSP1	2.30
EHHADH	-3.80	MIR125B-1	7.12	EID3	2.30
SOCS3	3.79	MIR20A	7.10	PXDC1	2.28
KLF4	3.78	SERPINE1	7.07	SPRY2	2.27
SGK1	3.74	MIR21	6.95	MIR21	2.23
ARF4	3.66	LOC100296849	6.81	LOC100300553	2.23
FGF2	3.59	CCK	6.80	NABP1	2.22
MIR221	3.58	SERPINA14	6.61	PLK3	2.22
DUSP5	3.55	FAM102B	6.40	SGK1	2.20
FAM102B	3.49	PRSS54	6.38	MAFF	2.16
PLAUR	3.48	LOC100140997	6.36	IPMK	2.16
PRSS54	3.47	KLF4	6.25	LOC100296849	2.13
RBM7	3.33	MIR19A	6.22	MYC	2.12
IHH	3.29	NRAP	6.17	MIR19B	2.10
TNFRSF12A	3.27	BMP2	6.06	FOS	2.05
NABP1	3.26	PLK2	6.03	RIPK4	2.05
MIR224	-3.21	FGF2	5.84	FGF1	2.03
LOC100296849	3.20	JUNB	5.81	GOS2	2.03
MMP3	3.18	MIRLET7A-2	5.65	MIR92A	2.02
PLK2	3.17	SOCS3	5.42	EGR1	1.96
LMO3	3.17	MIR17	5.39	TNFRSF21	1.94
BMP2	3.14	MAP3K8	5.37	EGR2	1.94
MIR21	3.12	ULBP11	5.35	DYRK3	1.92
LOC510442	3.11	ITGA5	5.35	ZBTB43	1.92
ANOS	-3.05	KRT14	5.28	MIR409A	1.91

**Table 3.2.** Top 50 genes from microarray analysis with highest relative expression in response to physiological (2.5MPa) and non-physiological (7MPa) magnitudes of load at 24h post-load. Relative gene expression in explants subjected to 2.5MPa **(A)** or 7MPa **(B)** when unloaded explants were used as a control, and 7MPa compared with 2.5MPa load **(C)**.

A. 2.5MPa vs unloaded		B. 7MPa vs unloaded		C. 7MPa vs 2.5MPa	
Gene	Fold change	Gene	Fold change	Gene	Fold change
LAMC2	7.07	LAMC2	19.27		
INHBA	4.24	CCK	13.28	GPRC5A	3.40
MSMP	-4.17	CDA	11.90	SGK1	2.73
CCDC39	-3.88	CHRD2	-11.49	RERG	-2.51
PSAT1	-3.87	INHBA	11.22	FERMT1	2.45
ALDH1L2	-3.68	FOSL1	8.92	CYTL1	-2.06
CDA	3.61	CPM	8.74	TRIM9	-2.06
CAV1	3.56	ABI3BP	-8.51	RCAN1	1.98
MT2A	3.55	MT2A	8.29		
ATF5	-3.53	TNFRSF11B	7.85	C17H4orf29	-1.80
PLAUR	3.43	PLAUR	7.19		
TNFRSF11B	3.39	ALOX12	7.07		
R3HDML	3.26	GPRC5A	6.79		
OSMR	3.19	ASPN	-6.73		
FOSL1	3.13	CAV1	6.68		
ANGPTL7	3.10	ATF5	-6.27		
GFAP	3.02	DCC	-6.15		
TSPAN2	2.95	ISLR	-5.87		
ARHGAP20	-2.85	VNN1	5.86		
MUSTN1	2.77	SLITRK6	-5.63		
ADH1C	-2.75	SERPINA14	5.61		
SLC7A11	-2.65	LSAMP	-5.59		
S100A2	2.61	LOC617833	5.43		
TEAD4	2.61	ALDH1L2	5.38		
STK38L	2.55	MIR221	5.29		
ARSI	2.47	FRMPD4	5.10		
TNFRSF12A	2.46	TNFAIP6	5.01		
CASP3	2.46	RGS16	5.00		
STAT4	-2.46	PLXDC1	-4.95		
GSTM1	-2.40	ACE2	-4.90		
SOCS3	2.38	MT1A	4.82		
ADAMTS9	-2.37	HBA	-4.81		
FRMPD4	2.35	HOPX	4.79		
PPP2R2B	-2.34	S100A2	4.72		
PDE5A	-2.34	SMPD3	-4.69		
RGCC	2.33	SGK1	4.65		
LOC520044	2.32	CRYAB	4.63		
EGR1	-2.22	HSD11B1	4.59		
NGEF	2.21	PTGS2	4.43		
TSPAN18	-2.16	ARHGAP20	-4.43		
JUNB	2.15	OSMR	4.42		
WARS	-2.14	PANX3	-4.41		
MVP	2.12	MSMP	-4.37		
KCNH1	-2.12	SNCAIP	4.33		
SYT4	-2.11	TNFRSF12A	4.32		
CMTM5	-2.04	SOCS3	4.31		
LOC507426	2.02	STK38L	4.30		
P2RX6	-2.00	GDF10	-4.29		
FAIM2	-1.99	ADIPOQ	4.28		
FADS1	1.98	HHIP	-4.26		

### 3.2.5. Classification of differentially expressed genes in explants subjected to 2.5MPa and 7MPa loading regimes into protein classes

To create a better understanding of the identified global mRNA changes in cartilage explants subjected to physiological and non-physiological loading magnitudes processed either at 4 or 24h post-load, differentially expressed genes were organised into protein classes using the PANTHER classification system (<http://www.pantherdb.org/>).

Functional classification of those genes which were significantly differentially expressed was performed according to the protein class to which the genes belong. The analysis indicates several protein classes which include the differentially expressed genes regulated by mechanical stimuli. The 3 biggest groups of protein class from each treatment were analysed in more detail.

Figure 3.9 illustrates the output of PANTHER analysis of differentially expressed genes in response to (i) 2.5MPa and (ii) 7MPa load relative to the unloaded control, and (iii) 7MPa load compared to the physiological (2.5MPa) magnitude of load in explants processed 4h post-load. Each segment represents the proportional distribution of the genes classified according to the different protein sub-classes, with the 3 or 4 most abundant groups discussed in more detail.

**4h post-load:** 778 genes responded significantly to a 2.5MPa load relative to the unloaded explants (Figure 3.9i). The 3 biggest protein classes in response to a physiological magnitude (2.5MPa) were nucleic acid binding molecules (13.7%; C), transcription factors (11.2%; D) and enzyme modulators (8.5%; A). In comparison, a 7MPa load induced the differential expression of 2,848 genes relative to unloaded explants (Figure 3.9ii). The 3 most abundant protein classes were: nucleic acid binding molecules (12.5%; C), transcription factors (7.9%; D) and transferases (7.7%; E).

The expression of only 76 genes were significantly altered between the 7MPa and 2.5MPa loading regimes (Figure 3.9iii), and of these the most abundant protein classes represented included equal distribution in: nucleic acid binding molecules (C) and transcription factors (D) (9.2%), followed equally by: kinases (B) and transferases (E) (6.6%).

2.5MPa (1Hz, 15 minutes) load: A 2.5MPa loading regime induced 778 genes, in which 107 were classified as nucleic acid binding molecules, however PANTHER software was only able to ascribe protein subclasses to 76 of these. Among these 76 genes, an almost even distribution was demonstrated by DNA binding proteins (39.5%) and RNA binding proteins (40.8%), whereas helicases and nucleases constituted respectively 11.8% and 7.9% of all nucleic acid binding proteins (Figure 3.10A).

The transcription factor chart was represented by 5 protein subclasses, with only 45 molecules out of the 87 classified. The greatest proportion (33.3%) was represented by zinc finger transcription factors and the smaller group (24.4%) was made up of transcription cofactors. The helix-turn-helix transcription factors constituted 15.6% of overall distribution, whereas even dispersal was represented by nuclear hormone transcription factors and basic helix-loop-helix transcription factors (13.3%; Figure 3.10B).

The results for the enzyme modulator protein class demonstrates 5 subgroups in which 61 out of the 66 genes were assigned. A significant majority were categorised as G-protein modulators (44.3%), and the next most abundant subgroups were: kinase modulators (21.3%), protease inhibitors (14.8%) and G-proteins (13.1%), whereas the smallest group was represented by phosphatase modulators (6.6%; Figure 3.10C).

7MPa (1Hz, 15minutes) load: Amongst the 2,848 genes with altered mRNA expression in response to a 7MPa load, 357 genes were classified as nucleic acid binding. Unfortunately, 72 out of the 357 genes were not annotated for PANTHER detection, but the other 285 molecules came from RNA binding proteins, DNA binding proteins, nucleases and helicases with a respective distribution of 51.2%, 31.2%, 9.8% and 7.7% (Figure 3.11A).

The second greatest group of regulated proteins was transcription factors which contained 220 molecules which fitted into this protein subclass. Most (45.6%) of the proteins were classified as zinc-finger transcription factors, the smaller group (25.2%) was transcription cofactors. The helix-turn-helix transcription factors (12.2%), nuclear hormones (8.2%) and basic helix-loop-helix transcription factors (6.1%) were 3 medium

size clusters, the smallest proportion was represented by basic leucine zipper transcription factors (2%) and HMG box transcription factors (0.7%) (Figure 3.11B).

The third group comprised 220 genes belonging to the transferases protein class and all of these molecules fitted to the available protein subclasses. The biggest group comprised kinase molecules (44.5%), followed by glycosyltransferases (17.3%), acetyltransferases (12.7%), acyltransferases (10%), methyl- and nucleotidyltransferases were induced equally (5.9%), and the smallest group was represented by transaminases (2.7%) and phosphorylases (0.9%; Figure 3.11C).

7MPa vs 2.5MPa (1Hz, 15minutes) load: This load comparison presented 76 differentially expressed genes, in which the most abundant groups were: nucleic acid binding proteins and transcription factors consisting of 7 genes each, however only 1 gene out of 7 from each protein group was recognised and classified as RNA binding protein for nucleic acid binding proteins and basic helix-loop-helix transcription factors for transcription factor group (Figure 3.12A-B). All 3 protein kinases involved in the next most abundant kinase group (8.9%; Figure 3.12C) were also classified as transferases, the group which in this experiment was created based on 5 molecules and also constituted 6.6% of overall gene distribution (Figure 3.12D).

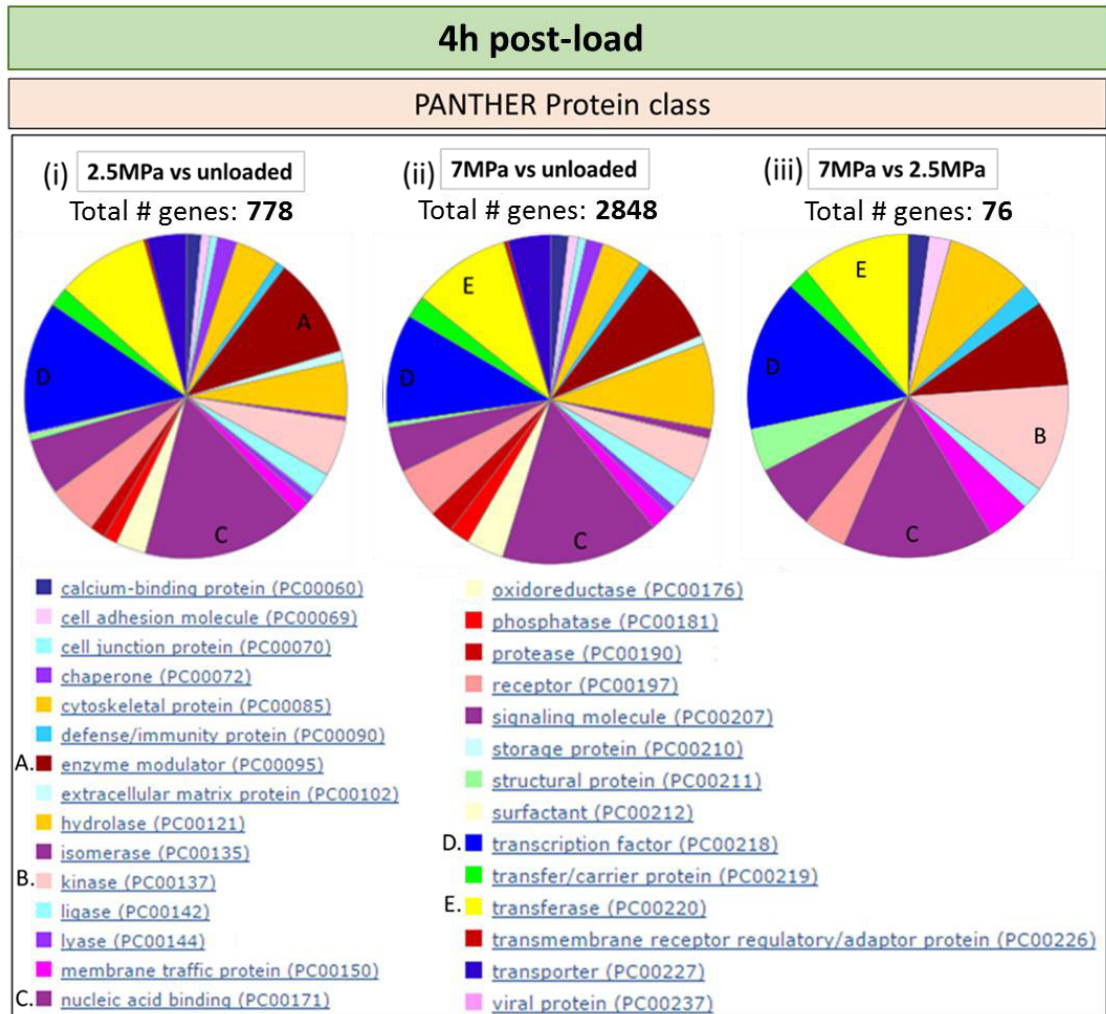


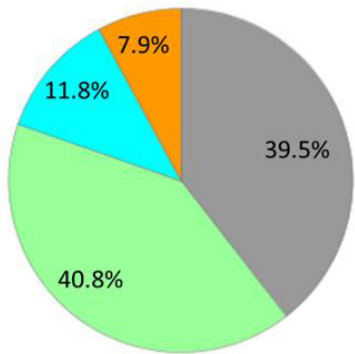
**Figure 3.9.** Classification, according to protein classes provided by PANTHER annotation, of differentially expressed genes at 4h post-load in articular cartilage subjected to 2.5MPa or 7MPa load (1Hz, 15 minutes). The pie chart represents the protein classes to which the differentially expressed genes were classified in response to 2.5MPa **(i)** or 7MPa **(ii)** load in comparison to unloaded explants. The chart also represents the protein classes attributed to genes significantly altered between the two loading regimes **(iii)**.

**4h post-load**

**2.5MPa vs unloaded**

**A. Nucleic acid binding molecules (13.7%)**

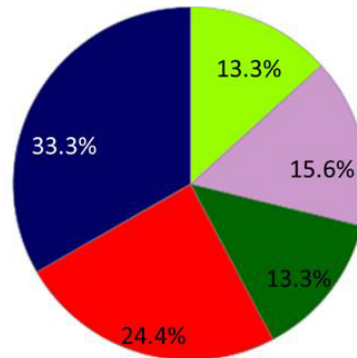
Total # genes: **107**  
Total # genes involved in subclasses: **76**



- [DNA binding protein \(PC00009\)](#)
- [RNA binding protein \(PC00031\)](#)
- [helicase \(PC00115\)](#)
- [nuclease \(PC00170\)](#)

**B. Transcription factors (11.2%)**

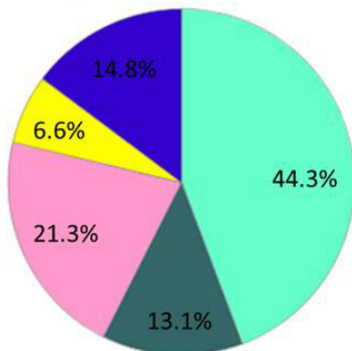
Total # genes: **87**  
Total # genes involved in subclasses: **45**



- [basic helix-loop-helix transcription factor \(PC00055\)](#)
- [helix-turn-helix transcription factor \(PC00116\)](#)
- [nuclear hormone receptor \(PC00169\)](#)
- [transcription cofactor \(PC00217\)](#)
- [zinc finger transcription factor \(PC00244\)](#)

**C. Enzyme modulators (8.5%)**

Total # genes: **66**  
Total # genes involved in subclasses: **61**



- [G-protein modulator \(PC00022\)](#)
- [G-protein \(PC00020\)](#)
- [kinase modulator \(PC00140\)](#)
- [phosphatase modulator \(PC00184\)](#)
- [protease inhibitor \(PC00191\)](#)

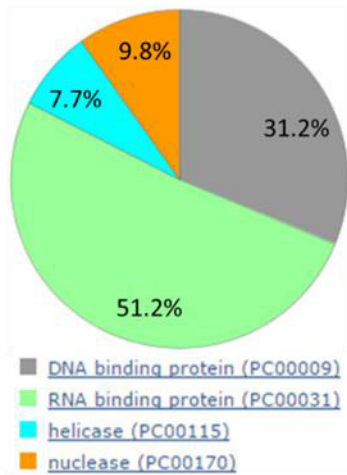
**Figure 3.10.** Pie charts demonstrating the characterisation of the differentially expressed genes according to protein class in response to a 2.5MPa load analysed 4h post-load. Unloaded explants were used as a control. Microarray data was classified using the PANTHER classification system, and the 3 most abundant groups are depicted.

**4h post-load**

**7MPa vs unloaded**

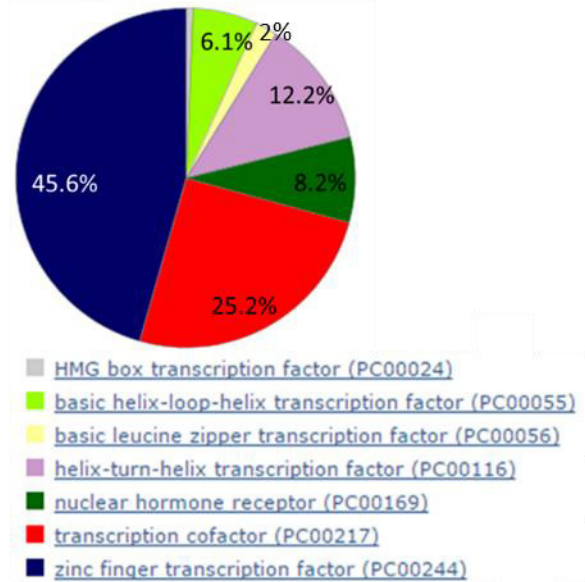
**A. Nucleic acid binding molecules (12.5%)**

Total # genes: **357**  
 Total # genes involved in subclasses: **285**



**B. Transcription factors (7.9%)**

Total # genes: **224**  
 Total # genes involved in subclasses: **220**



**C. Transferases (7.7%)**

Total # genes: **220**  
 Total # genes involved in subclasses: **220**

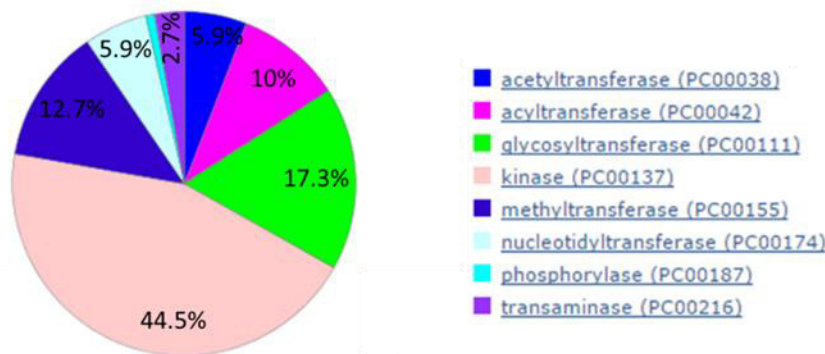


**Figure 3.11.** Pie charts demonstrating the characterisation of the differentially expressed genes according to protein class in response to a 7MPa load analysed 4h post-load. Unloaded explants were used as a control. Microarray data was classified using the PANTHER classification system, and the 3 most abundant groups are depicted.

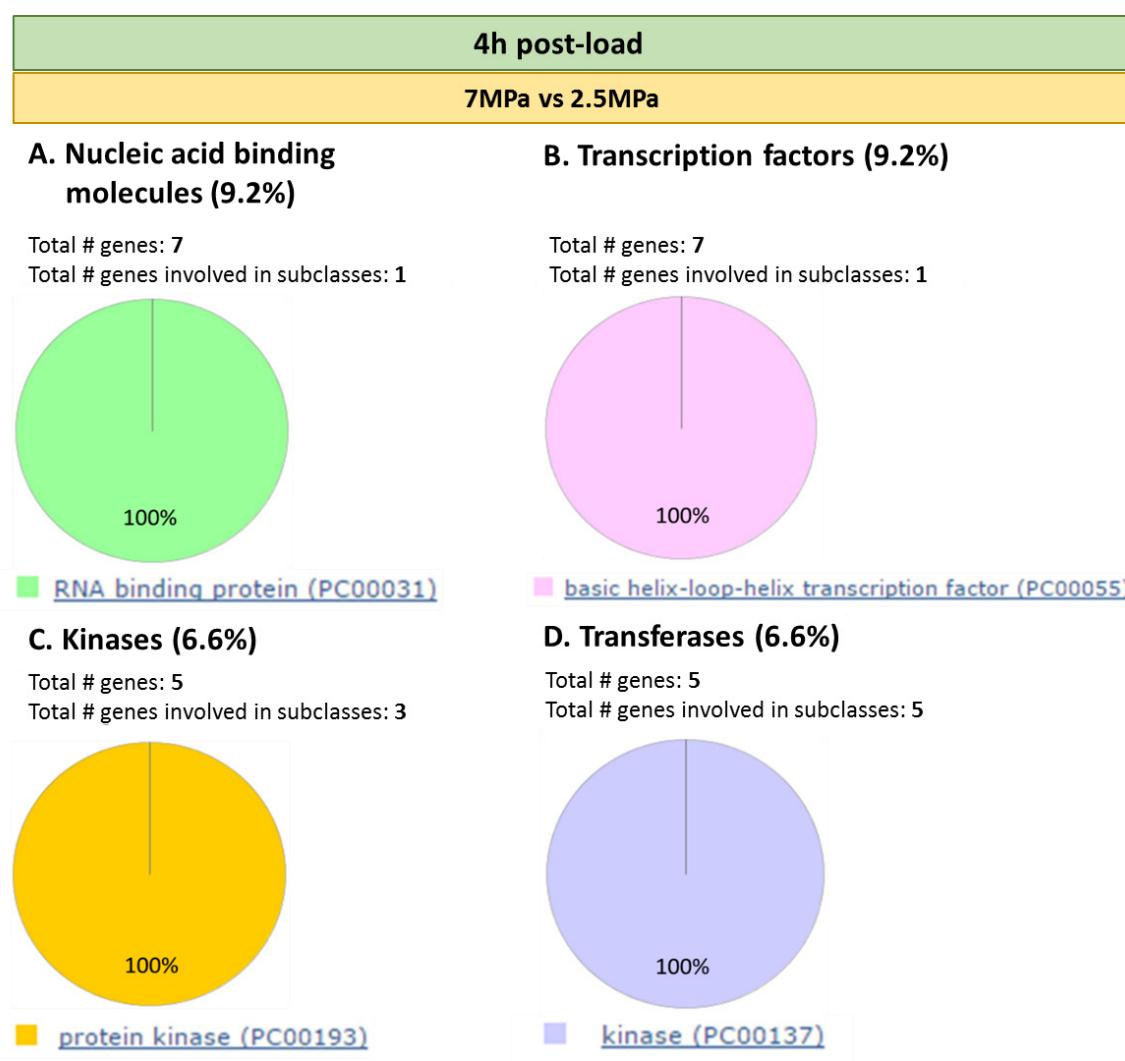


**Figure 3.12.** Pie charts demonstrating the characterisation of the differentially expressed genes according to protein class in response to a 7MPa load analysed 4h post-load. Explants subjected to 2.5MPa load were used as a control. Microarray data was classified using the PANTHER classification system, and the 4 most abundant groups are depicted.

Figure 3.13 illustrates the output of PANTHER analysis of differentially expressed genes in response to (i) 2.5MPa and (ii) 7MPa load relative to the unloaded control, and (iii) 7MPa load compared to the physiological (2.5MPa) load in explants processed 24h post-load. Each segment represents the proportional distribution of the genes classified according to the different protein sub-classes, with the 3 or 4 most abundant groups discussed in more detail.

**24h post-load:** By the later time point of 24h post-cessation of load, noticeably fewer genes were differentially expressed in response to the applied mechanical loads except for the 7MPa load (Figure 3.13).

2.5MPa (1Hz, 15 minutes) load: The 2.5MPa load (Figure 3.13i) induced significant alterations in the transcription of 91 genes in which 12.1% belonged to the signalling molecules (D). The next most abundant protein classes regulated by this loading regime were: hydrolases (9.9%; B), nucleic acid binding proteins (C) and transferases (E) contained evenly 8.8% of the 91 genes studied.

8 signalling molecules out of 11 were represented by cytokines (50%), membrane-bound signalling molecules (25%) and growth factors (25%) (Figure 3.14A).

The next greatest group of protein was hydrolases that contain 9 molecules, but only 7 of them fit the protein subclass. Most (42.8%) of the proteins were classified as proteases, the other subgroups were represented equally (14.3%) by deaminases, lipases, phosphatases and phosphodiesterases (Figure 3.14B).

Nucleic acid binding protein class was based on 6 genes out of 8 classified to this group. More than half (66.7%) of the explored genes were RNA binding proteins. The next subgroups represented evenly by 16.5% of molecules was DNA binding proteins and nucleases (Figure 3.14C).

The last group was transferase molecules in which 8 genes were involved, but cluster sizes of kinases (42.9%), glycosyltransferases (28.6%) and evenly abundant (14.3%) acetyltransferases and transaminases were created based on 7 genes (Figure 3.14D).

7MPa (1Hz, 15minutes) load: The largest protein class, accounting for 12% of the 1,995 genes differentially expressed in response to the 7MPa load (Figure 3.13ii) was represented by nucleic acid binding proteins. A significant majority of analysed molecules were categorised as RNA binding proteins (52.5%) and DNA binding proteins (40.1%), whereas the rest were represented by nucleases (6.8%) and helicases (0.6%) (Figure 3.15A).

In the group of hydrolases 157 genes were involved (7.9%), but only 110 were available using PANTHER software for classification. Among these 110 genes, more than half were classified as either phosphatases (31.8%) or proteases (30.9%). The next group that covered 12.7% was lipases. The smallest fraction of molecules accounted for esterases (8.2%), phosphodiesterases (6.4%), deaminases (3.6%) and glycosidases (2.7%), deacetylases (2.2%), phyrophosphatases and galactosidases (1.5%; Figure 3.15B).

The third most abundant protein class, created from genes significantly modulated in response to 7MPa load was enzyme modulators (7.5%). The distribution in this group was based on 127 genes despite the fact that 150 genes were originally classified to this group of receptors. Of these 127 molecules, almost half of the proteins were represented by G-protein modulators (48%). The next most abundant subgroups were: G-proteins (18.1%), protease inhibitors (16.5%), and kinase modulators (14.2%), whereas the smallest group was represented by phosphatase modulators (3.1%; Figure 3.15C).

7MPa vs 2.5MPa (1Hz, 15minutes) load: Interestingly, the comparison between 7MPa and 2.5MPa load (Figure 3.10iii) showed changes in the expression of 8 genes, however, the distribution of differentially expressed genes in this comparison was based on 6 molecules only. Although each gene represented a different protein class, the protein classes reflected in this data set included: calcium binding proteins, enzyme modulators, receptors, signalling molecules, transfer/carrier proteins and transferases which had also been evidenced when comparing transcriptional differences between the loaded and unloaded explants.

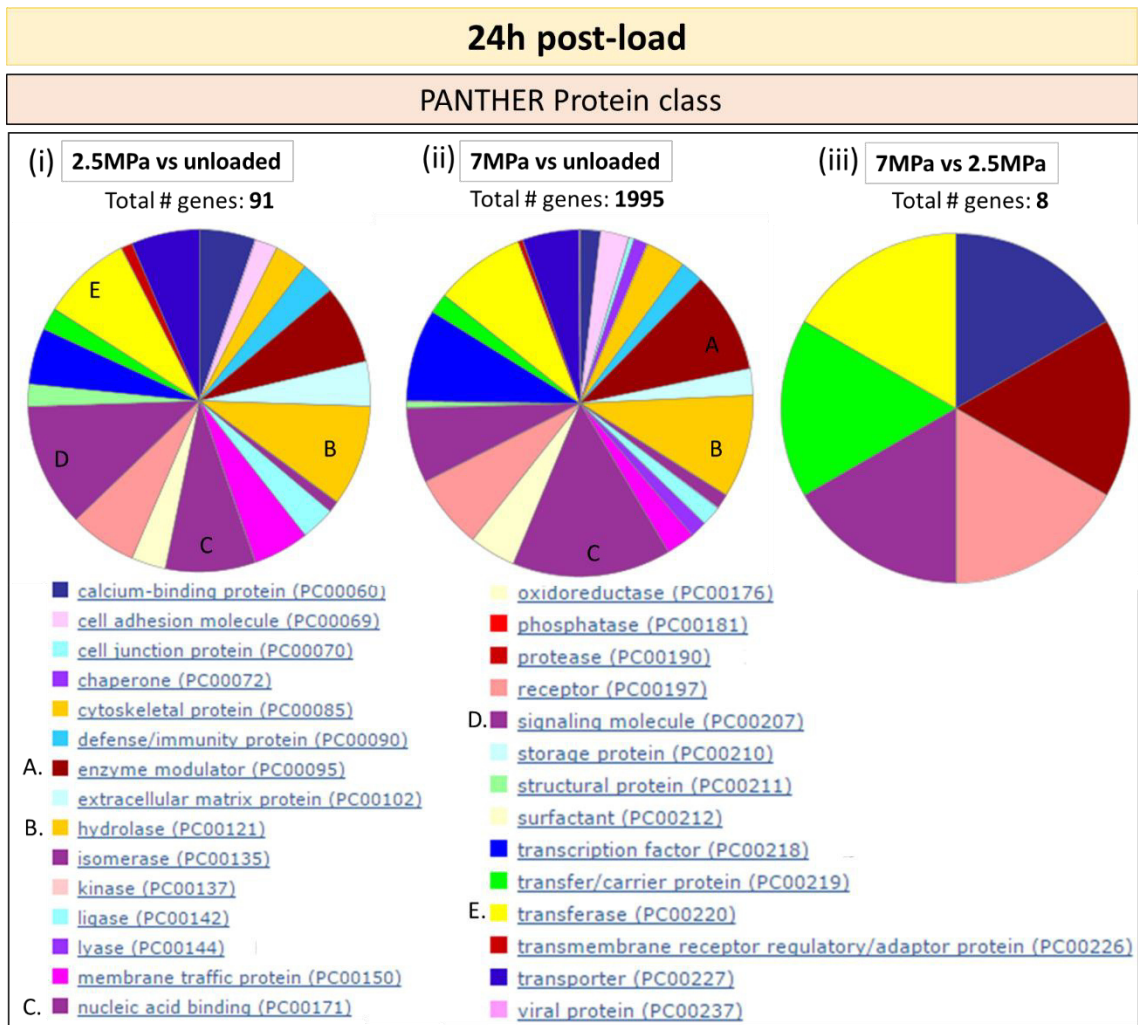
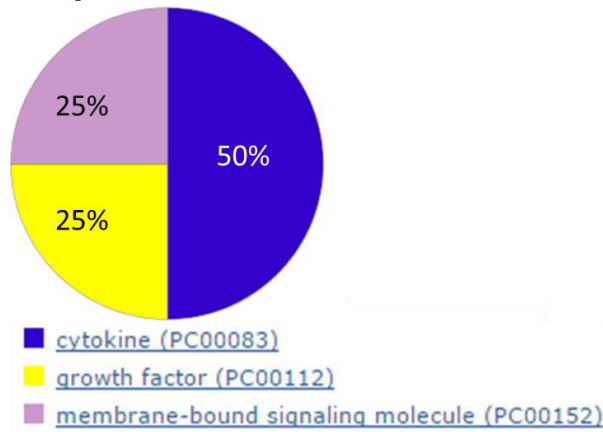


**Figure 3.13.** Classification, according to protein classes provided by PANTHER annotation, of differentially expressed genes at 24h post-load in articular cartilage subjected to 2.5MPa or 7MPa load (1Hz, 15 minutes). The pie chart represents the protein classes to which the differentially expressed genes were classified in response to 2.5 MPa **(i)** or 7MPa **(ii)** load in comparison to unloaded explants. The chart also represents the protein classes attributed to genes significantly altered between the two loading regimes **(iii)**.

24h post-load
2.5MPa vs unloaded

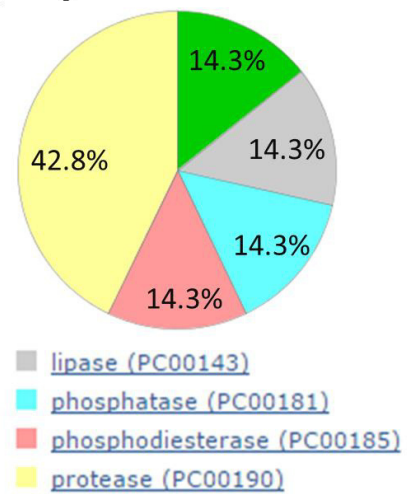
### A. Signalling molecules (12.1%)

Total # genes: 11  
Total # genes involved in subclasses: 8



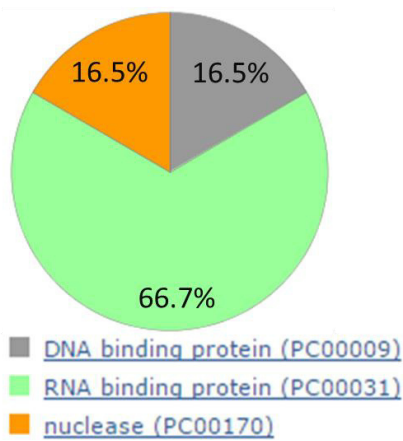
### B. Hydrolases (9.9%)

Total # genes: 9  
Total # genes involved in subclasses: 7



### C. Nucleic acid binding molecules (8.8%)

Total # genes: 8  
Total # genes involved in subclasses: 6



### D. Transferases (8.8%)

Total # genes: 8  
Total # genes involved in subclasses: 7

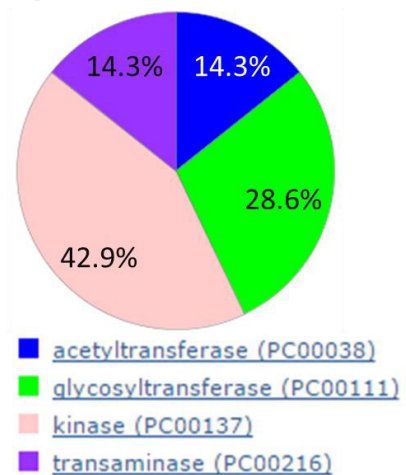
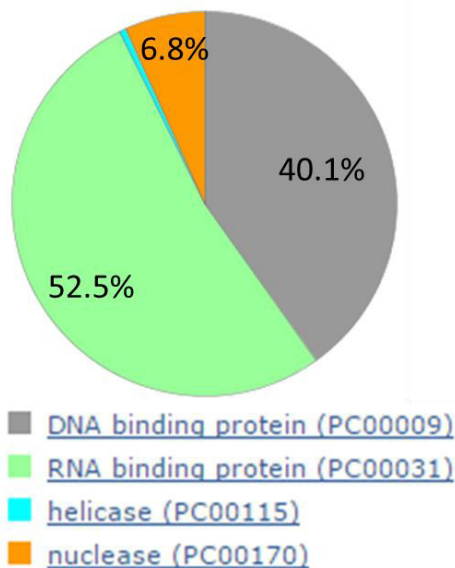


**Figure 3.14.** Pie charts demonstrating the characterisation of the differentially expressed genes according to protein class in response to a 2.5MPa load analysed 24h post-load. Unloaded explants were used as a control. Microarray data was classified using the PANTHER classification system, and the 4 most abundant groups are depicted.

<b>24h post-load</b>
<b>7MPa vs unloaded</b>

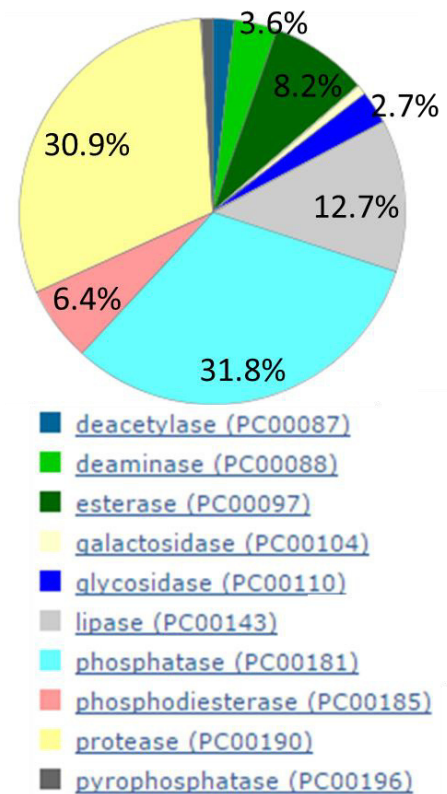
### A. Nucleic acid binding molecules (12%)

Total # genes: **240**  
Total # genes involved in subclasses: **177**



### B. Hydrolases (7.9%)

Total # genes: **157**  
Total # genes involved in subclasses: **110**



### C. Enzyme modulators (7.5%)

Total # genes: **150**  
Total # genes involved in subclasses: **127**

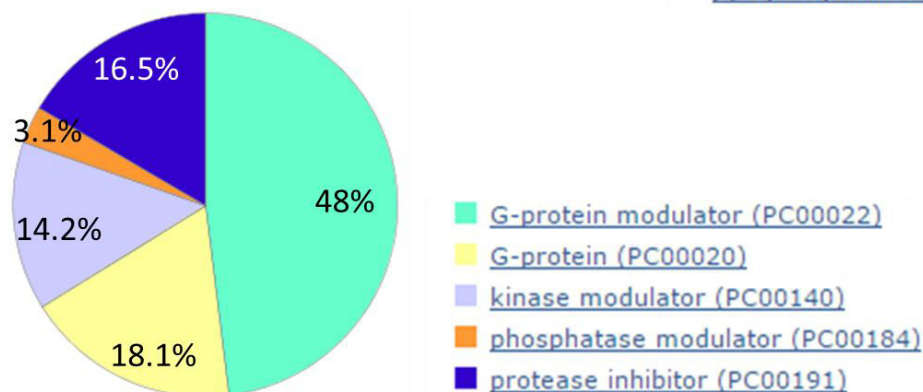


**Figure 3.15.** Pie charts demonstrating the characterisation of the differentially expressed genes according to protein class in response to a 7MPa load analysed 24h post-load. Unloaded explants were used as a control. Microarray data was classified using the PANTHER classification system, and the 3 most abundant groups are depicted.

### 3. 3. Discussion

Articular cartilage consists mainly of hyaluronan/proteoglycan and collagen type II networks which confers the tissue with viscoelastic properties, facilitating the dissipation of load that is placed on joints during movement and provides a frictionless surface for joint motion. Turnover of the cartilage matrix is maintained by an equilibrium of catabolic and anabolic processes; however, once the catabolic molecules i.e. MMPs, ADAMTSs are active over a prolonged period, the balance is shifted resulting in cartilage damage and ultimately tissue degradation.

One of the factors that maintains cartilage in a healthy and homeostatic condition is physiological levels of mechanical load. It is essential because it regulates chondrocyte activities to balance the expression of molecules that are needed for cartilage turnover. It has been shown that non-physiological load: either insufficient load (e.g. immobilisation or purely static load) or overload (e.g. sudden (traumatic) or prolonged (obesity)) leads to an imbalance in ECM turnover resulting in cartilage degeneration (Griffin and Guilak, 2005).

It is well known that many factors affect the response of chondrocytes to mechanical force (Bader et al., 2011, Lee and Bader, 1997), therefore the purpose of this experimental chapter was:

- **To identify low and high magnitudes of load that induce early transcriptional variations in anabolic/catabolic molecules in response to a short-term loading episode**
- **To identify more globally genes that are sensitive to load**
- **To identify more globally genes that are sensitive to load**

### **3.3.1. Identification and validation of appropriate reference genes that are unaffected by mechanical load**

Quantitative PCR (qPCR) is one of the most commonly used techniques in scientific studies due to its sensitivity in detection, and over the last decade the usage of this method to quantify mRNA levels increased from 8% to 88% (Bustin, 2000, Kozera and Rapacz, 2013, Thellin et al., 2009). qPCR may be a reliable method to assess the level of gene expression, but only if it is correctly optimised for the designed experiment (Thellin et al., 2009). One of the critical factors that is key to perform is a consistent analysis of reliable reference genes (Kozera and Rapacz, 2013). To select the most appropriate internal gene(s) for data normalisation, recommendations have been proposed by the MIQE guidelines concerning selection of reference gene(s): (i) experimental validation of reference gene stability and (ii) usage of at least three reference genes if there is no reason for using fewer (Bustin et al., 2009, Bustin et al., 2010). Reference genes are used to assess variations in studied gene expression levels induced by experimental parameters (McCulloch et al., 2012). In order to act as a reference gene, expression levels should be unaffected by the treatment regime being applied e.g. mechanical load (McCulloch et al., 2012). Using and normalising data to inappropriate reference genes can bear false positive or negative results, because an applied stimulus can affect the expression of not only the genes of interest but also the reference genes themselves (Dheda et al., 2004, Kozera and Rapacz, 2013). Historically, many scientific groups showing the effect of mechanical load on cartilage have normalised their data to common reference genes such as 18S, GAPDH and  $\beta$ -actin. These genes were normally chosen based on the literature, not by experimental optimisation of the most stable reference gene (McCulloch et al., 2012). Knowing how important the selection of endogenous reference genes is to obtain reliable qPCR results, it is surprising that only one group, prior to our study (Al-Sabah et al., 2016) tried to optimise the most suitable internal reference controls for chondrocytes subjected to mechanical stimulation. Lee et al. reported that 18S was the most appropriate from 5 tested putative reference genes (18S, GAPDH,  $\beta$ -actin,  $\beta$ -glucuronidase, and  $\beta$ -2 microglobulin) for articular chondrocytes and intervertebral discs subjected to mechanical load (Lee et al., 2005b).

As the selection of reference genes for a new experimental design needs to be confirmed experimentally (Bustin et al., 2010), I have taken a panel of reference genes (Anstaett et al., 2010) to assess their stability under the parameters I have used in the experimental setup. To identify the most stable reference genes, three independent experimental repeats of cartilage either subjected to different loading regimes or left unloaded were examined. qPCR data from each reference gene were analysed using RefFinder software (<http://fulxie.0fees.us/>) that combines 4 different algorithms: BestKeeper (Pfaffl et al., 2004), geNorm (Vandesompele et al., 2002), NormFinder (Andersen et al., 2004) and comparative  $\Delta C_t$  (Silver et al., 2006), to select the most stable reference genes on the basis of  $C_t$  values. The MIQE guidelines suggests use of at least three reference genes unless there is a reason to select less (Bustin et al., 2010). Several reports indicate the importance of selecting at least 2 reference genes for normalisation (Kozera and Rapacz, 2013, Nicot et al., 2005, Thellin et al., 2009, Vandesompele et al., 2002), because the use of only one internal reference gene can lead to relatively large errors and false results (Vandesompele et al., 2002). RefFinder analysis indicated that SDHA, YWHAZ and RPL4 were the most stable reference genes under the experimental conditions tested; because YWHAZ and RPL4 had similar levels of stability, YWHAZ was selected as the second reference gene for data normalisation. Therefore, all of the remaining data in this chapter were normalised to the geometric mean of the two most appropriate internal reference genes: SDHA and YWHAZ. GAPDH which is commonly used as an internal reference gene (Glare et al., 2002), and also previously utilised in cartilage mechanobiology studies, was classified as one of the least stable from the 8 tested and, therefore an inappropriate reference gene for data normalisation in loaded cartilage. This result is not surprising as GAPDH is an enzyme involved in glycolysis, providing the main source of energy production in chondrocytes. The unstable nature of GAPDH was also confirmed in other studies performed on canine (Maccoux et al., 2007) and human osteoarthritic articular cartilage (Pombo-Suarez et al., 2008), and in the differentiation of ATDC5 chondroprogenitor cells (Zhai et al., 2013). In contrast to most studies performed on chondrocytes, Silver et al. presented GAPDH as the most appropriate internal control for data normalisation in human reticulocytes (Silver et al., 2006).  $\beta$ -actin and 18S appear to have very similar levels of stability in my experimental design and both of them are relatively stable even though the actin cytoskeleton has

been shown to be reorganised in response to load (Blain, 2009, Knight et al., 2006). However,  $\beta$ -actin and 18S were classified as inappropriate internal controls for experiments with the ATDC5 cell line, with HPRT and PPIA recommended as the most suitable (Zhai et al., 2013), which contrasts to my observations in cartilage tissue under load. As can be seen, one endogenous reference gene can behave differently in different tissues and even in the same tissue when exposed to different stimuli, therefore it is absolutely essential to validate at least 2 potential reference genes for each experimental condition.

### **3.3.2. Characterisation of physiological and non-physiological magnitudes of load that induce transcriptional differences in chondrocyte response**

In most previously published studies, cartilage was subjected to load for different periods of time ranging from hours (h) (Kiraly et al., 1998, Parkkinen et al., 1993) to days (Lee and Bader, 1997, Mauck et al., 2000) or even weeks (Otterness et al., 1998, Pap et al., 1998). The purpose of this current study was to establish loading regimes to determine the earliest changes at the gene level induced by load.

To establish the required regimes, cartilage explants were loaded under three different magnitudes: 2.5MPa, 5MPa or 7MPa (1Hz, 15 minutes) and mRNA levels of markers of cartilage homeostasis measured 24h post-load. The aforementioned loading regimes were selected for testing based on previous studies (unpublished) and the literature where load  $\leq$ 5MPa was declared as physiological, whereas  $\geq$ 5MPa was reported as non-physiological/injurious (Arokoski et al., 2000, Hodge et al., 1986). To determine the magnitude of load that induces changes in cartilage homeostasis during normal movement, a frequency of 1Hz was applied as it is equivalent to fast walking (Bader et al., 2011). Application of load for 15 minutes appeared to be sufficient to observe changes at the mRNA level up to 24h post-cessation of load. To assess whether the applied load triggered changes at the transcriptional level and if so whether genes of molecules involved in anabolic or catabolic events were preferentially regulated, a panel of genes were selected that were either representative of anabolic (aggrecan, collagen type II, TIMP-1, TIMP-2 and TIMP-3) or catabolic (MMP-1, -3, -9, -13, ADAMTS-4, -5)

markers of cartilage metabolism; these genes were selected on the basis that they have previously been demonstrated to be influenced by mechanical load in articular cartilage (Blain et al., 2001, Blain, 2007, Kiraly et al., 1998, Kurz et al., 2001).

Analysis of mRNA levels in cartilage subjected to the different loading regimes demonstrated that aggrecan and collagen type II transcription were unaffected, when compared to the unloaded explants. Interestingly, several previous studies have shown the mechano-responsive character of these anabolic molecules (Grodzinsky et al., 2000, Kurz et al., 2001, Thomas et al., 2011), therefore it is likely that the period of loading was not long enough to induce transcriptional changes in these particular genes, corroborating a study that demonstrated that changes in aggrecan and collagen type II gene expression were dependent on the duration of load (Smith et al., 2000).

Increased MMP transcription can indicate an imbalance of ECM homeostasis, therefore to investigate whether any of the loading regimes initiate a catabolic molecules response, expression of specific MMPs that are known to be significantly altered under conditions of abnormal load were measured by qPCR. Neither 2.5MPa or 7MPa load affected the mRNA level of the collagenase MMP-1 which indicates that even if a non-physiological magnitude is applied to cartilage, but for too short a period of time, the tissue does not respond to it in agreement with Monfort et al. who showed that healthy cartilage subjected to normal load does not change MMP-1 expression (Monfort et al., 2006). However, surprisingly the 5MPa load significantly increased MMP-1 transcription suggesting its mechano-sensitive nature as previously reported (Fitzgerald et al., 2004, Leong et al., 2011). However, this data is contradictory as it is not clear why the highest load (7MPa) did not induce MMP-1 transcription similar to the 5MPa load.

MMP-3, which is able to activate itself and other MMPs - for example pro-collagenases (pro-MMP- 1, -13) and pro-gelatinases (pro-MMP-9, -2) (Johnson et al., 2011, Monfort et al., 2006, Ramos-DeSimone et al., 1999), moreover it has a capability to degrade collagen type II, IV, and IX, proteoglycans, laminin and fibronectin (Ye et al., 1996); was found to be up-regulated in explants subjected to either a 5MPa or 7MPa load. The mechano-sensitive nature of MMP-3 has been reported in previous studies (Blain, 2007,

Leigh et al., 2008, Monfort et al., 2006, Patwari et al., 2003) and qPCR confirmed this finding.

In my study, according to qPCR results MMP-9 and MMP-13 were significantly decreased in explants subjected to either a 2.5MPa or 5MPa load, whereas transcript levels were unaffected by a 7MPa load. These results, using the optimised loading regimes, corroborate the mechano-sensitive nature of MMP-9 and MMP-13 in cartilage explants. However, in contrast it has previously been shown that injurious static load (~20MPa applied for only 1 second) elevated MMP-9 expression (Lee et al., 2005c). Furthermore, when comparing the activity of MMP-13 in: (i) OA mouse knee subjected to moderate load versus an unloaded OA knee, (ii) non-OA loaded mouse knee to unloaded, MMP-13 expression was observed to decrease in response to physiological load (Hamamura et al., 2013). Decreased MMP-13 expression, as detected in my study, was also observed when physiological levels of tensile strain (3%, 0.25Hz) were applied for 4-24h to chondrocytes (Madhavan et al., 2006).

Proteoglycans are one of the first ECM molecules to undergo degradation in the process of cartilage degeneration, therefore measuring transcript levels of the catabolic enzymes that are the most effective aggrecanases may help to specify the early effects that applied load has on cartilage chondrocytes. ADAMTS-4 and ADAMTS-5 are reported as highly involved in aggrecan degeneration, although the contribution of these molecules to cartilage pathology remains unclear and appears to be species-dependant. Experiments conducted on ADAMTS-4 or -5 knock-out mice demonstrated that ADAMTS-5 is the major aggrecanase involved in mouse cartilage degeneration, as only ADAMTS-5 knock-out mice were protected from early aggrecan loss in an OA model induced by joint destabilisation (Glasson et al., 2004, Glasson et al., 2005, Stanton et al., 2005). In contrast to murine OA cartilage, ADAMTS-4 is suggested to be more important in human cartilage degradation as it is elevated in OA tissue (Malfait et al., 2002, Naito et al., 2007). Song et al. also showed higher expression of ADAMTS-4 compared to ADAMTS-5 in OA articular cartilage, however both enzymes were elevated in human OA cartilage (Song et al., 2007). Elevated expression of ADAMTS-4 and-5 in response to mechanical load corroborated data from a previous study which identified ADAMTS-4 as 2-fold elevated and ADAMTS-5 as the second most increased (40-fold) gene in bovine

cartilage subjected to injurious static load (~20MPa/1sec) (Lee et al., 2005c). Increased levels of ADAMTS-4 mRNA were observed under all of the loading regimes tested by qPCR suggesting that ADAMTS-4 is induced to regulate load-induced ECM turnover, whereas ADAMTS-5 responsiveness to only a non-physiological magnitude (7MPa) suggests that this ADAMTS is less committed to cartilage homeostasis than to cartilage degeneration.

In this study, the load-dependant nature of TIMP-1, TIMP-2 and TIMP-3 was also demonstrated. TIMP-1 and TIMP-3 expression was subtly up-regulated in response to the lowest load, and there was a greater increase in transcript levels in response to the 5MPa and 7MPa loads. This may mean that these TIMPs, as protease inhibitors, are synthesised to balance the production of catabolic molecules to maintain cartilage homeostasis, as all TIMPs are known to control the expression of many MMPs (Murphy, 2011); additionally, TIMP-3 is crucial in inhibiting ADAMTS-4 and ADAMTS-5 activities (Sahebjam et al., 2007). Surprisingly, TIMP-2 did not follow the trend of elevation in response to mechanical load. qPCR presented almost the same level of down-regulation in all tested loading regimes indicating that TIMP-2 in my experimental design was load-, but not magnitude-dependent.

The aim of the work described above was to optimise two individual loading regimes that induced different biochemical responses in cartilage chondrocytes. None of the loads tested altered the gene expression of selected anabolic molecules, however all of the assessed loading regimes differentially affected the gene expression of some catabolic molecules. Based on the transcriptional changes observed at the mRNA level I chose two loading regimes for further studies: (i) 2.5MPa load (1 Hz, 15 minutes) that induced a homeostatic response of chondrocytes to a normal (physiological) magnitude of load, and (ii) 7MPa load (1 Hz, 15 minutes) that led to elevated gene expression levels of some catabolic molecules. This loading magnitude dependent effect suggested that the 7MPa load can be considered as a potentially, high enough magnitude to induce a degradative response if it was applied for a prolonged period of time.

### **3.3.3. Global overview of genes that are sensitive to compressive mechanical load**

Although loading regimes that will be used for the subsequent identification of mechano-sensitive miRs were established, a comparison of transcriptional changes in explants processed either at 4h or 24h post-cessation of load was performed to identify global changes in mechano-sensitive genes and assess whether these effects were transitory or sustained. Changes in gene transcript levels in explants subjected to 2.5MPa or 7MPa (1Hz, 15 minutes) load and processed either at 4 or 24h after load were assessed using GeneChip® Bovine 1.0 ST arrays (all experimental work for explants processed at 4h post-load was conducted by Dr Aisha Al-Sabah).

The 24h post-load array results confirmed: (i) unchanged levels of aggrecan and collagen type II as shown in qPCR data, (ii) elevated level of MMP3, ADAMTS-4, TIMP-1/-3, (iii) decreased expression of TIMP-2 in response to 7MPa load. The microarray data showed also that the expression of a greater number of genes were significantly altered in cartilage 4h post-cessation of load compared to 24h suggesting that many genes present transitory transcriptional alterations in response to mechanical stimuli.

Transcription factor, FOS-like antigen (FOSL-1/Fra-1) has been noted in this study as one of the most load-dependent genes, showing increased expression with elevated magnitude of load at both tested time points. FOSL-1 dimerizes with proteins from the JUN family, JUNB which was also shown to be a load-dependent molecule, and JUND proteins forming the transcription factor AP-1 (Ijiri et al., 2008). This plays an important role in cartilage homeostasis as it was reported that activation of AP-1 reduces the expression of Sox-9, a major transcription factor controlling collagen type II expression (Hwang et al., 2005). Moreover, it has been also reported that 30 minutes of cyclic compression (1KPa, 1Hz) applied on chondrocytes increased AP-1 binding to MMP-3 and -13 resulting in their higher expression (Bader et al., 2011). As the role of FOSL-1 and JUNB in the regulation of cartilage homeostasis is clear, it is not surprising that both FOSL-1 (Thorfve et al., 2012) and JUNB (Rhee et al., 2016) are up-regulated in OA cartilage. My results additionally confirmed the mechano-sensitive nature of FOSL-1 in cartilage consistent with the findings in engineered cardiac tissue subjected to 48h of cyclic mechanical stretch (5% elongation, 0.5Hz) (Ye et al., 2013). FOSL-1 and JUNB were

also up-regulated at 4h post-load in rat bone following *in vivo* cyclic loading (13N, 2Hz, 3 minutes) (Mantila Roosa et al., 2011). As AP-1 is a series of dimeric complexes composed from the JUN and FOS family (Shaulian and Karin, 2002), and known to be early response transcription factors to mechanical stimuli, it is not surprising that previous studies demonstrated and also confirmed the mechano-sensitive nature of other molecules from the FOS family presented in this chapter (Haasper et al., 2008, Inoue et al., 2004, Thomas et al., 2011). Interestingly, a significant up-regulation of FOSB was observed only at 4h post-load, however FOS was found to be up-regulated at 24h in response to the 7MPa load only. These data suggest a load and time-dependent nature of FOSB and FOS transcription. The mechano-responsiveness of FOS has previously been reported with up-regulation at 4h post-load in chondrocytes subjected to 30 minutes of tensile strain (7.5%, 1Hz) (Thomas et al., 2011). In turn, Inoue et al. reported the mechano-inductive nature of FOSB in mice, showing increased FOSB expression in mouse hind limb bone after only 30 minutes (the highest expression by 2h) of re-loading in rotating cage after 4h tail-suspension (Inoue et al., 2004). Moreover, the mechano-sensitivity of FOSB was also demonstrated *in vitro* by its increased expression in response to fluid shear stress (100-120rpm, 30 minutes) in mouse osteoblasts (Inoue et al., 2004) and to 3 repeats per day of 2h cyclic stretching (2% or 8% elongation, 1 Hz) within 3 days in human bone marrow stromal cells (hBMSCs) (Haasper et al., 2008). All of these studies corroborate data demonstrating the mechano-responsive nature of the components of the AP-1 transcription factor.

The mechano-responsive nature of ADAMTS-1 demonstrated by Roosa et al. in *in vivo* loaded rat forelimb was also confirmed in this study (Mantila Roosa et al., 2011). This group reported that ADAMTS-1, which is a known catabolic molecule in articular cartilage as it cleaves cartilage proteoglycans (Kuno et al., 2000), is an early response gene (4h post-load) to cyclic mechanical loading (13N, 2Hz, 3 minutes); these results are also transient as the changes are not noticeable at later time points (Mantila Roosa et al., 2011). This study corroborates the mechano-sensitivity of ADAMTS-1 which was highly expressed at 4h post-load in explants subjected to both loading regimes, and the level of its expression decreased at the later time point showing 10-fold lower

expression at 24h post-load in response to 7MPa than at the 4h time point, with no change in response to a 2.5MPa load.

Another load- and time-dependent gene identified in this study is Inhibin Beta A (INHBA/ActivinA) which is an activator of anabolic SMAD2/3 pathway, and due to its anti-catabolic function it suppresses aggrecan degradation in cartilage (Alexander et al., 2007). INHBA plays an important role in cartilage turnover and is up-regulated in OA cartilage which suggests its effort to reactivate a leading role for SMAD2/3 above SMAD1/5/8 which becomes dominant in OA (Snelling et al., 2014). The only previous study showing sensitivity of INHBA to mechanical load was in human periodontal ligament cells subjected to cyclic deformation (12%, 6 seconds elongation every 90 seconds, 12h or 24h) (Pinkerton et al., 2008). This finding supports data showing that dynamic mechanical compression of healthy articular cartilage is a stimulator of TGF- $\beta$ /Smad2/3 signalling pathway (Madej et al., 2014) which is cartilage protective as it stimulates aggrecan and collagen type II synthesis (Swingler et al., 2012).

Interestingly, so far there is no publication about the mechano-sensitive nature of Laminin Subunit Gamma 2 (LAMC2) which according to microarray results performed on articular cartilage subjected to 2.5MPa and 7MPa (1Hz, 15 minutes) load and processed at 4 or 24h post-load is highly load-dependent. The closest data that confirms the influence of load on LAMC2 expression reported the increased expression of LAMC2 in human chondrocytes cultured in hypergravity (1.8g) conditions for 2h in comparison to normal gravity (1g) conditions (Wehland et al., 2015). Although studies on the tissues suggest that LAMC2 may play an important role in cartilage homeostasis, there are no publications on the role of LAMC2 in cartilage OA development. Garg et al. showed that LAMC2 binds to epidermal growth factor receptor (EGFR) and modulates its activity in anaplastic thyroid carcinoma (ATC); inhibition of LAMC2 partially blocks EGFR activation and its signalling pathway (Garg et al., 2014). This fact suggests that reduced expression of LAMC2 may also silence EGFR in articular cartilage and affect cartilage homeostasis, as it has been reported that DMM mice with reduced EGFR activity demonstrate enhanced cartilage degradation with higher expression of ADAMTS-5 and MMP-13 (Zhang et al., 2014a).

Although, there are no publications concerning the influence of Enoyl-CoA, Hydratase/3-Hydroxyacyl CoA Dehydrogenase (EHHADH) on cartilage homeostasis, it is known that enoyl-CoA hydratases are involved in fatty acid metabolism that provides energy for different cellular processes (Nelson, 2005), therefore it may play a crucial role in tissue homeostasis. This study corroborated the mechano-sensitive nature of EHHADH, as Chaillou et al. previously reported decreased expression of this gene in overload-induced hypertrophic skeletal muscles of the dorsal aspect of the lower hind limb (Chaillou et al., 2013).

Interestingly, this study is the first to demonstrate the mechano-sensitive nature of a number of other genes. Load- and time dependent ADAMTS-2 gene expression according to the microarray data has not yet been reported as mechano-responsive in the literature. This gene was down-regulated in response to 7MPa load at 24h only and was reported to be increased in OA cartilage (Kevorkian et al., 2004). ADAMTS-2 is a procollagen proteinase which processes the procollagens of fibrillar collagens to create collagen molecules used for generating fibrils (Alper et al., 2015, Kevorkian et al., 2004). The up-regulation of ADAMTS-2 in OA chondrocytes may be explained by increased production of collagen in OA chondrocytes likely to compensate for collagen type II loss (Kevorkian et al., 2004), whereas down-regulation in response to 7MPa indicates that a 7MPa (1Hz, 15 minutes) load is not sufficient to induce osteoarthritic damage and also it suggests that the 7MPa load inhibits pro-collagen processing in loaded cartilage.

The most increased gene in 7MPa loaded explants when compared to 2.5MPa loaded tissue was G Protein-Coupled Receptor Class C Group 5 Member A (GPC5A) also known as retinoic acid induced gene 1 (RAIG1) or retinoic acid induced three (RAI3). It was first found by Cheng et al. in 1998 in a human oral squamous carcinoma cell line as retinoic acid-inducible G protein binding receptor (Cheng and Lotan, 1998) and is known as an orphan receptor because its ligand remains unidentified (Acquafreda et al., 2009). Additionally, to date there are no papers indicating a role of GPC5A in cartilage homeostasis, but Harada et al. showed GPC5A as a putative binding partner of Frizzled proteins what suggests a possible role in activation of canonical and non-canonical Wnt signalling pathway (Acquafreda et al., 2009, Harada et al., 2007).

Ras-like and (o)Estrogen-Regulated Growth inhibitor (RERG) was the most decreased gene in explants subjected to a non-physiological load in comparison to a physiological loading magnitude. RERG is a highly oestrogen responsive gene and its expression is correlated with oestrogen receptor (ER) levels as it contains 2 ER binding sites in the promoter region (Key et al., 2006); furthermore, elevated and decreased mRNA levels were observed in a breast cancer cell line (MCF-7) treated with  $\beta$ -oestradiol or ER antagonist tamoxifen, respectively (Finlin et al., 2001). Therefore, the reduced expression of RERG can be explained by the fact that the expression level of ER $\alpha$  (ESR1) was also reduced in explants subjected to a 7MPa load with respect to 2.5MPa load, however this mRNA alteration was not statistically significant (1.37-fold: FDR=0.39) (data not shown). In cartilage, the same as in bone, ER $\alpha$  and ER $\beta$  are expressed and in the literature there is increasing evidence that ER $\alpha$ , which mediates most of the oestrogen function in bone such as synthesis of bone matrix proteins, osteoblast proliferation and promotion of osteoclast death, is activated in response to physiological mechanical load indicating that mechanical stimuli play an important role in bone homeostasis and density (Lee and Lanyon, 2004, Windahl et al., 2013). ER $\beta$  role in bone is still under investigation, however a recent study reported its antagonistic role towards ER $\alpha$  (Khalid and Krum, 2016). Although, there is no publication suggesting the mechano-responsive nature of ER in chondrocytes, the microarray data in the current study indicated mechanically-regulated expression of ER $\alpha$ . However, the transcriptional level of this gene was significantly decreased (1.28-fold: FDR=0.004) in explants subjected to a 7MPa load and processed at 24h post-load when compared to unloaded tissue (data available electronically). Explants subjected to either 2.5MPa or 7MPa loads and processed at 4h post-load or 2.5MPa load at 24h post-load did not show statistically significant changes in any of these genes which suggests that differential expression of ER $\alpha$  and RERG in cartilage is load- and period post-cessation of load dependent. Due to the increased activation of ER $\alpha$  in response to physiological mechanical stimuli in bone, the down-regulated mRNA expression in explants subjected to 7MPa (1Hz, 15 minutes) load suggests that this loading regime is too high to induce synthesis of ER $\alpha$ .

Prostate associated microseminoprotein (MSMP/ PC3-secreted microprotein), which was the most decreased gene observed in explants subjected to a 2.5MPa loading

regime processed at 24h post-load, has not previously been demonstrated to be mechano-responsive nor play an influence on cartilage homeostasis. However, it is believed to be involved in Akt phosphorylation and caspase activation in PC3 (prostate cancer cell line) suggesting an involvement in apoptosis (Pidgeon et al., 2002). Hence, the observation of decreased MSMP transcription over the 24h period suggests the load does not induce apoptosis reflecting my findings from live/dead explant staining (data not shown).

Another gene that was regulated in a load- and time-dependent manner in this study was chordin-like BMP inhibitor (CHL2/ CHRDL2). A greater down-regulation was observed in response to a 7MPa load in comparison to unloaded tissue than in response to a 2.5MPa load, 24h after loading, whereas the mRNA level of CHL2 at 4h post-load remained unchanged. Bone morphogenetic proteins (BMPs) were originally identified as factors promoting endochondral bone formation, however most recent studies have revealed that this protein family includes different molecules, including the growth factors (GDF) subfamily and collectively they are important in many organogenesis processes (Hogan, 1996, Nakayama et al., 2004, Tsumaki et al., 2002). Although the entire mechanism of influence of the BMP family on cartilage formation and development is still unclear, it is known that BMP-2, -4, -6 and -7, and GDF-5 are involved in cartilage development (Tsumaki et al., 2002). The activity of these BMP proteins is controlled by their receptors and inhibitors, and one of these inhibitors is CHL2 (Nakayama et al., 2004). CHL2 was identified as a negative regulator of cartilage formation from mesenchymal stem cells by reducing cartilage matrix accumulation and was identified only in the superficial layer of mouse embryo developing joint cartilage with very weak expression in adult mouse cartilage (Nakayama et al., 2004). Therefore, the down-regulation of CHL2 with high non-physiological load would potentially promote a cartilage repair mechanism in response to the potentially damaging load.

Microarray analysis of mechanically-regulated genes in explants subjected to 2.5MPa and 7MPa (1Hz, 15 minutes) load and processed at 4h or 24h post-load, showed also the mechano-responsiveness of several miRs including miR-221 and -222 that have already been shown as mechano-sensitive in weight bearing locations of bovine cartilage in stifle joints (Dunn et al., 2009).

### **3.3.4. Protein classes of differentially expressed genes in response to 2.5MPa and 7MPa loading regimes at 4h and 24h after loading**

To create a more organised picture of the identified global mRNA changes in cartilage explants subjected to physiological and non-physiological magnitudes of load and processed either at 4 or 24h post-load, the significantly altered genes were organised into protein classes using the online available PANTHER classification system (<http://www.pantherdb.org/>).

The grouped gene data performed using PANTHER showed that the greatest number of genes differentially expressed in explants processed at 4h post-load belong to nucleic acid binding proteins and transcription factors as these protein classes represent the top two most abundant of all the groups in explants subjected to both loading regimes. Explants processed at 24h post-load did not present such a similarity between loading regimes, but this might reflect the diversity of the more long-term transcriptional response to load. The most abundant protein subclasses in 24h post-load explants stimulated with a physiological (2.5MPa) magnitude were signalling molecules and hydrolases, whereas a non-physiological (7MPa) magnitude mostly induced the expression of molecules belonging to nucleic acid binding proteins and hydrolases.

The panel of all protein groups that were differentially expressed in response to 2.5MPa and 7MPa loads was similar in each condition suggesting that these protein groups are the most sensitive classes of molecules in response to mechanical stimuli in articular cartilage. The trend of greater transcriptional changes in explants subjected to 7MPa load than 2.5MPa suggests that these loading regimes may turn into degradative and biosynthetic/turnover load, respectively, if applied for long enough periods of time. For many of the mechano-responsive genes, their regulation is more pronounced at 4h compared to 24h post-load. The greater fold-changes observed at 4h relative to 24h suggest transitory mechanically-responsive effects on many genes e.g. FOSL-1 (4h post-load: 2.5MPa (6.94-fold), 7MPa (16.51-fold), 24h post-load: 2.5MPa (3.13-fold), 7MPa (8.92-fold); this is also supported by the fact that a greater number of genes show altered mRNA expression at 4h post-load as opposed to 24h post-cessation. It is yet to be determined whether or when the expression of this cohort of mechanically regulated

genes return to basal expression. Although the differentially regulated protein classes identified in response to a 7MPa load were comparable at both time points, subtle differences were observed in the protein classes identified at 4h and 24h post-cessation of the 2.5MPa load. This may be attributed to the transitory changes in expression levels of the mechanically-regulated genes identified at 24h following a 2.5MPa load. The difference in the top 3 most abundant protein classes in explants subjected to 2.5MPa load and processed at 4h versus 24h post-cessation may be attributed to (i) a less pronounced transcriptional response i.e. fold-change in expression, in cartilage subjected to a 2.5MPa load compared to a 7MPa load and (ii) the transitory mechano-regulation of many of these genes in explants subjected to 2.5MPa and processed 24h post-load. If my hypothesis is right, it would indicate that many of the genes belonging to nucleic acid binding proteins and transcription factors present transitory differential expression, whereas the changes in transferases are more sustained.

To summarise this subsection: these results demonstrate that the transcriptional response and associated protein classification is both load and time-dependant and this suggests that the timeframe to observe early transcriptional effects may be very different depending on the gene under investigation (Garg et al., 2014).

### 3.3.5. Summary:

- SDHA and YWHAZ are the most stable and appropriate reference genes, in cartilage explants subjected to different magnitudes of load, for data normalisation and reliable qPCR results.
- Transcriptional validation of mechano-responsive genes encoding anabolic and catabolic molecules has shown that: (i) 2.5MPa and 5MPa (1Hz, 15 minutes) loads triggered a response characteristic of homeostasis, whereas the (ii) 7MPa (1Hz, 15 minutes) loading regime induced predominantly catabolic genes, known to be highly expressed in OA cartilage, therefore it can be considered as potentially mechanically compromised. 2.5MPa and 7MPa (1Hz, 15 minutes) loading regimes were selected as representative of physiological and non-physiological magnitudes of load.
- Mechanical stimulation affects predominantly the transcriptional level of many nucleic acid binding and signalling molecules
- Time points post-cessation of load affect the transcriptional level of the studied genes. Differential expression of some genes was obvious only at 4 or 24h post-load, whereas other significantly altered molecules are differentially expressed at both time points however their levels of expression differ.

# Chapter 4

Identification of mechanically-regulated

miRs

## 4.1. Background

Mechanical force induces the expression of some genes that activate important pathways in articular cartilage to either maintain tissue homeostasis or promote a catabolic response, as previously explained in Chapter 3.

miRs are produced by all types of cells and control the expression of one third of all human genes (Lewis et al., 2005). Their sequences are highly conserved indicating the significance of their function; they are involved in the regulation of many biological processes such as apoptosis, proliferation, differentiation, development, cell cycle, cell metabolism and homeostasis (Miyaki et al., 2010). There is increasing evidence that alterations in miR levels are very often associated with changes in matrix molecule expression and may cause the development of many diseases (Soifer et al., 2007, Ardekani and Naeini, 2010). OA is one such disease that is characterised by altered miR expression levels when compared to healthy tissue (Araldi and Schipani, 2010, Goldring and Marcu, 2012, Pauley and Cha, 2011, Swingler et al., 2012).

It is well known that one of the main risk factors for OA development is abnormal mechanical load, but it is unknown whether non-physiological loading can influence ECM metabolism via miR activation.

Before I started my PhD study, only a few studies had reported the mechano-responsive nature of miRs in different cell types: airway smooth muscle cells (Mohamed et al., 2010), endothelial cells (Qin et al., 2010, Ni et al., 2011), trabecular meshwork cells (Luna et al., 2011b) and tendon fibroblasts (Mendias et al., 2012). To date, not many studies have been published on the mechano-sensitive character of miRs in articular cartilage or chondrocytes, and how their regulation may affect expression levels of downstream target genes. Guan et al. demonstrated that expression of miR-365 is significantly elevated in chicken and mouse primary chondrocytes subjected to a 24h mechanical stimulation (5% elongation, 1Hz, 15min/h) (Guan et al., 2011); furthermore, miR-365 was found to regulate chondrocyte differentiation via targeting of the central regulator of chondrocyte hypertrophy: histone deacetylase 4 (HDAC4) (Guan et al., 2011). Jin et al. identified miR-146a, a miR known to be differentially expressed in OA pathogenesis (Yamasaki et al., 2009), as being significantly increased,

in human chondrocytes subjected to a static 10MPa load (60 minutes), showing its influence on chondrocyte apoptosis by targeting SMAD4 (Jin et al., 2014). Dunn et al. demonstrated that expression of miR-221 and miR-222 were differentially up-regulated between anterior weight-bearing and posterior non-weight-bearing of medial femoral condyles of stifle joint providing further examples of cartilage mechano-responsive miRs (Dunn et al., 2009).

Based on these findings and the fact that mechanical load can promote either ECM homeostasis or degradation in cartilage, I hypothesised that chondrocytes differentially express many more miRs in response to load than have been discovered so far and that these specific mechano-responsive miRs induce homeostatic or catabolic effects in cartilage matrix composition, and hence affect functional integrity of the tissue.

To further investigate the mechano-responsive nature of miRs in chondrocytes subjected to mechanical load, Next Generation Sequencing (NGS) analysis was performed on miR libraries prepared from loaded and unloaded cartilage explants. As miRs are up-stream of their target genes, two different regimes (based on previous optimisation in Chapter 3) and three different time points post-cessation of load were examined to identify early events in the mechano-regulation of cartilage miRs.

**Summary of the aims of this experimental chapter:**

- **To identify and validate “early response” mechanically-regulated miRs in articular cartilage**

## 4.2. Results

### 4.2.1. Differential expression of miR-140, -221 and -222 at 24h post-load (7MPa only)

Prior to the submission of miR libraries for NGS analysis, the expression levels of miR-140, -221 and -222 were assessed by TaqMan qPCR on explants subjected to load (2.5MPa, 7MPa or unloaded) and analysed 2h and 24h post-load (Figure 4.1).

No changes were observed at the early (2h) time point for any of the miRs screened (Figure 4.1A,C,E), whereas significant changes in expression were present at 24h post-load. Although miR-140 levels appeared to be decreased in response to both loading regimes (Figure 4.1B), this was only statistically significant in explants subjected to a 7MPa load (1.38-fold:  $p=0.043$ ). Furthermore, miR-221 expression was significantly up-regulated (2.99-fold:  $p=0.029$ ) in explants subjected to a 7MPa load compared to unloaded tissue (Figure 4.1D). A noticeable, but not statistically significant up-regulation of miR-221 was also observed between explants subjected to 7MPa and 2.5MPa loads (2.77-fold:  $p=0.07$ ). A statistically significant up-regulation of miR-222 was observed in response to a 7MPa load when compared to unloaded explants (2.65-fold:  $p=0.001$ , Figure 4.1F). A comparison of miR-222 levels in explants subjected to 7MPa and 2.5MPa demonstrated a significantly greater expression of this miR with increasing load (2.36-fold:  $p=0.024$ ). Clearly, the selected miRs are responsive to increasing mechanical loads in articular cartilage.

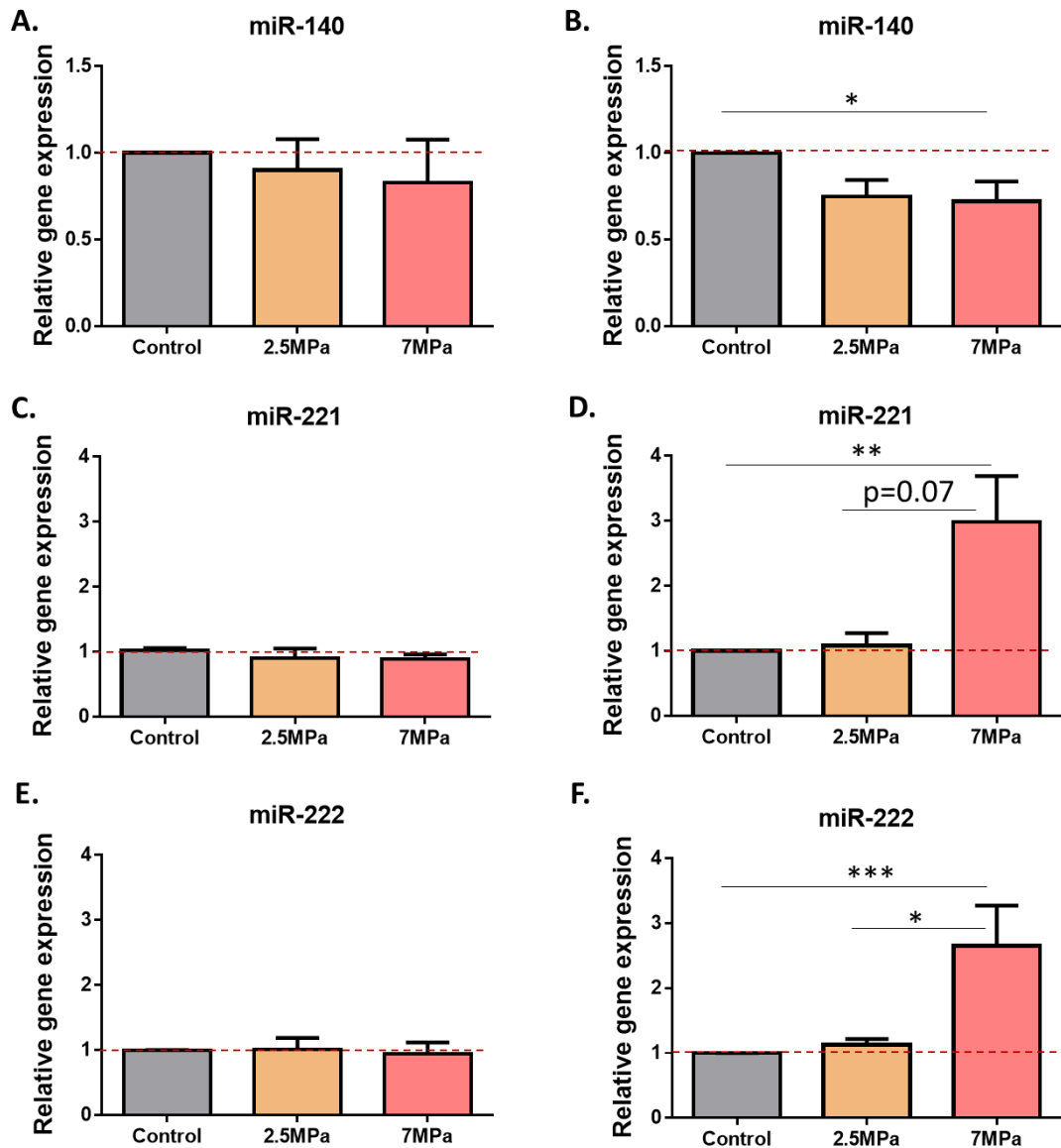


**Figure 4.1.** Relative expression levels of miR-140 (A,B), miR-221 (C,D) and miR-222 (E,F) in cartilage explants subjected to 2.5MPa or 7MPa load (1 Hz, 15 minutes) and analysed 2h (A,C,E) or 24h (B,D,F) post-load respectively; unloaded explants served as controls. Analysis of pooled samples (N = 3) that were either unloaded (n = 6) or were subjected to 2.5MPa (n = 6) or 7MPa (n = 6) load was conducted using qPCR with TaqMan™ Fast Advance technology; miR levels were normalised to the reference genes (SDHA, YWHAZ) and further normalised to the unloaded control tissue. Data are presented as mean ±SD (N = 3 pooled samples from independent experiments). Statistical analysis was performed using a 1-way ANOVA with Tukey's post hoc test. Key: Control - unloaded, 2.5MPa, 7MPa (loaded) [\* p<0.05, \*\* p≤0.01, \*\*\* p≤0.001].

#### **4.2.2. Identification of mechano-regulated miRs and time post-load required for differential expression of mechano-sensitive miRs**

Assessment of global changes in the expression of miRs in loaded and unloaded cartilage explants were performed using Next Generation Sequencing. Application of either a 2.5MPa or 7MPa load (1Hz, 15 minutes) and analysis conducted 2, 6 or 24h post-cessation of load elicited differing early transcriptional changes in many miRs when compared to the unloaded control cartilage.

NGS was performed in The Genome Analysis Centre™ (Norwich, UK) and the data was analysed by Andrew Skelton (Institute of Cellular Medicine, Newcastle University) using (i) a combination of RSamTools (Morgan, 2011) and ShortRead (Morgan et al., 2009) bioconductor packages to count aligned reads against a reference, and (ii) a DESeq2 algorithm to compare the expression of known miRs to identify mechano-responsive miRs. To detect differentially expressed miRs, it was necessary to know the raw number of reads of miRs in the representative samples for each parameter to calculate the average (base mean) from N = 3 individual repeats. Identification of mechano-sensitive miRs and the most appropriate time to observe such changes in miRs expression was assessed on the base mean from each loading regime and each time point post-cessation of load.

#### **4.2.2.1. Most abundant miRs in articular cartilage subjected to load**

The figures below illustrate the top 50 most abundantly expressed miRs in unloaded and loaded (2.5MPa and 7MPa) cartilage explants at 2h (Fig. 4.2A), 6h (Fig. 4.2B) and 24h (Fig. 4.2C) post-load. Several of the most abundant miRs detected are known to play very important roles in cartilage homeostasis, and their expression levels are reported to differ in OA tissue. To this group of miRs we can include for example: miR-27a (Akhtar et al., 2010), miR-27b (Yu et al., 2011), miR-125b (Matsukawa et al., 2013), miR-140 (Araldi and Schipani, 2010, Swingler et al., 2012), miR-148a (Vonk et al., 2014) and miR-455-3p (Swingler et al., 2012). The most abundantly expressed miRs under each loading regime and at all three time points were miR-140 and miR-148a.

Based on the number of reads of miR sequences in each sample, the mean of the reads was calculated as an average of 3 independent experiments. To assess for potential changes in the expression levels of the miRs, the counts were compared between unloaded and loaded or between different loading regimes at the three different time points post-cessation of load. miR transcripts that were identified as being significantly altered at 2, 6 or 24h post-load are presented (Table 4.1) along with their base mean numbers (Figure 4.5).

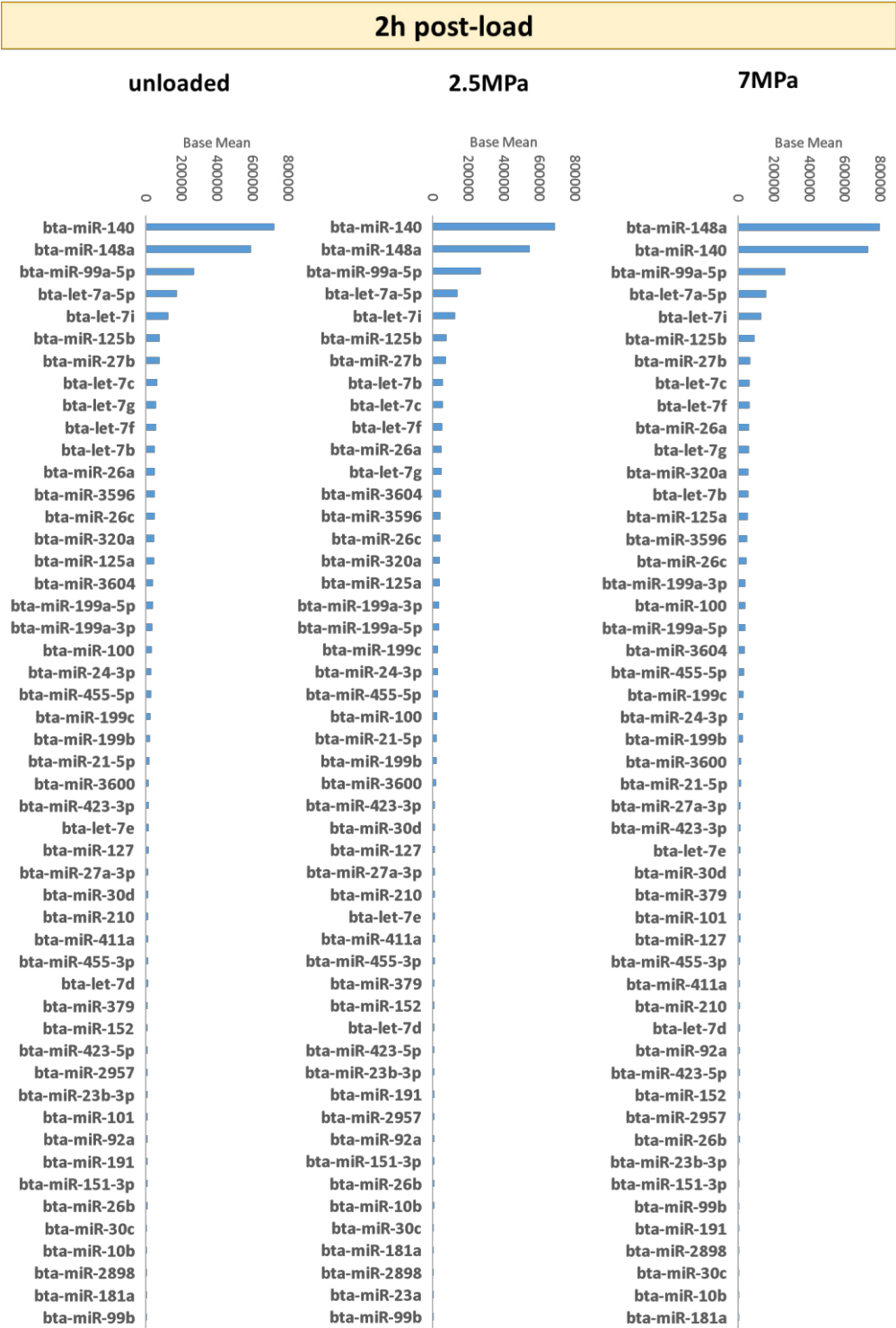


**Figure 4.2.** Top 50 most abundantly expressed miRNAs in articular cartilage at 2h post-load. Analysis of pooled samples that were either unloaded (n = 6) or were subjected to 2.5MPa (n = 6) or 7MPa (n = 6) load (1Hz, 15 minutes) was conducted by Next Generation Sequencing across all samples (N = 3).

## 6h post-load

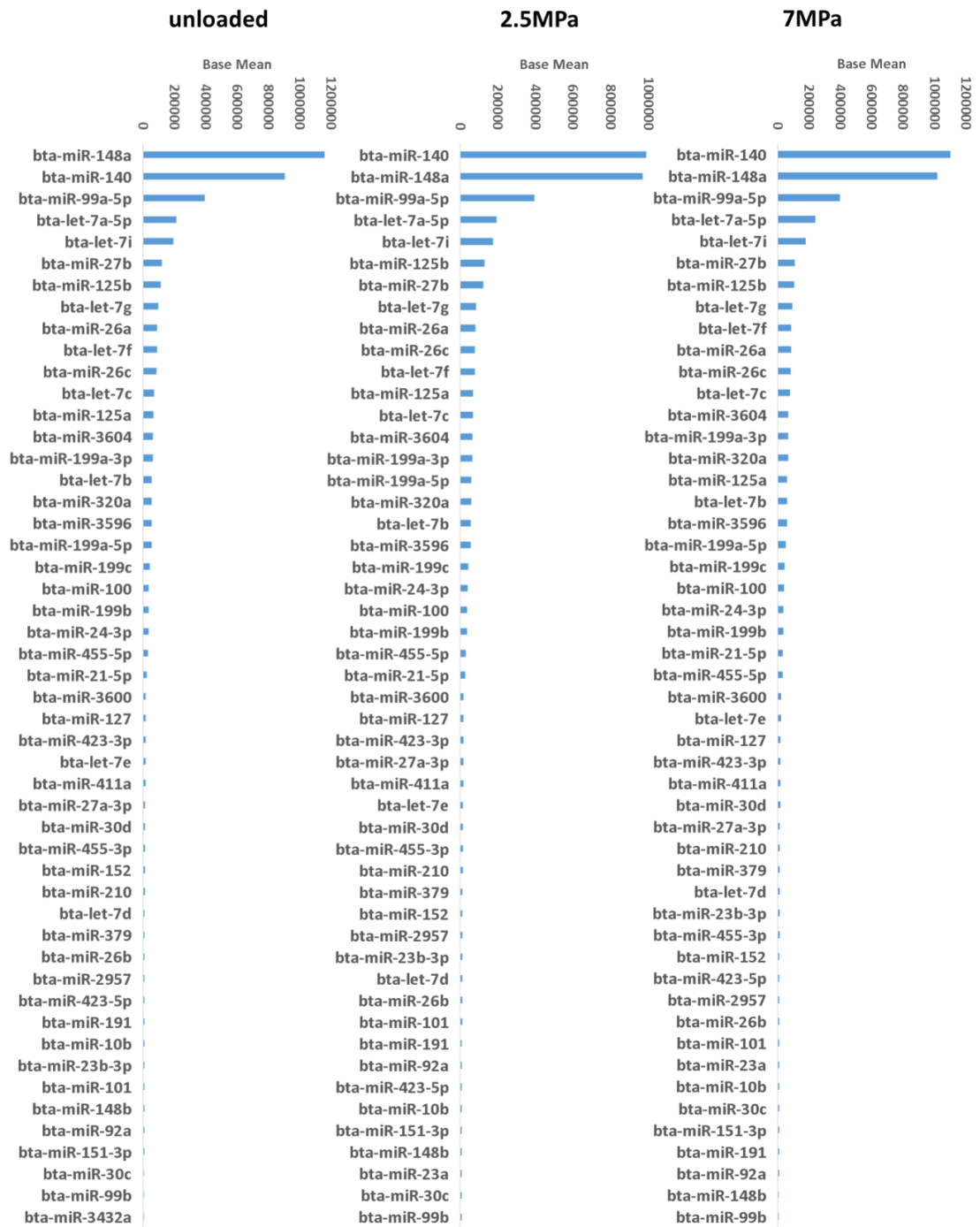


**Figure 4.3.** Top 50 most abundantly expressed miRNAs in articular cartilage at 6h post-load. Analysis of pooled samples that were either unloaded (n = 6) or were subjected to 2.5MPa (n = 6) or 7MPa (n = 6) load (1Hz, 15 minutes) was conducted by Next Generation Sequencing across all samples (N = 3).

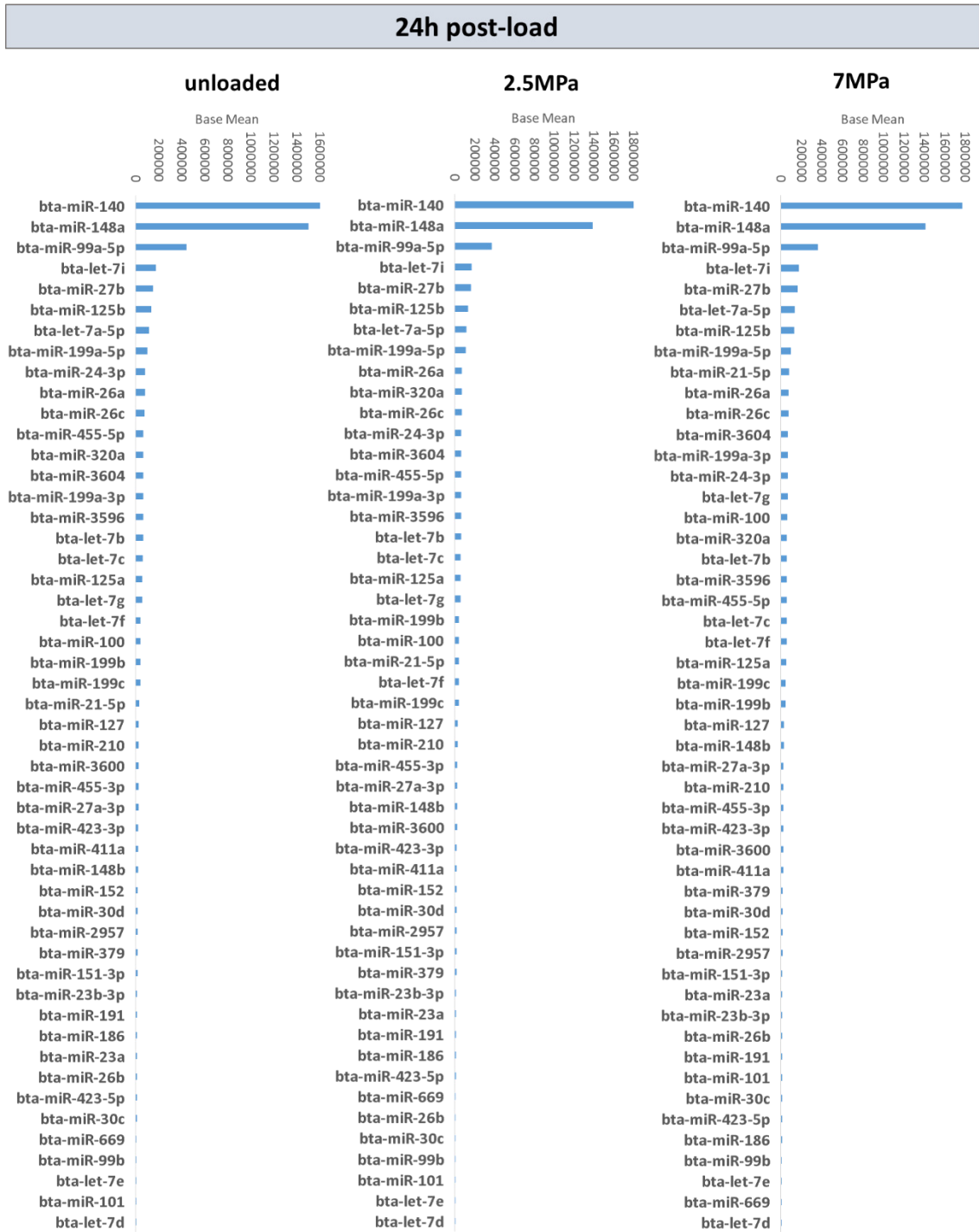


**Figure 4.4.** Top 50 most abundantly expressed miRNAs in articular cartilage at 24h post-load. Analysis of pooled samples that were either unloaded (n = 6) or were subjected to 2.5MPa (n = 6) or 7MPa (n = 6) load (1Hz, 15 minutes) was conducted by Next Generation Sequencing across all samples (N = 3).

**Table 4.1.** Mechanically regulated miRs identified in explants subjected to compressive load (2.5MPa or 7MPa, 1Hz, 15 minutes) compared to unloaded explants, and processed 2, 6 or 24h post-load (FDR  $\leq$  0.05).

<b>2h post-load</b>	<b>6h post-load</b>	<b>24h post-load</b>
bta-miR-23a	bta-miR-222	bta-miR-7
bta-miR-23b-3p	bta-miR-677	bta-miR-20a
bta-miR-27a-5p	bta-miR-486	bta-miR-21-5p
bta-miR-98	bta-miR-1249	bta-miR-27a-5p
bta-miR-148b	bta-miR-2889	bta-miR-100
bta-miR-1260b		bta-miR-155
bta-miR-2478		bta-miR-221
bta-miR-2898		bta-miR-222
		bta-miR-425-5p
		bta-miR-431
		bta-miR-451
		bta-miR-483
		bta-miR-495
		bta-miR-543
		bta-miR-760-3p
		bta-miR-2318
		bta-miR-2344

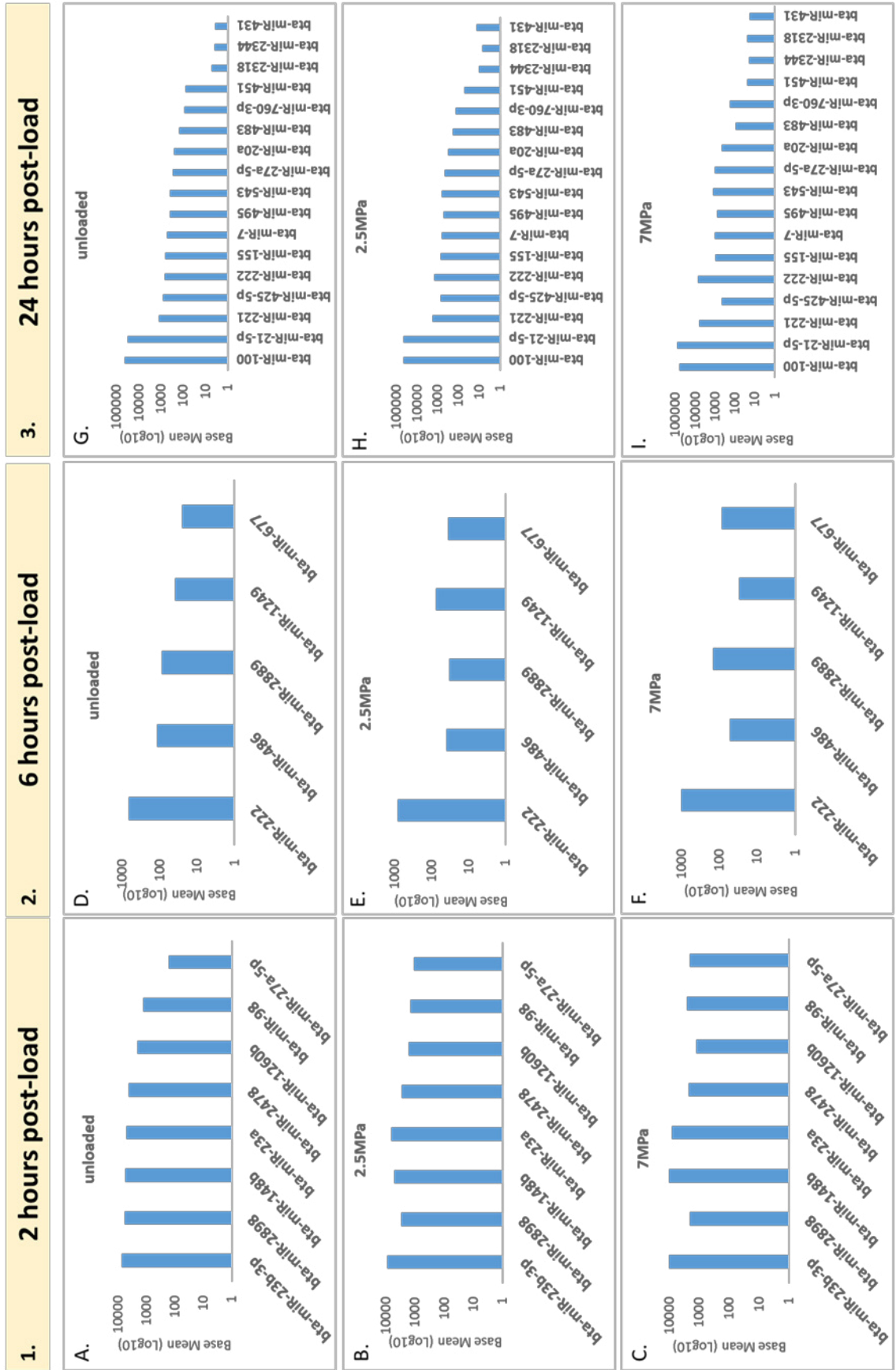


**Figure 4.5.** The base mean counts of all differentially expressed miRs when comparing expression levels between 7MPa and 2.5MPa vs unloaded or 7MPa vs 2.5MPa load. The mean base counts from three independent experiments for unloaded and loaded explants is presented according to: unloaded **(A,D,G)**, 2.5MPa load **(B,E,H)** and 7MPa load **(C,F,I)** at 2h **(1)**, 6h **(2)** and 24h **(3)** post-load.

**2h post-load:** Expression levels of miR-27a-5p (4.42-fold: FDR<0.001) and miR-2898 (1.73-fold: FDR=0.008) were significantly increased and decreased respectively in explants subjected to a 2.5MPa load in comparison to unloaded tissue (Figure 4.6A). A 7MPa load significantly elevated expression levels of miR-23a (1.46-fold: FDR=0.034), miR-23b-3p (1.54-fold: FDR=0.004), miR-27a-5p (7.09-fold: FDR<0.001), miR-98 (1.70-fold: FDR=0.001) and miR-148b (1.64-fold: FDR=0.039, Figure 4.6B); in contrast, identified miRs that were significantly down-regulated in response to a 7MPa load included miR-1260b (1.55-fold: FDR=0.025), miR-2478 (1.77-fold: FDR=0.001) and miR-2898 (2.45-fold: FDR<0.001, Figure 4.6B). However, there were no significant changes in miR levels when comparing the data obtained from the 2.5MPa versus 7MPa loads.

**6h post-load:** Very few changes in miR expression were observed after 6h post-cessation of load, however a 2.5MPa load decreased miR-486 expression (1.92-fold: FDR=0.002) in cartilage explants when compared to unloaded tissue (Figure 4.7A). In contrast, a 7MPa load elevated the levels of miR-222 (1.57-fold: FDR=0.008) and miR-667 (2.15-fold: FDR<0.001, Figure 4.7B). When comparing the two loading regimes directly, a 7MPa load induced higher expression of miR-667 (1.93-fold: FDR=0.001) and miR-2889 (2.39-fold: FDR<0.001), whilst reducing miR-1249 levels (1.78-fold: FDR=0.013) compared to the lower load of 2.5MPa (Figure 4.7C).

**24h post-load:** Analysis of miR expression 24h post-cessation of load indicated that only miR-222 was differentially increased (1.81-fold: FDR=0.003) in response to a 2.5MPa load when compared to unloaded explants (Figure 4.8A). In response to the 7MPa regime, many more miRNAs were mechanically regulated including elevation of: miR-7 (1.70-fold: FDR=0.017), miR-21-5p (2.27-fold: FDR<0.001), miR-27a-5p (3.02-fold: FDR<0.001), miR-100 (1.43-fold: FDR=0.048), miR-155 (1.47-fold: FDR=0.042), miR-221 (3.39-fold: FDR<0.001), miR-222 (7.41-fold: FDR<0.001), miR-431 (1.82-fold: FDR=0.030), miR-495 (1.78-fold: FDR<0.001), miR-543 (2.62-fold: FDR<0.001), miR-760-3p (1.72-fold: FDR=0.017), miR-2318 (1.85-fold: FDR=0.022) and miR-2344 (1.82-fold: FDR=0.030); miRs that were significantly decreased in response to a 7MPa load included: miR-425-5p (1.60-fold: FDR=0.010) and miR-451 (2.08-fold: FDR=0.002, Figure 4.8B). When directly comparing expression levels between the 2.5MPa and 7MPa loads, there

was significant up-regulation of miRs such as: miR-21-5p (1.72-fold: FDR=0.013), miR-27a-5p (2.03-fold: FDR<0.001), miR-221 (2.59-fold: FDR<0.001), miR-222 (4.09-fold: FDR<0.001) and miR-543 (1.73-fold: FDR=0.005), concomitant with down-regulation of miR-425-5p (1.49-fold: FDR=0.037) and miR-483 (1.79-fold: FDR=0.025, Figure 4.8C).

2h post-load

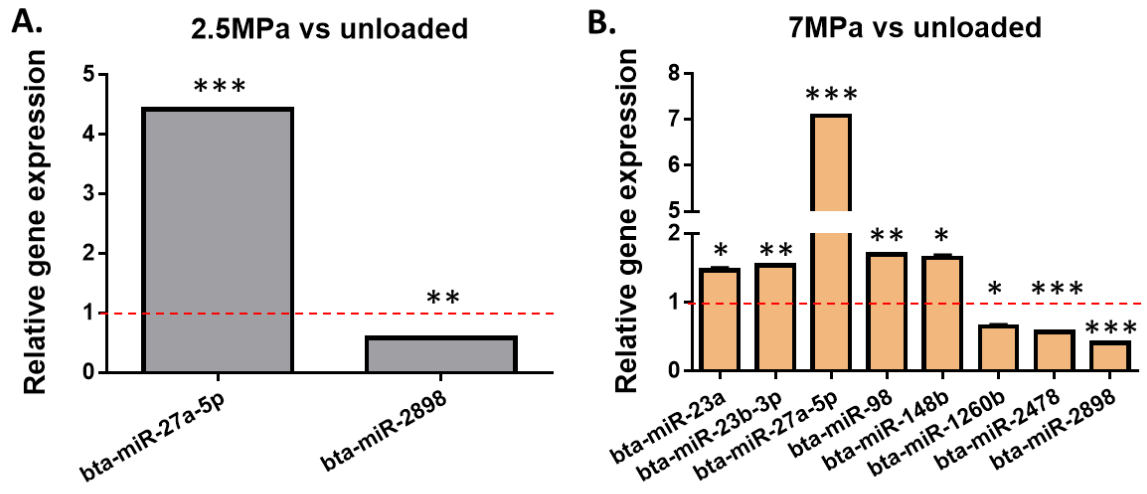


**Figure 4.6.** Differential expression of mechanically regulated miRNAs in explants subjected to either a 2.5MPa **(A)** or 7MPa **(B)** load and analysed at 2h post-load. Unloaded explants served as controls and the expression of each miR in these unloaded samples is presented as 1 (dotted line) **(A,B)**. Analysis of pooled samples that were either unloaded (n = 6) or were subjected to 2.5MPa (n = 6) or 7MPa (n = 6) load was conducted by Next Generation Sequencing. Results presented are the mean of three independent experiments (N = 3). Key: MPa - megapascal, vs - versus, [\* FDR≤0.05, \*\* FDR≤0.01, \*\*\* FDR≤0.001].

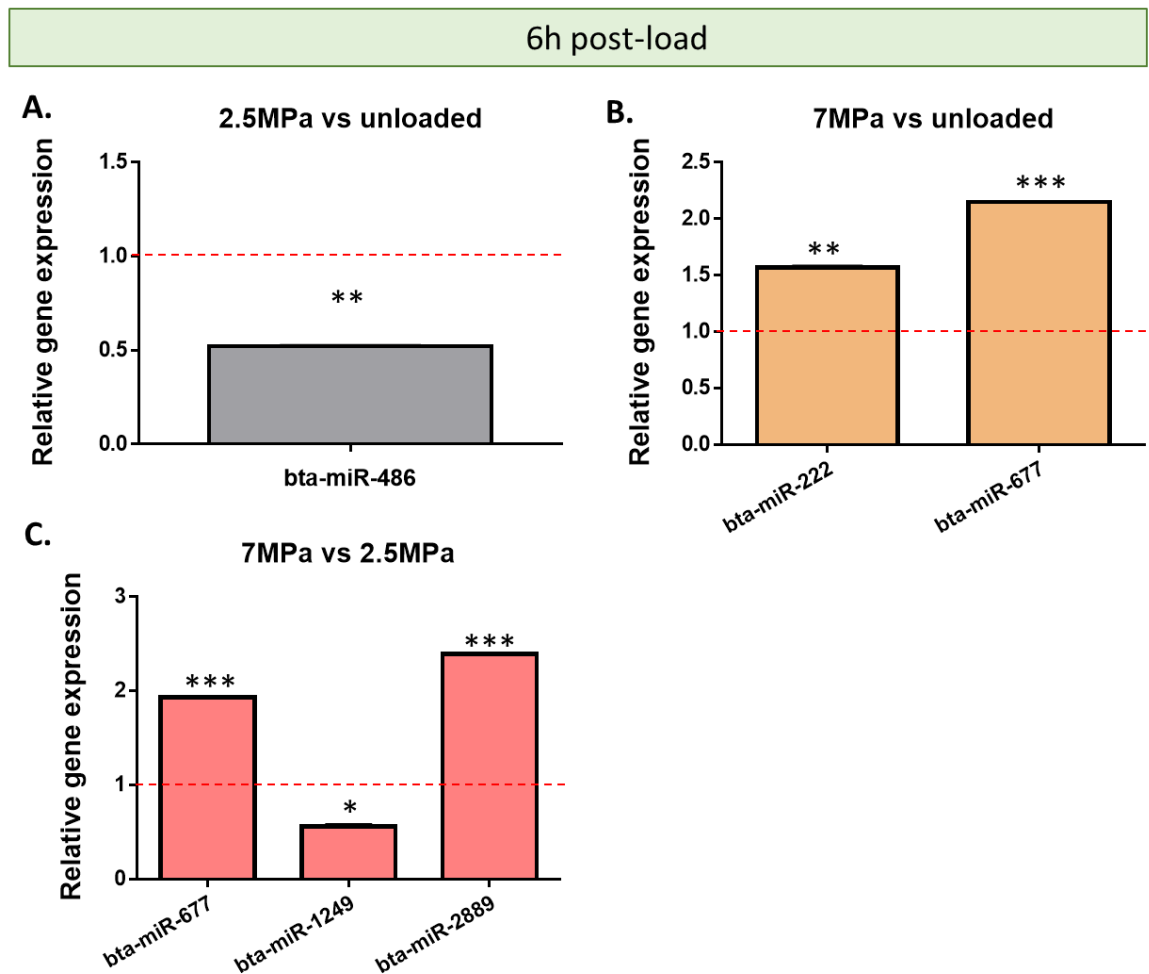


**Figure 4.7.** Differential expression of mechanically regulated miRNAs in explants subjected to either a 2.5MPa (A) or 7MPa (B) load and analysed at specific periods of 6h post-load. Unloaded explants served as controls and the expression of each miRNA in these unloaded samples is presented as 1 (dotted line) (A,B,C), however data were normalised to the 2.5MPa load when comparing the two loading regimes directly (C). Analysis of pooled samples that were either unloaded (n = 6) or were subjected to 2.5MPa (n = 6) or 7MPa (n = 6) load was conducted by Next Generation Sequencing. Results presented are the mean of three independent experiments (N = 3). Key: MPa - megapascal, vs - versus, [\* FDR≤0.05, \*\* FDR≤0.01, \*\*\* FDR≤0.001].

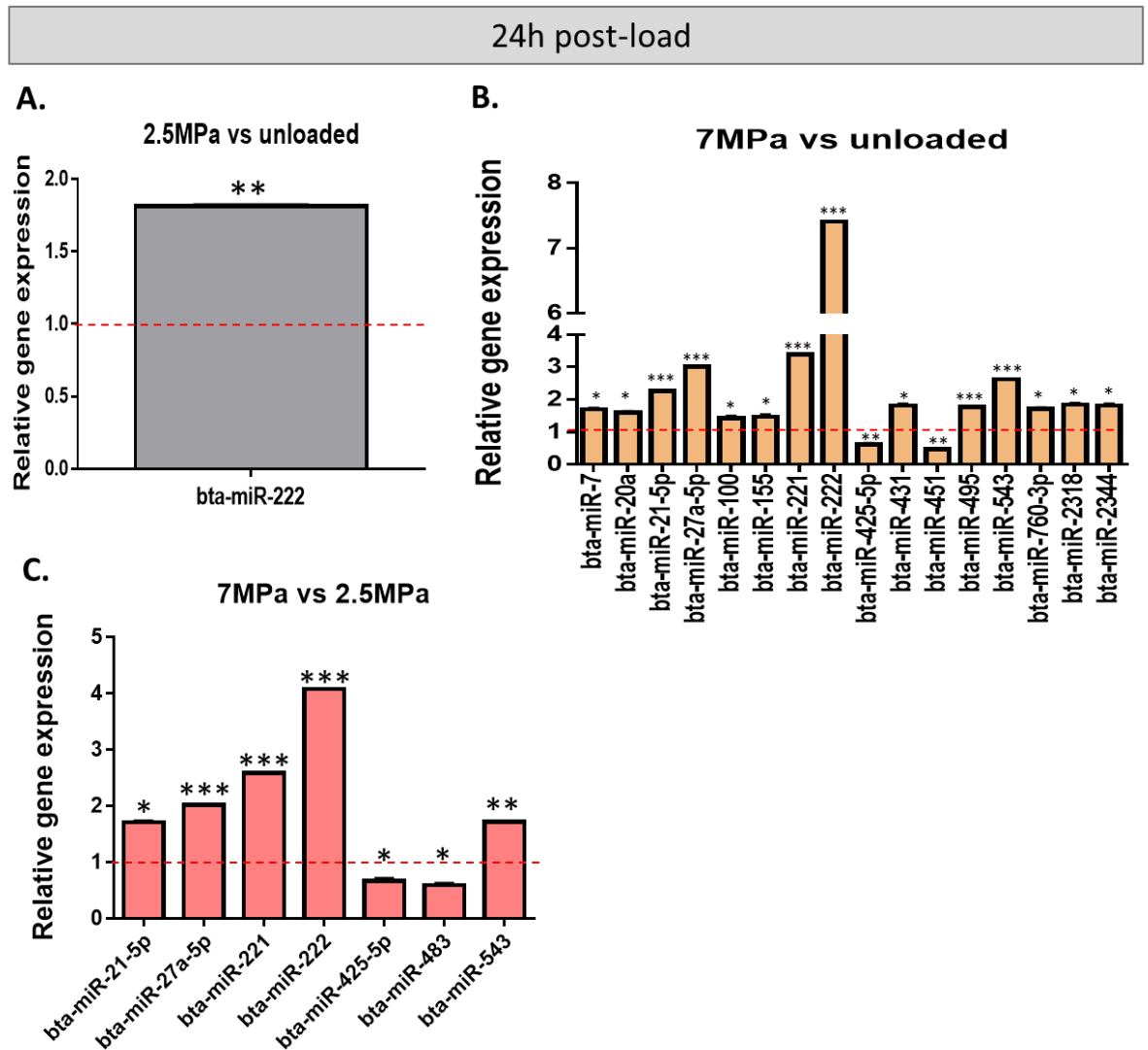


**Figure 4.8.** Differential expression of mechanically regulated miRs in explants subjected to either a 2.5MPa **(A)** or 7MPa **(B)** load and analysed at specific periods of 24h post-load. Unloaded explants served as controls and the expression of each miR in these unloaded samples is presented as 1 (dotted line) **(A,B,C)**, however data were normalised to the 2.5MPa load when comparing the two loading regimes directly **(C)**. Analysis of pooled samples that were either unloaded (n = 6) or were subjected to 2.5MPa (n = 6) or 7MPa (n = 6) load was conducted by Next Generation Sequencing. Results presented are the mean of three independent experiments (N = 3). Key: MPa - megapascal, vs - versus, [\* FDR≤0.05, \*\* FDR≤0.01, \*\*\* FDR≤0.001].

### **4.2.3. Validation of putative mechanically regulated miRs in articular cartilage**

Having identified mechanically-regulated miRs using NGS, the results were validated by quantitative PCR using TaqMan® technology. The results from the NGS indicated that most of the differentially regulated genes were present at 24h post-load (Figure 4.8), therefore this time point was focused on. miRs that demonstrated significant differences in expression in both comparisons i.e. unloaded vs loaded (2.5MPa or 7MPa) and 2.5MPa vs 7MPa loads were selected for validation. Validation was performed on three independent experiments (n = 6 explants per experiment) to confirm the NGS observations.

miR-21-5p presented a significantly differentiated expression (1.99-fold: p=0.034) in response to a 7MPa load, whereas 2.5MPa appeared to slightly increase miR-21-5p levels, however the change was not statistically significant (Figure 4.9A).

A significant increase in miR-27a-5p expression was observed in explants subjected to a 7MPa load when compared to the unloaded tissue (2.56-fold: p=0.001). There was also a significant response to increasing load with higher levels of miR-27a-5p in response to 7MPa load when compared to the 2.5MPa loading response (2.39-fold: p<0.001; Figure 4.9B).

Validation confirmed the elevated expression of miR-221 in explants subjected to the 7MPa load when compared to either the unloaded (3.89-fold: p<0.001) or 2.5MPa loading regime (2.55-fold: p=0.011; Figure 4.9C). In a similar manner, miR-222 was also significantly up-regulated in response to the 7MPa load when compared to either unloaded (3.78-fold: p<0.001) or the 2.5MPa regime (2.82-fold: p=0.002, Figure 4.9D). Interestingly, the qPCR analysis demonstrated that the lower load of 2.5MPa did not significantly affect the expression of either miR-221 or miR-222 when compared to the unloaded cartilage (Figure 4.9C and D), suggesting that they are responsive to higher loads only.

Of the remaining miRs, there was a high degree of variability in expression levels of miR-451 as demonstrated by the large error bars (Figure 4.10A). The observed reduction in miR-483, as detected by NGS, was confirmed when comparing the response of explants to 7MPa load versus unloaded (1.98-fold:  $p=0.047$ ; Figure 4.10B).

Expression of miR-543 was found to be significantly elevated in response to the 7MPa load, as detected by NGS (Figure 4.8B), however this differential regulation was not validated using qPCR (Figure 4.10C).

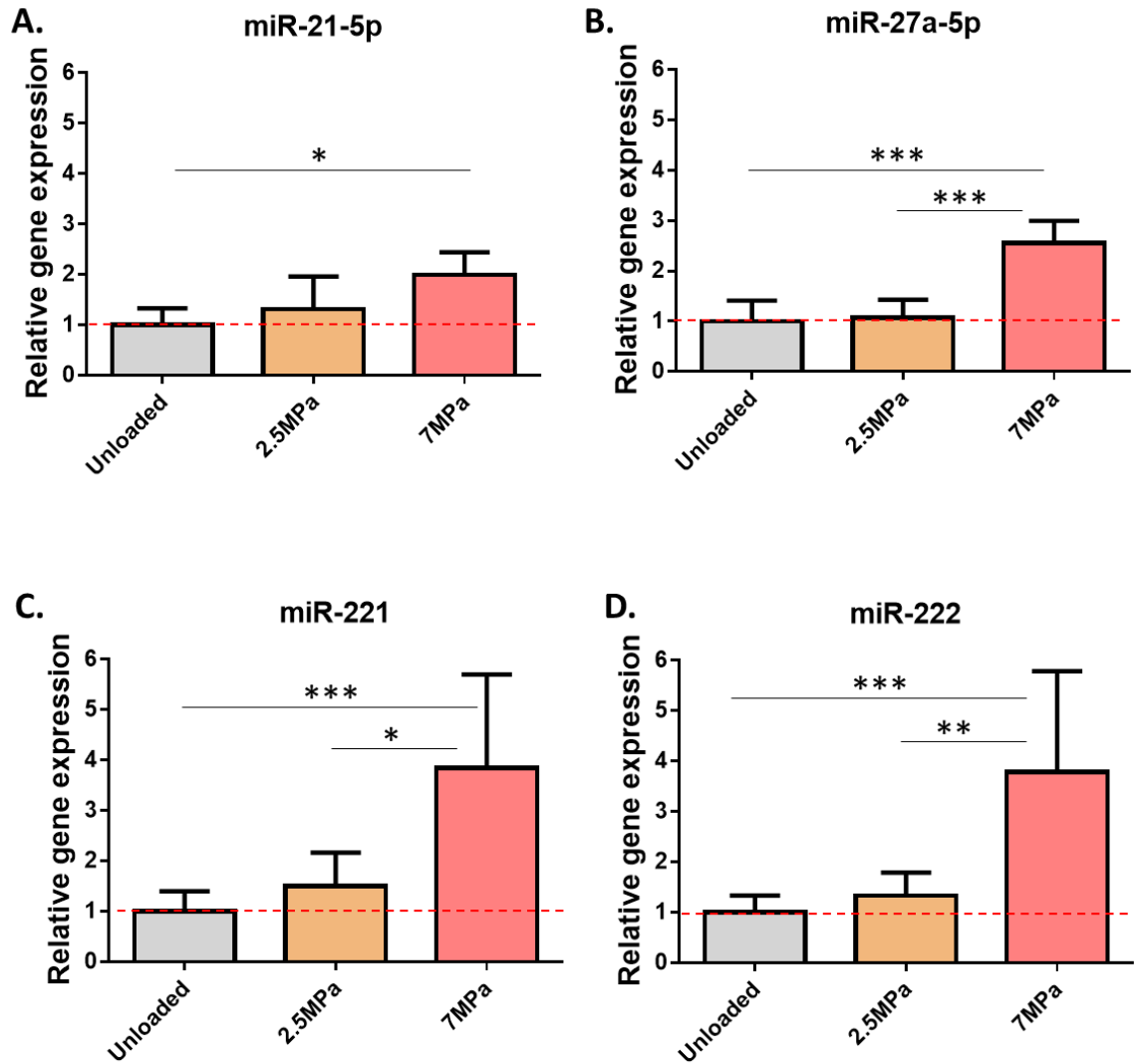


**Figure 4.9.** Validation of significant mechanically regulated mature miRNAs that were selected on the basis of NGS data. Analysis of samples that were either unloaded ( $n = 6$ ) or were subjected to 2.5MPa ( $n = 6$ ) or 7MPa ( $n = 6$ ) (1Hz, 15 minutes load) and processed 24h post-load was conducted using qPCR with TaqMan™ Fast Advance technology. miR levels were normalised to the geometric mean of 2 reference genes (SDHA, YWHAZ) and further normalised relative to the unloaded controls. Data are presented as mean  $\pm$ SD ( $n = 6$  explants) and is representative of 3 independent experiments for each miR: miR-21-5p (**A**), miR-27a-5p (**B**), miR-221 (**C**), miR-222 (**D**). Statistical analysis was performed using a 1-way ANOVA with Tukey's post hoc test. Key: unloaded (control), 2.5MPa, 7MPa (loaded) [ $*p \leq 0.05$ ,  $**p \leq 0.01$ ,  $***p \leq 0.001$ ].

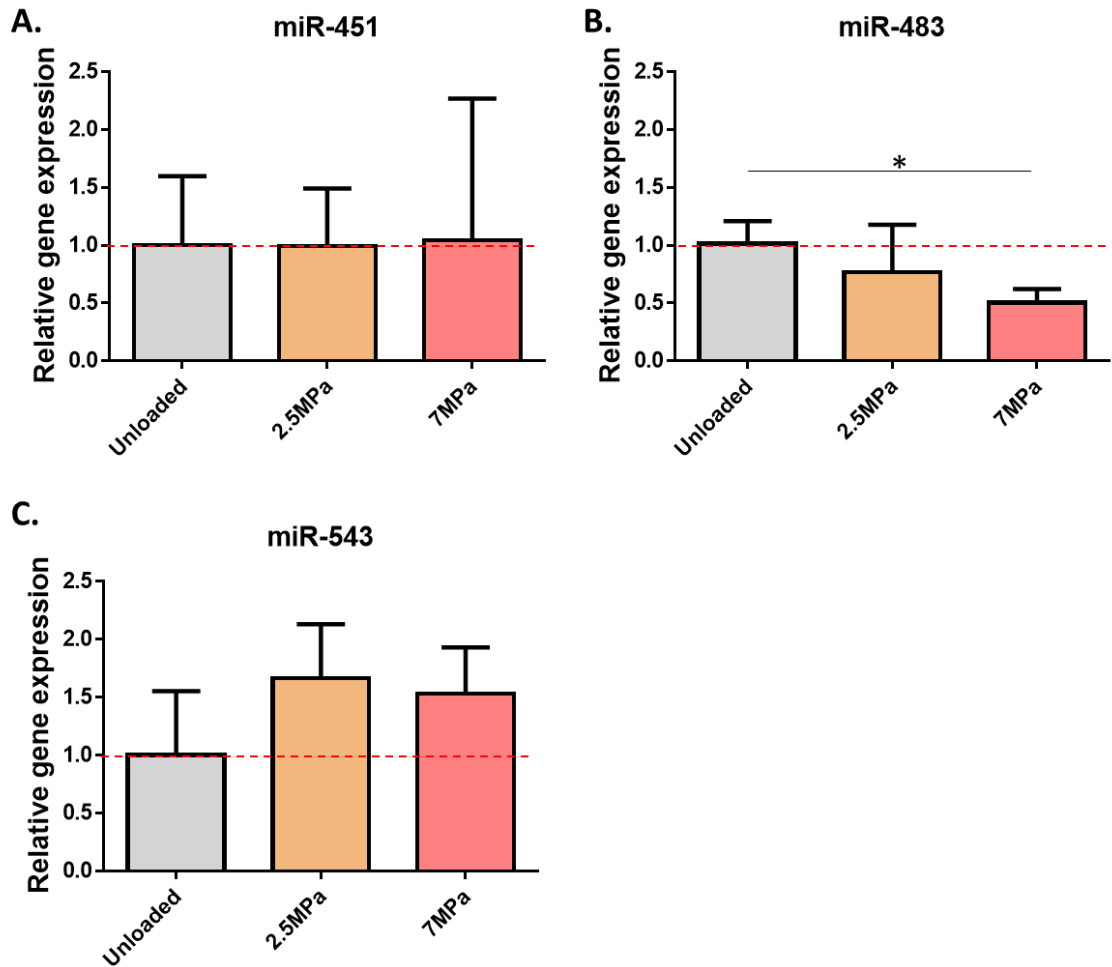


**Figure 4.10.** Validation of significant mechanically regulated mature miRNAs that were selected on the basis of NGS data. Analysis of samples that were either unloaded ( $n = 6$ ) or were subjected to 2.5MPa ( $n = 6$ ) or 7MPa ( $n = 6$ ) (1 Hz, 15 minutes load) and processed 24h post-load was conducted using qPCR with TaqMan™ Fast Advance technology. miR levels were normalised to the geometric mean of 2 reference genes (SDHA, YWHAZ) and further normalised relative to the unloaded controls. Data are presented as mean  $\pm$ SD ( $n = 6$  explants) and is representative of 3 independent experiments for each miR: miR-451 (**A**) miR-483 (**B**) and miR-543 (**C**). Statistical analysis was performed using a 1-way ANOVA with Tukey's post hoc test. Key: unloaded (control), 2.5MPa, 7MPa (loaded) [ $*p \leq 0.05$ ].

### 4.3. Discussion

Since 1993 when the miR molecule was initially discovered, the importance of these small non-coding RNA molecules has been widely reported. During this time, the role of miRs in articular cartilage has also been studied, and they are believed to have great significance in cartilage development, homeostasis and degradation (Mirzamohammadi et al., 2014). Of the many important factors that influence cartilage homeostasis, mechanical load is essential for the regulation of cartilage metabolism in order to keep cartilage in a healthy condition. Interestingly, there have only been a few studies that have investigated the mechano-sensitive character of miRs in articular chondrocytes including miR-146a (Jin et al., 2014), miR-221/-222 (Dunn et al., 2009) and miR-365 (Guan et al., 2011). With the knowledge that (i) some miRs are regulated by mechanical force in cartilage chondrocytes and (ii) expression of several miRs differ between healthy and OA cartilage the purpose of this experimental chapter was:

- **To identify cartilage miRs that respond to increasing mechanical load that may be potential regulators of genes involved in cartilage degeneration and OA development.**

Cartilage explants were subjected to 2.5MPa and 7MPa loads and were processed 2, 6 or 24h post-cessation of load. The same time points for analysis were applied to the unloaded explants that were used as controls. The time points chosen for this experiment were selected on the basis of the results from our previous studies, whereby the period of time post-cessation of load required to notice differential expression of mechano-regulated matrix genes was optimised (Chapter 3). In our preliminary, optimal timeframe identification experiment, periods of 4h, 8h and 24h post-cessation of load were appropriate to observe changes at the gene level of anabolic and catabolic molecules. As miRs are upstream of the target genes it was decided to select 2h, 6h and 24h as time points, as the miRs regulating anabolic and catabolic gene responses occurring in cartilage are likely to react more quickly to mechanical stimulation than matrix gene transcription.

#### **4.3.1. Preliminary examination of mechano-sensitive miRs**

Before establishing the global expression of miRs in the loaded explants by NGS, a preliminary experiment was performed to determine whether the previously reported mechano-sensitive miR-221 and miR-222 (Dunn et al. 2009) were regulated in my experimental mechanical loading system. In addition to miR-221 and miR-222, the expression levels of miR-140 was also quantified as it is reported to be one of the most important miRs in cartilage homeostasis (Miyaki et al., 2010). The qPCR data demonstrated the mechano-responsiveness of miR-221 and miR-222 confirming previously published studies (Dunn et al., 2009, Mohamed et al., 2010, Mendias et al., 2012). Interestingly, our preliminary results also indicated that the expression of miR-221 and miR-222 was only significantly increased when higher loads (7MPa) were applied, as they did not appear to be differentially regulated by the lower (2.5MPa) load in comparison to the unloaded. Surprisingly, miR-140 was also sensitive to mechanical stimulation and was significantly decreased in explants subjected to a 7MPa load compared to the unloaded explants when analysed after 24h. The mechano-sensitivity of miR-140 has been previously demonstrated in tendons (Mendias et al., 2012) and smooth muscle cells (Mohamed et al., 2010) but not in chondrocytes. In these studies, expression levels of miR-140 were significantly decreased in rat achilles tendons which were running for 30 minutes on an uphill treadmill with increasing elevation every 10 minutes (Mendias et al., 2012), and elevated in primary human airway smooth muscle cells subjected to 1h of cyclic stretch (1Hz, 0.5 seconds deformation/0.5 seconds relaxation) (Mohamed et al., 2010). These findings suggest that miR-140 expression is mechano-sensitive.

#### **4.3.2. Which miRs are the most abundant in articular cartilage?**

The NGS data was processed by Andrew Skelton (bioinformatician from Newcastle University) who performed all of the analyses. By using a combination of RSamTools (Morgan, 2011) and ShortRead (Morgan et al., 2009) bioconductor packages, the miRs present in the experimental material were detected and quantified which was the first necessary step prior to further analysis to determine whether the applied loading regimes affected the expression levels of cartilage miRs.

Of the top 50 most abundant miRs in articular cartilage (comparing data from loaded and unloaded tissue at all of the time points analysed) miR-140 and miR-148a were consistently present in the top two. This data are consistent with a previous study which demonstrated that one of the most highly expressed chondrocyte miRs is miR-140 (McAlinden et al., 2013). McAlinden et al. compared miR levels during the process of chondrogenesis and demonstrated that miR-140 is the most highly expressed miR in all three stages of the chondrocyte phenotype examined (precursor, differentiated and hypertrophic). Surprisingly, miR-148a that is known to play an important role in cartilage homeostasis by promoting the synthesis of collagen type II and inhibiting the mRNA levels of collagen type X, MMP-13 and ADAMTS-5 in the ECM (Vonk et al., 2014) was not present on the list of the top 30 most abundant miRs in any of the chondrocyte developmental stages examined (McAlinden et al., 2013). This was unexpected, especially because the results presented in this chapter demonstrate similar expression levels of miR-148a and miR-140 with some rotation in the top two places depending on the experimental condition.

#### **4.3.3. Identification of mechanically regulated miRs in articular cartilage**

NGS is widely used as a tool in both the clinical and research arena, and has revolutionised the field of genomics and molecular biology. It gives the opportunity to analyse the entire human genome within a few days (Ulahannan et al., 2013) and is characterised by a high sensitivity and reproducibility of data. Unfortunately, NGS and analysis of deep sequencing reads is not perfect and there are some risk factors that may affect the interpretation of data from deep sequencing, e.g. ligation bias of small RNAs during library preparation (Sorefan et al., 2012, Raabe et al., 2014) and incorrect mapping of genes to the reference genome (Ulahannan et al., 2013). To avoid false positive/negative results, miRs that are found to be significantly altered according to NGS data require validation. Three different periods post-cessation of load were examined to find the optimal timeframe to monitor the greatest number of significantly altered miRs in response to applied loads. The 2.5MPa loading regime, as was expected, altered expression of less miRs than the 7MPa load in all tested time points giving 2, 1 and 1 altered miRs at 2, 6 and 24h post-load, respectively, whereas the non-physiological

(7MPa) magnitude of load induced significant changes in expression levels in 8, 2 and 16 miRs at 2, 6 and 24h periods post-cessation of load, respectively. Levels of expression of only 3 and 7 miRs were changed respectively at 6 and 24h after the 7MPa load when normalised to 2.5MPa loading regimes, whereas no changes were observed at the earliest (2h) time point (Figure 4.6, 4.7, 4.8). The panel of miRs that were chosen for further validation were selected based on two criteria: (i) at least a 2-fold change in expression between loaded and unloaded explants or (ii) potential significance in OA development reported in the literature. As indicated, because most of the effects were observed at 24h post-cessation of load, the selected miRs were predominantly identified from this data set for validation. Normalisation of the qPCR data was performed against the geometric mean of the specific reference genes: SDHA and YWHAZ which had previously been established to be most stable in expression under the experimental system utilised. Most published studies analysing miRs expression level have used U6 spliceosomal RNA (U6) as a reference gene, however in my experimental system this gene was found to be unstable, therefore it was not used in my study.

Of the miRs identified by NGS and validated by qPCR, the most robustly altered miRs regulated by mechanical load (7MPa) are miR-221 and miR-222; these miRs were up-regulated by almost 4-fold in comparison to unloaded controls and approximately 2.5-fold when compared to 2.5MPa load. These results corroborate the mechano-sensitive nature of miR-221 and miR-222 as demonstrated in our preliminary experiments and in previously published studies (Dunn et al., 2009, Mendias et al., 2012). Dunn et al. (2009) demonstrated that the level of these miRs is increased in the superficial zone of anterior weight-bearing cartilage when compared to either the posterior non-weight bearing superficial zone or middle zone of anterior weight-bearing tissue in bovine stifle joint (Dunn et al., 2009).

Another mechano-responsive miR was miR-21-5p that presented increased expression in response to high load (7MPa). These novel results in chondrocytes are consistent with several other studies that have reported on the mechano-regulation of miR-21 (Song et al., 2012, Weber et al., 2010, Zhou et al., 2011). Song et al. (2012) exposed human aortic smooth muscle cells to elevated tensile strain (16%, 1Hz, 12h) which induced increased expression of miR-21 (tao Song et al., 2012). Other groups have shown that steady

laminar shear stress (LSS; 15 dynes/cm<sup>2</sup>) (Weber et al., 2010) and oscillatory shear stress (OSS; 0.5 ± 4 dynes/cm<sup>2</sup>) (Zhou et al., 2011) applied to human umbilical vein endothelial cells elevated miR-21 expression, whereas pulsatile shear stress (PSS; 12 ± 4 dynes/cm<sup>2</sup>) inhibited the expression of miR-21 at the transcriptional level (Zhou et al., 2011). However, to date, there are no published reports on the response of miR-21 to mechanical load in cartilage chondrocytes making this a novel finding.

Another NGS-identified miR which was found to be significantly elevated in response to high loads (7MPa) was miR-27a-5p. The human genome contains two miR-27 genes: miR-27a and miR-27b, but the mature product of these miRs differ by only one nucleotide in the 3' UTR region leaving the seed region unchanged (Demolli et al., 2013). The novel finding that miR-27a is mechanically regulated in chondrocytes, corroborates the findings of other groups who demonstrated that both miR-27a and miR-27b were up-regulated in endothelial cells subjected to 18h and 24h laminar flow (15 dynes/cm<sup>2</sup>) (Urbich et al., 2012).

The results of the NGS and qPCR validation indicated that miR-483 levels were significantly reduced in response to high loads (7MPa), but interestingly, to date there is no published data referring to the mechano-responsiveness of this miR in any cell type, again reflecting the novelty of this finding.

The role of these validated miRs in cartilage homeostasis and/or OA development will be described in further depth in Chapter 5.

#### **4.3.4. Summary:**

- The most abundantly expressed miRs in articular cartilage are: miR-140 and miR-148 and their expression remains constant irrespective of the magnitude of compressive load or period post-cessation of load
- Differential expression of miRs in articular cartilage were most evident at 24h post-cessation of load and were magnitude-dependent i.e. most miRs were affected by the higher 7MPa load only
- miR-221 and miR-222 were confirmed as being mechano-sensitive in cartilage chondrocytes as previously reported (Dunn et al., 2009)
- Novel findings that miR-21-5p, miR-27a-5p and miR-483 are mechanically regulated in cartilage chondrocytes

# Chapter 5

Identification of direct targets of  
mechanically-regulated miRs

## 5.1. Background

NGS and qPCR validation performed in Chapter 4 identified a number of mechanically-regulated miRs in articular cartilage: miR-21-5p, miR-27a-5p, miR-221 and miR-222. Although the identification of mechano-sensitive miRs in articular cartilage was one of the objectives of this PhD, an awareness of the existence of these differentially-regulated miRs and knowledge of their reported functions is not enough to have an input into understanding the correlation between miRs, mechanical load and OA pathogenesis.

Although the function of miRs is clear i.e. controlling the level of target molecule expression in cells by regulation of their genes at the post-transcriptional level, a working mechanism of gene target recognition is still not completely understood. The target genes are recognised by miRs based on the miR:mRNA base pairing that does not have to be perfectly matched. The target sites (allocated on mRNA) that allow miRs to control mRNA expression can be classified into four groups: (i) 5'- dominant canonical, (ii) 5'- dominant seed only, (iii) 3'-compensatory (Brennecke et al., 2005) and (iv) centred (Shin et al., 2010) as described below.

The canonical site is well paired at both the 5' and 3' ends. The dominant seed only site has perfect base pairing at the most evolutionary conserved miR sequence called the "seed region" (Lewis et al., 2003) positioned at the miR 5' end, with little or no 3' miR pairing (Brennecke et al., 2005). The 3' compensatory site depends on strong pairing to the miR 3' end, to compensate for mismatches or short base pairing to the seed region (Brennecke et al., 2005). The centred site is a sequence of at least 11 base pairs that perfectly match to the miR at the following nucleotide positions: 4-14 or 5-15 and lack the seed region and 3'-compensatory complementarity (Shin et al., 2010). As the abundance of both 3'-compensatory and centred sites is relatively low compared to seed-matched sites (Shin et al., 2010), the seed region at the miR 5' end is commonly acknowledged as the most important sequence in mRNA targeting (Thomson et al., 2011).

Focusing on the seed region that is the main area of binding, it must be paired to a seed-matched site that is mostly allocated at the 3' UTR target mRNA, however a small

subset of miRs are also able to control expression of some genes by targeting the 5'UTR (Lee et al., 2009) or coding region of mRNA (Brümmer and Hausser, 2014). Although targeting mRNA can occur in three different locations (3'UTR, 5'UTR and coding regions) that usually contains at least one type of seed-matched site (6mer, 7mer-m8, 7mermA1, 8mer), the most effective protein reduction occurs as a result of miR binding to the 3'UTR (Baek et al., 2008, Fang and Rajewsky, 2011, Bartel, 2009) with a minimum of one 7mer-m8 seed-matched site in the mRNA (Baek et al., 2008, Grimson et al., 2007).

To explore the functional role of a specific miR and determine their influence on target genes, precise target prediction is essential. To identify miR target molecules, bioinformatic approaches are commonly used and these are the most popular prediction programmes: TargetScan (Lewis et al., 2003), miRanda (Betel et al., 2008) and PicTar (Krek et al., 2005). Each programme uses its own algorithm to identify target genes of a selected miR, therefore unfortunately, the results when compared between different online prediction systems are not always the same (Sethupathy et al., 2006).

Computational prediction of target mRNA is the first step in the identification of specific miR:mRNA interactions, but unfortunately it is not good enough to use it as the only way of identifying target genes. One of the biggest problems with using prediction algorithms to identify target genes is that these programmes are focused on searching mRNAs containing target sites in their 3'UTR, ignoring 5'UTR and coding regions (Thomson et al., 2011, Moqadam et al., 2013). In addition, the algorithms select target genes based on the exact seed site complementarity, paying no attention to other groups of target sites that can still result in gene repression (described at the beginning of this chapter) (Moqadam et al., 2013). In addition, one mRNA might be regulated by more than one miR and multiple miRs may have to act together to affect individual protein expression (Thomson et al., 2011). This means that apart from bioinformatic analysis, all biological outcomes of a miR:mRNA interaction must be examined experimentally to observe the real influence of a miR on potential target molecules.

**Summary of the aims of this experimental chapter:**

- **Establish whether the identified mechano-sensitive miRs control the expression of ECM molecules that have an involvement in cartilage homeostasis and/or OA development**

## **5.2. Results**

NGS analysis of miR levels in articular cartilage explants subjected to different loading regimes identified several miRs as being mechanically-regulated, which were subsequently confirmed by qPCR validation (Chapter 4). The next step was to identify the downstream target genes of the miRs selected for further exploration which included miR-21-5p, miR-27a-5p, miR-221 and miR-222. The choice of miR-21-5p, miR-27a-5p, miR-221 and miR-222 over the other differentially-regulated miRs was made based on their: (i) mRNA level in loaded explants compared to unloaded tissue and (ii) published reports of their differential expression levels in OA cartilage compared to healthy tissue. In addition to using a computational algorithm for prediction of putative target genes (<http://www.targetscan.org/>), these targets were also validated experimentally to confirm the TargetScan results. To examine experimentally the direct regulation of predicted downstream target genes by the miRs, manipulation of the expression levels of selected miRs was required.

### **5.2.1. Evaluation of cellular uptake of siRNA**

Before manipulation of miR-21-5p, -27a-5p, -221 and -222 expression levels was performed in primary bovine chondrocytes, the ability of the cells to take up the siRNA was examined using the same experimental conditions planned for miR-21-5p, -27a-5p, -221 and -222 manipulation. Isolated primary chondrocytes were transfected as a monolayer for 48h, and the extent of cellular uptake of Cy3<sup>™</sup>- anti-miR<sup>™</sup> negative control #1 was visualised by fluorescence microscopy. The transfection efficiency was found to be almost 100% for the delivery of siRNA into chondrocytes (Figure 5.1).

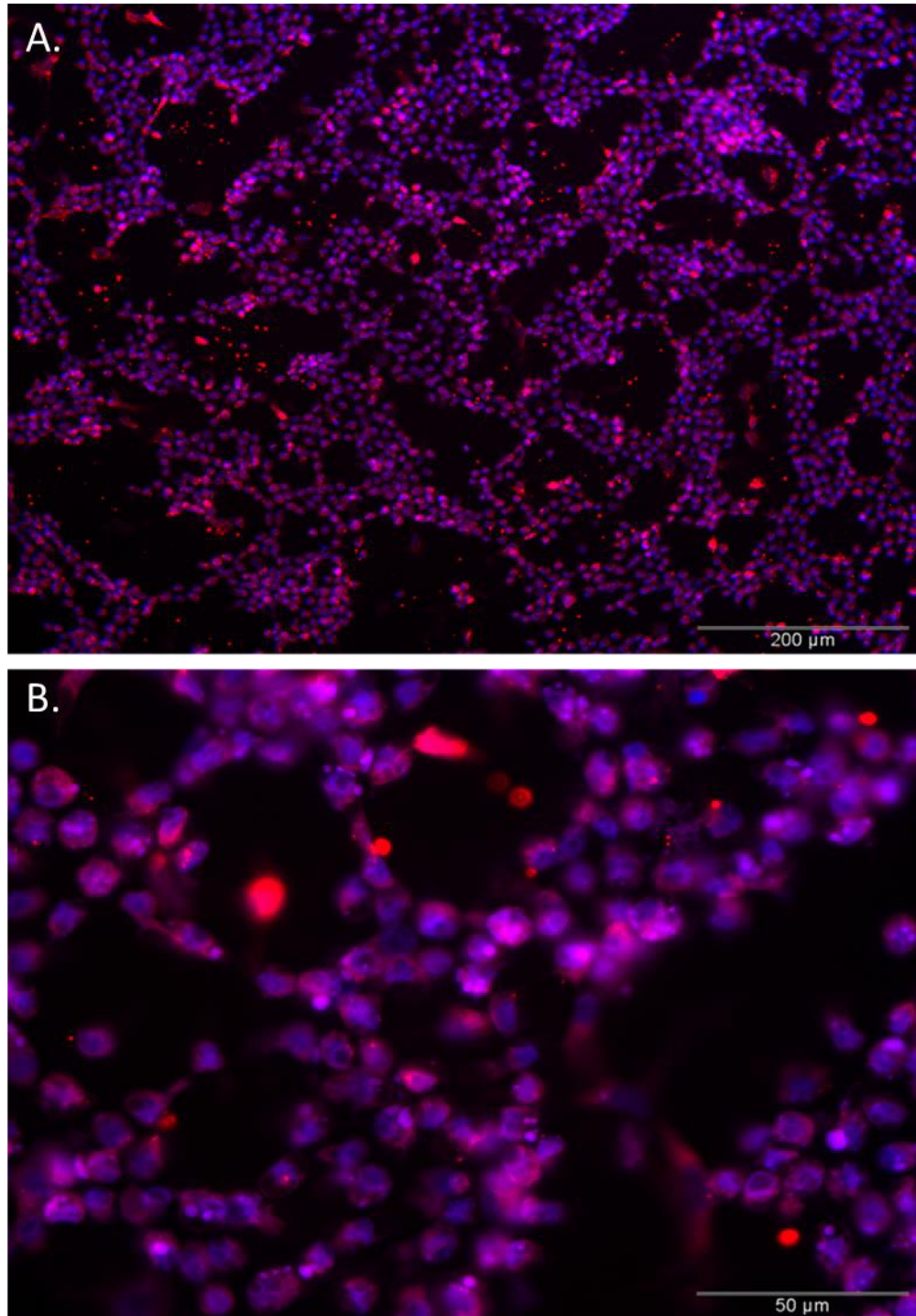


**Figure 5.1.** Cellular uptake of siRNA over a 48h transfection period. The efficiency of chondrocyte transfection was assessed by Cy3™- anti-miR™ negative control #1 (red) counterstained with DAPI to locate the nuclei (blue) and visualised using fluorescence microscopy. Purple represents transfected cells. Low (A) and high (B) power images of representative cells [Scale bars = 200μm and 50μm respectively].

### 5.2.2. Transfection efficiency of miR inhibitors/mimics

Having assessed the transfection efficiency of primary chondrocytes using an anti-miR™ negative control #1 oligo, the next step was to determine whether the transfection conditions were equally conducive to transfecting a high number of cells using the functional siRNAs to examine the downstream influence on their target genes. The effectiveness of the transfection process on the expression levels of the specific miRs were assessed prior to investigating the direct targets of the selected miRs. qPCR was conducted on cells transfected with inhibitors/mimics of miRs of interest to evaluate the relative expression levels compared to their respective non-targeting controls. In addition, as well as assessing miR inhibitor/mimic transfection experiments, the response of cells to the process of transfection itself was examined.

**Transfection reagent effect:** Primary chondrocytes were transfected with: (i) DharmaFECT1™ transfection reagent only (referred to herein as Mock), (ii) DharmaFECT1™ and Negative Control #1 (non-targeting inhibitor control) or (iii) DharmaFECT1™ and AllStars negative control siRNA (non-targeting mimic control). The levels of miR-21-5p, miR-27a-5p, miR-221 and miR-222 were evaluated in transfected cells using cells treated with non-targeting controls as the baseline control level. The expression levels of miR-21-5p (Figure 5.2A), miR-221 (Figure 5.4A) and miR-222 (Figure 5.5A) did not alter appreciably in either the mock cells or the non-targeting inhibitor/mimic controls compared to untreated controls. Also, miR-27a-5p (Figure 5.3A) did not show statistically significant changes between non-targeting inhibitor control and untreated cells.

Transfection efficiency of functional miRs was assessed by comparison of their expression in cells transfected with their modulators: inhibitors/mimics and cells transfected with non-targeting inhibitor/mimic, respectively.

**miR-21-5p:** Both miR-21-5p inhibitor and mimic affected miR-21-5p expression levels. Although, the knock-down activity of miR-21-5p inhibitor was small, the alteration in miR-21-5p expression in inhibited cells was still significant (1.39-fold:  $p=0.02$ ; Figure 5.2B). In contrast to miR-21-5p inhibitor, miR-21-5p mimic significantly increased miR-21-5p levels (142.32-fold:  $p<0.001$ ; Figure 5.2C).

**miR-27a-5p:** The response of miR-27a-5p expression in primary chondrocytes to miR-27a-5p inhibitor transfection was surprising as the level of miR-27a-5p was slightly down-regulated in one experiment but the change did not reach statistical significance (1.52-fold:  $p=0.39$ ; Figure 5.3B), whereas the second experiment showed a statistically significant up-regulation (3.59-fold:  $p=0.002$ ; Figure 5.3B) of this miR. Due to these unexpected results potential target genes of miR-27a-5p were not examined in the current study.

**miR-221:** miR-221 expression was significantly altered in response to transfection with either the miR-221 inhibitor or miR-221 mimic. As with the miR-21-5p experiment, the effect of miR-221 inhibitor was subtle and resulted in a 2.48-fold decrease in miR-221 expression ( $p=0.01$ ; Figure 5.4B), whereas the specific mimic significantly increased miR-221 levels (289.5-fold:  $p<0.001$ ; Figure 5.4C).

**miR-222:** Delivery of either miR-222 inhibitor or miR-222 mimic to cells also influenced the level of miR-222. Interestingly, miR-222 inhibitor acted more effectively than miR-21-5p or miR-221 on their target sequences, knocking down miR-222 expression by 9.08-fold ( $p<0.001$ ; Figure 5.5B). A significant increase in miR-222 levels was also observed in the presence of the miR-222 mimic (82.45-fold:  $p<0.001$ ; Figure 5.5C).

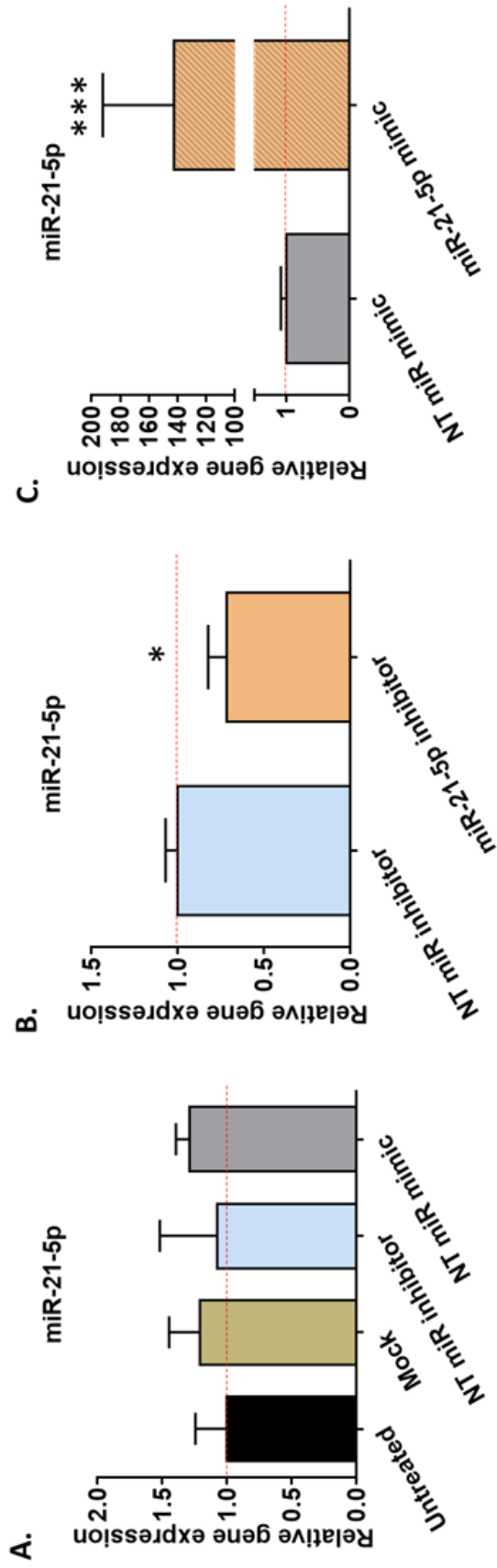


**Figure 5.2.** Expression level of miR-21-5p in response to 48h of transfection. Untreated cells were used as a control for cells transfected with either Dharmafect1 only (Mock) or non-targeting miR inhibitor/mimic (**A**). Cells transfected with 50nM non-targeting miR inhibitor was used as a control to assess relative expression of miR-21-5p in cells transfected with 50nM mirVana® miR-21-5p inhibitor (**B**) or 50nM non-targeting miR mimic was used as a control for miScript miRNA-21 mimic (**C**). miR levels were assessed using qPCR. All data were normalised to the geometric mean of reference genes HPRT and YWHAZ and relative to either untreated or non-targeting controls respectively. Results presented are mean  $\pm$  SD. Statistical analysis was performed using a 1-way ANOVA with Tukey's post hoc test (n = 3 cell culture wells). [\* p $\leq$ 0.05, \*\*\* p $\leq$ 0.001].

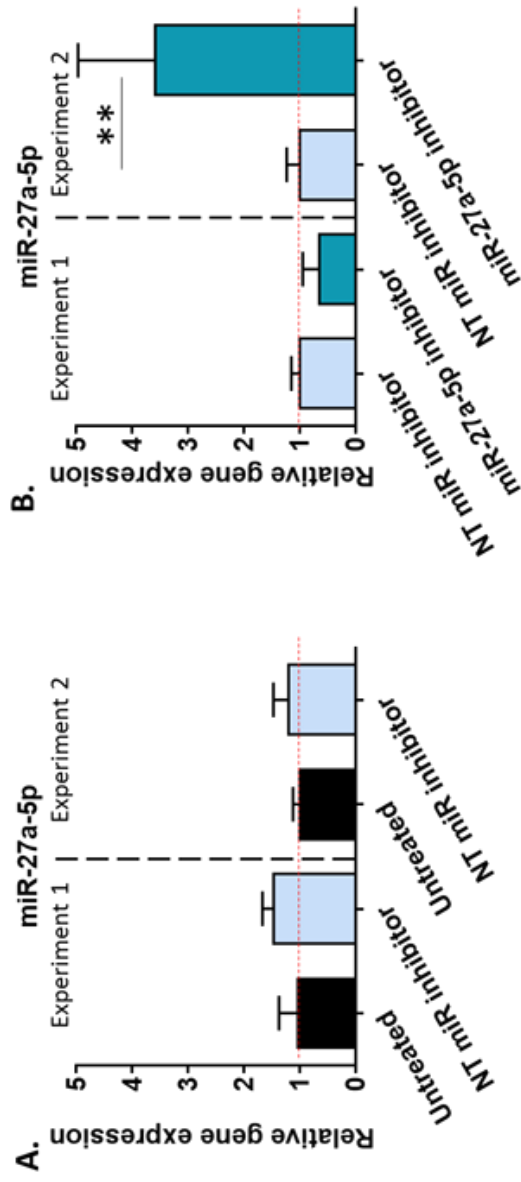


**Figure 5.3.** Expression level of miR-27a-5p in response to 48h of transfection. Untreated cells were used as a control for cells transfected with a non-targeting miR inhibitor (**A**). Cells treated with 50nM non-targeting miR inhibitor was used as a control to assess relative expression of miR-27a-5p in cells transfected with 50nM mirVana® miR-27a-5p inhibitor (**B**). miR levels were assessed using qPCR and results are presented as two independent experiments. All data were normalised to the geometric mean of reference genes HPRT and YWHAZ and relative to either untreated or non-targeting controls respectively. Results presented are mean  $\pm$  SD. Statistical analysis was performed using a 1-way ANOVA with Tukey's post hoc test ( $n = 3$  cell culture wells). [ $** p \leq 0.01$ ].

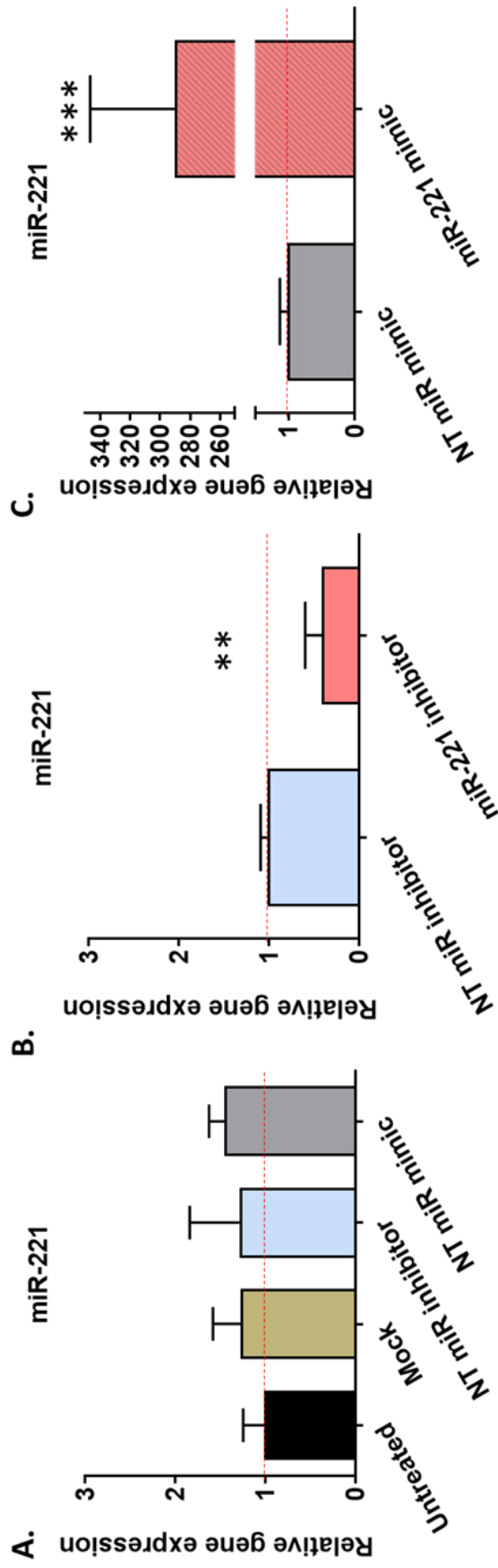


**Figure 5.4.** Expression level of miR-221 in response to 48 h of transfection. Untreated cells were used as a control for cells transfected with either Dharmafect1 only (Mock) or non-targeting miR inhibitor/mimic (A). Cells treated with 50nM non-targeting miR inhibitor was used as a control to assess relative expression of miR-221 in cells transfected with 50nM mirVana® miR-221 inhibitor (B) or 50nM non-targeting miR mimic was used as a control for miScript miRNA-221 mimic (C). miR levels were assessed using qPCR. All data were normalised to the geometric mean of reference genes HPRT and YWHAZ and relative to either untreated or non-targeting controls respectively. Results presented are mean  $\pm$  SD. Statistical analysis was performed using a 1-way ANOVA with Tukey's post hoc test (n = 3 cell culture wells). [\*\* p $\leq$ 0.01, \*\*\* p $\leq$ 0.001].

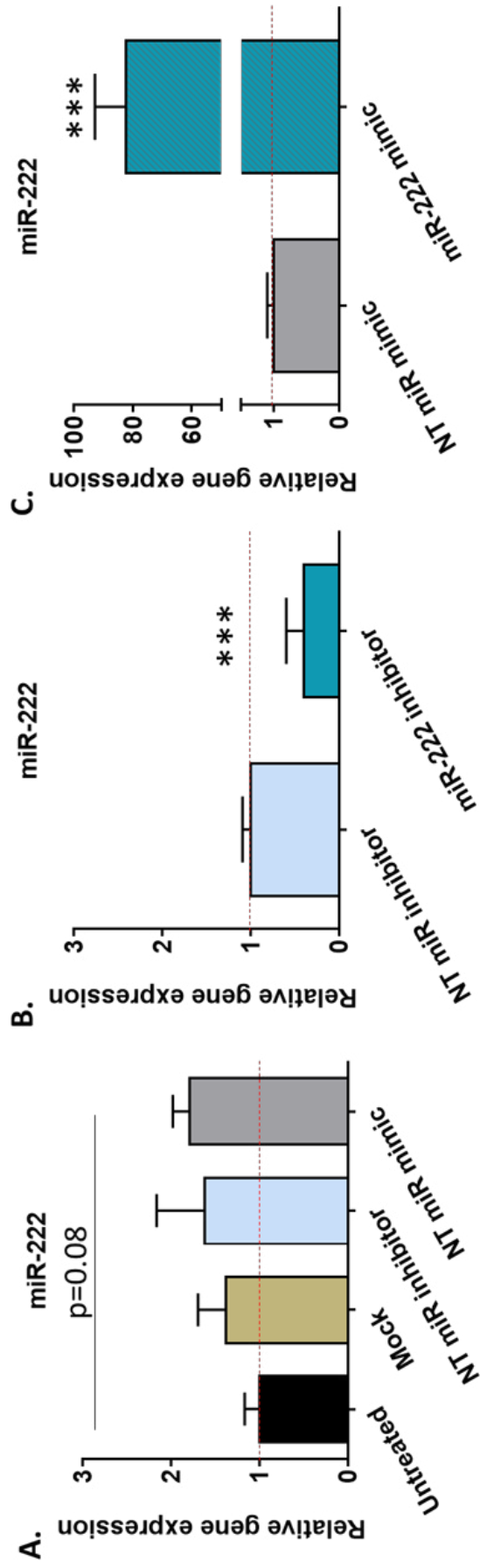


**Figure 5.5.** Expression level of miR-222 in response to 48 h of transfection. Untreated cells were used as a control for cells transfected with either Dharmafect1 only (Mock) or non-targeting miR inhibitor/mimic (**A**). Cells treated with 50nM non-targeting miR inhibitor was used as a control to assess relative expression of miR-222 in cells transfected with 50nM mirVana® miR-222 inhibitor (**B**) or 50nM non-targeting miR mimic was used as a control for miScript miRNA-222 mimic (**C**). miR levels were assessed using qPCR. All data were normalised to the geometric mean of reference genes HPRT and YWHAZ and relative to either untreated or non-targeting controls respectively. Results presented are mean  $\pm$  SD. Statistical analysis was performed using a 1-way ANOVA with Tukey's post hoc test. (n = 3 cell culture wells). [\*\*\* p<math>\leq 0.001</math>].

### **5.2.3. Impact of transfection on cell morphology and viability**

To confirm that variations in gene expression was a specific effect of manipulating miR levels and not a specific effect on cell differentiation/metabolism, the cell phenotype was examined. Morphology of cells incubated for 48h in transfection reagent with 50nM final concentration of siRNA was assessed by light microscopy. As expected, the morphology of all cells remained unchanged (circular) in comparison to untreated cells that were used as a control (Figure 5.6). The results indicate that the transfection reagents do not affect cell phenotype and that changes in target mRNA levels are attributed to the effects of manipulating miR expression directly.

As it is quite common that too high concentration of transfection reagents may have a toxic influence on cells, cell death was assessed using a viability assay. The Live/Dead® Assay, in conjunction with confocal microscopy, was used to assess the effect on chondrocyte viability of a 48h period of transfection, in the presence or absence of 50nM miR inhibitors/mimics (Figure 5.7). Although representative images showed higher levels of cell death as evidenced by increased ethidium homodimer-1 labelling in cells subjected to miR-221 mimic (Figure 5.7I) and miR-222 mimic (Figure 5.7J), the average percentage of live (Figure 5.8A) or dead (Figure 5.8B) cells calculated from 6 individual regions of each transfection treatment or untransfected cells showed no statistically significant changes in cell viability/death in any of the treatments when compared to untreated cells indicating that the transfection and concentrations of miR inhibitors/mimics were non-toxic.

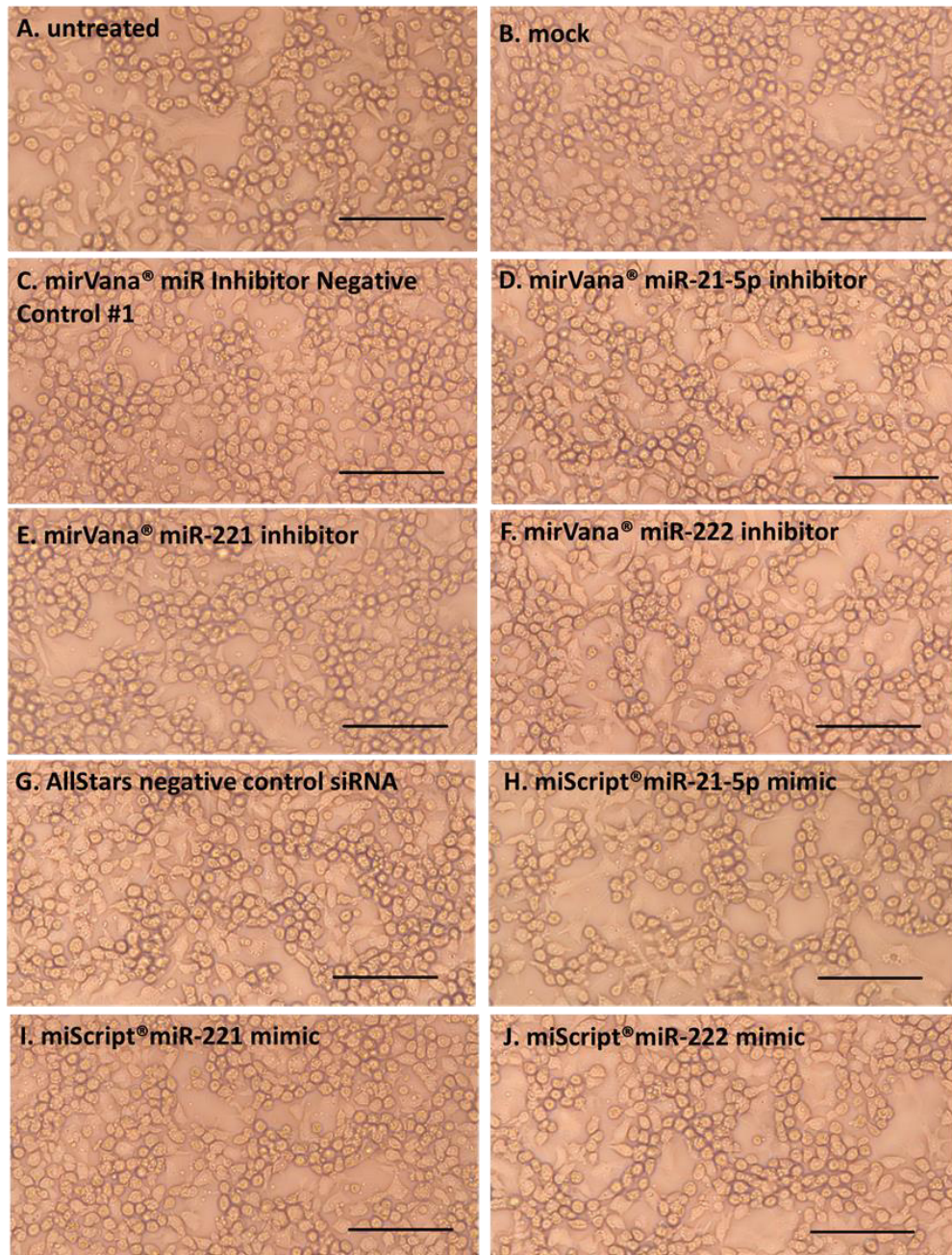
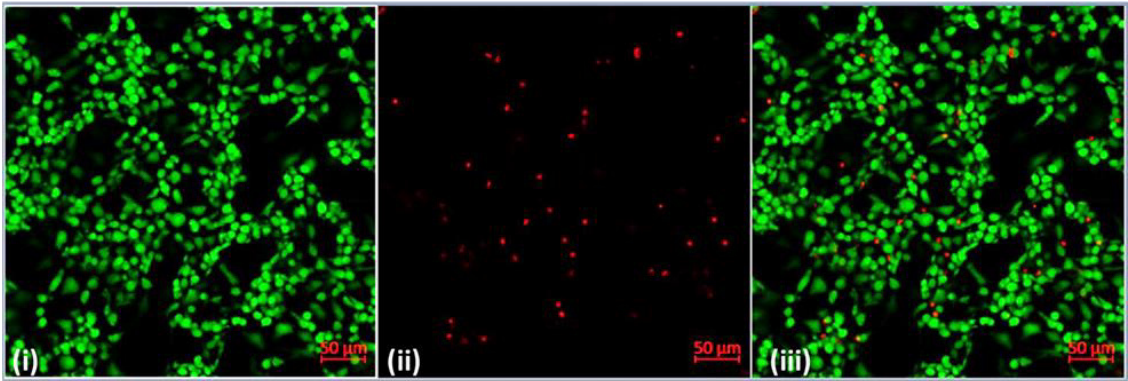
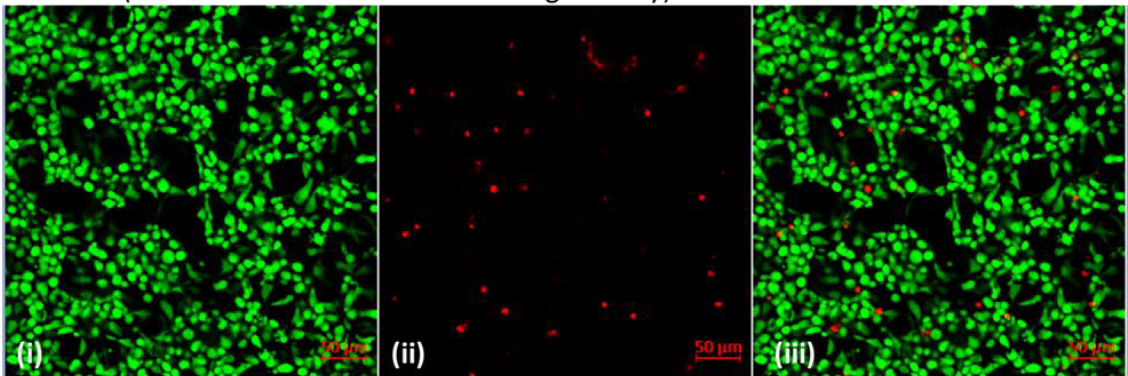


**Figure 5.6.** Morphology of untreated or transfected primary chondrocytes. Monolayers of transfected or untreated cells were incubated at 37°C for 48h. Untreated primary chondrocytes **(A)** were used as a control for healthy cell morphology. Transfected cells were treated either with transfection reagent only (mock) **(B)**, or 50nM inhibitors/mimics: mirVana® miR Inhibitors: Negative Control #1 **(C)**, miR-21-5p **(D)**, miR-221 **(E)**, miR-222 **(F)**, miScript® miR Mimics: 50nM AllStars negative control siRNA **(G)**, miR-21-5p **(H)**, miR-221 **(I)**, miR-222 **(J)**. Images were taken using a light microscope. Scale bar = 100µm.

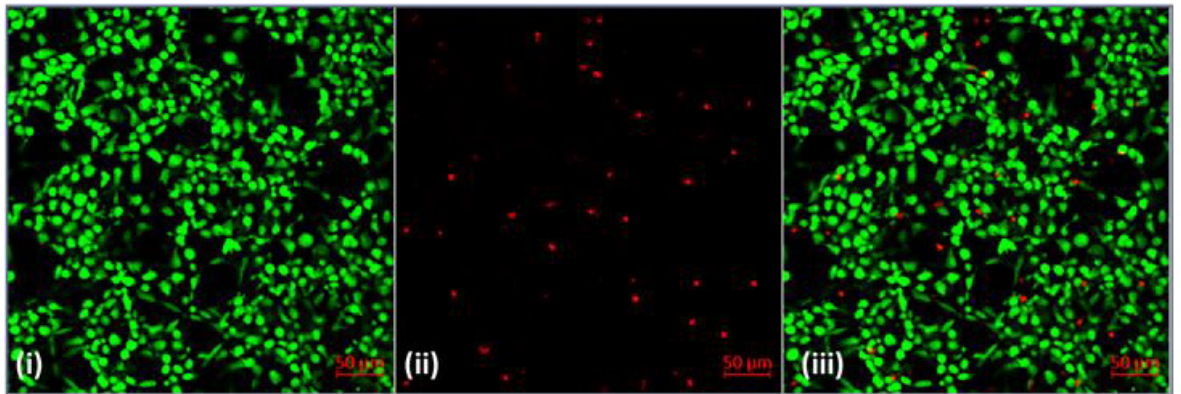
**A. Untreated (non-transfected) cells**



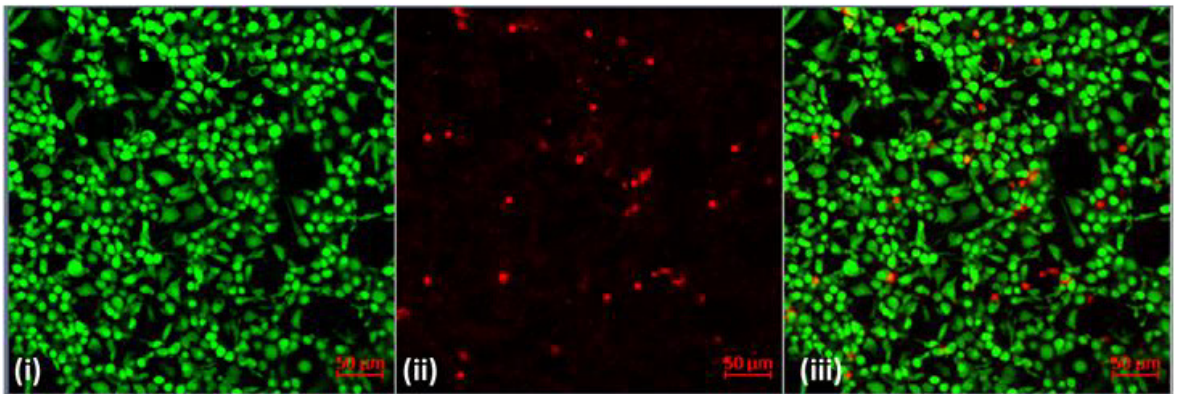
**B. Mock (Transfected with transfection reagent only) cells**



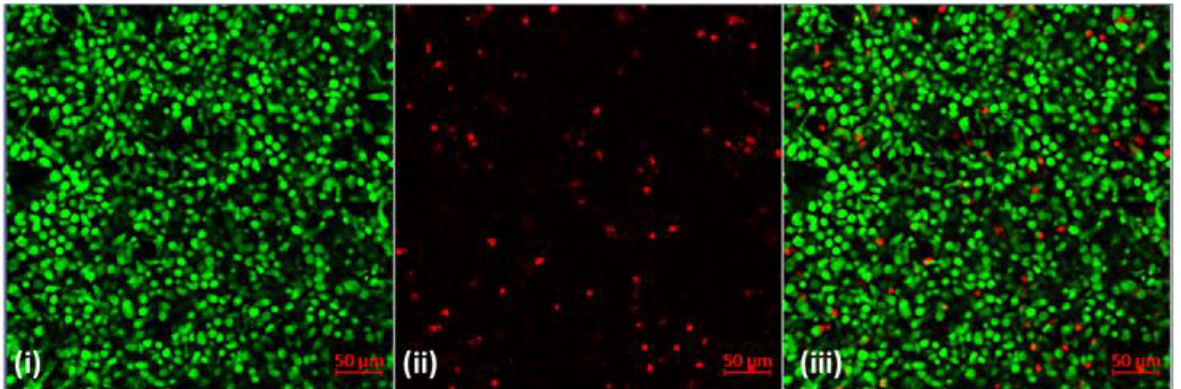
C. Cells transfected with 50nM of non-targeting miR control (mirVana® miR Inhibitor Negative Control #1)



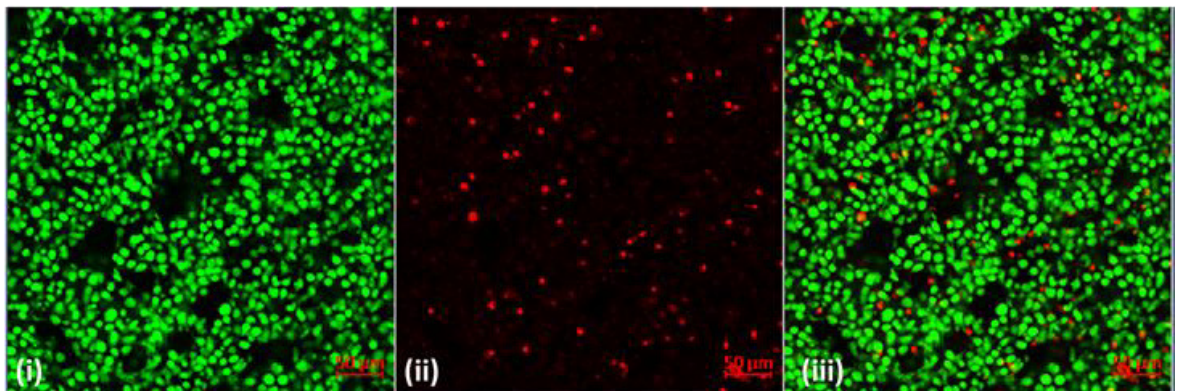
D. Cells transfected with 50nM of mirVan® miR-21-5p inhibitor



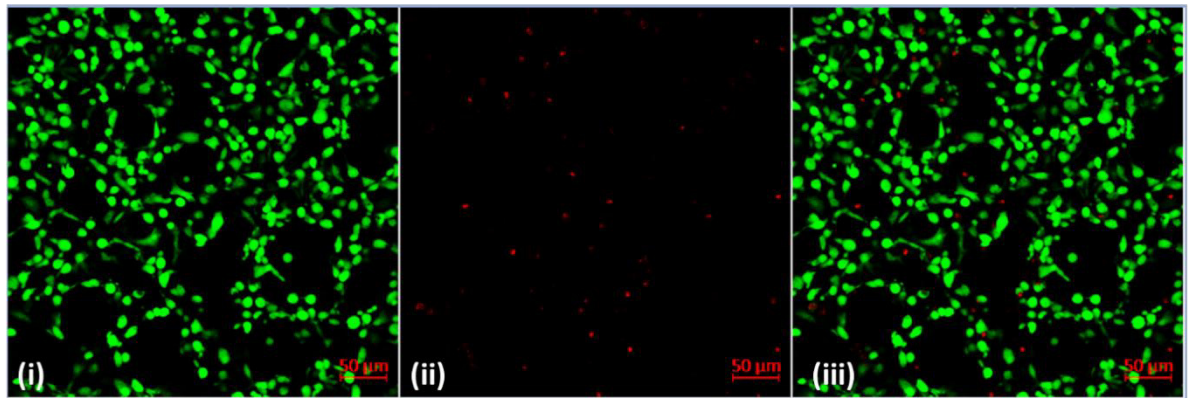
E. Cells transfected with 50nM of mirVan® miR-221 inhibitor



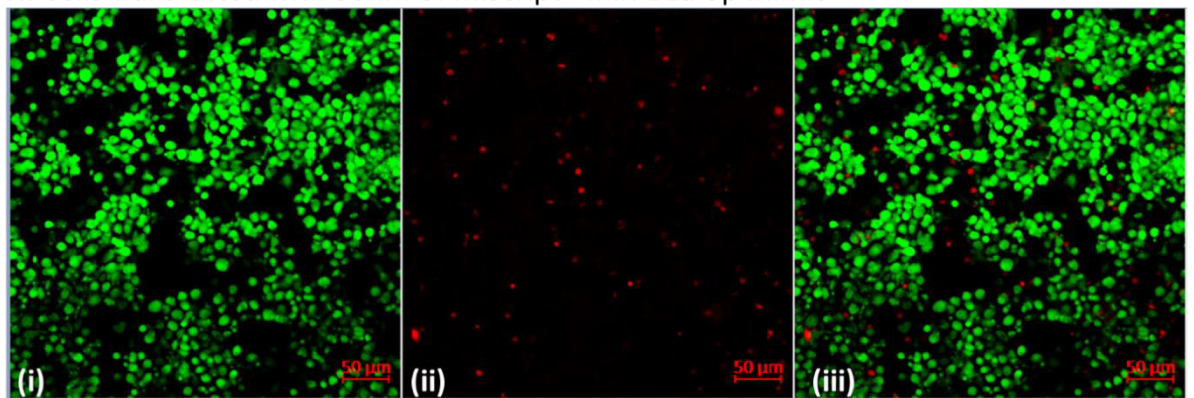
F. Cells transfected with 50nM of mirVan® miR-222 inhibitor



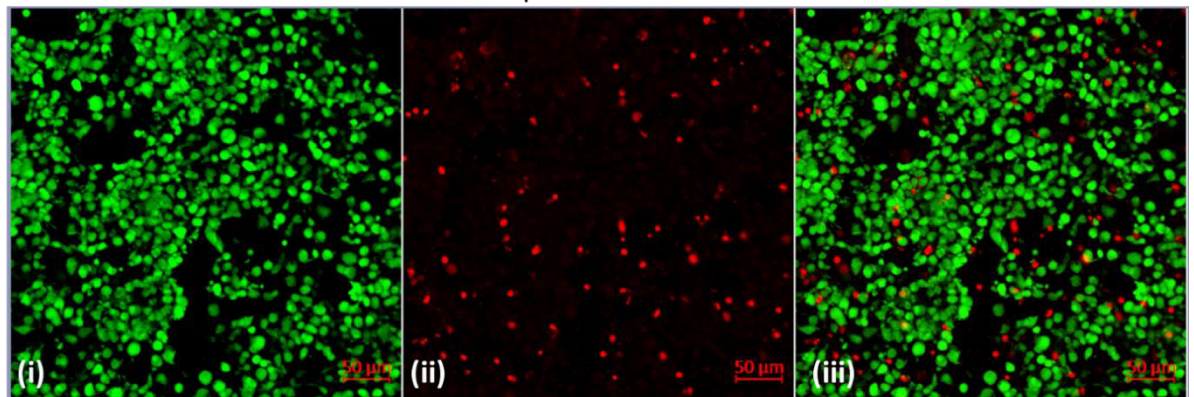
**G.** Cells transfected with 50nM of non-targeting miR control (AllStars negative control siRNA)



**H.** Cells transfected with 50nM of miScript® miR-21a-5p mimic



**I.** Cells transfected with 50nM of miScript® miR-221 mimic



**J.** Cells transfected with 50nM of miScript® miR-222 mimic

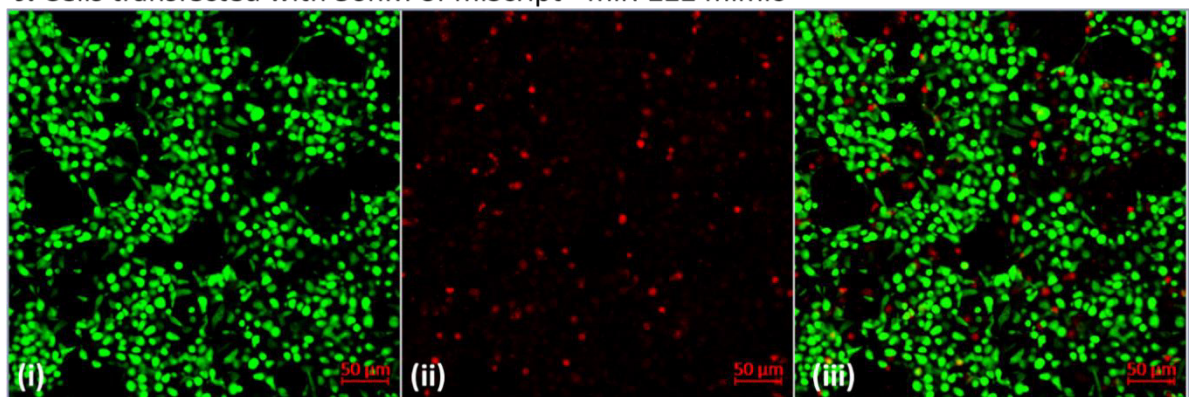


**Figure 5.7.** Representative images of Live/Dead<sup>®</sup> assay to monitor cell viability in chondrocytes either left as untreated **(A)**, cells transfected with transfection reagent only **(B)**, 50nM mirVana<sup>®</sup> miR Inhibitor Negative Control #1 **(C)**, 50nM mirVana<sup>®</sup> miR Inhibitors: miR-21 **(D)**, miR-221 **(E)**, miR-222 **(F)**, 50nM AllStars negative control siRNA **(G)** or 50nM miScript<sup>®</sup> miR Mimics: miR-21-5p **(H)**, miR-221 **(I)**, miR-222 **(J)**. Confocal images of cells labelled with CalceinAM or Ethidium homodimer-1 present abundance of live and dead cells respectively. Representative images for each treatment show either separate results for live cells **(i)** and dead cells **(ii)** or an overlay of both channels **(iii)**. Scale bar = 50µm.

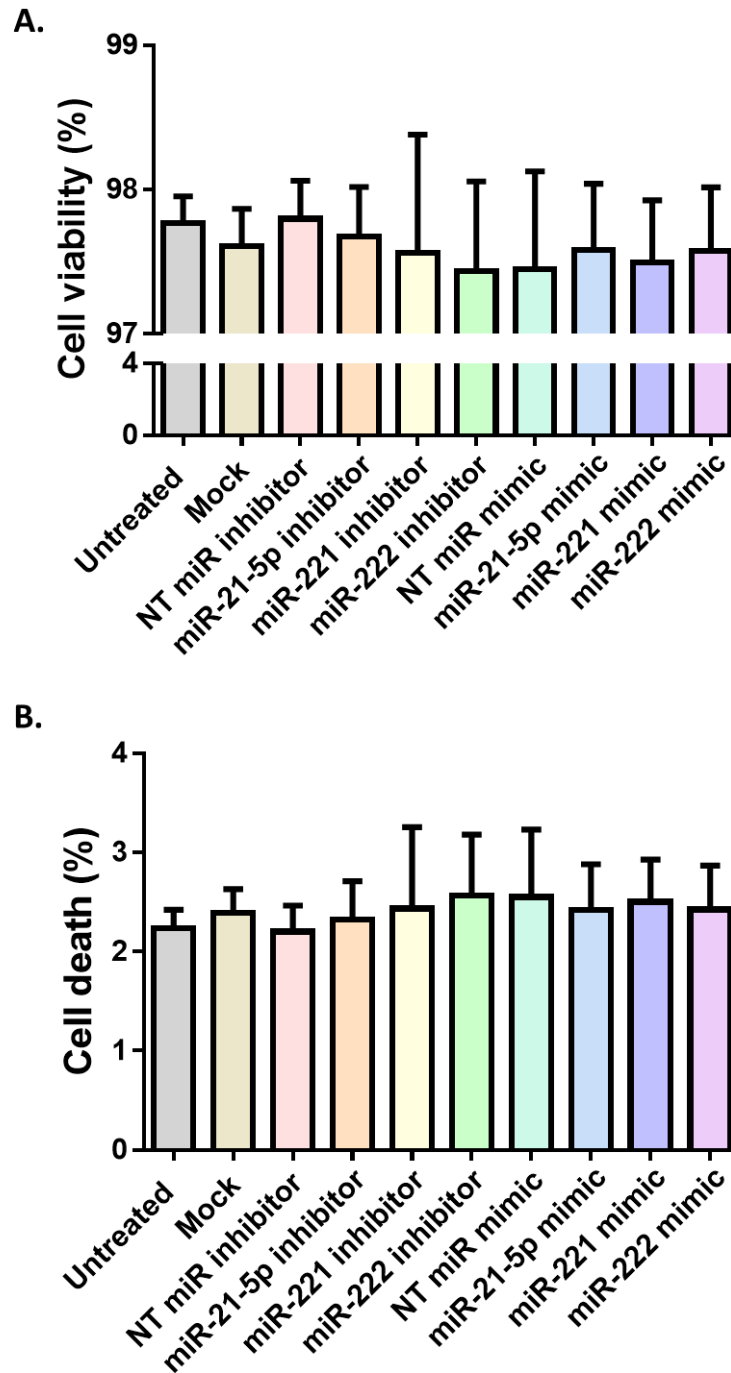


**Figure 5.8.** Calculation of cell viability (A) and death (B) expressed as a % of live (CalceinAM) and dead (Ethidium homodimer-1) cells compared to % of total cell number (CalceinAM and Ethidium homodimer-1) of untreated and transfected primary chondrocytes, as assessed by Live/Dead® assay. Cell viability was determined 48h post-transfection and was visualised by confocal microscopy (Figure 5.5). Number of live/dead cells was calculated using Image J. Data are presented as mean  $\pm$ SD (n = 6 individual images) and analysed using a 1-way ANOVA.

#### **5.2.4. Differential expression of Wnt signalling components in response to inhibition of miR-21-5p, miR-221 and miR-222**

As the manipulation of the miRs by inhibitors/mimics efficiently modified miR levels without affecting cell morphology or viability, the next step was to determine the direct target genes of miR-21-5p, miR-221 and miR-222.

A few studies have been reported, in cell types other than chondrocytes, implicating these miRs of interest in the regulation of genes involved in Wnt/ $\beta$ -catenin signalling pathways (Corr, 2008, Kawakita et al., 2014, Li et al., 2013, Wu et al., 2015, Zheng et al., 2012). To establish which of the Wnt related molecules are potential target genes of these miRs, the transcriptional levels of Wnt/ $\beta$ catenin signalling components were examined in chondrocytes transfected with miR inhibitors using custom-built bovine specific Wnt signalling PCR arrays designed by Dr Aisha Al-Sabah (Cardiff University). The PCR array contained 84 Wnt related genes including: targets of Wnt signalling, molecules of canonical Wnt signalling, Wnt/ $\text{Ca}^{2+}$  pathway, planar cell polarity (PCP) pathway and inhibitors of Wnt signalling (a complete gene list is shown in the Appendix 1 - 3). Array data were normalised to HPRT1 and YWHAZ reference genes that were present on the array using the online Qiagen Data Analysis centre software (<http://pcrdataanalysis.sabiosciences.com/pcr/arrayanalysis.php>).

Surprisingly, transcript levels of FOSL1, PITX2 and Wnt2B were differentially expressed as a result of the transfection procedure itself, as determined by comparing the gene profile of the untreated cells to the non-targeting inhibitor control (Figure 5.9); therefore, these genes were excluded from the panel of putative target genes. Alterations in gene expression in response to inhibition of miR-21-5p, miR-221 or miR-222 were normalised to cells treated with the non-targeting inhibitor control and the data presented as at least a 2-fold change in gene expression in cells transfected with functional inhibitors.

**miR-21-5p targets:** miR-21-5p inhibitor increased MMP-7 transcription (2.7-fold). Surprisingly, many more genes were down-regulated including DKK1 and DKK3 (canonical Wnt signalling) and FOXN1 (developmental process) (2.53-fold; Figure 5.10).

**miR-221 targets:** Only one Wnt-related gene was differentially expressed by more than 2-fold in cells transfected with miR-221 inhibitor and that was Wnt3A (canonical Wnt signalling and Wnt/Ca<sup>2+</sup> signalling) which was elevated (2.2-fold; Figure 5.11). Surprisingly, this inhibitor did not reduce the transcript levels of any of the genes measured.

**miR-222 targets:** Predictably, as miR-222 has the same seed region as miR-221, Wnt3A transcription was increased (2.67-fold) in response to miR-222 inhibition (Figure 5.12). In contrast to miR-221, miR-222 down-regulated 13 genes including AXIN2 (3.15-fold, canonical Wnt signalling) and GSK3A (2.72-fold, canonical Wnt signalling).

Although, data from inhibition of miR-21-5p and miR-222 demonstrate a greater number of repressed genes than those with increased expression, an interesting observation is that some genes are down-regulated in both cases: APC (canonical Wnt signalling), AXIN2 (canonical Wnt signalling, Wnt signalling target gene), CTNNB1 (canonical Wnt signalling, cell growth and proliferation), DKK3 (canonical Wnt signalling), FOXN1 (cell growth and proliferation) and FRZB (Wnt binding protein).

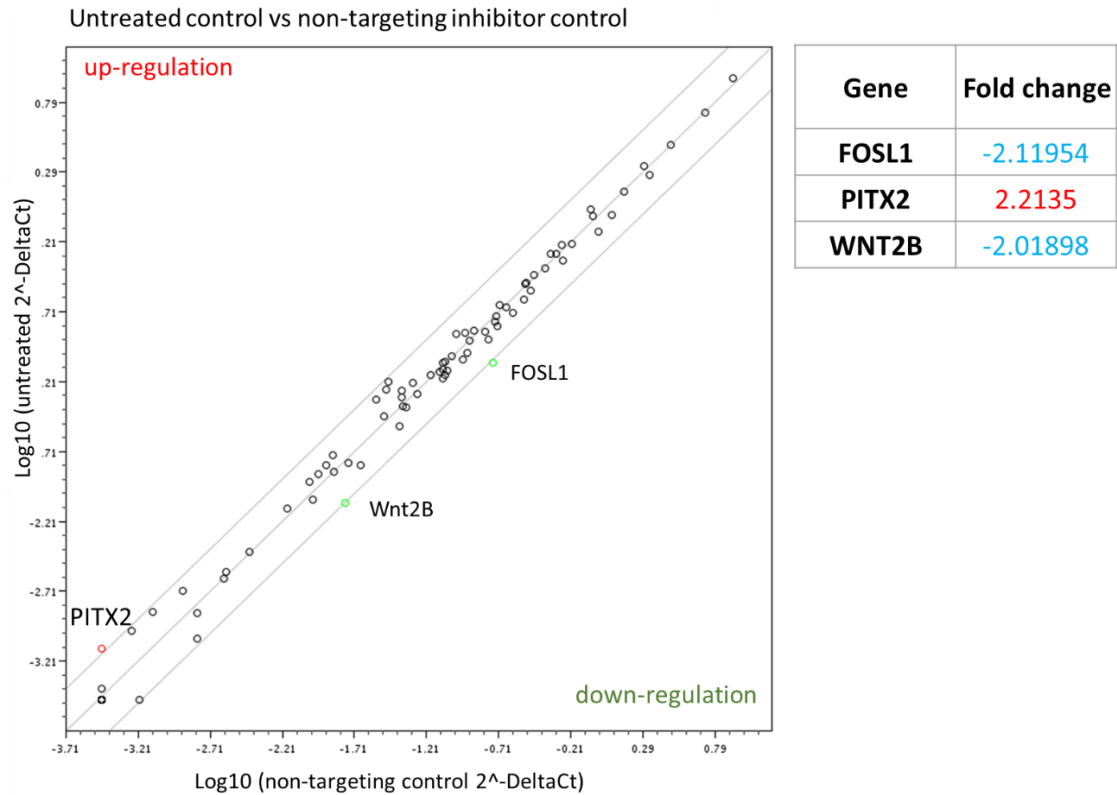


**Figure 5.9.** Scatterplots of Qiagen Wnt signalling PCR array data comparing the transcriptional profile of Wnt-related genes between untreated and cells transfected with non-targeting inhibitor (mirVana® miR Inhibitor Negative Control #1 miR). Cells were transfected for 48h with 50nM inhibitor, RNA extracted and PCR arrays performed. Data represents a single experiment, in which n = 3 cell culture wells per treatment. A single array was performed with representation of each treatment from pooled samples. Gene expression was normalised to the geometric mean of reference genes (HPRT1, YWHAZ) and relative to the untransfected control. The lines on the graph represent a 2-fold change in gene expression, and the fold-change of identified targets are listed in the accompanying table.

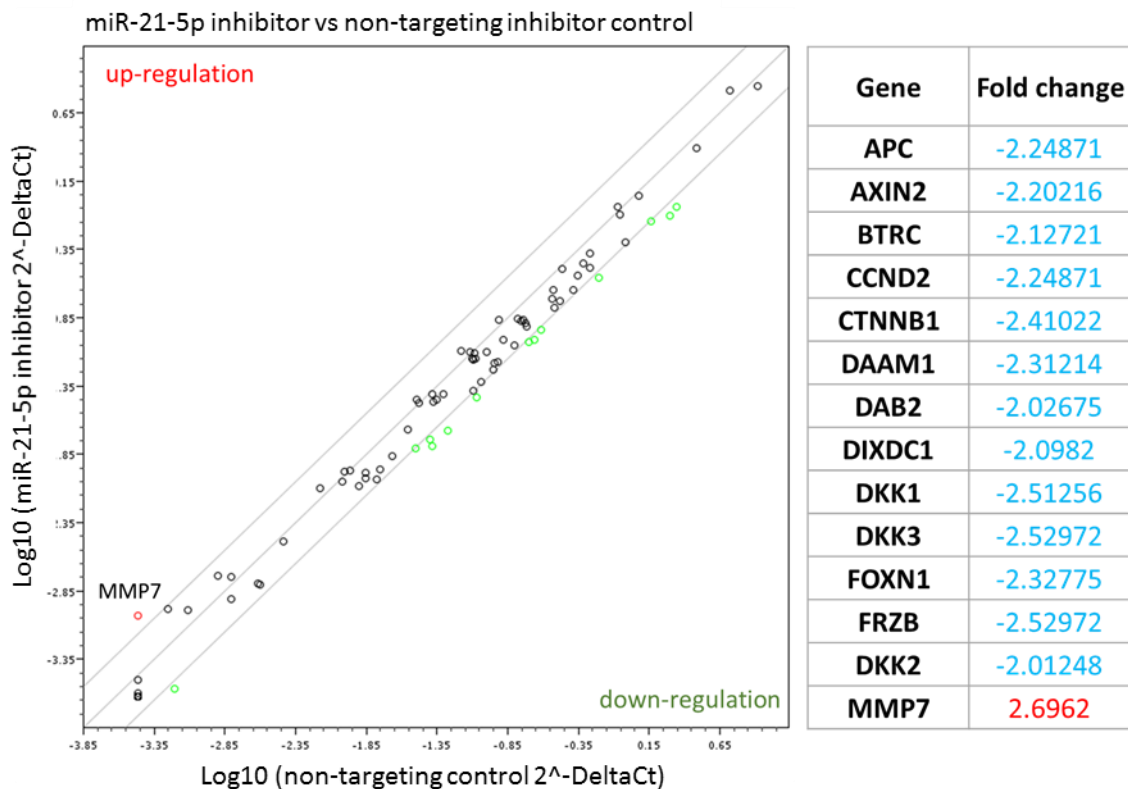


**Figure 5.10.** Scatterplots of Qiagen Wnt signalling PCR array data comparing the transcriptional profile of genes between transfected cells with miR-21-5p inhibitor and non-targeting miR inhibitor. Cells were transfected for 48h with 50nM inhibitor, RNA extracted and PCR arrays performed. Data represents a single experiment, in which  $n = 3$  cell culture wells per treatment. A single array was performed with representation of each treatment from pooled samples. Gene expression was normalised to the geometric mean of reference genes (HPRT1, YWHAZ) and relative to the non-targeting inhibitor control. The lines on the graph represent a 2-fold change in gene expression, and the fold-change of identified targets are listed in the accompanying table.

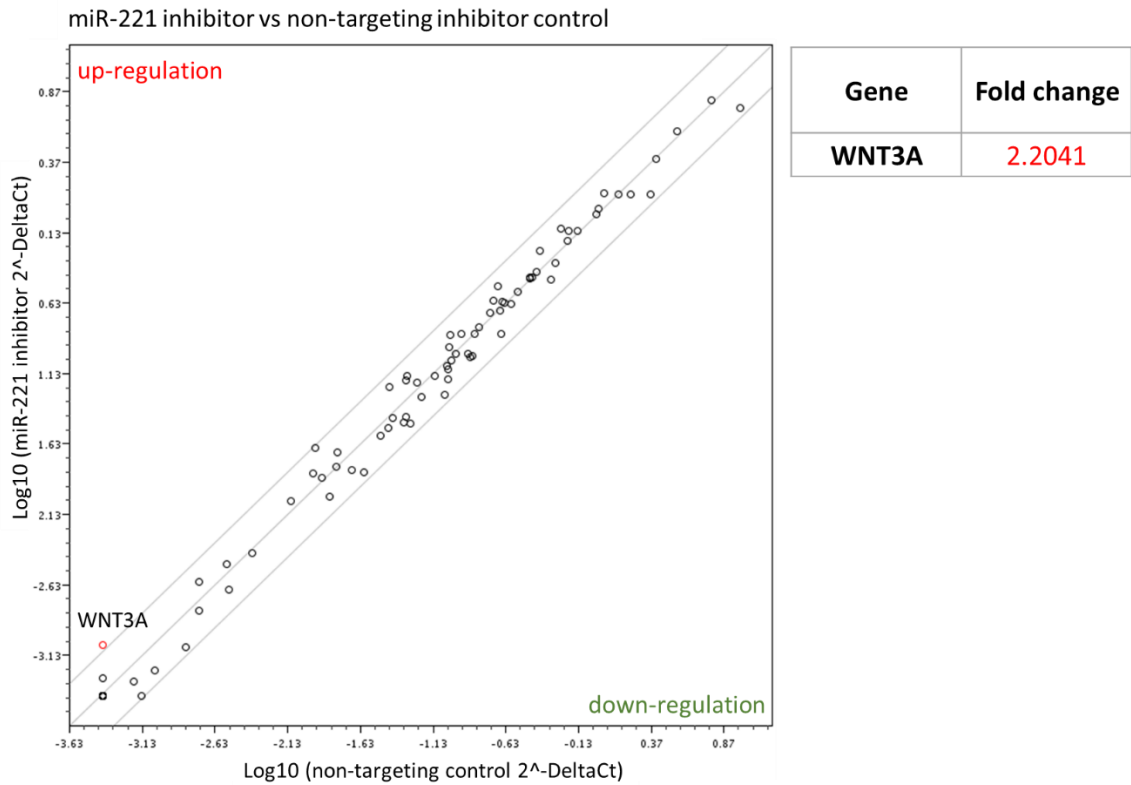


**Figure 5.11.** Scatterplots of Qiagen Wnt signalling PCR array data comparing the transcriptional profile of genes between transfected cells with miR-221 inhibitor and non-targeting miR inhibitor. Cells were transfected for 48h with 50nM inhibitor, RNA extracted and PCR arrays performed. Data represents a single experiment, in which  $n = 3$  cell culture wells per treatment. A single array was performed with representation of each treatment from pooled samples. Gene expression was normalised to the geometric mean of reference genes (HPRT1, YWHAZ) and relative to the non-targeting inhibitor control. The lines on the graph represent a 2-fold change in gene expression, and the fold-change of identified targets are listed in the accompanying table.

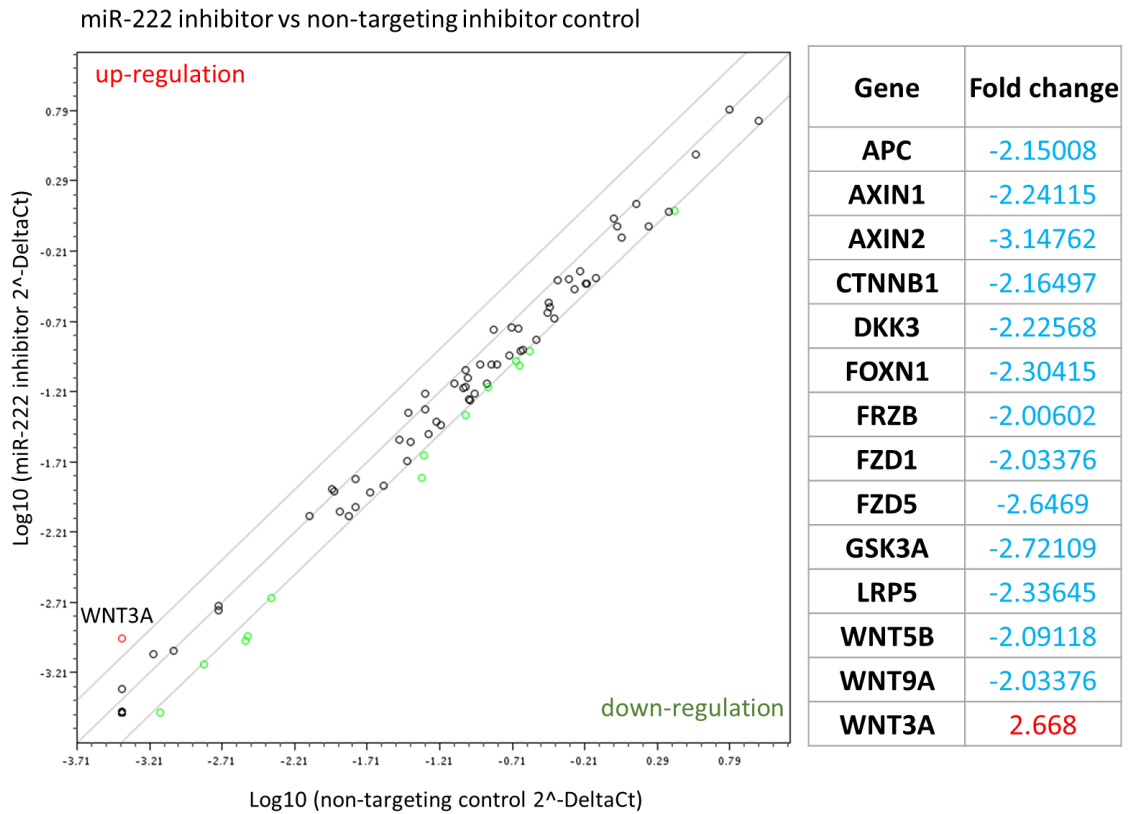


**Figure 5.12.** Scatterplots of Qiagen Wnt signalling PCR array data comparing the transcriptional profile of genes between transfected cells with miR-222 inhibitor and non-targeting miR inhibitor. Cells were transfected for 48h with 50nM inhibitor, RNA extracted and PCR arrays performed. Data represents a single experiment, in which  $n = 3$  cell culture wells per treatment. A single array was performed with representation of each treatment from pooled samples. Gene expression was normalised to the geometric mean of reference genes (HPRT1, YWHAZ) and relative to the non-targeting inhibitor control. The lines on the graph represent a 2-fold change in gene expression, and the fold-change of identified targets are listed in the accompanying table.

### **5.2.5. Quantitative PCR validation of miR-21-5p, miR-221 and miR-222 target genes identified from the PCR arrays**

Expression levels of identified genes that were differentially expressed using Wnt signalling arrays were validated using SybrGreen® qPCR. Alterations in target gene expression in response to manipulation of miR-21-5p, miR-221 or miR-222 levels were normalised to cells treated with the respective non-targeting control. The impact of transfection itself was assessed by comparing untreated control cells to cells treated with: (i) DharmaFECT1™ transfection reagent only (Mock), (ii) DharmaFECT1™ and Negative Control #1 (non-targeting inhibitor control) or (iii) DharmaFECT1™ and AllStars negative control siRNA (non-targeting mimic control).

Putative target genes were selected for validation based on the following criteria: (i) at least a 2-fold change in transcript levels between cells transfected with functional miR inhibitor and non-targeting control, (ii) mRNA level of putative target gene is elevated in cells treated with the functional miR inhibitor compared to the non-targeting control. The second criteria was crucial as the aim of this chapter was to identify direct target genes of mechano-sensitive miR-21-5p, miR-221 and miR-222. Based on these criteria, only two genes were selected for validation: MMP-7 and Wnt3A. Although neither MMP-7 nor Wnt3A mRNA contain miR-21-5p, miR-221 or miR-222 seed sites (according to TargetScan software), the genes were selected for validation as the predictive software only searches for target sites in the 3'UTR.

The transfection process itself did not significantly affect expression of MMP-7 (Figure 5.13A); furthermore, there was no change in MMP-7 expression in cells transfected with either miR-21-5p inhibitor or mimic (Figure 5.13B). Although transfection reagent alone, in the presence or absence of the non-targeting inhibitor control, did not affect Wnt3A gene expression compared to untransfected cells (Figure 5.14A), interestingly, transfection with the non-targeting mimic control increased expression of Wnt3A in comparison to both untreated cells (3.98-fold;  $p=0.024$ ) and non-targeting inhibitor control (2.91-fold;  $p=0.079$ ). However, neither miR-221 inhibitor or miR-221 mimic (Figure 5.14B), or miR-222 inhibitor or miR-222 mimic affected Wnt3A transcript levels (Figure 5.14C).

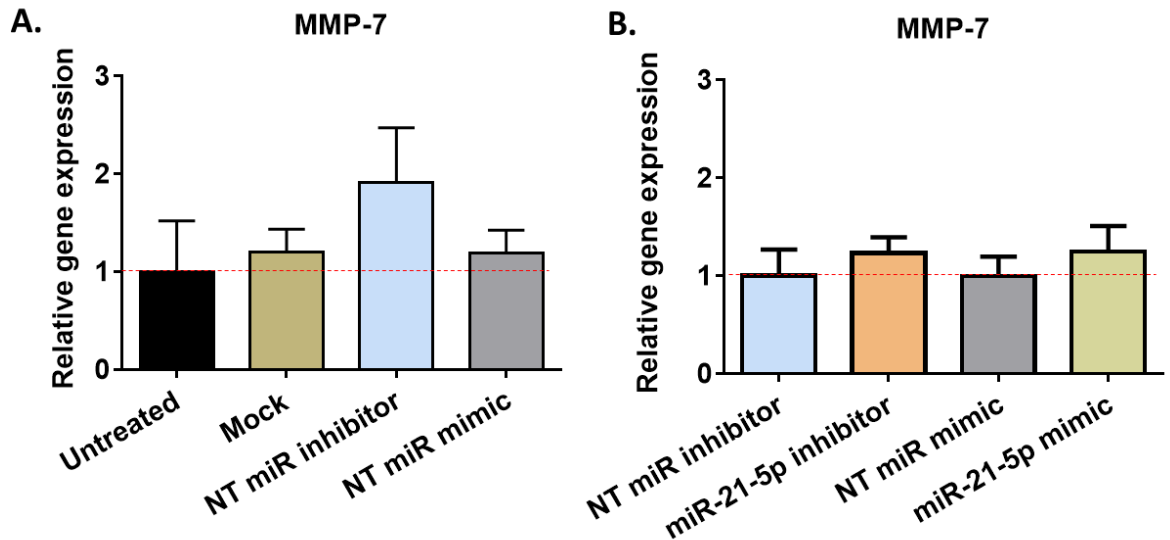


**Figure 5.13.** Validation of MMP-7, a component of the Wnt signalling pathway, as a putative target gene of miR-21-5p. Expression levels of MMP-7 was assessed by qPCR in cells transfected with transfection reagent only or non-targeting inhibitor/mimic **(A)** and miR-21-5p inhibitor/mimic **(B)**. All data were normalised to the geometric mean of reference genes HPRT and YWHAZ and to the respective controls, which were either untreated **(A)** or cells transfected with non-targeting miR inhibitor/mimic **(B)**. Results are presented as mean of independent wells  $\pm$  SD ( $n = 3$  cell culture wells). Statistical analysis was performed using a 1-way ANOVA with Tukey's post hoc test. Key: NT - non-targeting.

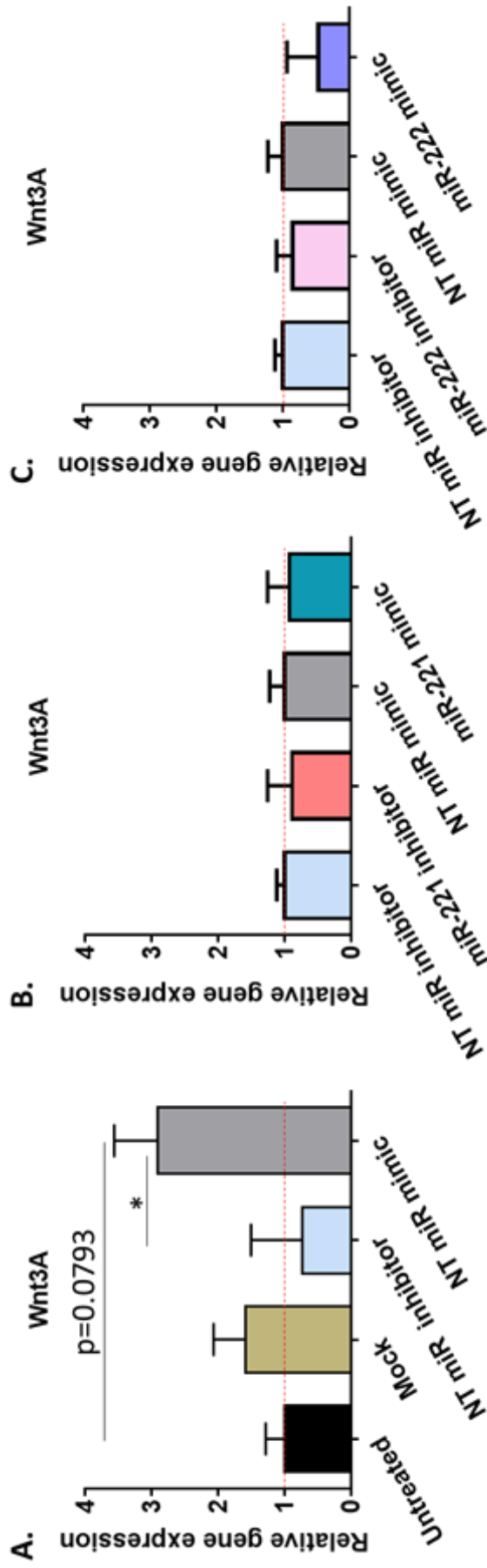


**Figure 5.14.** Validation of Wnt3A, a component of the WNT signalling pathway, as a putative target gene of miR-221 and -222. Expression levels of Wnt3A was assessed by qPCR in cells transfected with transfection reagent only or non-targeting inhibitor/mimic (**A**), miR-221 inhibitor/mimic (**B**) or miR-222 inhibitor/mimic (**C**). All data were normalised to the geometric mean of reference genes HPRT and YWHAZ and to the respective controls, which were either untreated (**A**) or cells transfected with non-targeting miR inhibitor/mimic (**B,C**). Results are presented as mean of independent wells  $\pm$  SD (n = 3 cell culture wells). Statistical analysis was performed using a 1-way ANOVA with Tukey's post hoc test. Key: NT - non-targeting, [\* p $\leq$ 0.05].

### 5.2.6. Identification of miR-21-5p, miR-221 and miR-222 target genes using Next Generation Sequencing

As the expression of selected Wnt signalling components present on the custom-built PCR array did not identify any candidate target genes from cells transfected with functional miR inhibitors, an analysis of global gene changes was conducted using NGS. Extracted RNA from untreated cells or cells treated with 50nM non-targeting siRNA or miR-21-5p/miR-221/miR-222 inhibitors was analysed via Illumina deep sequencing conducted in the School of Biosciences, Cardiff University. The average number of reads obtained from sequencing was  $\sim 42.9 \times 10^6$  per library and they were analysed by Dr Daniel Pass using R Statistical programming software available on Bioconductor. All raw reads were aligned to the bovine reference genome (UMD3.1). To observe global changes in mRNA levels, expression levels of genes in cells treated with functional miR inhibitors was normalised against the non-targeting controls. Genes that were significantly altered in cells with non-targeting siRNA compared to untreated cells were excluded from the panel of putative target genes as they were identified as being sensitive to the transfection procedure itself (data available electronically). As the Benjamini-Hochberg adjusted p-values (FDR) at a threshold of  $\leq 0.05$  presented a limited number of differentially expressed genes, the list of putative target genes was expanded by selecting them according to fold change instead of the False Discovery Rate (FDR), and genes that were increased by a minimum 1.5-fold were taken into consideration as target genes of tested miRs.

Table 5.1 and 5.2 indicate the top 5 most up-regulated and down-regulated genes, respectively, in cells transfected with miR-21-5p inhibitor. Surprisingly, the gene that was elevated the most (4.9-fold: FDR=0.51) was U1 (U1 spliceosomal RNA). This gene is involved in intron removal and processing of mRNA splicing that occurs in the nucleus. The most reduced gene was Insulin Like Growth Factor Binding Protein 2 (IGFBP2) (3.31-fold: FDR=0.51) that binds Insulin Like Growth Factors (IGF-1 and IGF-2) which seems to be one of the most important growth factors in articular cartilage as IGF-1 stimulates synthesis of ECM molecules, mostly collagen type II and proteoglycans (Starkman et al., 2005).

Unexpectedly, the top 5 most significantly up-regulated genes in response to inhibition of either miR-221 (Table 5.3) or miR-222 (Table 5.5) are genes involved in mRNA processing in the nucleus. U1, as identified in cells treated with miR-21-5p inhibitor, exhibited the greatest transcriptional up-regulation in response to inhibition of both miR-221 (2,333-fold: FDR<0.001) and miR-222 (1,209-fold: FDR<0.001). Inhibition of miR-221 significantly reduced the expression of several genes including a Wnt signalling ligand: SFRP2 (Secreted Frizzled-Related Protein 2, 2.94-fold: FDR=1; Table 5.4) which was the most reduced. IGFBP2, similar to the cell response observed for miR-21-5p inhibition was the most down-regulated gene (2.83-fold: FDR=1) in response to miR-222 reduction (Table 5.6).

**Table 5.1.** Top 5 most highly elevated genes in response to miR-21-5p knock-down. The table presents the greatest fold change of differentially expressed genes that were normalised to the non-targeting inhibitor control, the p value and False Discovery Rate (FDR - adjusted p value).

<b>Top 5 most highly elevated genes as an effect of miR-21-5p knock-down</b>				
<b>Gene</b>	<b>Gene name</b>	<b>Fold change</b>	<b>p value</b>	<b>FDR</b>
<b>U1</b>	U1 spliceosomal RNA	4.92	0.00	0.51
<b>snoU13</b>	U13 small nucleolar RNA	3.89	0.37	1.00
<b>U3</b>	U3 small nucleolar RNA	3.87	1.00	1.00
<b>NPPA</b>	Natriuretic Peptide A	3.43	0.06	1.00
<b>U5</b>	U5 spliceosomal RNA	3.00	0.20	1.00

**Table 5.2.** Top 5 most highly reduced genes in response to miR-21-5p knock-down. The table presents the greatest fold change of differentially expressed genes that were normalised to non-targeting inhibitor control, the p value and False Discovery Rate (FDR - adjusted p value).

<b>Top 5 most highly reduced genes as an effect of miR-21-5p knock-down</b>				
<b>Gene</b>	<b>Gene name</b>	<b>Fold change</b>	<b>p value</b>	<b>FDR</b>
<b>IGFBP2</b>	Insulin Like Growth Factor Binding Protein 2	-3.31	0.00	0.51
<b>TTR</b>	Transthyretin	-2.86	0.01	1.00
<b>SFRP2</b>	Secreted Frizzled-Related Protein 2	-2.16	0.07	1.00
<b>PPP1R14A</b>	Protein Phosphatase 1 Regulatory Inhibitor Subunit 14A	-1.99	0.04	1.00
<b>TMEM86B</b>	Transmembrane Protein 86B	-1.97	0.04	1.00

**Table 5.3.** Top 5 most highly elevated genes in response to miR-221 knock-down. The table presents the greatest fold change of differentially expressed genes that were normalised to non-targeting inhibitor control, the p value and False Discovery Rate (FDR - adjusted p value).

<b>Top 5 most highly elevated genes as an effect of miR-221 knock-down</b>				
<b>Gene</b>	<b>Gene name</b>	<b>Fold change</b>	<b>p value</b>	<b>FDR</b>
<b>U1</b>	U1 spliceosomal RNA	<b>2333.74</b>	0.00	0.00
<b>U5</b>	U5 spliceosomal RNA	<b>861.50</b>	0.00	0.00
<b>U3</b>	U3 small nucleolar RNA	<b>720.88</b>	0.00	0.00
<b>U3</b>	U3 small nucleolar RNA	<b>492.28</b>	0.00	0.00
<b>snoU13</b>	U13 small nucleolar RNA	<b>175.95</b>	0.00	0.00

**Table 5.4.** Top 5 most highly reduced genes in response to miR-221 knock-down. The table presents the greatest fold change of differentially expressed genes that were normalised to non-targeting inhibitor control, the p value and False Discovery Rate (FDR - adjusted p value).

<b>Top 5 most highly reduced genes as an effect of miR-221 knock-down</b>				
<b>Gene</b>	<b>Gene name</b>	<b>Fold change</b>	<b>p value</b>	<b>FDR</b>
<b>SFRP2</b>	Secreted Frizzled-Related Protein 2	<b>-2.94</b>	0.01	1.00
<b>TTR</b>	Transthyretin	<b>-2.91</b>	0.00	1.00
<b>IGFBP2</b>	Insulin Like Growth Factor Binding Protein 2	<b>-2.89</b>	0.00	0.32
<b>CLEC4F</b>	C-Type Lectin Domain Family 4 Member F	<b>-2.85</b>	0.45	1.00
<b>C8orf22</b>	Chromosome 8 Open Reading Frame 22	<b>-2.45</b>	0.04	1.00

**Table 5.5.** Top 5 most highly elevated genes in response to miR-222 knock-down. The table presents the greatest fold change of differentially expressed genes that were normalised to non-targeting inhibitor control, the p value and False Discovery Rate (FDR - adjusted p value).

Top 5 most highly elevated genes as an effect of miR-222 knock-down				
Gene	Gene name	Fold change	p value	FDR
<b>U1</b>	U1 spliceosomal RNA	1209.41	0.00	0.00
<b>U3</b>	U3 small nucleolar RNA	817.69	0.00	0.00
<b>U5</b>	U5 spliceosomal RNA	686.85	0.00	0.00
<b>U3</b>	U3 small nucleolar RNA	670.94	0.00	0.00
<b>U1</b>	U1 spliceosomal RNA	176.10	0.00	0.00

**Table 5.6.** Top 5 most highly reduced genes in response to miR-222 knock-down. The table presents the greatest fold change of differentially expressed genes that were normalised to non-targeting inhibitor control, the p value and False Discovery Rate (FDR - adjusted p value).

Top 5 most highly reduced genes as an effect of miR-222 knock-down				
Gene	Gene name	Fold change	p value	FDR
<b>IGFBP2</b>	Insulin Like Growth Factor Binding Protein 2	-2.83	0.45	1.00
<b>CLEC4F</b>	C-Type Lectin Domain Family 4 Member F	-2.72	0.00	0.64
<b>KIF26A</b>	Kinesin Family Member 26A	-2.42	0.28	1.00
<b>TTR</b>	Transthyretin	-2.33	0.03	1.00
<b>CACNG4</b>	Calcium Voltage-Gated Channel Auxiliary Subunit Gamma 4	-2.31	0.05	1.00

The aim of the work described in this chapter was to identify direct target genes regulated by the mechano-sensitive miR-21-5p, miR-221 and miR-222. As the expression levels of direct target genes should be inversely proportional to the level of knocked-down miRs, only up-regulated genes ( $\geq 1.5$ -fold) with p value  $\leq 0.05$ , despite a FDR=1 were taken from the lists of putative genes (Tables 5.7-5.9) for validating their expression as downstream targets of miR-21-5p, miR-221 and miR-222.

To inhibit the activity of a gene, the miR must bind either totally or partially to a specific site within the mRNA of the direct target. In order to establish which genes contain specific target sites (Tables 5.7-5.9), the computational prediction program TargetScan was used. The TargetScan algorithm recognises conserved and poorly conserved 6mer, 7merA1, 7mer-m8 and 8mer seed sites within the examined 3'UTR of the mRNA.

Using this software in conjunction with the NGS data (Table 5.7), 28 genes were identified as putative target genes for miR-21-5p. From the panel of recognised target genes, 7 transcripts had conserved seed sites, 18 contained poorly conserved seed sites, and 3 included both conserved and poorly conserved sites. Using TargetScan and analysis of NGS data from cells transfected with miR-221 inhibitor (Table 5.8), 3 putative target genes were identified with conserved and poorly conserved seed sites, 7 with conserved sites only and 17 transcripts that contained poorly conserved sites only. By a similar process, inhibition of miR-222 elevated the expression of 24 transcripts recognised as target genes (Table 5.9). Amongst these 24 mRNA sequences, 5 genes had conserved sites only, 16 contained poorly conserved sites, whereas both conserved and poorly conserved sites were present in 3 genes.

**Table 5.7.** Up-regulated genes ( $\geq 1.5$ -fold) in cells transfected with miR-21-5p inhibitor compared to expression in the non-targeting inhibitor control, as identified using NGS. Key: Genes highlighted with green contain conserved seed site(s), yellow contain poorly conserved seed site(s), and orange contain conserved seed site(s) and poorly conserved seed site(s), FDR - False Discovery Rate (p adjusted).

miR-21-5p knock-down vs non-targeting control							
Genes up-regulated at least 1.5-fold				Genes up-regulated at least 1.5-fold			
Gene	Fold change	p value	FDR	Gene	Fold change	p value	FDR
U1	4.92	0.000	0.51	TIMP3	1.60	0.074	1
snoU13	3.89	0.367	1	KALRN	1.60	0.076	1
U3	3.87	1.000	1	CR2	1.60	0.481	1
NPPA	3.43	0.057	1	COL4A5	1.60	0.054	1
U5	3.00	0.200	1	ITGB8	1.59	0.080	1
SYN3	2.71	0.025	1	NFAT5	1.59	0.012	1
IGSF5	2.52	0.033	1	EPHA5	1.59	0.244	1
CATIP	2.35	0.024	1	PLA2G4F	1.58	0.109	1
S100A12	2.28	0.200	1	EML6	1.58	0.142	1
SPP1	2.28	0.016	1	PDGFC	1.58	0.054	1
COL4A6	2.20	0.045	1	ZBED6	1.58	0.004	1
SPDYA	2.15	0.026	1	KIAA1549	1.58	0.018	1
SEMA3D	2.01	0.014	1	FOXRED2	1.58	0.131	1
DGKH	2.00	0.003	1	SCN2A	1.58	0.109	1
UNC80	1.95	0.086	1	DCX	1.57	0.097	1
SPRY4	1.91	0.024	1	SLC6A12	1.57	0.312	1
PAPPA2	1.91	0.025	1	PCDHB13	1.56	0.065	1
TRIM66	1.86	0.093	1	PCDHB4	1.56	0.309	1
SULF1	1.85	0.017	1	PCDHB15	1.55	0.111	1
DLK2	1.85	0.128	1	FAM84A	1.55	0.120	1
TRH	1.83	0.108	1	SCRN3	1.55	0.071	1
C17orf67	1.82	0.209	1	GPX3	1.55	0.057	1
U12	1.79	0.385	1	NPTX1	1.55	0.384	1
DMXL2	1.76	0.123	1	NEK10	1.55	0.140	1
ALOX12	1.76	0.031	1	ABHD2	1.54	0.009	1
WDPCP	1.75	0.100	1	TENM1	1.54	0.355	1
CSAR2	1.75	0.090	1	CD163	1.53	0.178	1
TNFRSF11B	1.74	0.064	1	SLC10A5	1.53	0.329	1
KCTD21	1.73	0.165	1	MAP3K2	1.53	0.016	1
NOG	1.73	0.204	1	KCNQ5	1.53	0.047	1
HTR3E	1.72	0.136	1	ZKSCAN4	1.53	0.093	1
ZNF699	1.72	0.047	1	RAB20	1.53	0.254	1
CSF2RB	1.72	0.099	1	HIPK2	1.53	0.110	1
SPIN4	1.71	0.050	1	SLC4A4	1.53	0.145	1
U6	1.71	0.074	1	RPS6KA3	1.53	0.020	1
GALNT15	1.71	0.145	1	EFCAB6	1.52	0.229	1
UBN2	1.70	0.008	1	KCNN4	1.52	0.258	1
ADGRV1	1.70	0.099	1	DNAH3	1.52	0.203	1
ZBTB20	1.70	0.039	1	ANKRD50	1.52	0.070	1
SLC6A6	1.70	0.084	1	PGM2L1	1.51	0.121	1
USF3	1.69	0.003	1	PLAG1	1.51	0.161	1
NAV3	1.68	0.092	1	HAS3	1.51	0.146	1
HIVEP3	1.67	0.037	1	AGO3	1.51	0.034	1
NT5E	1.67	0.017	1	ADAMTS9	1.51	0.183	1
LIFR	1.65	0.023	1	SMOX	1.51	0.103	1
ADAMTS8	1.65	0.853	1	CA5B	1.51	0.038	1
CPEB3	1.65	0.056	1	NALCN	1.50	0.333	1
PCSK6	1.65	0.047	1	PIK3CB	1.50	0.141	1
SPNS2	1.65	0.090	1	LETM2	1.50	0.145	1
ASB14	1.64	0.240	1	FGF1	1.50	0.249	1
EPHA4	1.64	0.104	1	CMKLR1	1.50	0.014	1
SEMA6D	1.64	0.035	1	AK9	1.50	0.242	1
KIAA2022	1.63	0.061	1				
FGF1	1.63	0.293	1				
TNC	1.62	0.070	1				
CDA	1.61	0.102	1				
PAPPA	1.61	0.042	1				
CEMIP	1.61	0.050	1				
EFNB3	1.61	0.247	1				

**Table 5.8.** Up-regulated genes ( $\geq 1.5$ -fold) in cells transfected with miR-221 inhibitor compared to expression in the non-targeting inhibitor control, as identified using NGS. Key: Genes highlighted with green contain conserved seed site(s), yellow contain poorly conserved seed site(s), and orange contain conserved seed site(s) and poorly conserved seed site(s), FDR - False Discovery Rate (p adjusted).

miR-221 knock-down vs non-targeting control												
Genes up-regulated at least 1.5-fold				Genes up-regulated at least 1.5-fold				Genes up-regulated at least 1.5-fold				
Gene	Fold change	p value	FDR	Gene	Fold change	p value	FDR	Gene	Fold change	p value	FDR	
U1	2333.74	0.000	0.00	CACHD1	1.78	0.095	1.00	ADAM8	1.59	0.149	1.00	
U5	861.50	0.000	0.00	MEX3A	1.77	0.106	1.00	ITGA3	1.59	0.083	1.00	
U3	720.88	0.000	0.00	ADIPOQ	1.77	0.014	1.00	KCNH1	1.59	0.154	1.00	
U3	492.28	0.000	0.00	TIMP3	1.77	0.031	1.00	SEMA6B	1.59	0.116	1.00	
snoU13	175.95	0.000	0.00	CEMIP	1.76	0.020	1.00	ANKRD50	1.58	0.047	1.00	
U1	157.56	0.000	0.00	SULF1	1.75	0.030	1.00	RAPH1	1.58	0.006	1.00	
U1	86.49	0.000	0.00	TPBG	1.75	0.069	1.00	SEMA6D	1.58	0.050	1.00	
U3	83.07	0.000	0.00	RUFY4	1.74	0.075	1.00	NAV3	1.58	0.137	1.00	
U12	65.51	0.000	0.00	DMXL2	1.74	0.125	1.00	SLC6A6	1.58	0.137	1.00	
U5	38.17	0.000	0.00	C12orf66	1.74	0.033	1.00	SLC29A1	1.57	0.015	1.00	
U1	23.98	0.000	0.00	C17orf67	1.73	0.250	1.00	ANKRD61	1.57	0.223	1.00	
CATIP	4.63	0.000	0.04	SLC6A12	1.73	0.216	1.00	RAB20	1.57	0.229	1.00	
HIST1H1E	4.34	0.001	0.90	SCUBE3	1.71	0.037	1.00	CDKN1A	1.57	0.025	1.00	
SYN3	4.09	0.002	1.00	ARC	1.70	0.154	1.00	ETV4	1.57	0.097	1.00	
NPPA	3.61	0.047	1.00	HIPK2	1.70	0.046	1.00	FGF1	1.56	0.329	1.00	
DLK2	3.46	0.002	1.00	CORO2A	1.70	0.114	1.00	RRP8	1.56	0.030	1.00	
PLA2G4F	3.46	0.000	0.02	SPDYA	1.70	0.124	1.00	S100A12	1.56	0.509	1.00	
bta-mir-27a	3.35	0.003	1.00	HAS3	1.69	0.065	1.00	CSPG4	1.55	0.028	1.00	
bta-mir-23a	3.18	0.009	1.00	NEB	1.69	0.048	1.00	DOT1L	1.55	0.022	1.00	
TFR2	3.16	0.000	0.32	HTR3E	1.68	0.152	1.00	CRELD1	1.55	0.088	1.00	
ISG20	2.47	0.453	1.00	C8H9orf152	1.68	0.096	1.00	RUNX2	1.55	0.014	1.00	
SPRY4	2.43	0.002	1.00	KALRN	1.67	0.051	1.00	AGO3	1.54	0.025	1.00	
U8	2.41	0.002	1.00	HS6ST1	1.67	0.068	1.00	RPS6KA3	1.54	0.017	1.00	
IGSF5	2.31	0.053	1.00	SLC13A5	1.67	0.363	1.00	LPAR3	1.54	0.067	1.00	
SPP1	2.29	0.015	1.00	USF3	1.67	0.004	1.00	ASB14	1.54	0.303	1.00	
ALOX12	2.23	0.002	1.00	UNC80	1.67	0.187	1.00	bta-mir-2443	1.54	0.143	1.00	
CDHR5	2.23	0.168	1.00	SLC35E4	1.66	0.149	1.00	CATSPER2	1.54	0.169	1.00	
ZBTB20	2.22	0.002	1.00	KIAA1549	1.66	0.009	1.00	KMT2D	1.53	0.021	1.00	
CSF2RB	2.10	0.025	1.00	CYTL1	1.65	0.027	1.00	SDK2	1.53	0.025	1.00	
KCNN3	2.09	0.018	1.00	ST6GAL1	1.65	0.017	1.00	SPATA21	1.53	0.228	1.00	
KCNN4	2.08	0.047	1.00	RPP40	1.65	0.037	1.00	SH2B2	1.53	0.186	1.00	
BAIAP2L2	2.07	0.023	1.00	BDKRB2	1.65	0.020	1.00	UBN2	1.52	0.037	1.00	
ADAMTS8	2.07	0.761	1.00	SMAD7	1.65	0.027	1.00	SLC5A12	1.52	0.110	1.00	
SPNS2	2.00	0.019	1.00	GALNT15	1.64	0.173	1.00	PLCXD2	1.52	0.368	1.00	
DGKH	1.99	0.003	1.00	NT5E	1.64	0.021	1.00	ITGB8	1.52	0.112	1.00	
NPAS1	1.99	0.026	1.00	SPRED2	1.64	0.017	1.00	ZMAT3	1.52	0.106	1.00	
ZBTB32	1.99	0.093	1.00	SEMA4B	1.63	0.039	1.00	PLAG1	1.52	0.156	1.00	
NOG	1.96	0.119	1.00	SLC25A41	1.63	0.180	1.00	FN1	1.52	0.044	1.00	
HIVEP3	1.96	0.006	1.00	SMG9	1.63	0.017	1.00	LETM2	1.52	0.131	1.00	
PAPPA2	1.93	0.022	1.00	GPX3	1.63	0.034	1.00	KIAA1671	1.52	0.052	1.00	
C5AR2	1.91	0.050	1.00	SPRED3	1.63	0.143	1.00	VEGFC	1.52	0.193	1.00	
TRH	1.90	0.087	1.00	UPP1	1.63	0.182	1.00	AEN	1.52	0.128	1.00	
NPTX1	1.88	0.207	1.00	PDGFC	1.63	0.041	1.00	VEGFA	1.51	0.144	1.00	
TNFRSF11B	1.87	0.037	1.00	CPAMD8	1.62	0.067	1.00	LIFR	1.51	0.065	1.00	
SEMA3D	1.85	0.030	1.00	USP31	1.62	0.040	1.00	COL6A3	1.50	0.046	1.00	
EFNB3	1.83	0.140	1.00	SLC10A5	1.62	0.260	1.00	DNAH3	1.50	0.218	1.00	
PAPPA	1.82	0.011	1.00	IKZF4	1.62	0.067	1.00	IGSF9B	1.50	0.262	1.00	
CDA	1.82	0.041	1.00	EPHA2	1.61	0.011	1.00	PHOSPHO1	1.50	0.293	1.00	
SMOX	1.82	0.018	1.00	DCLRE1B	1.61	0.020	1.00	STAC3	1.50	0.279	1.00	
TNC	1.81	0.026	1.00	PCSK6	1.61	0.059	1.00	CCND1	1.50	0.162	1.00	
CDC14A	1.81	0.025	1.00	CRACR2B	1.61	0.138	1.00	CXADR	1.50	0.105	1.00	
CMKLR1	1.81	0.000	0.31	DUSP6	1.60	0.039	1.00	EPHA4	1.50	0.183	1.00	
STK32B	1.80	0.026	1.00	GLDC	1.60	0.066	1.00					
COL4A6	1.80	0.139	1.00	TLR2	1.60	0.115	1.00					
PHF7	1.79	0.032	1.00	FOXA2	1.60	0.079	1.00					
ABHD2	1.79	0.000	0.33	S100A2	1.60	0.033	1.00					
GOLGA7B	1.78	0.134	1.00	CA5B	1.59	0.019	1.00					

**Table 5.9.** Up-regulated genes ( $\geq 1.5$ -fold) in cells transfected with miR-222 inhibitor compared to expression in the non-targeting inhibitor control, as identified using NGS. Key: Genes highlighted with green contain conserved seed site(s), yellow contain poorly conserved seed site(s), and orange contain conserved seed site(s) and poorly conserved seed site(s), FDR - False Discovery Rate (p adjusted).

miR-222 knock-down vs non-targeting control							
Upregulated at least 1.5-fold				Upregulated at least 1.5-fold			
Gene	Fold change	p value	FDR	Gene	Fold change	p value	FDR
U1	1209.41	0.000	0.00	NPTX1	1.69	0.293	1.00
U3	817.69	0.000	0.00	NEB	1.68	0.050	1.00
U5	686.85	0.000	0.00	TNFRSF11B	1.68	0.083	1.00
U3	670.94	0.000	0.00	TEX14	1.66	0.086	1.00
U1	176.10	0.000	0.00	EPHA4	1.66	0.095	1.00
U3	135.45	0.000	0.00	SLC13A5	1.66	0.364	1.00
snoU13	129.09	0.000	0.00	LIFR	1.65	0.025	1.00
U1	105.19	0.000	0.00	MYB	1.64	0.369	1.00
U5	58.96	0.000	0.00	AEN	1.63	0.073	1.00
U12	46.85	0.000	0.00	SPRED3	1.63	0.146	1.00
U1	32.48	0.000	0.00	CATSPER2	1.63	0.116	1.00
bta-mir-23a	6.60	0.000	0.03	ST6GAL1	1.63	0.021	1.00
bta-mir-27a	6.41	0.000	0.01	DQX1	1.62	0.142	1.00
HIST1H1E	4.01	0.003	1.00	USF3	1.61	0.007	1.00
TFR2	3.48	0.000	0.10	ADGRV1	1.60	0.145	1.00
PLA2G4F	3.30	0.000	0.03	USP31	1.59	0.048	1.00
CATIP	3.14	0.002	1.00	SEMA3D	1.59	0.098	1.00
NPPA	2.57	0.143	1.00	MC2R	1.59	0.078	1.00
SPDYA	2.56	0.006	1.00	SMOX	1.59	0.065	1.00
ZBTB32	2.54	0.024	1.00	WNK3	1.59	0.145	1.00
SYN3	2.52	0.036	1.00	KCNN3	1.59	0.136	1.00
U8	2.39	0.002	1.00	DCLRE1B	1.59	0.024	1.00
CDHR5	2.34	0.140	1.00	SEMA6D	1.58	0.048	1.00
C17orf67	2.26	0.089	1.00	MDN1	1.58	0.011	1.00
IGSF5	2.22	0.064	1.00	FGF1	1.58	0.318	1.00
DLK2	2.19	0.047	1.00	RUFY4	1.58	0.145	1.00
CSF2RB	2.03	0.031	1.00	IMPG2	1.57	0.088	1.00
SPNS2	1.96	0.023	1.00	GALNT15	1.57	0.218	1.00
ALOX12	1.95	0.011	1.00	NEK10	1.57	0.135	1.00
COL4A6	1.94	0.093	1.00	HIPK2	1.56	0.091	1.00
HTR3E	1.94	0.071	1.00	ZBTB37	1.56	0.102	1.00
ZBTB20	1.94	0.011	1.00	ZBTB25	1.56	0.092	1.00
S100A12	1.92	0.313	1.00	SLC25A41	1.56	0.226	1.00
DGKH	1.92	0.005	1.00	ZNF416	1.56	0.171	1.00
DMXL2	1.92	0.074	1.00	SMG1	1.55	0.010	1.00
SPRY4	1.92	0.022	1.00	NABP1	1.55	0.085	1.00
SLC46A2	1.87	0.374	1.00	GOLGA7B	1.55	0.255	1.00
LAMC2	1.86	0.306	1.00	KMT2D	1.54	0.019	1.00
KCTD21	1.86	0.121	1.00	CPAMD8	1.54	0.101	1.00
PHF7	1.86	0.023	1.00	CACNA1A	1.54	0.103	1.00
SPP1	1.86	0.067	1.00	SCN2A	1.54	0.137	1.00
C5AR2	1.85	0.062	1.00	PEG3	1.53	0.234	1.00
UBN2	1.83	0.003	1.00	SLC5A12	1.53	0.106	1.00
KCNN4	1.83	0.102	1.00	MAP3K2	1.53	0.016	1.00
RRP8	1.82	0.003	1.00	ZKSCAN2	1.53	0.096	1.00
DNAH3	1.80	0.073	1.00	SCRN3	1.53	0.081	1.00
HIVEP3	1.80	0.017	1.00	RAPH1	1.52	0.012	1.00
ASB14	1.80	0.164	1.00	EVI2B	1.52	0.273	1.00
PAPPA2	1.78	0.046	1.00	CEMIP	1.52	0.085	1.00
ISG20	1.76	0.654	1.00	ZBED6	1.51	0.009	1.00
NAALADL1	1.76	0.086	1.00	ANKRD61	1.51	0.273	1.00
NAV3	1.75	0.069	1.00	GTF2A1	1.51	0.016	1.00
CDA	1.75	0.055	1.00	FN1	1.51	0.048	1.00
MYBPH	1.74	0.064	1.00	NT5E	1.51	0.054	1.00
CDC14A	1.73	0.038	1.00	GCFC2	1.50	0.069	1.00
PAPPA	1.73	0.020	1.00	NFAT5	1.50	0.028	1.00
MEX3A	1.71	0.122	1.00	AGO3	1.50	0.036	1.00
HAS3	1.71	0.059	1.00				
ZMAT3	1.70	0.043	1.00				

### **5.2.7. Quantitative PCR validation of target genes of miR-21-5p, -221 and -222 identified from the NGS**

A panel of putative target genes has been identified, genes that are differentially expressed i.e. mRNA levels increase in cells treated with miR-21-5p, miR-221 or miR-222 inhibitors, and using TargetScan the 3'UTR sequences are predicted to contain the seed sites, suggestive of direct gene targets for further validation. Putative genes were chosen for validation based on the following criteria: (i) at least a 1.5-fold increase in transcript levels in response to specific miR inhibition, (ii) no effect on gene expression between non-targeting control and non-transfected control, (iii) contains at least 1 conserved seed site for a specific miR, (iv) Fischer's exact test p-values  $\leq 0.05$ . Although a few of the target genes did not meet all of these criteria, they had been previously validated, by other groups, using experimental approaches hence their selection.

Transcript levels of selected genes were assessed on RNA extracted from cells treated with miR-21-5p, miR-221 or miR-222 inhibitors or their equivalent mimics. Experimental validation should present the appropriate transcriptional response in the cells transfected with siRNA, namely being elevated expression with miR inhibitors and reduced levels with miR mimics. Validation was conducted using either SybrGreen® or TaqMan® quantitative PCR. The impact of transfection reagents on the gene levels was evaluated by comparing the relative expression in cells treated with (i) transfection reagent only (mock), or (ii) transfection reagent and non-targeting siRNAs (non-targeting controls) to untreated control cells. Transcriptional levels of genes of interest were normalised to the geometric mean of the reference genes HPRT and YWHAZ (which were found to maintain stable expression under the experimental conditions) and relative to inhibitor/mimic non-targeting control.

**miR-21-5p:** 4 putative targets of miR-21-5p with varying numbers of seed sites were selected for validation: (i) mRNA polyadenylation factor: CPEB3, (ii) signalling antagonist: SPRY4, (iii) matrix metalloproteinase: MMP-13 and (iv) metalloproteinase inhibitor: TIMP-3 (Table 5.10).

**Table 5.10.** List of putative target genes of miR-21-5p. The list was created based on NGS data and computational target gene prediction using TargetScan.

Gene ID	Gene name	Conserved sites				Poorly conserved sites				6mer sites
		total	8mer sites	7mer-m8 sites	7mer-A1 sites	total	8mer sites	7mer-m8 sites	7mer-A1 sites	
CPEB3	cytoplasmic polyadenylation element binding protein 3	2	1	1	0	0	0	0	0	0
MMP13	matrix metalloproteinase 13 (collagenase 3)	0	0	0	0	1	0	1	0	0
SPRY4	sprouty homolog 4 (Drosophila)	1	0	1	0	0	0	0	0	1
TIMP3	TIMP metalloproteinase inhibitor 3	2	2	0	0	0	0	0	0	0

CPEB3 transcription was highly reduced by the non-targeting mimic compared to other controls: untreated (2.77-fold:  $p < 0.001$ ), mock (2.31-fold:  $p < 0.001$ ) and non-targeting inhibitor (2.71-fold:  $p = 0.001$ ; Figure 5.15A). CPEB3 mRNA level was elevated in response to miR-21-5p inhibition in a manner approaching significance (1.22-fold:  $p = 0.068$ ), confirming the NGS data (Table 5.7), and was significantly decreased when treated with miR mimic (1.52-fold:  $p = 0.015$ ) compared to the respective non-targeting controls (Figure 5.15B).

Expression of SPRY4 mRNA did not change in response to mimic control, but surprisingly, was significantly increased in both mock cells (4.08-fold:  $p < 0.001$ ) and in response to inhibitor control (4.21-fold:  $p < 0.001$ ) when compared to untreated cells (Figure 5.16A). SPRY4 mRNA levels were elevated in response to the miR-21-5p mimic (1.5-fold:  $p = 0.046$ ) when compared to its respective non-targeting control (Figure 5.16B); miR-21-5p inhibitor did not affect SPRY4 transcription.

The non-targeting miR inhibitor also appeared to affect MMP-13 expression, elevating MMP-13 mRNA levels compared to the untreated control (2.06-fold:  $p = 0.026$ ) and mimic control (1.99-fold:  $p = 0.036$ ; Figure 5.17A). Although the NGS data did not indicate a  $\geq 1.5$ -fold increase in MMP-13 expression in response to miR-21-5p inhibition, the qPCR data demonstrated a significant 1.99-fold increase ( $p = 0.007$ ) compared to the non-targeting control, with no effect of mimic treatment (Figure 5.17B).

For TIMP-3 expression, there was reduced mRNA levels in the mimic control when compared with mock (2.08-fold:  $p=0.024$ ) or non-targeting inhibitor (2.07-fold:  $p=0.023$ ), although its expression remained unchanged from untreated control (Figure 5.18A). Validation of TIMP-3 confirmed the results of NGS (1.61-fold,  $p=0.074$ ; Table 5.7) showing an up-regulation in response to miR-21-5p inhibitor (1.51-fold:  $p=0.01$ ), and a significant reduction in response to miR-21-5p mimic (2.11-fold:  $p=0.006$ ; Figure 5.18B) compared to their respective non-targeting controls.

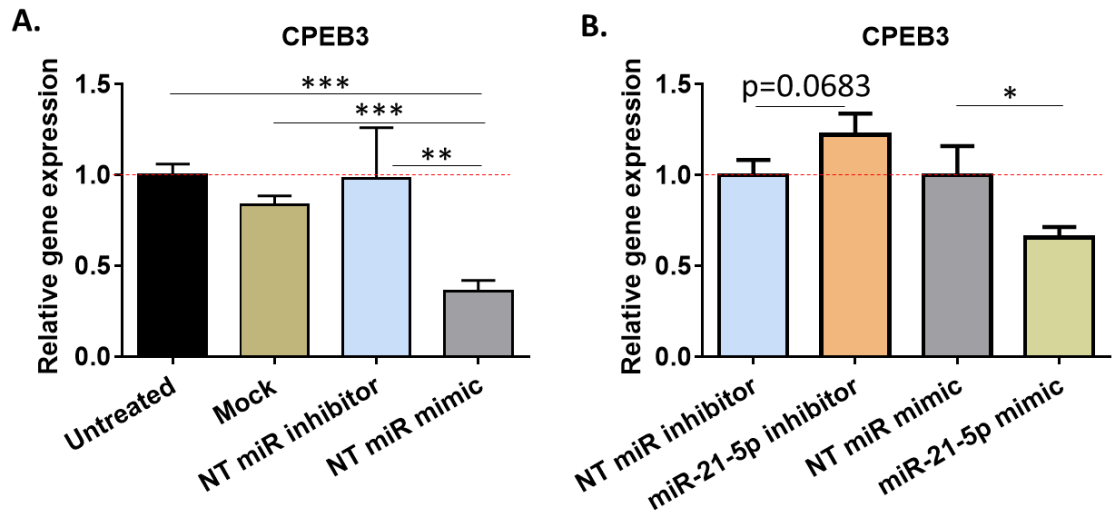


**Figure 5.15.** Validation of CPEB3 - a putative target gene of miR-21-5p. Expression of CPEB3 in cells transfected with: transfection reagent only or non-targeting inhibitor/mimic **(A)** and miR-21-5p inhibitor/mimic **(B)** was assessed by TaqMan<sup>®</sup> qPCR. All data were normalised to the geometric mean of the reference genes HPRT and YWHAZ and to the respective control: either untreated **(A)** or transfected with non-targeting miR-inhibitor/mimic **(B)** cells. Data is presented as mean  $\pm$  SD (n = 3 cell culture wells) and is representative of 3 independent experiments. Statistical analysis was performed using a 1-way ANOVA with Tukey's post hoc test. Key: NT - non-targeting, [\*  $p \leq 0.05$ , \*\*  $p \leq 0.01$ , \*\*\*  $p \leq 0.001$ ].

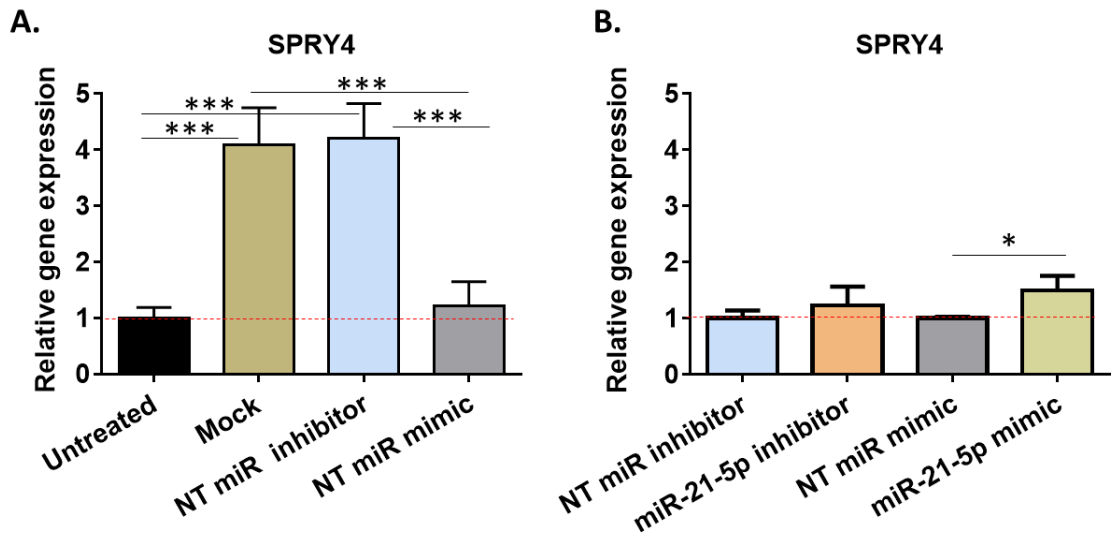


**Figure 5.16.** Validation of SPRY4 - a putative target gene of miR-21-5p. Expression of SPRY4 in in cells transfected with: transfection reagent only or non-targeting inhibitor/mimic **(A)** and miR-21-5p inhibitor/mimic **(B)** was assessed by SYBRgreen® qPCR. All data were normalised to the geometric mean of the reference genes HPRT and YWHAZ and to the respective control: either untreated **(A)** or transfected with non-targeting miR-inhibitor/mimic **(B)** cells. Data is presented as mean  $\pm$  SD (n = 3 cell culture wells) and is representative of 3 independent experiments. Statistical analysis was performed using a 1-way ANOVA with Tukey's post hoc test. Key: NT - non-targeting, [\* p $\leq$ 0.05, \*\*\* p $\leq$ 0.001].

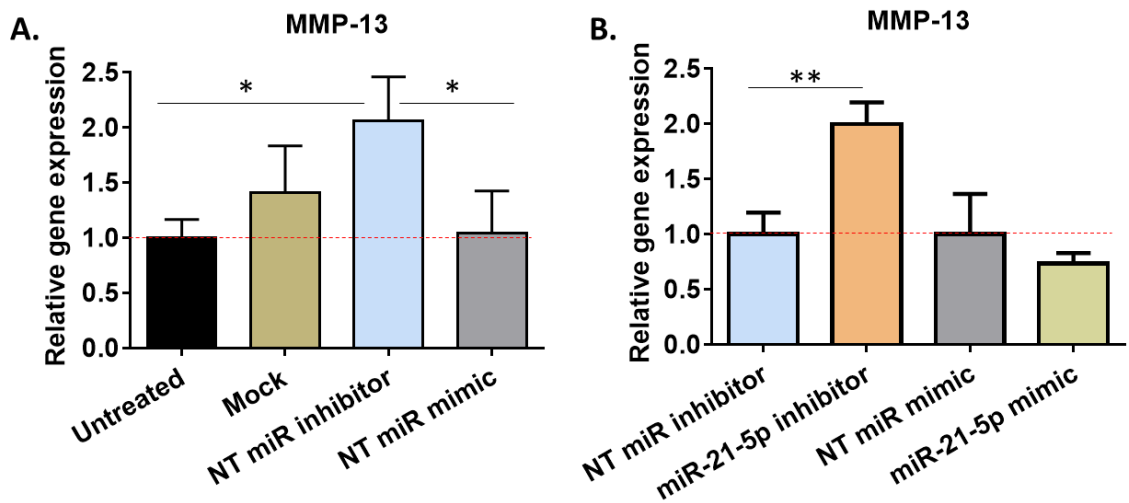


**Figure 5.17.** Validation of MMP-13 - a putative target gene of miR-21-5p. Expression of MMP-13 in cells transfected with: transfection reagent only or non-targeting inhibitor/mimic **(A)** and miR-21-5p inhibitor/mimic **(B)** was assessed by SYBRgreen® qPCR. All data were normalised to the geometric mean of the reference genes HPRT and YWHAZ and to the respective control: either untreated **(A)** or transfected with non-targeting miR-inhibitor/mimic **(B)** cells. Data is presented as mean  $\pm$  SD (n = 3 cell culture wells) and is representative of 3 independent experiments. Statistical analysis was performed using a 1-way ANOVA with Tukey's post hoc test. Key: NT - non-targeting, [\*  $p \leq 0.05$ , \*\*  $p \leq 0.01$ ].

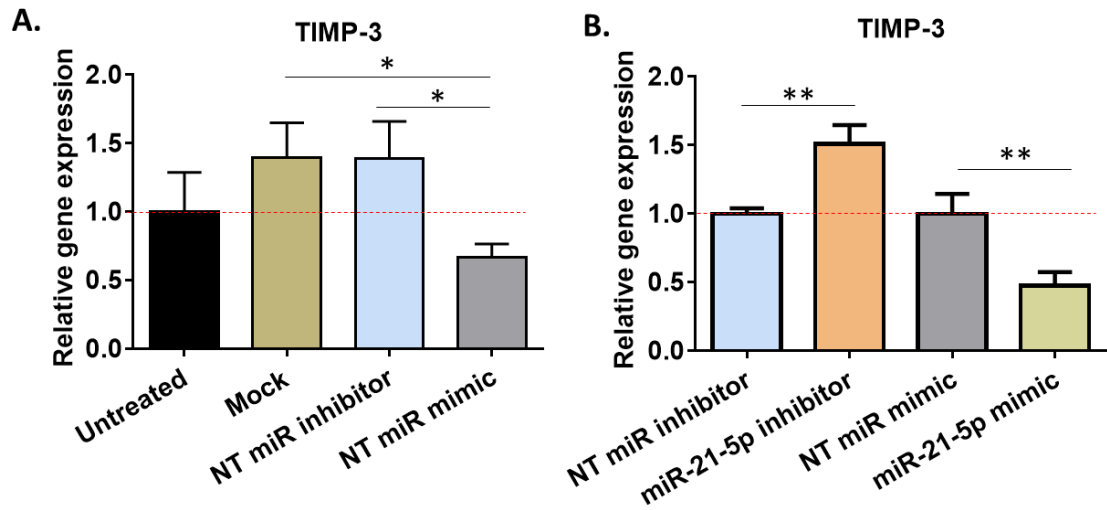


**Figure 5.18.** Validation of TIMP-3 - a putative target gene of miR-21-5p. Expression of TIMP-3 in cells transfected with: transfection reagent only or non-targeting inhibitor/mimic **(A)** and miR-21-5p inhibitor/mimic **(B)** was assessed by SYBRgreen® qPCR. All data were normalised to the geometric mean of the reference genes HPRT and YWHAZ and to the respective control: either untreated **(A)** or transfected with non-targeting miR-inhibitor/mimic **(B)** cells. Data is presented as mean  $\pm$  SD (n = 3 cell culture wells) and is representative of 3 independent experiments. Statistical analysis was performed using a 1-way ANOVA with Tukey's post hoc test. Key: NT - non-targeting, [\*  $p \leq 0.05$ , \*\*  $p \leq 0.01$ ].

**miR-221 and miR-222:** As the seed regions of miR-221 and miR-222 are identical, expression of selected putative target genes were validated for both. The panel of potential targets of these miRs includes transcription factor: Runx2, signalling antagonist: SPRY4, mRNA polyadenylation factor: CPEB3, cytokine/type I cytokine receptor/immunity protein: LIFR, and the metalloproteinase inhibitor: TIMP-3 (Table 5.11). MMP-13 and HDAC4, despite not having seed sites in the 3'UTR for miR-221 or miR-222, were also validated as they have been identified as target genes controlled by miR-222 (Song et al., 2015).

**Table 5.11.** List of putative target genes of miR-221 and miR-222. The list was created based on NGS data and computational target gene prediction using TargetScan.

Gene ID	Gene name	Conserved sites				Poorly conserved sites				6mer sites
		total	8mer sites	7mer-m8 sites	7mer-A1 sites	total	8mer sites	7mer-m8 sites	7mer-A1 sites	
CPEB3	cytoplasmic polyadenylation element binding protein 3	2	1	1	0	0	0	0	0	0
LIFR	leukemia inhibitory factor receptor alpha	2	1	1	0	0	0	0	0	1
RUNX2	runt-related transcription factor 2	1	0	0	1	1	0	1	0	0
SPRY4	sprouty homolog 4 (Drosophila)	0	0	0	0	1	0	0	1	1
TIMP3	TIMP metalloproteinase inhibitor 3	2	0	1	1	0	0	0	0	0

The effect of transfection reagents on SPRY4 mRNA expression was as previously described for miR-21-5p manipulation. Although SPRY4 was identified from the NGS data as one of the significant highly up-regulated genes in response to miR-221 and miR-222 inhibition, these changes were not confirmed by qPCR (Figure 5.19B and C). SPRY4 mRNA expression is visibly elevated when treated with the functional inhibitors, but the changes are not statistically significant. Surprisingly, no significant elevation of SPRY4 is observed in response to the miR-222 mimic (Figure 5.19C).

Runx2 appears to be sensitive to the transfection process itself showing reduced mRNA levels in the mock cells compared to the untreated control (1.43-fold:  $p=0.047$ ) and non-targeting inhibitor (1.55-fold:  $p=0.011$ ; Figure 5.20A). Runx2 was identified from the NGS data as being noticeably but not statistically significantly elevated in response to miR-221/-222 inhibition (Table 5.8), and has been experimentally validated as a target gene of hsa-miR-222-3p (Yan et al., 2016) which contains an identical nucleotide sequence as bta-miR-222. Therefore, the qPCR validation data were totally surprising as both miR-221 and miR-222 inhibitors down-regulated Runx2 transcripts relative to the non-targeting miR inhibitor control, however the differentially expressed gene was statistically significant (2.42-fold:  $p=0.048$ ) in response to miR-221 inhibitor only (Figure 5.20B). The expression of Runx2 was not significantly affected by either the miR-221 mimic (Figure 5.20B) or the miR-222 mimic (Figure 5.20C).

CPEB3 sensitivity to the transfection process (Figure 5.21A) is as described above for miR-21-5p validation. There was a significant decrease in CPEB3 mRNA levels in response to the miR-221 mimic (1.51-fold:  $p=0.016$ ; Figure 5.21B) compared to the non-targeting control. However, the miR-221 inhibitor (Figure 5.21B), or either the miR-222 inhibitor or mimic did not affect CPEB3 transcription (Figure 5.21C).

LIFR transcription was unaffected by transfection itself as none of the treatments significantly altered its expression (Figure 5.22A). Up-regulation in LIFR mRNA levels was observed in the NGS data for both miR-221 (1.51-fold:  $p=0.07$ ) and miR-222 (1.65-fold:  $p=0.03$ ), and this was confirmed by qPCR in response to the miR-221 inhibitor (1.31-fold:  $p=0.014$ ; Figure 5.22B). In contrast, miR-222 inhibition appeared to slightly elevate LIFR mRNA levels but this was not statistically significant, although miR-222 mimic significantly reduced LIFR transcription (1.51-fold;  $p=0.03$ ; Figure 5.22C).

Differential expression of TIMP-3 transcription was induced by transfection itself (Figure 5.23A) as discussed above for miR-21-5p validation. TIMP-3 seems to be a direct target of both miR-221/-222 (Table 5.11). It was also up-regulated by inhibition of miR-221 (1.76-fold:  $p=0.03$ ; Table 5.8) and miR-222 (1.45-fold:  $p=0.16$ ; Table 5.9). Increased TIMP-3 transcription in response to knock-down of miR-221 (1.54-fold:  $p=0.003$ ; Figure 5.23B) and miR-222 (1.29-fold:  $p=0.025$ ; Figure 5.23C) was confirmed.

Furthermore, there were significant reductions in TIMP-3 mRNA in cells treated with miR-221 mimic (2.11-fold;  $p=0.006$ ; Figure 5.23B) and miR-222 mimic (2.17-fold;  $p=0.006$ ; Figure 5.23C) when compared to the mimic control.

Despite HDAC4 and MMP-13 not meeting any of the criteria set for validation of putative targets of the selected miRs, their responses to miR-221 and miR-222 siRNAs were assessed. The reason why these genes were taken into consideration was that previously miR-222 had been identified as regulating MMP-13 expression by targeting HDAC4 (Song et al., 2015). Results from the NGS experiment did not identify HDAC4 as being differentially expressed in response to transfection itself or the miR-221 and miR-222 inhibitors (data not shown); furthermore, the qPCR validation confirmed these findings (Figure 5.24A), and also confirmed that HDAC4 transcription was unaffected by over-expression of either miR-221 (Figure 5.24B) or miR-222 (Figure 5.24C).

MMP-13 sensitivity to transfection reagents (Figure 5.25A) is as previously described above for miR-21-5p validation. Although the deep sequencing data indicated no significant increase in MMP-13 transcription in response to knock-down of miR-221 (1.31-fold:  $p=0.416$ ) and miR-222 (1.39-fold:  $p=0.309$ ), surprisingly, the qPCR validation showed definite up-regulation of MMP-13 mRNA levels in response to both inhibitors: miR-221 (2.41-fold:  $p<0.001$ ; Figure 5.25B) and miR-222 (1.76-fold:  $p=0.027$ ; Figure 5.25C). In contrast, overexpression of either miR-221 (Figure 5.25B) or miR-222 (Figure 5.25C) did not affect MMP-13 transcript levels.

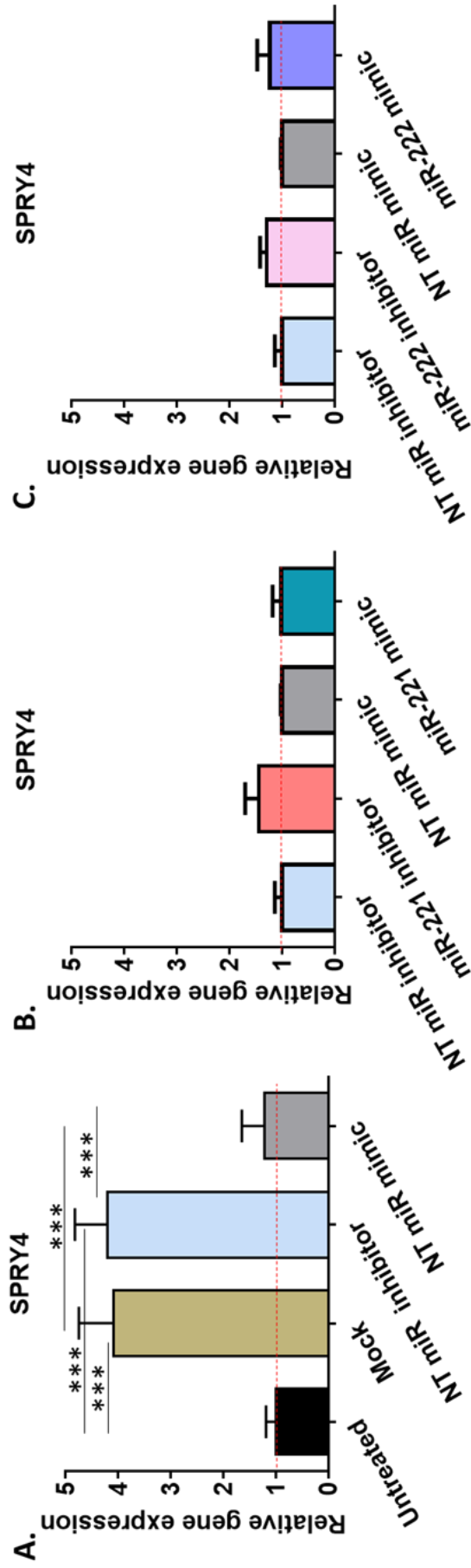


**Figure 5.19.** Validation of SPRY4 – a putative target gene of miR-221 and miR-222. Expression of SPRY4 in cells transfected with: transfection reagent only or non-targeting inhibitor/mimic (**A**), miR-221 inhibitor/mimic (**B**) and miR-222 inhibitor/mimic (**C**) was assessed by SYBR® green qPCR. All data were normalised to the geometric mean of the reference genes HPRT and YWHAZ and to the respective control: either untreated (**A**) or transfected with non-targeting miR-inhibitor/mimic (**B, C**) cells. Data is presented as mean  $\pm$  SD ( $n = 3$  cell culture wells) and is representative of 3 independent experiments. Statistical analysis was performed using a 1-way ANOVA with Tukey's post hoc test. Key: NT - non-targeting, [\*\*\*  $p < 0.001$ ].

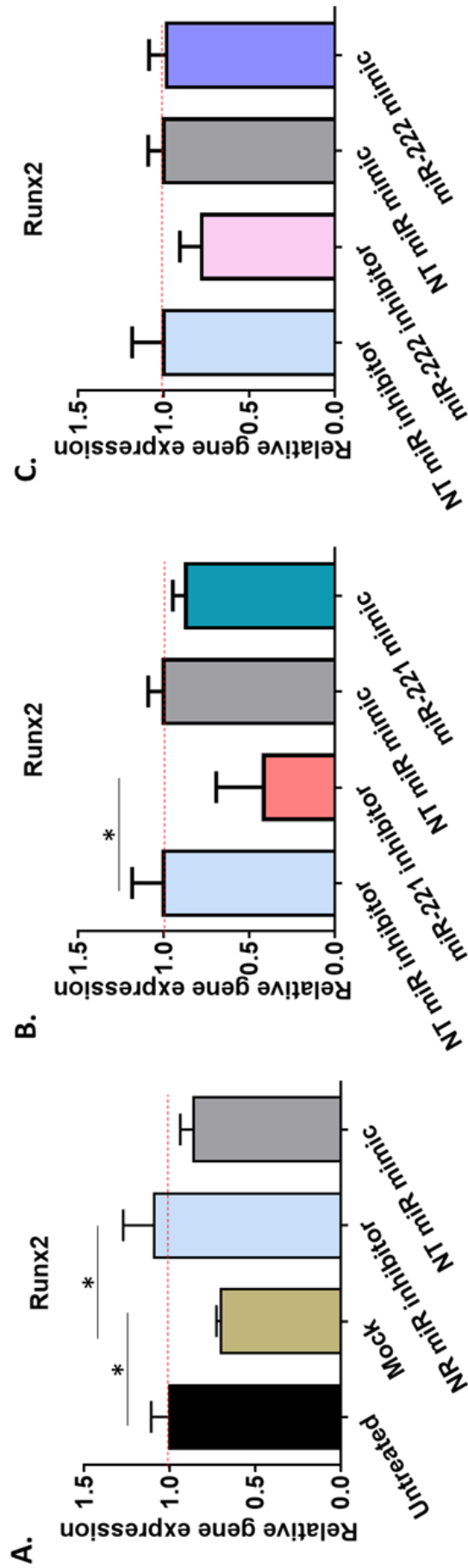


**Figure 5.20.** Validation of Runx2 – a putative target gene of miR-221 and -222. Expression of Runx2 in cells transfected with: transfection reagent only or non-targeting inhibitor/mimic (**A**) and miR-221 inhibitor/mimic (**B**), miR-222 inhibitor/mimic (**C**) was assessed by SYBR® green qPCR. All data were normalised to the geometric mean of the reference genes HPRT and YWHAZ and to the respective control: either untreated (**A**) or transfected with non-targeting miR-inhibitor/mimic (**B, C**) cells. Data is presented as mean  $\pm$  SD ( $n = 3$  cell culture wells) and is representative of 3 independent experiments. Statistical analysis was performed using a 1-way ANOVA with Tukey's post hoc test. Key: NT - non-targeting, [\*  $p \leq 0.05$ ].

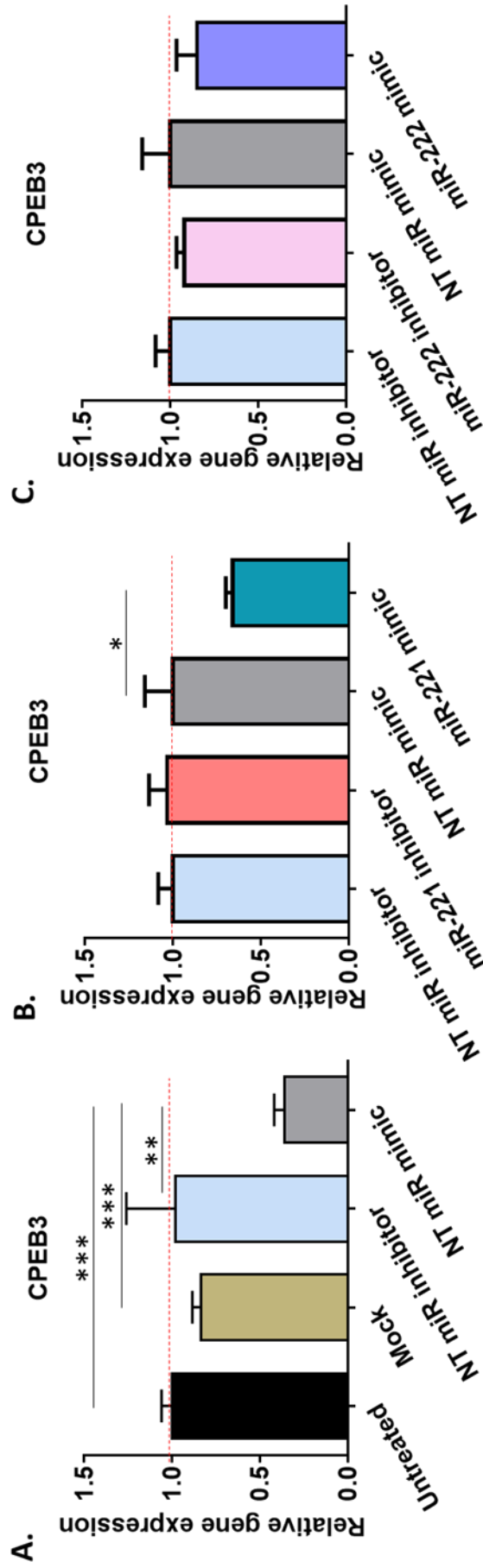


**Figure 5.21.** Validation of CPEB3 - putative target gene of miR-221 and -222. Expression of CPEB3 in cells transfected with: transfection reagent only or non-targeting inhibitor/mimic (**A**), miR-221 inhibitor/mimic (**B**) and miR-222 inhibitor/mimic (**C**) was assessed by TaqMan® qPCR. All data were normalised to the geometric mean of the reference genes HPRT and YWHAZ and to the respective control: either untreated (**A**) or transfected with non-targeting miR-inhibitor/mimic (**B, C**) cells. Data is presented as mean  $\pm$  SD (n = 3 cell culture wells) and is representative of 3 independent experiments. Statistical analysis was performed using a 1-way ANOVA with Tukey's post hoc test. Key: NT - non-targeting, [\* p $\leq$ 0.05, \*\* p $\leq$ 0.01, \*\*\* p $\leq$ 0.001].

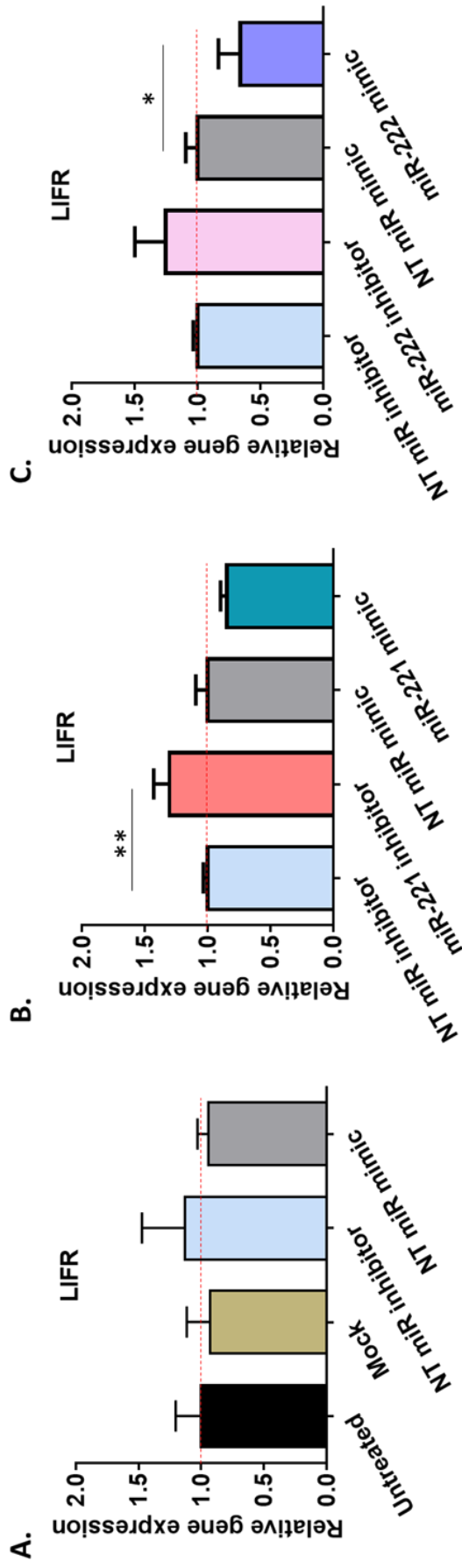


**Figure 5.22.** Validation of LIFR – a putative target gene of miR-221 and -222. Expression of LIFR in cells transfected with: transfection reagent only or non-targeting inhibitor/mimic (**A**), miR-221 inhibitor/mimic (**B**) and miR-222 inhibitor/mimic (**C**) was assessed by TaqMan® qPCR. All data were normalised to the geometric mean of the reference genes HPRT and YWHAZ and to the respective control: either untreated (**A**) or transfected with non-targeting miR-inhibitor/mimic (**B, C**) cells. Data is presented as mean  $\pm$  SD (n = 3 cell culture wells) and is representative of 3 independent experiments. Statistical analysis was performed using a 1-way ANOVA with Tukey's post hoc test. Key: NT - non-targeting, [\* p $\leq$ 0.05, \*\* p $\leq$ 0.01, \*\*\* p $\leq$ 0.001].

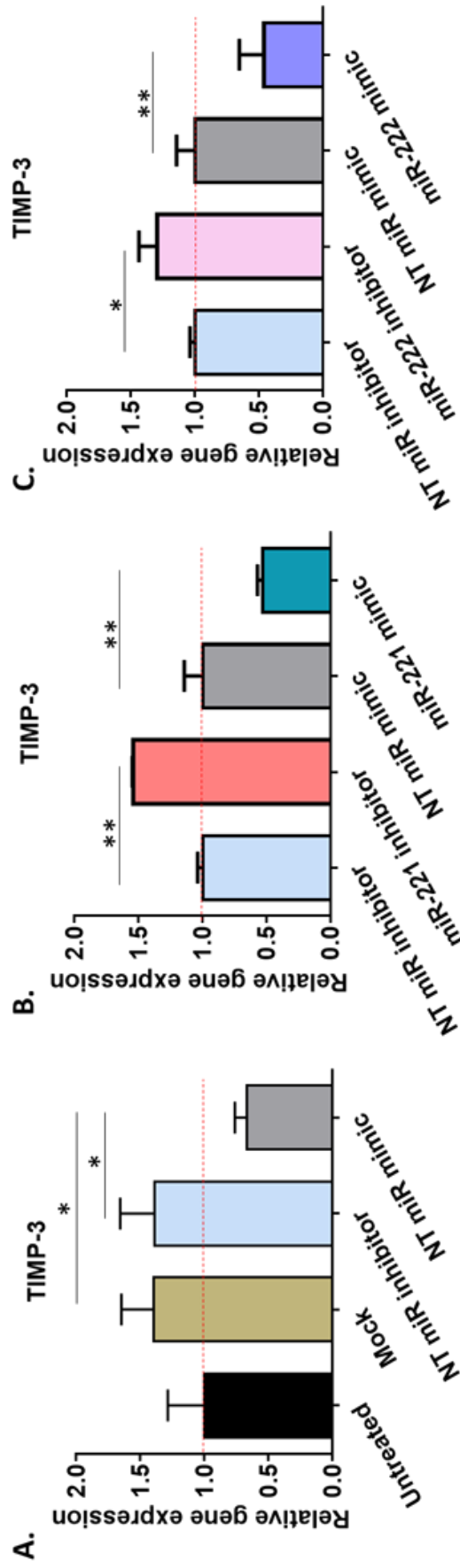


**Figure 5.23.** Validation of TIMP-3 – a putative target gene of miR-221 and -222. Expression of TIMP-3 in cells transfected with: transfection reagent only or non-targeting inhibitor/mimic (**A**), miR-221 inhibitor/mimic (**B**) and miR-222 inhibitor/mimic (**C**) was assessed by SYBR<sup>®</sup> green qPCR. All data were normalised to the geometric mean of the reference genes HPRT and YWHAZ and to the respective control: either untreated (**A**) or transfected with non-targeting miR-inhibitor/mimic (**B, C**) cells. Data is presented as mean  $\pm$  SD (n = 3 cell culture wells) and is representative of 3 independent experiments. Statistical analysis was performed using a 1-way ANOVA with Tukey's post hoc test. Key: NT - non-targeting [\* p $\leq$ 0.05, \*\* p $\leq$ 0.01].

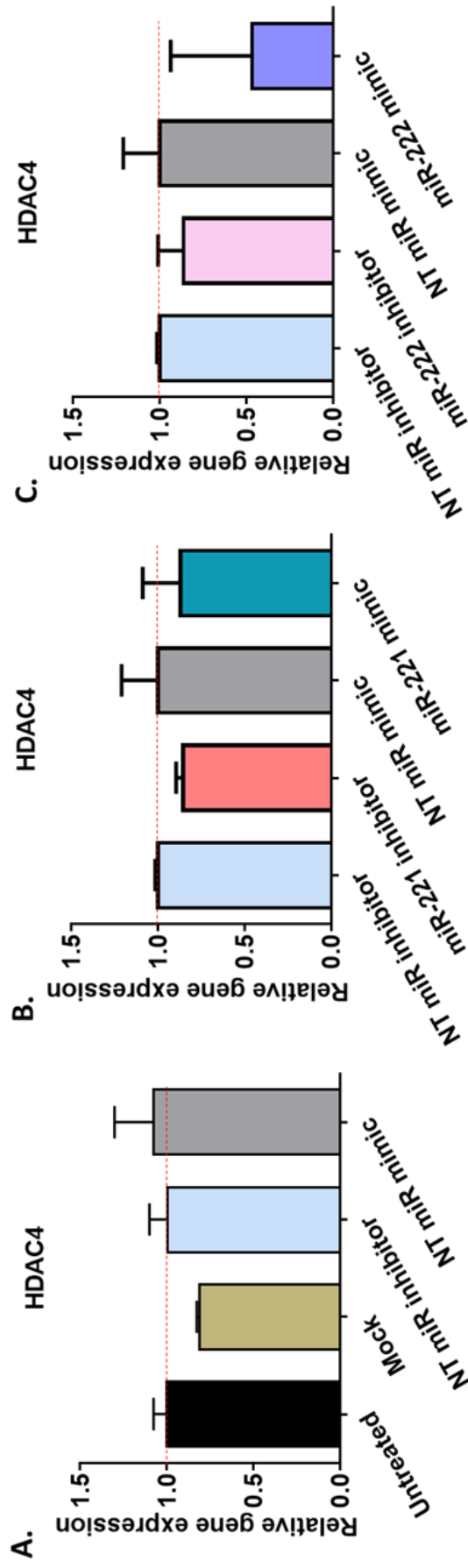


**Figure 5.24.** Validation of HDAC4 - a putative target gene of miR-221 and -222. Expression of HDAC4 in cells transfected with: transfection reagent only or non-targeting inhibitor/mimic (**A**), miR-221 inhibitor/mimic (**B**) and miR-222 inhibitor/mimic (**C**) was assessed by SYBR® green qPCR. All data were normalised to the geometric mean of the reference genes HPRT and YWHAZ and to the respective control: either untreated (**A**) or transfected with non-targeting miR-inhibitor/mimic (**B, C**) cells. Data is presented as mean  $\pm$  SD (n = 3 cell culture wells) and is representative of 3 independent experiments. Statistical analysis was performed using a 1-way ANOVA with Tukey's post hoc test. Key: NT - non-targeting

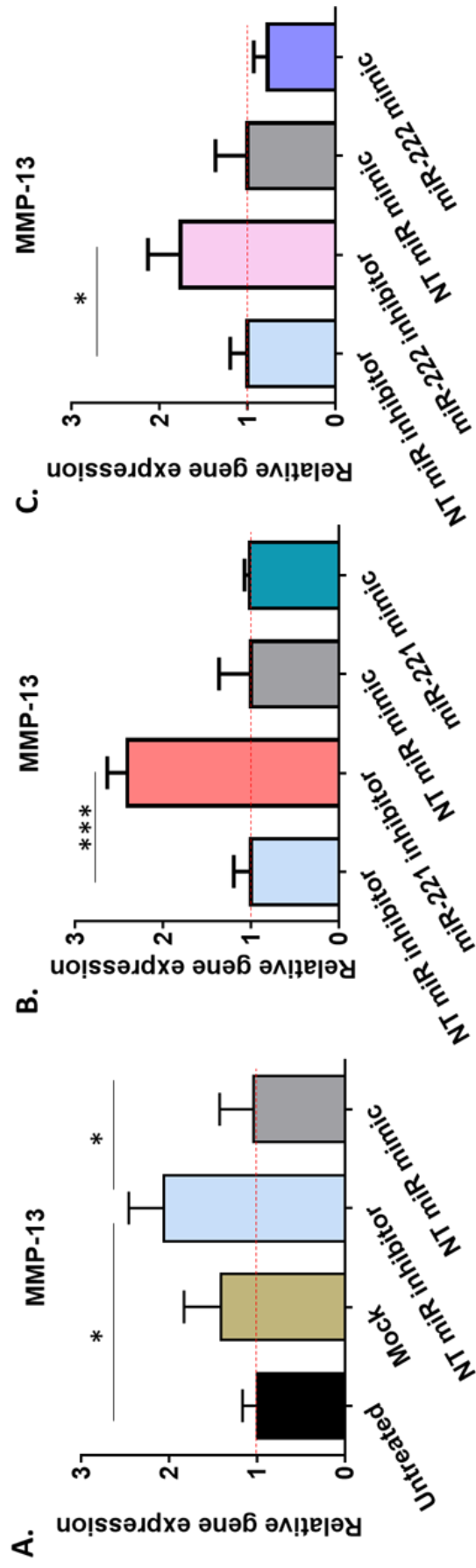


**Figure 5.25.** Validation of MMP-13 – a putative target gene of miR-221 and -222. Expression of MMP-13 in cells transfected with: transfection reagent only or non-targeting inhibitor/mimic (**A**), miR-221 inhibitor/mimic (**B**) and miR-222 inhibitor/mimic (**C**) was assessed by SYBR<sup>®</sup> green qPCR. All data were normalised to the geometric mean of the reference genes HPRT and YWHAZ and to the respective control: either (**A**) untreated or (**B, C**) transfected with non-targeting miR-inhibitor/mimic cells. Data is presented as mean  $\pm$  SD (n = 3 cell culture wells) and is representative of 3 independent experiments. Statistical analysis was performed using a 1-way ANOVA with Tukey’s post hoc test. Key: NT - non-targeting, [\* p $\leq$ 0.05, \*\*\* p $\leq$ 0.001].

### 5.3. Discussion

miRs are small, highly conserved and non-coding molecules having regulatory functions in many crucial biological processes i.e. proliferation, differentiation, signal transduction, immune responses and carcinogenesis (Bartel, 2009). The importance of miRs in living organisms is strengthened by the fact that they are coded by roughly 1% of animal genes and they are very often highly conserved across different species (Brennecke et al., 2005). Moreover miRs control expression of approximately one third of all human genes (Lewis et al., 2003), therefore it is not surprising that alterations in miR levels is very often associated with changes in expression of matrix molecules and may cause the development of many diseases (Soifer et al., 2007, Ardekani and Naeini, 2010). One of the diseases that is characterised by altered expression of some miRs compared to healthy tissue is OA (Araldi and Schipani, 2010, Crowe et al., 2016, Goldring and Marcu, 2012, Le et al., 2016, Pauley and Cha, 2011, Swingler et al., 2012).

Although miRs biological importance is clear, the mechanism of target gene recognition and regulation remains not well explained. Nowadays, it is known that miR control of gene expression is based on the miR complementarity to at least one of the target seed sites: 6mer, 7mer-m8, 7mermA1, 8mer (Brennecke et al., 2005, Fang and Rajewsky, 2011). Moreover, there is some evidence that mammalian miRs can regulate expression of genes by complementary binding to their 5'UTR mRNA (Lee et al., 2009) or coding region mRNA (Brümmer and Hausser, 2014), but base-pairing to 3'UTR mRNA with a minimum of one 7mer-m8 seed-matched site in the mRNA is still thought to be the dominant manner of target genes regulation (Baek et al., 2008, Fang and Rajewsky, 2011, Bartel, 2009).

Based on miR abilities of binding to short complementary sequences of mRNA, it is not surprising that a single miR can putatively regulate transcription of hundreds of genes and that one mRNA can be targeted by many different miRs (Lewis et al., 2003).

Knowing that miR-21-5p, -221 and -222 are: (i) responsive to non-physiological (7MPa, 1Hz, 15 minutes) magnitude of load and (ii) miR-21 alters in expression in OA cartilage compared to healthy tissue, the purpose of this experimental chapter was to:

- **Determine whether mechano-sensitive miR-21-5p, -221 and -222 regulate the expression of ECM molecules that have an involvement in cartilage homeostasis and/or OA development.**

Unfortunately, computational prediction of target genes of miRs is not good enough, because (i) prediction algorithms search for complementarity to seed region sequences in the 3' UTR of mRNA only, (ii) each prediction software uses different algorithms not always giving the same results, (iii) most softwares do not contain the database for the bovine genome. Therefore, in order to establish which genes are truly controlled by specific miRs, experimental evaluation is necessary. Initially, mammalian miRs were believed to regulate expression of their target genes mainly via inhibition of mRNA translation. However, studies by Baek et al. and Selbach et al. using proteomics and microarray methods, suggested that mRNA degradation of target genes of miRs may be a major manner of miR activity, as changes in protein expression of target genes were associated with variations in mRNA levels of these molecules (Baek et al., 2008, Selbach et al., 2008). Based on these studies, identification of direct target genes of mechano-sensitive miR-21-5p, -221 and -222 was conducted by assessment of putative target gene mRNA levels.

The functional analysis of mechano-responsive miRs in articular chondrocytes selected from chapter 4 was performed by monitoring relative expression of genes in chondrocytes subjected to manipulation of miR-21-5p, -221 and -222 levels.

### **5.3.1. Transfection, toxicity and quantification of manipulated miRs**

The preliminary transfection of bovine primary articular chondrocytes performed to assess the transfection efficiency was taken from published siRNA transfection conditions (Crowe et al., 2016) and confirmed a highly efficient delivery system and therefore were applied to functional siRNA transfection. The chondrocytes were exposed to 50nM miR-21-5p, -221, -222 inhibitors/mimics and miR-27a-5p inhibitor transfection for 48h. The analysis performed directly after this transfection period corroborated high intracellular uptake showing significant knock-down or overexpression of miR in cells treated with specific miR-21-5p, miR-221 and miR-222

mimics/inhibitors, respectively when compared to their non-targeting controls. However, surprisingly the miR-27a-5p presented statistically significant up- and not down-regulation of miR-27a-5p gene level in response to theoretically knock-down treatment, therefore searching of miR-27a-5p targets became impossible in this circumstance.

As too high a concentration of transfection reagents may induce cell death (Masotti et al., 2009), the effect of the cationic lipid transfection reagent only and with 50nM siRNA was assessed following a 48h transfection. Unchanged chondrocyte morphology (rounded cells) of transfected cells and similar level (~97.7%) of cell viability and (~2.3%) of cell death in treated and untreated cells measured using Live/Dead assay confirmed that transfection and concentrations of miR inhibitors/mimics were non-toxic and enough to induce changes in miR levels.

### **5.3.2. Differential expression of Wnt signalling components in response to inhibition of miR-21-5p, miR-221 and miR-222**

Having confirmed that transfection conditions do not affect cell morphology and viability of primary articular chondrocytes, identification of direct target genes of miR-21-5p, -221 and -222 was the next step and the goal of this chapter. Based on the previously published influence of these miRs on the expression of Wnt/ $\beta$ catenin signalling pathway components (Corr, 2008, Kawakita et al., 2014, Li et al., 2013, Wu et al., 2015, Zheng et al., 2012), the profile of Wnt signalling molecules in chondrocytes subjected to miR manipulation was assessed. The study was conducted using a custom-built bovine specific Wnt signalling PCR array designed by Dr. Aisha Al-Sabah (Cardiff University). The array included 84 Wnt signalling related genes that were grouped according to their function: targets of Wnt signalling, molecules of canonical Wnt signalling, Wnt/ $\text{Ca}^{2+}$  pathway, planar cell polarity (PCP) pathway and inhibitors of Wnt signalling. To eliminate false results of the chondrocytic response to functional miR level reduction, the gene expression profile was firstly compared between cells treated with non-targeting siRNA and untransfected cells. The effect of miR-21-5p, -221 and -222 knock-down was assessed by comparison of transcript profile in cells transfected with functional siRNA to non-targeting siRNA control.

Genes: FOSL1, PITX2 and Wnt2B were excluded from functional siRNA versus non-targeting siRNA comparison, as they presented altered expression levels in cells treated with non-targeting siRNA compared to untransfected cells, suggesting a sensitivity of these genes to transfection itself. As miR inhibitor binds to its complementary miR and reduces its activity, the expression of the direct target gene of this miR should be elevated. Surprisingly, results of the Wnt signalling PCR array for all tested miRs presented a greater number of decreased genes in cells treated with specific miR inhibitors than elevated ones. This data suggests that these down-regulated genes are down-stream of direct targets of examined miRs.

miR-21 is upregulated in OA cartilage (Zhang et al., 2014b) and was reported to be an upstream gene of some Wnt signalling pathway components (Kawakita et al., 2014, Wu et al., 2015). miR-21-5p inhibition reduced expression levels of 13 molecules, whereas only 1 gene (MMP-7) was upregulated. Despite MMP-7 not containing a target site in its 3'UTR and having not been indicated by TargetScan as a target gene of miR-21-5p, it was taken for validation. The reason for this decision was that target prediction algorithms are focused on the 3'UTR and four target sites ignoring the 5'UTR, protein coding region and mismatched sequences (Thomson et al., 2011). Unfortunately, validation data corroborated TargetScan results in that MMP-7 is not a direct target of miR-21-5p ([http://www.targetscan.org/vert\\_71/](http://www.targetscan.org/vert_71/)). Although, this experiment did not reach the appointed goal to find direct target genes of miR-21-5p, it confirmed a positive correlation of miR-21 with  $\beta$ -catenin, a key molecule in the Wnt signalling pathway, observed in previous studies performed on human lung cancer cells and Lewis lung carcinoma in mice (Wu et al., 2015). Surprisingly, the data presented also demonstrated positive regulation with the Wnt antagonist gene: dickkopf 2 (DKK2); this response is contradictory with Kawakita's observation of up-regulation of this gene in a human tongue cancer cell line transfected with miR-21 inhibitor (Kawakita et al., 2014).

Studies performed on human prostate cell lines and glioma cells demonstrated that respectively miR-221 (Zheng et al., 2012) and -222 (Li et al., 2013, Corr, 2008) also control the Wnt/ $\beta$ -catenin signalling pathway. In my experiment down-regulation of miR-221 and -222 slightly elevated expression of a few genes, but only Wnt3A, a gene which does not contain a seed site for any of these miRs in its 3'UTR, crossed the cut off

of a 2-fold increase. Due to the potential of other seed sites, as was mentioned in the case of MMP-7 up-regulation in response to miR-21-5p inhibition, Wnt3A was selected for validation, however the validation did not confirm the Wnt signalling array data. Zheng et al. reported a negative correlation between miR-221 and dishevelled 2 (DVL2) (Zheng et al., 2012) suggesting that, despite the minor up-regulation of this gene (1.26-fold) in response to miR-221 knock-down in my experiment, the change in expression was real, however this gene was also not validated. Studies by Li et al. showed an ability of miR-222 to regulate the expression of  $\beta$ -catenin and other downstream genes of the Wnt/ $\beta$ -catenin pathway by inhibition of its direct target DKK2, a known Wnt antagonist (Li et al., 2013); however results presented in this chapter did not corroborate these findings. Surprisingly, down-regulation of miR-222 expression in articular chondrocytes showed a reduction in expression of the following genes: DKK2 (data not shown), Axis Inhibition Protein 2 (Axin2) and Frizzled Class Receptor 1 (FZD1) which contain seed sites for miR-222 thus making these data difficult to rationalize.

### **5.3.3. qPCR validation of miR-21-5p, miR-221 and miR-222 target genes identified using Next Generation Sequencing**

Although Wnt signalling pathway arrays presented variations in gene expression, the results showed mostly positive correlation between altered genes (even those containing specific seed sites for examined miRs) and inhibited miRs indicating that these genes are not direct targets of tested miRs.

As the purpose of this chapter was to identify direct target genes of miR-21-5p, -221 and -222, the global changes in mRNA levels in cells transfected with functional miR inhibitors was assessed via Illumina Next Generation Sequencing. Cells treated with non-targeting siRNA were used as a control. Untreated cells were used as an additional control to assess the influence of transfection itself on gene expression. Genes that were significantly altered in cells with non-targeting siRNA compared to untreated cells and their FDR was less than 5%, were excluded from the panel of putative target genes as they were deemed sensitive to the transfection process. Originally, differentially expressed genes were selected based on the Benjamini-Hochberg corrected adjusted p-values ( $FDR \leq 0.05$ ), however because of the very limited number of significantly

altered genes, which were not direct targets as they do not have seed sites for the tested miRs, genes with at least a 1.5-fold up-regulation were considered for further studies in order to determine direct targets. Although, the FDR suggested extremely high rates of false positives for most of the differentially expressed genes, some of these genes were selected for further studies using the fold change cut off because expression of selected putative target genes was individually validated by qPCR.

The NGS data without the additional target site prediction analysis presented a number of spliceosomal and small nucleolar RNAs located in the nucleus as significantly up-regulated genes in response to miR-21-5p, -221 and -222 knock-down, with U1 spliceosomal RNA as the most elevated gene in cells with miR reduction. Although, there is evidence that some miRs i.e. miR-21 (Meister et al., 2004), -206 (Politz et al., 2006) and -709 (Tang et al., 2012) are present in the cell nucleus in their mature form, with miR-206 even being localised in the nucleolus (Politz et al., 2006), to date there is no publication confirming the control function of any miRs in nuclear non-coding RNAs. U1, U5 (Wassarman and Steitz, 1992) and U12 (Hall and Padgett, 1996) are involved in intron removal and mRNA splicing, whereas small nucleolar RNAs: U3 and U13 are engaged in nucleolar processing of pre-18S ribosomal RNA (Tyc and Steitz, 1989). Although, Meister et al. (2004) reported that 20% of mature miR-21 was localised in the nucleus of HeLa cells (Meister et al., 2004), the U1 gene does not contain a seed site for this miR excluding it as a miR-21-5p direct target. None of the spliceosomal or nucleolar RNA, or miR, or protein coding genes that were statistically ( $FDR \leq 0.05$ ) and significantly up-regulated in response to miR-221/-222 contain seed sites complementary to seed regions of these miRs, nor have they been localised anywhere else than the cytoplasm. Therefore, at this stage these up-regulated genes must be considered as either false positive results or potential indirect target genes.

The goal of this chapter was to establish which genes that were differentially detected in the NGS data are direct targets of mechano-responsive miR-21-5p, -221 and -222. A loss/gain of function theory used for the identification of target genes assumes the inversely proportional expression of target genes of up- or down-regulated miRs. Although some down-regulated transcripts may be indirect targets of examined inhibited miRs, these genes were excluded from the further analysis. Molecules that

were at least 1.5-fold up-regulated were considered as putative targets, from which a few genes were selected for further studies in order to validate their response to miR-21-5p, miR-221 and miR-222 manipulation.

The true direct target mRNA of miR must have at least one complementary seed site. Therefore, to eliminate indirect targets or false positive results, TargetScan - the computational prediction algorithm was used to search potential gene targets based on their conserved and poorly conserved 6mer, 7merA1, 7mer-8m and 8mer seed sites within their 3'UTR mRNA.

Among the genes presenting at least a 1.5-fold change (Tables 5.7 - 5.9), few genes with at least 1 conserved seed site for a specific miR were selected for further validation. All selected genes based on the above criteria were also validated for other tested miRs if they contained any seed site complementary to the miR seed region sequence and was up-regulated in response to miR inhibition even if not reaching the 1.5-fold criteria. Moreover, additional genes that were experimentally proven by other groups as a target gene of miR-21 or miR-221/-222 were also selected for validation.

Potential direct target gene validation was conducted on original mRNA from cells transfected with miR inhibitors sent for NGS and on cells treated with miR mimics as an additional control of a true response to miR manipulation. Relative gene expression was normalised to non-targeting siRNA controls.

A number of genes were either up-regulated or down-regulated in response to miR inhibitors or miR mimics, respectively, suggesting they are direct targets. Matrix metalloproteinase-13 (MMP-13), which was significantly decreased in 2.5MPa (Chapter 3), is highly expressed by hypertrophic chondrocytes and is involved in cartilage degradation by proteolytic cleavage of collagen type II (Billinghurst et al., 1997, Poole et al., 2002) and aggrecan (Fosang et al., 1996) was activated by miR-21-5p inhibitor having only one poorly conserved 7mer-8m seed site. Also, it was induced by miR-221 and 222 inhibitors which corroborates the observation that miR-222 knock-down elevates the expression of MMP-13 (Song et al., 2015). However, this regulation was indirect and it was conducted through positive correlation with HDAC4 which was reported by luciferase assay to be a direct target gene of miR-222 (Song et al., 2015). Although,

HDAC4 was a proven direct target of miR-222 (Song et al., 2015), qPCR validation of this gene in chondrocytes transfected with both miR-222 inhibitor and mimic in this current study did not confirm this result which is surprising and difficult to explain.

One 8mer and one 7mer-m8 conserved seed site for miR-221/222 is present in leukemia inhibitory factor receptor alpha (LIFR). This molecule combined with a signal transducer gp130 is involved in inducing the Mitogen-Activated Protein Kinase (MAPK) Pathway (Schiemann et al., 1995, Thoma et al., 1994) which is required for cartilage formation and maturation (Bobick and Kulyk, 2008, Mariani et al., 2014), therefore it was selected for validation. Moreover, it has shown mechano-sensitivity in response to 7MPa load presenting up-regulation (1.69-fold; FDR=0.01) at 4h post-load (Chapter 3). Although, the gene showed statistically significant changes in response only to miR-221 inhibitor and miR-222 mimic, noticeable but not statistically important changes were also seen in miR-221 mimic and miR-222 inhibitor. Although, there is no evidence in the literature that LIFR is targeted by the miRs used in this study, the trend of alteration (up-regulation in response to miR inhibitor and down-regulation to miR mimic) in this experiment suggests that it would be worth assessing the correlation between miR-221/222 and LIFR expression using alternative methods of searching for miR target genes.

Although, the transcription factor Runx2 is weakly expressed in immature chondrocytes, its expression is elevated in pre- and hypertrophic cells (Kim et al., 1999, Komori, 2010). Moreover Runx2, which is elevated in OA cartilage, directly regulates MMP-13 which is involved in cartilage matrix degradation, efficiently degrading collagen type II (Billingham et al., 1997, Poole et al., 2002) and aggrecan (Fosang et al., 1996). This transcription factor contains one 7mer-A1 conserved and one 7mer-m8 poorly conserved site for miR-221/-222, suggesting it is a target of this miR. Yan et al. (2016) reported that hsa-miR-222-3p, which contains an identical nucleotide sequence as bta-miR-222 and has the same seed region as bta-miR-221, controls Runx2 at the protein level in human bone marrow stromal osteoprogenitor cells (Yan et al., 2016). Although, NGS performed on miR-221/-222 knock-down chondrocytes presented Runx2 as a target gene of miR-221/222, qPCR validation did not confirm previous findings. The results of Yan et al. were based on protein levels of Runx2, whereas in my study I assessed the quantity of Runx2 transcripts and as miRs can control gene expression via

repression of translation without interfering at the mRNA level, it may be a reason for these two conflicting results.

Out of 4 and 7 tested putative target genes for miR-21-5p and miR-221/-222, respectively, only TIMP-3 showed a statistically significant elevation and down-regulation respectively to miR-21-5p, -221 and -222 inhibitors and mimics transfection. CPEB3 may be also considered as a real target gene of miR-21-5p, because its statistically significant reduction was observed in response to miR-21-5p mimic and up-regulation presented in miR-21 knock-down cells was approaching significance ( $p=0.068$ ).

TIMP-3 has a wide range of inhibitory capabilities (Murphy, 2011). It represses TACE/ADAM-17 (Amour et al., 1998), ADAM-10 (Amour et al., 2000) that are able to convert pro-TNF $\alpha$  into the active cytokine TNF $\alpha$  which is involved in chronic autoimmune and inflammatory diseases, i.e. rheumatoid arthritis (Amour et al., 1998) and ADAM-12 (Loechel et al., 2000) which inhibits chondrocyte proliferation in human OA cartilage (Okada et al., 2008). Sahebjam et al. performed histological analysis of aggrecan and collagen type II in a knee joint of TIMP-3 knock-out mice and showed significant degradation of these two ECM components in knock-out mice compared to wild type mice (Sahebjam et al., 2007). This result suggests that TIMP-3 is essential for maintaining cartilage homeostasis by regulation of aggrecanase (ADAMTS-4 and -5) and collagenase (MMP-1, -8 and -13) activity (Sahebjam et al., 2007). TIMP-3 is known to be down-regulated in experimentally induced temporomandibular joint osteoarthritis in rats (Li et al., 2014) and in human OA chondrocytes (Dehne et al., 2009); furthermore, it appears to be a direct target of miR-21-5p, -221 and -222, however it was up-regulated in explants subjected to both 2.5MPa and 7MPa loads which coincided with elevated levels of these miRs. These conflicting findings may be explained by different experimental systems (cartilage explants for mechanical load/primary chondrocytes for identification of miRs targets) used in this study and masking effects of other load-induced genes on miR-21-5p, -221 and -222 influence on TIMP-3 expression. The level of TIMP-3 transcripts assessed by qPCR was altered according to the rule indicating that expression of a real target of a miR must be inversely proportional to the tested miR inhibitors and mimics. This result is consistent with already existing data from experiments performed on other cells or tissue; e.g. miR-21 has been shown to be a

TIMP-3 regulator in glioma cell lines (Gabriely et al., 2008), esophageal carcinoma cell line (Wang et al., 2013b) and human renal carcinoma cell line (Zhang et al., 2011). In turn miR-221 and -222 regulated TIMP-3 expression in lung and liver cancer tissue and cell lines (Garofalo et al., 2009), papillary thyroid carcinoma tissue (Yang et al., 2013) and human glioblastoma cells (Zhang et al., 2012). So far, there is no publication reporting miR-21, -221 and -222 as regulators of TIMP-3 in articular cartilage. The facts that TIMP-3 (i) affects the activity of aggrecanases and collagenases (Nagase et al., 2006), (ii) is down-regulated in OA cartilage (Li et al., 2014) and (iii) is validated by qPCR as a target gene of the overexpressed miR-21 reported to be elevated in OA cartilage (Zhang et al., 2014b) and mechano-sensitive miR-221/-222 (Dunn et al., 2009) strongly implicates these miRs as having a role in OA development.

A novel finding is the regulation of CPEB3 by miR-21-5p. CPEB3 has been mainly identified in neural tissues as a modifier of post-translational/post-transcriptional molecule expression, however due to the function it plays in those tissue, I believe it can also affect cartilage integrity. In neurons of CPEB3 knock-out mice an increased expression/activity of glutamate NMDA receptor (NMDAR) has been identified resulting in induced  $Ca^{2+}$  influx (Chao et al., 2013). NMDAR is a non-selective cation channel and was first shown to occur in human chondrocytes in 2004 (Salter et al., 2004). NMDAR is implicated in cartilage mechanotransduction and the  $Ca^{2+}$  influx through NMDAR is believed to be one of the major activators of many signalling pathways e.g. PI3K/AKT and MAPK (Salter and Lee, 2010a). CPEB3 is a nucleocytoplasm-shuttling protein that is predominantly localised in the cytoplasm, however the activation of NMDAR translocates and accumulates CPEB3 in the nucleus where it binds and suppresses signal transducer activated transcription 5b (STAT5b) transcription factor (Peng et al., 2010). STAT5b has been identified as a stimulator of EGFR gene transcription, therefore CPEB3 knock-down elevated EGFR expression through higher activity of STAT5b in neuron nuclei (Peng et al., 2010). EGFR is involved in the control of cartilage homeostasis by inducing the PI3K/AKT and MAPK signalling pathways (Peng et al., 2010). Moreover, induction of OA by destabilisation of the medial meniscus (DMM) in EGFR knock-down mice demonstrated higher up-regulation of ADAMTS-5 and MMP-13 and a reduced level of aggrecan in comparison to DMM model of wild type mice (Zhang et al., 2014a). In the

microarray data (available electronically) of explants loaded with 2.5MPa and 7MPa, EGFR was shown to be significantly down-regulated in response to 2.5MPa and 7MPa (1.52-fold: FDR=0.033, 1.6-fold: FDR=0.007, respectively) 4h post-load and 24h post-load with 7MPa load (1.49-fold: FDR=0.021). However, neither CPEB3 nor NMDAR mRNA levels were differentially regulated in loaded explants even though miR-21-5p was significantly elevated in response to 2.5MPa (3.12-fold: FDR>0.001) and 7MPa (6.95-fold: FDR>0.001) at 4h post-load and 7MPa load at 24h post-load (2.28-fold: FDR=0.002). These findings suggest that even though CPEB3 has been validated as a direct target of miR-21-5p in transfected primary chondrocytes, the effect of this miR activity in a more complex system i.e. tissue may be weakened by the activity of other molecules. This study also confirmed the mechano-sensitive nature of EGFR which has been reported in statically (10% elongation, 5 minutes) (Kippenberger et al., 2005) and dynamically (30% elongation, 0.5Hz, 10 minutes) (Correa-Meyer et al., 2002) loaded epidermal cells, however the current study was the first to show EGFR mechano-responsiveness in chondrocytes.

The work described in this chapter investigated potential direct targets of the mechano-sensitive miR-21-5p, -221 and -222. There are a few experimental methods that are recommended for use to validate functional target molecules of miRs including: qPCR, western-blotting and luciferase reporter assay. Both qPCR and western-blotting assess co-expression of miR and putative targets respectively at the gene and protein levels, whereas a luciferase reporter assay determines direct interaction between a miR and a target gene (Kuhn et al., 2008, Thomson et al., 2011). As one miR is able to control many genes and the purpose of this study was to find as many molecules that are targeted by selected miRs that potentially play important roles in cartilage homeostasis/pathology as possible, the Wnt signalling array and Next Generation Sequencing based on mRNA level assessment was used. The choice of these methods was driven by the fact that at least 84% of miRs control the expression of their targets through mRNA destabilisation (Guo et al., 2010) and that the majority of alterations at the protein level of target molecules are reflected by changes in their transcript abundance (Baek et al., 2008, Selbach et al., 2008). Although transcript destabilisation based methods can determine direct target genes, the biggest drawback of these

methods is that both the direct and indirect targets are identified simultaneously. To establish which putative differentially regulated genes identified by NGS data are direct targets the combined approach of computational target prediction and gene validation is necessary, both NGS and array analysis give more global views on genes and affected pathways in response to miR variations.

This chapter showed that TIMP-3, which contains target sites for the studied miR-21-5p, -221 and -222 was regulated by all tested miRs, whereas CPEB3 seems to be targeted by miR-21-5p only. Although these genes were up-regulated and down-regulated respectively in response to miR overexpression or inhibition, they should be validated by at least one more method to confirm them as direct target genes (Kuhn et al., 2008).

#### **5.3.4. Summary:**

- Transfection conditions (transfection reagent concentration and 48h transfection) is non-toxic for primary chondrocytes
- DharmaFECT1 (cationic lipid transfection reagent) and non-targeting siRNAs affect expression of most studied genes
- miR-21-5p is a regulator of TIMP-3 and CPEB3
- miR-221 and miR-222 control expression of TIMP-3

# Chapter 6

General discussion

## 6.1. Importance of miRs in articular cartilage homeostasis

miRs are small non-coding molecules with an ability to control the expression of their target genes; therefore they play important roles in many biological processes and their dysregulation can lead to a large range of diseases (Bartel, 2009). Recent studies have demonstrated that miRs are actively involved in maintaining the balance between anabolic and catabolic processes occurring in articular cartilage by regulating the expression of ECM molecules either directly or by secondary signalling processes (Diaz-Prado et al., 2012, Swingler et al., 2012, Tuddenham et al., 2006). Therefore, due to the highly important role of miRs in the maintenance of cartilage turnover many groups have studied their involvement in degenerative diseases including OA.

OA is a multi-factorial and prevalent chronic joint disease that leads to cartilage degeneration, thickening of subchondral bone and osteophyte formation (Thyssen et al., 2015). Several risk factors that contribute to the development of OA include ageing, abnormal mechanical load, joint injury, obesity, inflammation and genetic predisposition (Goldring and Marcu, 2009). OA is the most common form of arthritis and results in an imbalance of biosynthetic and degenerative activities in chondrocytes, with increased expression and activation of proteolytic enzymes that degrade the main components of cartilage: namely collagen and proteoglycans (Goldring and Marcu, 2009). Apart from an increased mRNA level and activity of proteolytic enzymes such as the MMPs and ADAMTSs in OA (Goldring and Marcu, 2009), recent studies have investigated differences in the expression of miRs in healthy and OA articular cartilage tissue. Among significantly down-regulated miRs in OA chondrocytes are: miR-27a/b (Akhtar et al., 2010), miR-125b (Matsukawa et al., 2013) and miR-142-3p (Wang et al., 2016a); in contrast miR-9 (Jones et al., 2009), miR-98 (Jones et al., 2009), miR-22 (Iliopoulos et al., 2008), miR-23a-3p (Kang et al., 2016), miR-30a (Chang et al., 2016), miR-139 (Hu et al., 2016) and miR-455 (Swingler et al., 2012) expression is increased with the OA disease. miR-146a whose influence on cartilage homeostasis is described in more detail in Section 1.5.1.6.2 is elevated in the early stages of degeneration but is decreased in end-stage OA (Yamasaki et al., 2009). Findings concerning the differential expression of miR-140 in OA cartilage are conflicting with studies reporting both repressed (Miyaki et al., 2009, Miyaki et al., 2010, Tardif et al., 2009) and elevated

(Swingler et al., 2012) levels of this miR in diseased cartilage, however both data may be right and miR-140 expression similar to miR-146a may be OA-stage dependent as the stage of OA cartilage utilised in these studies may have been different (Le et al., 2013). This miR is one of the most important in OA development as it is implicated in chondrogenesis (Karlsen et al., 2013, Miyaki et al., 2009, Miyaki et al., 2010) and cartilage development and homeostasis (Miyaki et al., 2010, Miyaki et al., 2009, Nakamura et al., 2011). Therefore, dysregulation of miR-140 expression in chondrocytes leads to stimulation of several genes involved in chondrocyte hypertrophy: Runx2 and Mef-2 which are regulated by HDAC-4 that is a direct target of this miR (Swingler et al., 2012, Tuddenham et al., 2006) or in cartilage matrix degradation: ADAMTS-5 (Araldi and Schipani, 2010, Miyaki et al., 2010, Miyaki et al., 2009), IGFBP-5 (Tardif et al., 2009) which was previously discussed (Section 1.5.1.6).

During every day movement the joints are subjected to different categories of mechanical stimuli such as tensile, hydrostatic and shear stress, however a compressive load is the dominant stimulus applied on the weight bearing joint. Different types of load have different impacts on cartilage integrity; normal “physiological” load helps to maintain the functional integrity of articular cartilage and joint homeostasis by balancing biosynthetic and degenerative activities in chondrocytes (Goldring and Marcu, 2009). In contrast, abnormal “non-physiological” loads induce elevated gene expression of catabolic molecules (e.g. MMPs, ADAMTS) which can lead to cartilage degradation and result in OA development (Bader et al., 2011).

One of the primary risk factors for the initiation and development of OA is a combination of abnormal mechanical load (e.g. excessive or diminished joint contact) and an inflammatory response to mechanical stress (e. g. IL-1-induced cellular catabolism) (Torzilli et al., 2011). To date, there are limited studies on the mechano-regulation of miRs in cartilage, but previous studies in articular cartilage (Section 1.5.1.8) have shown that miR-146a (Jin et al., 2014), miR-221/-222 (Dunn et al., 2009) and miR-365 (Guan et al., 2011) are sensitive to mechanical load. Moreover, the mechano-responsive nature of a number of miRs, for example miR-19a (Qin et al., 2010), miR-663 (Ni et al., 2011), miR-24 (Luna et al., 2011b), miR-208a (Wang et al., 2013a), miR-16, -26a and -140

(Mohamed et al., 2010), miR-378 and miR-100 (Mendias et al., 2012) was also reported in cell types other than chondrocytes (Section 1.5.1.7).

Therefore, I hypothesised that: ***(i) mechanical compression applied to cartilage explants induces a differential miR response involved in maintaining cartilage integrity, (ii) the alteration in expression of mechanically-regulated miRs occurs in a load-dependent manner, (iii) differentially expressed miRs in response to a higher load may have a potential involvement in cartilage degeneration and development of OA.***

To verify the hypothesis, the aims of this PhD project were to:

1. establish regimes utilising “physiological” and “non-physiological” magnitudes of load *in vitro*, that (i) induce transcription of genes involved in ECM turnover/catabolism, and (ii) have the potential to induce biosynthetic and degradative changes at the protein level if applied for a suitably prolonged period of time
2. determine which miRs expressed in explant chondrocytes are sensitive to mechanical stimuli
3. establish whether there is any relationship between expression of mechanically-sensitive miRs and molecules involved in cartilage pathophysiology

## **6.2. SDHA and YWHAZ are the most appropriate reference genes in mechanically loaded cartilage explants**

Minimum Information for Publication of Quantitative Real-Time PCR Experiments (MIQE) guidelines advises use of at least three experimentally validated reference genes for an individual experimental design for normalisation of qPCR data indicating that usage of only one reference gene is unacceptable as it increases the chance of getting false results (Bustin et al., 2009, Bustin et al., 2010). Reference genes are used to determine the differences in studied gene expression levels stimulated by experimental factors (McCulloch et al., 2012), therefore reference gene expression levels must be stable and unaffected by the treatment regime being applied e.g. mechanical load (McCulloch et al., 2012). Identification of reference genes for the loading regimes utilised that were appropriate for use in qPCR normalisation were investigated. Very few 'mechanobiology' groups have analysed the appropriateness of the reference genes used for transcript quantification, therefore using a panel of eight reference genes, qPCR was utilised to ascertain which of these genes remained constant in their expression in response to the different loading regimes to be used in this study. Using RefFinder software, SDHA was identified as the most stable reference gene across the loading regimes tested with YWHAZ as second; in contrast, GAPDH and HPRT were deemed to be the least stable under these experimental conditions. These findings were published this year (Al-Sabah et al., 2016), and thus in this thesis gene expression in loaded and unloaded explants were normalised to SDHA and YWHAZ, having been identified as the most appropriate in this model system.

## **6.3. Identification of physiological and non-physiological magnitudes of cyclic compressive load**

Before identification of mechano-sensitive miRs that are potentially involved in cartilage integrity, optimisation of load magnitudes was necessary to determine loading regimes that regulate the expression of ECM genes which have been implicated in cartilage homeostasis or OA development. Furthermore, the periods of loading also needed to be investigated to identify regimes in which early transcriptional changes induced by short periods of cyclic compression could be detected. Although there are many publications

reporting on compressive load-induced alterations in the expression of key ECM molecules involved in cartilage homeostasis *in vivo* (Kiviranta et al., 1987, Jortikka et al., 1997, Otterness et al., 1998, Palmoski and Brandt, 1981, Palmoski et al., 1979) and *in vitro* (Fitzgerald et al., 2008, Kiraly et al., 1998, Kurz et al., 2001, Palmoski and Brandt, 1984), this first step was necessary as all of the changes reported in these studies occurred after hours of mechanical load/immobilisation.

In my preliminary study, early transcriptional changes that suggests turnover or induction of catabolism in response to load was observed after load was applied for 15 minutes, at a frequency of a fast walking pace (1Hz) (Bader et al., 2011). Having selected these parameters for time and frequency, the loading regimes were further optimised to take into account the magnitude of load – for this peak stresses of 2.5MPa, 5MPa and 7MPa were applied to the explants. These peak stresses were selected based on previously reported studies. In the literature  $\leq 5$ MPa magnitude is considered as a physiological load (Fehrenbacher et al., 2003, Grodzinsky et al., 2000), whereas magnitudes above 5MPa are considered as injurious (Fehrenbacher et al., 2003). The loading regimes i.e. applied magnitudes were examined to identify experimental regimes capable of inducing changes in the expression of ECM molecules at the transcriptional level, with the potential to induce alterations at the protein level if the load was applied for longer periods of time. ADAMTS-4 transcription was up-regulated both in response to 2.5MPa and 5MPa loads, but significant up-regulation of other catabolic molecules such as MMP-1 and -3 was only observed at 5MPa, therefore I considered a 2.5MPa to be physiological magnitude. Despite the up-regulation of some catabolic molecules with a 5MPa load compared with the 2.5MPa load, I did not consider this magnitude as abnormal. The reason this decision was made was that with a 5MPa load ADAMTS-5 mRNA levels were not elevated and expression of MMP-9 and -13 were down-regulated. The substantially increased expression of catabolic genes in response to 7MPa load compared with the lower loads confirmed that the 7MPa load should be used as representative of a non-physiological magnitude of load. To summarise, a loading magnitude of 2.5MPa was selected to represent a physiological (normal) magnitude and 7MPa as a non-physiological magnitude.

### **6.3.1. Time dependent transcriptional response of mechano-sensitive genes**

One of the aims of chapter 3 was to identify, using a global perspective involving microarray analysis, mechano-sensitive genes in articular cartilage subjected to the selected 2.5MPa and 7MPa loading regimes. In addition, to establish the stability of transcriptional changes of mechanically-regulated genes, the analysis of mechano-sensitive gene expression was performed at 4h and 24h time points post-cessation of load. These time points were selected based on the preliminary experiments performed in our lab (data not shown) and the literature showing differential expression of mechano-sensitive genes such as (i) MMP-3, -13, ADAMTS-4 in primary bovine chondrocytes subjected to tensile strain (7.5% elongation, 1Hz, 30 minutes) and processed 4h post-load (Thomas et al., 2011), and (ii) MMP-3 reported to be elevated in bovine cartilage explants subjected to a single impact load (50% final strain at a velocity of 1 mm/second) as early as 2h however the peak of 250-fold elevation occurred at 24 hours post-load (Lee et al., 2005c).

As was expected, the microarray results confirmed some previous data presented in the load optimisation experiments and demonstrated significantly higher expression of MMP-3, ADAMTS-4, TIMP-1 and -3 in explants subjected to 7MPa when compared to unloaded tissue at 24h post-load. However, neither the 2.5MPa load at the 24h time point, nor the 2.5MPa and 7MPa loads at 4h post-load presented changes in these genes. Furthermore, at both time points post-cessation of load the 7MPa loading regime stimulated the expression of a greater number of mechano-sensitive genes than 2.5MPa. The data showed differential expression of (i) 2,848 and 778 genes in response to 7MPa and 2.5MPa (1Hz, 15minutes) loads, respectively, at 4h post-load and (ii) 1,995 and 91 genes in response to 7MPa and 2.5MPa (1Hz, 15minutes) loading regimes, respectively, at 24h post-load.

The microarray data suggest that some genes, for example aggrecan and collagen, whose levels were not significantly altered either in load optimisation or microarray data may need longer periods of load to modulate their differential expression as has previously been reported by Fitzgerald et al. They reported a time-dependent transcriptional response to mechanical stimulation showing that bovine explants

subjected to a cyclic compression (3% deformation, 0.1Hz) for 24h induced significant elevations in aggrecan, collagen type II, MMP3 and ADAMTS-5 expression, whereas the same load applied for shorter periods of time (1, 4 or 8h) did not affect their mRNA levels (Fitzgerald et al., 2006); these explants were processed directly after application of load.

The microarray findings indicated that differential transcription of many mechanically-regulated genes in this study requires different periods post-cessation of load to present changes at the mRNA level; moreover, most of the differentially-regulated genes were altered in a load dependent manner indicating a transitory effect of mechanical stimuli. To these genes belong, for example, FOSB presenting elevated expression at 4h only in response to both loading regimes (2.5MPa: 8.89-fold: FDR>0.001, 7MPa: 40.31-fold: FDR>0.001) or ESR1 (ER $\alpha$ ) which was significantly decreased in response to 7MPa load at 24h post-load (2.8-fold, FDR=0.004). Other molecules, for example, FOSL-1 and JUNB showed differential expression at both time-points. FOSL-1 was up-regulated in explants subjected to 2.5MPa (6.94-fold: FDR>0.001) and 7MPa loads (16.51-fold: FDR>0.001) processed at 4h post-load; in turn, explants loaded with 2.5MPa and 7MPa magnitudes and processed at 24h post-load showed elevation of this gene in the following manner: 3.13-fold: FDR>0.001 (2.5MPa) and 8.92-fold: FDR>0.001 (7MPa). JUNB was upregulated by 4.11-fold (FDR>0.001) and 5.81-fold (FDR>0.001) at 4h post load in response to 2.5MPa and 7MPa, respectively, while at 24h post-load JUNB was still elevated in response to 2.5MPa load (2.15-fold: FDR>0.001) and 7MPa load (2.61-fold: FDR>0.001), and had not returned to basal expression levels.

In my experiments, transcription factors were one of the most abundant protein classes of differentially expressed genes in explants subjected to 2.5MPa and 7MPa loads and processed 4h post-load. The 24h time point also showed a large group of this type of molecule, although not as many as observed at 4h, however this was only in response to the 7MPa load. These results corroborate published data concerning mainly FOS and JUN family members suggesting that transcription factors are early-response molecules to mechanical stimuli (Bougault et al., 2012, Lee et al., 2005c). This effect can be explained by the fact that as they are molecules that regulate the transcription of other genes they must be affected first to stimulate transcriptional changes in their downstream genes. Bougault et al. reported that FOS and JUN family members were

up-regulated directly after 30 minutes of compressive load (range 20-40KPa, 0.5Hz) applied on 3D chondrocyte constructs (Bougault et al., 2012). Lee et al. showed that injuries static load (50% final strain at a velocity of 1 mm/second) increased the expression level of c-FOS (~120-fold) and c-JUN (~40-fold) in bovine articular cartilage explants within 1h after load and after 4h post-load their elevated expression decreased by 3-fold and remained at this level of expression for 24h (Lee et al., 2005c). In turn, Roosa et al. also observed a rapid response in the increased expression of the AP1 transcription factor components, such as FOSL-1 and JUNB after only 4h from the application of the single loading episode (13N, 2Hz, 3 minutes) on rat forelimb bone (Mantila Roosa et al., 2011). The early responsiveness of AP1 components was confirmed in my mechanical loading model, whereby significant elevations in FOSB, FOSL-1, JUNB and JUND transcripts in explants subjected to both utilised loading regimes and processed at 4h post-cessation was observed. Results from the current study demonstrated sustained up-regulation of FOSL-1 and JUNB showing their increased expression at 24h post-load; however, the effect was transitory as the relative fold changes of these genes were twice and 4 times lower in FOSL-1 and JUNB in response to both loading regimes in comparison to the explants subjected to the same loads but processed at 4h post-load. FOSB and JUND were not significantly altered by the 24h time point.

The molecular classification performed using PANTHER software showed that both mechanical loads (2.5MPa or 7MPa, 1Hz, 15 minutes) and both times post-cessation of load (4h and 24h) induced the expression of similar protein classes in loaded explants indicating that these protein groups are the most sensitive to mechanical compression in articular cartilage. Although, the sizes of most of these protein groups differed in each condition, there were some protein classes demonstrating similar proportions. Explants subjected to 7MPa load and processed either at 4h or 24h post-load presented comparable proportions of the most abundant protein classes. Interestingly, cartilage loaded with 2.5MPa and processed at 4h post-load presented a similar distribution to the most abundant protein groups induced in the 7MPa loaded explants processed at 4h and 24h post-load; whereas, noticeable differences were observed in the top 3 most abundant protein classes identified in cartilage loaded with 2.5MPa when comparing 4h

versus 24h post-load. These differences may be attributed to (i) the temporary changes in gene expression of some mechanically-regulated molecules identified in explants subjected to load and (ii) the lower fold-changes of mechanically-regulated molecules in explants subjected to 2.5MPa compared to 7MPa. These data suggest that the transferase protein group does not contain as many temporary mechano-regulated molecules as nucleic acid binding proteins and transcription factors. Transferases were identified as the only class out of these most abundant protein groups of mechano-sensitive molecules that occurred in all loaded explants processed either at 4h or 24h post-load. In turn, nucleic acid binding proteins and transcription factor sub-classes were similarly regulated in explants subjected to 7MPa load at both time points and in the 2.5MPa loaded explants processed at 4h post-load; however, these protein classes were not amongst the most abundant groups of mechanically-regulated proteins in explants subjected to a 2.5MPa load and analysed at the later time-point.

The microarray results and PANTHER analysis suggest that the transcript levels of mechanically-regulated molecules and associated protein classification is load- and time-dependant indicating that the timeframe to observe early transcriptional effects of mechanical stimuli may be very different depending on the gene under investigation (Garg et al., 2014).

#### **6.4. 24h time point is the most appropriate to observe differentially expressed miRs**

Experiments presented in Chapter 4 focused on identifying mechanically-regulated miRs in articular cartilage that are involved in maintaining cartilage homeostasis. One of the aims of this study was to identify early mechano-responsive miRs in articular cartilage that control important cartilage homeostasis genes. To date, there is no publication suggesting which time point is the most appropriate to observe changes in the expression of mechanically-regulated miRs, therefore RNA was extracted from cartilage explants 2h, 6h and 24h after being subjected to physiological (2.5MPa) or non-physiological (7MPa) magnitude of loads and expression of miRs quantified. Pooled samples were sent for NGS followed by analysis by the bioinformatician (Andrew

Skelton, Newcastle University). Assessment of miR expression levels using the NGS method was chosen over microarray analysis as NGS provides more detailed information about the transcriptomes, therefore NGS data may be used for future investigation i.e. novel mechano-responsive miRs in cartilage, whereas arrays deliver limited results containing only those genes that are present on the array platform.

Although, all time points (2h, 6h, 24h) analysed using the NGS method initially revealed mechano-sensitive miRs, the RNA extracted at 24h post-load presented the greatest number of 17 differentially expressed miR genes, therefore this period post-load cessation was selected for further analysis. NGS of miRs had been conducted before the microarray technique was utilised to compare global changes in mechano-sensitive genes in explants processed either at 4h or 24h post-load. From the microarray, it was determined that cartilage processed at both 4 and 24h post-load would allow for changes in miR expression to be observed. Surprisingly, the microarray data demonstrated many more significantly regulated miRs in response to load at 4h post-load than 24h post-cessation showing 76 and 21 differently expressed miRs at earlier and later time points, respectively. RNA from the 4h post-load explants was extracted using Qiagen RNeasy mini kits, whereas total RNA isolation from tissue processed at 2h, 6h and 24h post-load cessation was performed using a mirVana™ miRNA isolation kit which may have affected the outcome. If this supposition is real, then these findings suggest that either the silica membrane in the Qiagen RNeasy mini kit columns bind short sequences of RNA, and not only >200bp as it is designed for, or the findings of the microarray performed on the 4h time point are the result of partial RNA degradation. It is highly unlikely that it is the latter explanation as the RIN scores for the RNA integrity exceeded 8 indicating excellent RNA quality.

## 6.5. Differential regulation of cartilage miRs in response to cyclic compressive load

According to the number of reads generated from the NGS data, the most abundantly expressed miR in cartilage, presenting  $\sim 1.2 \times 10^6$  as the average number of reads in all explants and time points, is miR-140. It has also been shown to be the most highly expressed miR in all three stages of the human chondrocyte phenotype (precursor, differentiated and hypertrophic) (McAlinden et al., 2013). Crowe et al. showed that even in OA cartilage the most highly expressed miR is miR-140, and further detailed that: (i) miR-140-3p is the most abundant miR in cartilage ( $\sim 4 \times 10^6$  numbers of reads per  $10 \times 10^6$  of reads) and (ii) miR-140-5p is the 3<sup>rd</sup> most highly expressed miR presenting  $\sim 2 \times 10^5$  numbers of reads per  $10 \times 10^6$  of reads (Crowe et al., 2016). miR-140 also presented a large difference in expression between articular chondrocytes and mesenchymal stem cells (MSC) concomitant with a parallel increase in Sox9 and collagen type II transcription during chondrogenesis (Miyaki et al., 2009). This miR was reported to play a crucial role in cartilage development and homeostasis (Araldi and Schipani, 2010, Miyaki et al., 2009, Miyaki et al., 2010, Nakamura et al., 2011, Tardif et al., 2009, Tuddenham et al., 2006). Apart from its involvement in decreased proliferation and premature chondrocyte differentiation leading to endochondral bone growth defects resulting in dwarfism (Miyaki et al., 2010, Nakamura et al., 2011), miR-140 plays a critical role in maintaining cartilage homeostasis and integrity by targeting ADAMTS-5 (Miyaki et al., 2010, Miyaki et al., 2009, Araldi and Schipani, 2010), HDAC4 (Tuddenham et al., 2006, Swingler et al., 2012) and IGFBP-5 (Tardif et al., 2009).

Surprisingly, miR-148a that was expressed in my experimental samples at a similar level to miR-140 ( $\sim 1.2 \times 10^6$  average number of reads) was not on the list of the 30 most abundantly expressed miRs in any of the chondrocyte developmental stages (McAlinden et al., 2013). miR-148a is important in maintaining cartilage integrity as it (i) inhibits chondrocyte hypertrophy via targeting collagen type X and MMP-13, (ii) reduces expression of ADAMTS-5 and (iii) elevates collagen type II mRNA levels (Vonk et al., 2014).

Unexpectedly, a significant reduction in miR-140 expression was observed in the cartilage explants subjected to a 7MPa load and analysed 24h post-cessation in an initial

screening using qPCR; however, this observation was not confirmed by the NGS data even though the material used for the NGS analysis was the pooled RNA that had been utilised for the qPCR (Chapter 4). Although, qPCR is a more sensitive technique than NGS and the mechano-regulation of miR-140 has also been reported in human airway smooth muscle cells 12h post-cessation of cyclic stretch (12%, 1Hz, 1h) (Mohamed et al., 2010), this miR was not selected for further studies as it is already well described in the literature. However, miR-140 is imperative for cartilage homeostasis as (i) miR-140 knock-out mice show growth defects and an abnormal skeletal phenotype as defined by shortening of the long bones and craniofacial deformities (Miyaki et al., 2010, Nakamura et al., 2011), (ii) ADAMTS-5 is a direct target of miR-140 and was significantly increased in miR-140 knock-out mice and significantly decreased in miR-140 transgenic mice (Miyaki et al., 2010) and (iii) miR-140 targets HDAC4 (Tuddenham et al., 2006, Swingler et al., 2012) which is a corepressor of Runx-2 and Mef-2 that are fundamental for chondrocytes hypertrophy and bone formation (Swingler et al., 2012), and IGFBP-5 (Tardif et al., 2009). Therefore, with additional time it would be worthwhile further validating its expression in individual samples to confirm its mechano-responsiveness. This knowledge might be beneficial in better understanding how abnormal load might modify miR-140 expression and induce cartilage degeneration, especially because miR-140 has already been shown to regulate genes involved in OA pathology and its expression is known to be altered in OA chondrocytes compared to healthy cells, probably in an OA stage dependent manner (Gibson and Asahara, 2013).

NGS analysis identified a total of 17 differentially expressed known miRs in cartilage explants when comparing the response of physiological and non-physiological magnitudes of load processed at 24h post-load to unloaded tissue. The investigation of novel miRs was not conducted as it was not the purpose of this study. Due to time constraints, only 7 miRs were selected for validation based on two criteria: (i) at least a 2-fold change in expression between loaded and unloaded explants or (ii) potential significance in OA development reported in the literature. In agreement with previous studies in several cell types (not necessarily in chondrocytes), qPCR validation indicated the mechano-responsive nature of miR-21-5p, miR-27a-5p, miR-221 and miR-222, and also miR-483 that has not previously been reported as being mechanically-regulated.

Expression levels of these miRs were reported to be altered in OA cartilage when compared to healthy tissue (up-regulation of miR-21 (Zhang et al., 2014b), -483-3p/-5p (Gibson and Asahara, 2013, Qi et al., 2013), and down-regulation of miR-27a (Tardif et al., 2009) and miR-222 (Song et al., 2015)) indicating that they affect chondrocyte metabolic activities and cartilage homeostasis. These miRs have putative and experimentally proven targets including: GDF-5 (Zhang et al., 2014b), TIMP-3 (Wang et al., 2013b), MMP-13 (<http://www.targetscan.org>) for miR-21; MMP-13 and insulin-like growth factor-binding protein 5 (IGFBP-5) (Tardif et al., 2009) for miR-27a; TIMP-3 (Zhang et al., 2012) for miR-221/-222; Mdm2 (Kim et al., 2010) for miR-221; HDAC4 (Song et al., 2015) and DKK2 (Li et al., 2013) for miR-222 separately; collagen type VI, GDF-5 and TIMP-3 (<http://www.targetscan.org>) for miR-483, hence a few of them were selected for further studies.

#### **6.6. Functional analysis of mechano-sensitive miRs in transfected primary chondrocytes**

Having validated mechano-sensitive miRs, Chapter 5 was focused on determining the functional consequences of differential expression of these miRs in chondrocyte mechano-transduction. For this purpose, primary cartilage chondrocytes were transfected with miR inhibitors or non-targeting siRNA and the level of gene expression assessed by: (i) custom designed Wnt signalling arrays and (ii) NGS, where cells treated with non-functional siRNA or with transfection reagent only were used as controls. The rationale for analysing the profile of Wnt signalling genes in the transfected chondrocytes was based on previous studies demonstrating the influence of these miRs on the expression of Wnt/ $\beta$ catenin signalling pathway components (Corr, 2008, Kawakita et al., 2014, Li et al., 2013, Wu et al., 2015, Zheng et al., 2012). Furthermore, our laboratory has previously demonstrated that components of the Wnt/ $\beta$ -catenin signalling pathways are extremely sensitive to these loading conditions (A. Al-Sabah, Cardiff University PhD) and regulation of several of the canonical and non-canonical Wnt molecules were evident in the microarrays performed (Chapter 3). Unexpectedly, the Wnt signalling PCR array demonstrated mostly down-regulated genes in response to

treatment with miR inhibitors, hence excluding these genes as direct targets of the selected miRs although they could well be regulated indirectly - but this remains to be elucidated. Additionally, it was found that in the transfected cells genes that were selected for validation based on a  $\geq 2$ -fold up-regulation turned out to be false positives. Although, the Wnt signalling arrays produced unexpected and contradictory data to the published literature, I believe that the positive correlation of miR-21-5p with  $\beta$ -catenin detected in this experiment is real and hence has the ability to manipulate Wnt signalling in mechanically-stimulated chondrocytes. This hypothesis is based on a previous study which demonstrated that although miR-21 knock-down did not alter  $\beta$ -catenin expression in a human lung cancer cell line, elevated mRNA and protein levels of  $\beta$ -catenin was observed in response to overexpressed miR-21 (Wu et al., 2015). Additionally, the same group showed higher expression of both miR-21 and  $\beta$ -catenin in Lewis lung carcinoma in mice compared to normal lung cells (Wu et al., 2015). Furthermore, the negative correlation between miR-221 and DVL2, which is a key intracellular stimulator of the Wnt signalling pathway (Smalley et al., 2005), identified in the Wnt qPCR array and previously demonstrated in human prostate carcinoma cell lines (Zheng et al., 2012) also adds to this being a real result and should be investigated in future studies. Moreover, there is a possibility that the positive correlation between the reduced expression level of a miR and its target gene may be an effect of: (i) indirect regulation by the miR targeting the upstream genes that do not belong to the Wnt signalling pathway or were not present on the array, but affected the expression of Wnt components or (ii) influence of transfection itself. Despite the comparison of the non-targeting siRNA control vs untreated Wnt arrays not showing many transcriptional changes, the gene validation performed in Chapter 5 demonstrated statistically significant variations in some of the gene transcripts caused by either cationic lipid transfection reagent only or the non-targeting siRNA controls.

The aim of the final experimental chapter was to identify direct targets of the validated mechanically-regulated miR-21-5p, miR-221 and miR-222 to elucidate potential involvement in cartilage homeostasis and OA pathogenesis. Therefore, because the experiment conducted on the custom-built Wnt signalling array did not identify direct target genes of the selected miRs, an analysis of global gene changes in the same set of

transfected and untreated cells was conducted using NGS to establish functional effects of these miRs on chondrocyte metabolism. Unexpectedly, the sequencing data demonstrated no statistically significant genes ( $FDR \leq 0.05$ ) for miR-21-5p or only a few whose expression was statistically significant and inversely proportional to the level of miR-221 (U1, U3, U5, U12, snoU13, CATIP and PLA2G4F) and miR-222 (U1, U3, U5, U12, snoU13, PLA2G4F, mir-23a and mir-27a). To wider the panel of putative target genes of tested miRs, I selected a few differentially but not statistically significant genes, based on the criteria described in Chapter 5, to check their expression in primary chondrocytes transfected with inhibitors or mimics of miR-21-5p, miR-221 and miR-222.

From 4 potential target genes (CPEB3, MMP-13, SPRY4, TIMP-3) of miR-21-5p selected for validation, TIMP-3 and CPEB3 were identified as real targets, whereas miR-221/-222 showed targeting of TIMP-3 out of 7 tested molecules (CPEB3, HDAC4, LIFR, MMP-13, RUNX2, SPRY4, TIMP-3).

### **6.7. Mechano-regulation of miR-21-5p and its potential role in OA pathogenesis**

My finding that miR-21-5p is mechanically regulated in cartilage chondrocytes in response to a non-physiological magnitude of load is corroborated by previous publications. Elevated miR-21 expression was previously reported in human aortic smooth muscle cells subjected to cyclic tensile strain (16%, 1Hz, 12 hours) (tao Song et al., 2012). Moreover, its increased level was also seen in human umbilical vein endothelial cells in response to steady laminar shear stress (15 dynes/cm<sup>2</sup>) (Weber et al., 2010) and oscillatory shear stress ( $0.5 \pm 4$  dynes/cm<sup>2</sup>) (Zhou et al., 2011), while pulsatile shear stress ( $12 \pm 4$  dynes/cm<sup>2</sup>) decreased miR-21 transcript levels (Zhou et al., 2011). There is however no published information about the mechano-sensitive nature of miR-21 in chondrocytes indicating that the responsiveness of miR-21-5p in cartilage to a non-physiological loading magnitude (7MPa) is a novel finding. The fact that (i) mechanical induction of miR-21-5p in chondrocytes occurred in explants subjected to 7MPa load only and (ii) up-regulation of miR-21 is observed in OA pathology (Zhang et al., 2014b) indicate that miR-21-5p could be a potential biomarker of OA

pathophysiology caused by abnormal mechanical load. miR-21 has been experimentally proven to control OA development by direct targeting of growth differentiation factor 5 (GDF-5), which is known to be reduced in OA cartilage (Zhang et al., 2014b). As GDF-5 has been reported to increase chondrocyte proliferation in later stages of skeletal development (Francis-West et al., 1999), the lower synthesis of this gene may weaken the capability of cartilage repair. The fact that GDF-5 expression is inhibited by mechano-sensitive miR-21 may suggest that this miR:mRNA correlation is involved in OA development induced by abnormal mechanical load. Although, in my study of direct miR targets, GDF-5 was not on the list of differentially expressed genes affected by miR-21-5p inhibition (Chapter 5), it would be worth checking this finding in my experimental model. In terms of data obtained from my study, the novel findings of TIMP-3 and CPEB3 regulation in cartilage by the mechano-sensitive miR-21-5p only reinforces the involvement that this miR has in cartilage homeostasis and pathology. TIMP-3 regulates the activity of aggrecanases (ADAMTS-4 and -5) and all MMPs (Murphy, 2011); therefore it is not surprising that its expression is down-regulated in OA cartilage (Dehne et al., 2009, Li et al., 2014) which may be an effect of miR-21-5p activity. Furthermore, the inversely proportional co-expression of miR-21 and TIMP-3 has been already reported in glioma cell lines (Gabriely et al., 2008), oesophageal (Wang et al., 2013b) and human renal (Zhang et al., 2011) carcinoma cell lines. In turn, CPEB3 which modifies molecule expression at the post-translational (Huang et al., 2014) and post-transcriptional level (Peng et al., 2010) has mainly been identified in neural tissue and has not been reported as a regulator of cartilage homeostasis yet. However, as CPEB3 knock-down or knock-out murine neurons respectively induce the expression of EGFR (Peng et al., 2010) and NMDAR (Chao et al., 2013) which activates anabolic PI3K/AKT and catabolic MAPK signalling pathways (Huang et al., 2014, Peng et al., 2010), I assume that CPEB3 plays a significant role in maintaining cartilage integrity. This study is the first to demonstrate CPEB3 regulation by miR-21-5p and identify the CPEB3 transcript as a direct target of this miR.

## **6.8. Is miR-221/-222 sensitivity to non-physiological magnitudes of load involved in controlling turnover of cartilage molecules?**

Out of the validated miRs, miR-221 and miR-222 presented the greatest response to a 7MPa load compared to unloaded explants and those subjected to a physiological magnitude of load (2.5MPa). These results supported my preliminary qPCR data demonstrating the mechano-regulation of miR-221/-222 in cartilage and corroborate a previously published study whereby elevated levels of these miRs were observed in anterior weight-bearing compared to posterior non-weight-bearing regions of the medial femoral condyles of bovine stifle joints (Dunn et al., 2009). Although the role of miR-221/-222 in cartilage remains not well understood, there are some publications indicating their potentially important function in cartilage biology. miR-221 regulates chondrogenesis in mesenchymal cells by inhibition of Mdm2 expression (Kim et al., 2010). Down-regulation of Mdm2 increased Slug protein activity inhibiting proliferation of chondroprogenitor cells (Kim et al., 2010, Lolli et al., 2014). Therefore, these findings may indicate that an elevated level of miR-221 expression negatively affects chondrocyte differentiation and cartilage development. This hypothesis is supported by another study which showed that silencing of miR-221 promoted chondrogenesis in hMSC pellet culture without the addition of the chondrogenic inducer TGF- $\beta$  (Lolli et al., 2016). Moreover, this group also reported that miR-221 silenced hMSC, embedded in alginate and inserted into osteochondral defects in osteochondral biopsies that were subsequently implanted subcutaneously onto the backs of nude mouse improved cartilage repair compared to untransfected hMSCs or no cell alginate controls (Lolli et al., 2016). Furthermore, both miR-221 (Wang et al., 2016b) and miR-222 (Li et al., 2013) have been reported to affect the Wnt/ $\beta$ -catenin signalling pathway by direct targeting of the WNT inhibitor Dickkopf-2 (DKK2). Knock-down of miR-221 in an oesophageal cancer cell line reduced Wnt/ $\beta$ -catenin activity via targeting of DKK2 (Wang et al., 2016b). In turn, overexpression of miR-222 in glioma cell lines led to inhibition of DKK2 and activation of the Wnt/ $\beta$ -catenin pathway i.e. elevation of  $\beta$ -catenin protein levels, whereas down-regulation of miR-222 induced the opposite effect (Li et al., 2013). Moreover, miR-222 has been shown to control cartilage destruction via HDAC4 mediated control of MMP-13 expression in OA cartilage (Song et al., 2015). This group

reported decreased miR-222 expression in OA chondrocytes in which HDAC4, the direct target of this miR and regulator of MMP-13 expression, was elevated, whereas overexpression of miR-222 in OA chondrocytes significantly reduced the level of both these genes (Song et al., 2015). They also reported that intra-articular injection of lentivirus expressing miR-222 into DMM mice joints notably decreased expression of MMP-13 and cartilage degradation (Song et al., 2015). Unfortunately, experiments conducted in my study cannot confirm this previously published data, because (i) NGS data from cells treated with miR-221 inhibitor demonstrated a 1.33-fold up-regulation of Mdm2 which did not cross the cut off of a 2-fold increase and therefore was not selected for validation, (ii) DKK2 remained unchanged in the Wnt signalling array in response to miR-221 knock-down at the time points analysed and (iii) DKK2 was observed to be down-regulated in the Wnt signalling array for miR-222 knock-down (1.87-fold) which argues against the loss of function theory stating that a real target gene must be inversely proportional to the inhibited miR, and (iv) HDAC4 did not respond to miR-222 level manipulation indicative of being a direct target. TIMP-3 was validated at the gene level as a direct target of both miR-221 and miR-222 corroborating previous findings in lung and liver cancer tissue and cell lines (Garofalo et al., 2009), papillary thyroid carcinoma tissue (Yang et al., 2013) and human glioblastoma cells (Zhang et al., 2012). In my study only TIMP-3 was confirmed to be a genuinely direct target gene of miR-221/-222 in chondrocytes.

### **6.9. Differential regulation of miR-21-5p, miR-221 and miR-222 in loaded cartilage explants does not inhibit expression of their direct target TIMP-3**

The findings from this study have demonstrated the (i) elevated expression of miR-21-5p, miR-221 and miR-222 in response to non-physiological (7MPa) magnitudes of compressive load (Chapter 4) and (ii) validation by qPCR that TIMP-3 is a direct target of these miRs (Chapter 5), suggesting that up-regulation of these miRs in response to a non-physiological peak load may play an important role in cartilage degradation by reduction of TIMP-3 levels. Interestingly, to my surprise TIMP-3 mRNA expression is increased in cartilage explants subjected to a 7MPa load (Chapter 3) concomitant with

up-regulation of the aforementioned miRs. However, it is unclear how this discrepancy in findings has arisen. There is good evidence to believe however that TIMP-3 is a real target of miR-21-5p, miR-221 and miR-222 in primary chondrocytes, because it has also been experimentally verified in cell types other than chondrocytes (Gabriely et al., 2008, Garofalo et al., 2009, Wang et al., 2013b, Yang et al., 2013, Zhang et al., 2012, Zhang et al., 2011). It may well be that a more complex system such as *in situ* cartilage tissue, as opposed to primary chondrocytes or cell lines, subjected to exogenous stimulation activates the response of so many genes that the strength of the repressive roles of miR-21-5p, miR-221 and miR-222 may be masked by other genes and become too weak to inhibit TIMP-3 in this explant system. The other possibility that might explain the simultaneous elevation of both the tested miRs and TIMP-3 is a regulatory loop i.e. elevated TIMP-3 expression induces higher expression of miR-21-5p, miR-221 and miR-222 with the purpose of reducing TIMP-3 levels in the cell over time.

#### **6.10. Future directions**

Despite the study providing informative and novel data on the sensitivity of miRs to mechanical load which was the main goal of this PhD thesis, there are some aspects that could be further explored to gain a better understanding of the effect of mechanical load on chondrocyte metabolism and cartilage degradation/OA development.

In my experiments I used immature bovine cartilage derived from 1-3 weeks old calves, however future studies would utilise mature bovine cartilage to investigate whether the observations here are evident in skeletally mature tissue. The reasons why I decided to use immature cartilage were: 1. Higher chondrocyte number in immature tissue facilitating greater yields of extracted total RNA, 2. Less variability in age indicating a similar mechanical stimulation history. However, the comparative studies should be performed to determine whether the skeletal maturation status of cartilage affects expression of mechanically-regulated miRs, especially because some miRs are developmental stage dependent. Additionally, it would be interesting to do this study also on human cartilage and compare it to differentially expressed miRs in OA cartilage.

This kind of comparison would be a better model to identify mechano-sensitive miRs involved in OA onset, as the comparison would be made on the same species. All my experiments were conducted in an *in vitro* model, therefore it would be interesting to characterise miRs response in an *in vivo* experimental model. An *in vivo* model widely used in mechano-biology and cartilage degradation studies is the surgical destabilisation of the medial meniscus (DMM) in mice and this could be utilised to establish the influence of abnormal load on miR expression levels (Gardiner et al., 2015, Glasson et al., 2007, O’Conor et al., 2016). Another *in vivo* model of load-induced cartilage degeneration which could be used to assess mechanical effects on miR expression is a non-surgical rupture of the murine anterior cruciate ligament (ACL) which induces joint instability and subsequent cartilage loss. This ACL rupture model, which represents a phenotype akin to that of human post-traumatic OA involves swelling and inflammation as an early response to a single episode of mechanical load (12N, 1.4mm/s) and extensive cartilage degradation, as well as bone remodelling, by 3 weeks post-rupture (Blain et al., unpublished observations). Using this model, the mechanical influences on miR regulation could be analysed at defined time points of cartilage degeneration i.e. early versus late stage degradation; this is something that is currently being undertaken in the lab to inform on mechanically-regulated miRs in disease progression.

The aim of this study was to find early response mechano-sensitive miRs that are involved in cartilage homeostasis and play an important role in cartilage degeneration caused by degradative load. For this purpose, based on the literature and optimisation studies, two magnitudes of load that can induce “physiological” and “non-physiological” responses at the gene level were selected, with the proviso that these magnitudes have the potential to activate anabolic/catabolic response at the protein level if applied for prolonged periods of time. The loading regimes I chose to determine early events in miR regulation was appropriate as miR genes are non-protein coding molecules and do not need time for translation. However, it would be interesting to compare the expression of miRs that are differentially expressed at the beginning of a potentially physiological or non-physiological load and then at the stage where the load becomes biosynthetic or degradative respectively, and further compare these miRs with those that are

differentially expressed in OA cartilage. This type of comparison would be very helpful in identification of early miR biomarkers of degradative load.

One of the significantly elevated miRs in response to a non-physiological magnitude of load (7MPa) was miR-27a-5p (2.56-fold:  $p=0.001$ ). This novel finding of miR-27a-5p mechano-sensitivity in chondrocytes has only been previously demonstrated in endothelial cells subjected to 18h, 24h or 72h of laminar shear stress (15 dynes/cm<sup>2</sup>) (Urbich et al., 2012). Moreover, the information that: (i) miR-27a-5p is mechanically regulated in chondrocytes and (ii) miR-27a is decreased in human OA chondrocytes and indirectly regulates expression of MMP-13 and insulin-like growth factor-binding protein 5 IGFBP-5 (Tardif et al., 2009) suggest that this miR may have an influence on cartilage homeostasis and progression of load dependent OA. In my study, although cells were transfected with miR-27a-5p inhibitor under the same experimental conditions as chondrocytes treated with the other miR inhibitors, miR-27a-5p presented an unstable trend of expression showing both up-regulated and down-regulated miR-27a-5p levels in response to this transfection which was completely unexpected. As miR-27a expression is reduced in OA chondrocytes (Tardif et al., 2009), it would be worth repeating the transfection of chondrocytes using a new batch of miR inhibitor or miR mimic to establish the direct targets of this mechanically-regulated miR.

Although my study is the first to demonstrate the novel mechano-regulation of miR-483, which is an equivalent of hsa-miR-483-3p, due to time and cost limitations, I have not experimentally searched for its targets although prediction software indicates the following targets: collagen type VI, GDF-5 and TIMP-3 (<http://www.targetscan.org>). However it would be worth trying to identify these target genes, especially because miR-483-3p/-5p is known to be up-regulated in OA cartilage (Gibson and Asahara, 2013, Qi et al., 2013), has been reported to target aggrecan (Iliopoulos et al., 2008) and is positively correlated with MMP-13 and IL-1 $\beta$  (Qi et al., 2013).

It would also be very interesting to confirm the findings of miR-125b and miR-455 whose expressions were observed to be elevated (miR-125b-1) or decreased (miR-125b-2, miR-455) from the microarray data (analysis performed on explants 4h post-cessation of load), as these miRs are reported to be differentially expressed in OA cartilage

(Matsukawa et al., 2013, Swingler et al., 2012). miR-125b whose direct target is ADAMTS-4 has been shown to be down-regulated in OA chondrocytes and was able to significantly suppress IL-1 $\beta$  induced ADAMTS-4 levels (Matsukawa et al., 2013). These findings may suggest that elevated expression of miR-125b-1 controls ADAMTS-4 mRNA levels in 4h post-load explants subjected to both 2.5MPa and 7MPa loads, therefore its level remained unchanged at this time point, whereas elevated expression of ADAMTS-4 in tissue processed 24h after load may be an effect of the unaltered level of this miR (microarray data available electronically). In turn, miR-455 was reported to be up-regulated in OA chondrocytes and able to control the TGF $\beta$ /SMAD2/3 signalling pathway, for example: BMP binding protein inhibitor chordin-like 1 (CHRDL1) (Swingler et al., 2012) which was down-regulated at 24h post-load in explants subjected to a 7MPa load (microarray data available electronically). Therefore, it would be interesting to assess their expression in explants processed at 24h post-load, despite the fact that they were not identified as being differentially regulated by 24h post-load in microarray and NGS analysis. It would also be worth validating miR-21-5p, miR-27a-5p, miR-221 and miR-222 in cartilage explants at 4h post-load as the microarray analysis implied their differential expression at this earlier time point. If these mechano-sensitive miRs present at 24h post-cessation of load are also significantly regulated at this earlier 4h time point, it would be worth considering using earlier time points for future miRs studies.

Future studies should also examine TIMP-3 and CPEB3 as target genes of miR-21-5p, miR-221/miR-222 and miR-21-5p respectively using techniques other than qPCR to confirm that they are real targets of these miRs. Such techniques might include performing (i) Western-blotting to establish whether the protein levels of these targets is affected by miR expression manipulation, however this method does not distinguish direct and secondary targets and (ii) luciferase assay which is commonly used for determination of direct interaction of miR:mRNA at the gene level. Based on the fact that miR inhibits post-transcriptional process of its target mRNA, the luciferase - 3'UTR construct should show less activity than the negative control, if the 3'UTR contains specific binding sites for the tested miR.

## **6.11. Conclusion**

The aim of this PhD project was to identify mechano-sensitive miRs in articular cartilage that are involved in controlling genes that play key roles in cartilage homeostasis/degradation. This study confirms the mechano-regulatory nature of miR-221/-222 and demonstrates novel findings of the mechano-regulation of miR-21-5p, miR-27a-5p and miR-483 in cartilage explants. Moreover, my work is the first to identify TIMP-3 as a target of miR-21-5p, miR-221/-222 and CPEB3 as a direct target of miR-21-5p in primary chondrocytes. I believe that my findings provide important information in our understanding of cartilage mechanotransduction and that this is only the beginning of future studies aimed at identifying biomarkers in cartilage of load-induced OA which may provide therapeutic potential for OA treatment.

# Bibliography

- ACHARYA, C., YIK, J. H., KISHORE, A., VAN DINH, V., DI CESARE, P. E. & HAUDENSCHILD, D. R. 2014. Cartilage oligomeric matrix protein and its binding partners in the cartilage extracellular matrix: interaction, regulation and role in chondrogenesis. *Matrix Biology*, 37, 102-111.
- ACQUAFREDA, T., SOPRANO, K. J. & SOPRANO, D. R. 2009. GPRC5A: A potential tumor suppressor and oncogene. *Cancer Biol Ther*, 8, 963-5.
- AGARWAL, S., DESCHNER, J., LONG, P., VERMA, A., HOFMAN, C., EVANS, C. H. & PIESCO, N. 2004. Role of NF- $\kappa$ B transcription factors in antiinflammatory and proinflammatory actions of mechanical signals. *Arthritis & rheumatism*, 50, 3541-3548.
- AKANJI, O., SAKTHITHASAN, P., SALTER, D. & CHOWDHURY, T. 2010. Dynamic compression alters NF $\kappa$ B activation and I $\kappa$ B- $\alpha$  expression in IL-1 $\beta$ -stimulated chondrocyte/agarose constructs. *Inflammation research*, 59, 41-52.
- AKHTAR, N., RASHEED, Z., RAMAMURTHY, S., ANBAZHAGAN, A. N., VOSS, F. R. & HAQQI, T. M. 2010. MicroRNA-27b regulates the expression of matrix metalloproteinase 13 in human osteoarthritis chondrocytes. *Arthritis & Rheumatism*, 62, 1361-1371.
- AL-SABAH, A. 2014. *The role of canonical and non-canonical WNT signalling pathways in load induced cartilage degradation*. Cardiff University.
- AL-SABAH, A., STADNIK, P., GILBERT, S., DUANCE, V. & BLAIN, E. 2016. Importance of reference gene selection for articular cartilage mechanobiology studies. *Osteoarthritis and Cartilage*, 24, 719-730.
- ALEXANDER, S., WATT, F., SAWAJI, Y., HERMANSSON, M. & SAKLATVALA, J. 2007. Activin A is an anticatabolic autocrine cytokine in articular cartilage whose production is controlled by fibroblast growth factor 2 and NF- $\kappa$ B. *Arthritis & Rheumatism*, 56, 3715-3725.
- ALPER, M., AYDEMIR, A. T. & KÖÇKAR, F. 2015. Induction of human ADAMTS-2 gene expression by IL-1 $\alpha$  is mediated by a multiple crosstalk of MEK/JNK and PI3K pathways in osteoblast like cells. *Gene*, 573, 321-327.
- AMIN, A. R. & ABRAMSON, S. B. 1998. The role of nitric oxide in articular cartilage breakdown in osteoarthritis. *Current opinion in rheumatology*, 10, 263-268.
- AMOUR, A., KNIGHT, C. G., WEBSTER, A., SLOCOMBE, P. M., STEPHENS, P. E., KNÄUPER, V., DOCHERTY, A. J. & MURPHY, G. 2000. The in vitro activity of ADAM-10 is inhibited by TIMP-1 and TIMP-3. *FEBS letters*, 473, 275-279.
- AMOUR, A., SLOCOMBE, P. M., WEBSTER, A., BUTLER, M., KNIGHT, C. G., SMITH, B. J., STEPHENS, P. E., SHELLEY, C., HUTTON, M. & KNÄUPER, V. 1998. TNF- $\alpha$  converting enzyme (TACE) is inhibited by TIMP-3. *FEBS letters*, 435, 39-44.
- ANDERS, S., PYL, P. T. & HUBER, W. 2014. HTSeq—a Python framework to work with high-throughput sequencing data. *Bioinformatics*, btu638.
- ANDERSEN, C. L., JENSEN, J. L. & ØRNTOFT, T. F. 2004. Normalization of real-time quantitative reverse transcription-PCR data: a model-based variance estimation approach to identify genes suited for normalization, applied to bladder and colon cancer data sets. *Cancer research*, 64, 5245-5250.
- ANDREWS, S. 2010. FastQC: A quality control tool for high throughput sequence data. *Reference Source*.
- ANSTAETT, O. L., BROWNLIE, J., COLLINS, M. E. & THOMAS, C. J. 2010. Validation of endogenous reference genes for RT-qPCR normalisation in bovine lymphoid cells (BL-3) infected with Bovine Viral Diarrhoea Virus (BVDV). *Veterinary immunology and immunopathology*, 137, 201-7.
- ARALDI, E. & SCHIPANI, E. 2010. MicroRNA-140 and the silencing of osteoarthritis. *Genes & development*, 24, 1075-80.
- ARDEKANI, A. M. & NAEINI, M. M. 2010. The role of microRNAs in human diseases. *Avicenna journal of medical biotechnology*, 2, 161.

- AROKOSKI, J., JURVELIN, J., VÄÄTÄINEN, U. & HELMINEN, H. 2000. Normal and pathological adaptations of articular cartilage to joint loading. *Scandinavian journal of medicine & science in sports*, 10, 186-198.
- ASPBERG, A. 2012. The different roles of aggrecan interaction domains. *Journal of Histochemistry & Cytochemistry*, 60, 987-996.
- ATTUR, M., AL-MUSSAWIR, H. E., PATEL, J., KITAY, A., DAVE, M., PALMER, G., PILLINGER, M. H. & ABRAMSON, S. B. 2008. Prostaglandin E2 exerts catabolic effects in osteoarthritis cartilage: evidence for signaling via the EP4 receptor. *The Journal of Immunology*, 181, 5082-5088.
- BADER, D. L., SALTER, D. M. & CHOWDHURY, T. T. 2011. Biomechanical influence of cartilage homeostasis in health and disease. *Arthritis*, 2011, 979032.
- BAEK, D., VILLÉN, J., SHIN, C., CAMARGO, F. D., GYGI, S. P. & BARTEL, D. P. 2008. The impact of microRNAs on protein output. *Nature*, 455, 64-71.
- BARTEL, D. P. 2009. MicroRNAs: target recognition and regulatory functions. *Cell*, 136, 215-233.
- BARTER, M. J., BUI, C. & YOUNG, D. A. 2012. Epigenetic mechanisms in cartilage and osteoarthritis: DNA methylation, histone modifications and microRNAs. *Osteoarthritis Cartilage*, 20, 339-49.
- BATEMAN, J. F., ROWLEY, L., BELLUOCIO, D., CHAN, B., BELL, K., FOSANG, A. J. & LITTLE, C. B. 2013. Transcriptomics of wild-type mice and mice lacking ADAMTS-5 activity identifies genes involved in osteoarthritis initiation and cartilage destruction. *Arthritis & Rheumatism*, 65, 1547-1560.
- BENJAMINI, Y. & HOCHBERG, Y. 1995. Controlling the false discovery rate: a practical and powerful approach to multiple testing. *Journal of the Royal Statistical Society. Series B (Methodological)*, 289-300.
- BENNINGHOFF, A. 1925. Form und Bau der Gelenkknorpel in ihren Beziehungen zur Funktion. *Cell and Tissue Research*, 2, 783-862.
- BENTLEY, J. K., DENG, H., LINN, M. J., LEI, J., DOKSHIN, G. A., FINGAR, D. C., BITAR, K. N., HENDERSON JR, W. R. & HERSHENSON, M. B. 2009. Airway smooth muscle hyperplasia and hypertrophy correlate with glycogen synthase kinase-3 $\beta$  phosphorylation in a mouse model of asthma. *American Journal of Physiology-Lung Cellular and Molecular Physiology*, 296, L176.
- BEREZIKOV, E., CHUNG, W.-J., WILLIS, J., CUPPEN, E. & LAI, E. C. 2007. Mammalian mirtron genes. *Molecular cell*, 28, 328-336.
- BERNSTEIN, E., KIM, S. Y., CARMELL, M. A., MURCHISON, E. P., ALCORN, H., LI, M. Z., MILLS, A. A., ELLEDGE, S. J., ANDERSON, K. V. & HANNON, G. J. 2003. Dicer is essential for mouse development. *Nature genetics*, 35, 215-217.
- BETEL, D., WILSON, M., GABOW, A., MARKS, D. S. & SANDER, C. 2008. The microRNA.org resource: targets and expression. *Nucleic acids research*, 36, D149-D153.
- BHATTACHARYYA, S., HABERMACHER, R., MARTINE, U., CLOSS, E. & FILIPOWICZ, W. Stress-induced reversal of microRNA repression and mRNA P-body localization in human cells. Cold Spring Harbor symposia on quantitative biology, 2006. Cold Spring Harbor Laboratory Press, 513-521.
- BHOSALE, A. M. & RICHARDSON, J. B. 2008. Articular cartilage: structure, injuries and review of management. *Br Med Bull*, 87, 77-95.
- BILLINGHURST, R. C., DAHLBERG, L., IONESCU, M., REINER, A., BOURNE, R., RORABECK, C., MITCHELL, P., HAMBOR, J., DIEKMANN, O. & TSCHESCHE, H. 1997. Enhanced cleavage of type II collagen by collagenases in osteoarthritic articular cartilage. *Journal of Clinical Investigation*, 99, 1534.
- BLAIN, E. J. 2007. Mechanical regulation of matrix metalloproteinases. *Front Biosci*, 12, 507-527.

- BLAIN, E. J. 2009. Involvement of the cytoskeletal elements in articular cartilage homeostasis and pathology. *International journal of experimental pathology*, 90, 1-15.
- BLAIN, E. J., ALI, A. Y. & DUANCE, V. C. 2010. Boswellia frereana (frankincense) suppresses cytokine-induced matrix metalloproteinase expression and production of pro-inflammatory molecules in articular cartilage. *Phytotherapy research : PTR*, 24, 905-12.
- BLAIN, E. J., GILBERT, S. J., WARDALE, R. J., CAPPER, S. J., MASON, D. J. & DUANCE, V. C. 2001. Up-regulation of matrix metalloproteinase expression and activation following cyclical compressive loading of articular cartilage in vitro. *Archives of biochemistry and biophysics*, 396, 49-55.
- BLOM, A. B., BROCKBANK, S. M., VAN LENT, P. L., VAN BEUNINGEN, H. M., GEURTS, J., TAKAHASHI, N., VAN DER KRAAN, P. M., VAN DE LOO, F. A., SCHREURS, B. W. & CLEMENTS, K. 2009. Involvement of the Wnt signaling pathway in experimental and human osteoarthritis: Prominent role of Wnt-induced signaling protein 1. *Arthritis & Rheumatism*, 60, 501-512.
- BOBICK, B. E. & KULYK, W. M. 2008. Regulation of cartilage formation and maturation by mitogen-activated protein kinase signaling. *Birth Defects Research Part C: Embryo Today: Reviews*, 84, 131-154.
- BONNANS, C., CHOU, J. & WERB, Z. 2014. Remodelling the extracellular matrix in development and disease. *Nature reviews Molecular cell biology*, 15, 786-801.
- BORODINA, T., ADJAYE, J. & SULTAN, M. 2011. A strand-specific library preparation protocol for RNA sequencing. *Methods Enzymol*, 500, 79-98.
- BOUGAULT, C., AUBERT-FOUCHER, E., PAUMIER, A., PERRIER-GROULT, E., HUOT, L., HOT, D., DUTERQUE-COQUILLAUD, M. & MALLEIN-GERIN, F. 2012. Dynamic compression of chondrocyte-agarose constructs reveals new candidate mechanosensitive genes. *PLoS One*, 7, e36964.
- BOURBOULIA, D. & STETLER-STEVENSON, W. G. Matrix metalloproteinases (MMPs) and tissue inhibitors of metalloproteinases (TIMPs): Positive and negative regulators in tumor cell adhesion. *Seminars in cancer biology*, 2010. Elsevier, 161-168.
- BRAMEIER, M., HERWIG, A., REINHARDT, R., WALTER, L. & GRUBER, J. 2011. Human box C/D snoRNAs with miRNA like functions: expanding the range of regulatory RNAs. *Nucleic acids research*, 39, 675-686.
- BRENNECKE, J., STARK, A., RUSSELL, R. B. & COHEN, S. M. 2005. Principles of microRNA–target recognition. *PLoS Biol*, 3, e85.
- BREW, K. & NAGASE, H. 2010. The tissue inhibitors of metalloproteinases (TIMPs): an ancient family with structural and functional diversity. *Biochimica et Biophysica Acta (BBA)-Molecular Cell Research*, 1803, 55-71.
- BRIGGS, M. D., BELL, P. A. & PIROG, K. A. 2015. The utility of mouse models to provide information regarding the pathomolecular mechanisms in human genetic skeletal diseases: The emerging role of endoplasmic reticulum stress (Review). *International journal of molecular medicine*, 35, 1483-1492.
- BRONNER, I. F., QUAIL, M. A., TURNER, D. J. & SWERDLOW, H. 2014. Improved protocols for illumina sequencing. *Current Protocols in Human Genetics*, 18.2. 1-18.2. 42.
- BROWN, R. & JONES, K. 1990. The synthesis and accumulation of fibronectin by human articular cartilage. *The Journal of rheumatology*, 17, 65-72.
- BROWNE, J. E. & BRANCH, T. P. 2000. Surgical alternatives for treatment of articular cartilage lesions. *Journal of the American Academy of Orthopaedic Surgeons*, 8, 180-189.
- BRÜMMER, A. & HAUSSER, J. 2014. MicroRNA binding sites in the coding region of mRNAs: Extending the repertoire of post-transcriptional gene regulation. *Bioessays*, 36, 617-626.
- BUCKWALTER, J. A., MANKIN, H. J. & GRODZINSKY, A. J. 2005. Articular cartilage and osteoarthritis. *Instructional course lectures*, 54, 465-80.

- BUSCHMANN, M. D., GLUZBAND, Y. A., GRODZINSKY, A. J. & HUNZIKER, E. B. 1995. Mechanical compression modulates matrix biosynthesis in chondrocyte/agarose culture. *Journal of cell science*, 108, 1497-1508.
- BUSTIN, S. A. 2000. Absolute quantification of mRNA using real-time reverse transcription polymerase chain reaction assays. *Journal of molecular endocrinology*, 25, 169-193.
- BUSTIN, S. A., BEAULIEU, J.-F., HUGGETT, J., JAGGI, R., KIBENGE, F. S., OLSVIK, P. A., PENNING, L. C. & TOEGEL, S. 2010. MIQE precis: Practical implementation of minimum standard guidelines for fluorescence-based quantitative real-time PCR experiments. *BMC molecular biology*, 11, 1.
- BUSTIN, S. A., BENES, V., GARSON, J. A., HELLEMANS, J., HUGGETT, J., KUBISTA, M., MUELLER, R., NOLAN, T., PFAFFL, M. W. & SHIPLEY, G. L. 2009. The MIQE guidelines: minimum information for publication of quantitative real-time PCR experiments. *Clinical chemistry*, 55, 611-622.
- CAO, K., WEI, L., ZHANG, Z., GUO, L., ZHANG, C., LI, Y., SUN, C., SUN, X., WANG, S. & LI, P. 2014. Decreased histone deacetylase 4 is associated with human osteoarthritis cartilage degeneration by releasing histone deacetylase 4 inhibition of runt-related transcription factor-2 and increasing osteoarthritis-related genes: a novel mechanism of human osteoarthritis cartilage degeneration. *Arthritis research & therapy*, 16, 1.
- CARVALHO, B. S. & IRIZARRY, R. A. 2010. A framework for oligonucleotide microarray preprocessing. *Bioinformatics*, 26, 2363-2367.
- CATERSON, B., FLANNERY, C. R., HUGHES, C. E. & LITTLE, C. B. 1999. Mechanisms of proteoglycan metabolism that lead to cartilage destruction in the pathogenesis of arthritis. *Drugs Today (Barc)*, 35, 397-402.
- CATERSON, B., FLANNERY, C. R., HUGHES, C. E. & LITTLE, C. B. 2000. Mechanisms involved in cartilage proteoglycan catabolism. *Matrix Biol*, 19, 333-44.
- CATERSON, B. & LOWTHER, D. A. 1978. Changes in the metabolism of the proteoglycans from sheep articular cartilage in response to mechanical stress. *Biochimica et Biophysica Acta (BBA)-General Subjects*, 540, 412-422.
- CHAILLOU, T., LEE, J. D., ENGLAND, J. H., ESSER, K. A. & MCCARTHY, J. J. 2013. Time course of gene expression during mouse skeletal muscle hypertrophy. *Journal of Applied Physiology*, 115, 1065-1074.
- CHANG, C.-F., RAMASWAMY, G. & SERRA, R. 2012. Depletion of primary cilia in articular chondrocytes results in reduced Gli3 repressor to activator ratio, increased Hedgehog signaling, and symptoms of early osteoarthritis. *Osteoarthritis and Cartilage*, 20, 152-161.
- CHANG, T., XIE, J., LI, H., LI, D., LIU, P. & HU, Y. 2016. MicroRNA-30a promotes extracellular matrix degradation in articular cartilage via downregulation of Sox9. *Cell proliferation*, 49, 207-218.
- CHAO, H.-W., TSAI, L.-Y., LU, Y.-L., LIN, P.-Y., HUANG, W.-H., CHOU, H.-J., LU, W.-H., LIN, H.-C., LEE, P.-T. & HUANG, Y.-S. 2013. Deletion of CPEB3 enhances hippocampus-dependent memory via increasing expressions of PSD95 and NMDA receptors. *The Journal of Neuroscience*, 33, 17008-17022.
- CHENG, Y. & LOTAN, R. 1998. Molecular cloning and characterization of a novel retinoic acid-inducible gene that encodes a putative G protein-coupled receptor. *J Biol Chem*, 273, 35008-15.
- CLARK, J. M. 1985. The organization of collagen in cryofractured rabbit articular cartilage: a scanning electron microscopic study. *Journal of orthopaedic research*, 3, 17-29.
- CORR, M. 2008. Wnt- $\beta$ -catenin signaling in the pathogenesis of osteoarthritis. *Nature Clinical Practice Rheumatology*, 4, 550-556.

- CORREA-MEYER, E., PESCE, L., GUERRERO, C. & SZNAJDER, J. I. 2002. Cyclic stretch activates ERK1/2 via G proteins and EGFR in alveolar epithelial cells. *American Journal of Physiology-Lung Cellular and Molecular Physiology*, 282, L883-L891.
- COWLAND, J. B., HOTHER, C. & GRONBAEK, K. 2007. MicroRNAs and cancer. *APMIS : acta pathologica, microbiologica, et immunologica Scandinavica*, 115, 1090-106.
- CROWE, N., SWINGLER, T., LE, L., BARTER, M., WHEELER, G., PAIS, H., DONELL, S., YOUNG, D., DALMAY, T. & CLARK, I. 2016. Detecting new microRNAs in human osteoarthritic chondrocytes identifies miR-3085 as a human, chondrocyte-selective, microRNA. *Osteoarthritis and Cartilage*, 24, 534-543.
- DAI, L., ZHANG, X., HU, X., ZHOU, C. & AO, Y. 2012. Silencing of microRNA-101 prevents IL-1beta-induced extracellular matrix degradation in chondrocytes. *Arthritis research & therapy*, 14, R268.
- DARLING, E. M. & ATHANASIOU, K. A. 2005. Rapid phenotypic changes in passaged articular chondrocyte subpopulations. *Journal of orthopaedic research : official publication of the Orthopaedic Research Society*, 23, 425-32.
- DAS, R. H., JAHR, H., VERHAAR, J. A., VAN DER LINDEN, J. C., VAN OSCH, G. J. & WEINANS, H. 2008. In vitro expansion affects the response of chondrocytes to mechanical stimulation. *Osteoarthritis Cartilage*, 16, 385-91.
- DEHNE, T., KARLSSON, C., RINGE, J., SITTINGER, M. & LINDAHL, A. 2009. Chondrogenic differentiation potential of osteoarthritic chondrocytes and their possible use in matrix-associated autologous chondrocyte transplantation. *Arthritis research & therapy*, 11, 1.
- DELLETT, M., HU, W., PAPADAKI, V. & OHNUMA, S. I. 2012. Small leucine rich proteoglycan family regulates multiple signalling pathways in neural development and maintenance. *Development, growth & differentiation*, 54, 327-340.
- DEMOLLI, S., STARK, K., DODDABALLAPUR, A., BOON, R. A., DOEBELE, C., ECKERT, A., KORFF, T., HECKER, M., MASSBERG, S. & KALUZA, D. 2013. Shear Stress-Regulated Mir-27a/b Controls Pericyte Recruitment: Implications for Vessel Maturation. *Circulation*, 128, A14910.
- DESNOYERS, L., ARNOTT, D. & PENNICA, D. 2001. WISP-1 binds to decorin and biglycan. *Journal of Biological Chemistry*, 276, 47599-47607.
- DHEDA, K., HUGGETT, J. F., BUSTIN, S. A., JOHNSON, M. A., ROOK, G. & ZUMLA, A. 2004. Validation of housekeeping genes for normalizing RNA expression in real-time PCR. *Biotechniques*, 37, 112-119.
- DIAZ-PRADO, S., CICIONE, C., MUINOS-LOPEZ, E., HERMIDA-GOMEZ, T., OREIRO, N., FERNANDEZ-LOPEZ, C. & BLANCO, F. J. 2012. Characterization of microRNA expression profiles in normal and osteoarthritic human chondrocytes. *BMC Musculoskelet Disord*, 13, 144.
- DOBACZEWSKI, M., CHEN, W. & FRANGOIANNIS, N. G. 2011. Transforming growth factor (TGF)- $\beta$  signaling in cardiac remodeling. *Journal of molecular and cellular cardiology*, 51, 600-606.
- DOUDNA, J. A. & RATH, V. L. 2002. Structure and function of the eukaryotic ribosome: the next frontier. *Cell*, 109, 153-156.
- DOUGLAS, T., HEINEMANN, S., BIERBAUM, S., SCHARNWEBER, D. & WORCH, H. 2006. Fibrillogenesis of collagen types I, II, and III with small leucine-rich proteoglycans decorin and biglycan. *Biomacromolecules*, 7, 2388-2393.
- DUANCE, V. 1983. Surface of articular cartilage: immunohistological studies. *Cell biochemistry and function*, 1, 143-144.
- DUDEK, K. A., LAFONT, J. E., MARTINEZ-SANCHEZ, A. & MURPHY, C. L. 2010. Type II collagen expression is regulated by tissue-specific miR-675 in human articular chondrocytes. *Journal of Biological Chemistry*, 285, 24381-24387.

- DUNN, W., DURAIN, G. & REDDI, A. H. 2009. Profiling microRNA expression in bovine articular cartilage and implications for mechanotransduction. *Arthritis and rheumatism*, 60, 2333-9.
- ENDER, C., KREK, A., FRIEDLÄNDER, M. R., BEITZINGER, M., WEINMANN, L., CHEN, W., PFEFFER, S., RAJEWSKY, N. & MEISTER, G. 2008. A human snoRNA with microRNA-like functions. *Molecular cell*, 32, 519-528.
- EVANGELISTA, M., TIAN, H. & DE SAUVAGE, F. J. 2006. The hedgehog signaling pathway in cancer. *Clinical Cancer Research*, 12, 5924-5928.
- EYRE, D. 2002. Collagen of articular cartilage. *Arthritis Res*, 4, 30-5.
- FANG, Z. & RAJEWSKY, N. 2011. The impact of miRNA target sites in coding sequences and in 3'UTRs. *PLoS One*, 6, e18067.
- FEHRENBACHER, A., STECK, E., RICKERT, M., ROTH, W. & RICHTER, W. 2003. Rapid regulation of collagen but not metalloproteinase 1, 3, 13, 14 and tissue inhibitor of metalloproteinase 1, 2, 3 expression in response to mechanical loading of cartilage explants in vitro. *Archives of biochemistry and biophysics*, 410, 39-47.
- FERNANDES-SILVA, M. M., CARVALHO, V. O., GUIMARAES, G. V., BACAL, F. & BOCCHI, E. A. 2012. Physical exercise and microRNAs: new frontiers in heart failure. *Arquivos brasileiros de cardiologia*, 98, 459-66.
- FILIPOWICZ, W., JASKIEWICZ, L., KOLB, F. A. & PILLAI, R. S. 2005. Post-transcriptional gene silencing by siRNAs and miRNAs. *Current opinion in structural biology*, 15, 331-41.
- FINLIN, B. S., GAU, C. L., MURPHY, G. A., SHAO, H., KIMEL, T., SEITZ, R. S., CHIU, Y. F., BOTSTEIN, D., BROWN, P. O., DER, C. J., TAMANOI, F., ANDRES, D. A. & PEROU, C. M. 2001. RERG is a novel ras-related, estrogen-regulated and growth-inhibitory gene in breast cancer. *J Biol Chem*, 276, 42259-67.
- FITZGERALD, J. B., JIN, M., CHAI, D. H., SIPARSKY, P., FANNING, P. & GRODZINSKY, A. J. 2008. Shear- and compression-induced chondrocyte transcription requires MAPK activation in cartilage explants. *J Biol Chem*, 283, 6735-43.
- FITZGERALD, J. B., JIN, M., DEAN, D., WOOD, D. J., ZHENG, M. H. & GRODZINSKY, A. J. 2004. Mechanical compression of cartilage explants induces multiple time-dependent gene expression patterns and involves intracellular calcium and cyclic AMP. *J Biol Chem*, 279, 19502-11.
- FITZGERALD, J. B., JIN, M. & GRODZINSKY, A. J. 2006. Shear and compression differentially regulate clusters of functionally related temporal transcription patterns in cartilage tissue. *Journal of Biological Chemistry*, 281, 24095-24103.
- FOSANG, A. J., LAST, K., KNÄUPER, V., MURPHY, G. & NEAME, P. J. 1996. Degradation of cartilage aggrecan by collagenase-3 (MMP-13). *FEBS letters*, 380, 17-20.
- FRANCIS-WEST, P., ABDELFATTAH, A., CHEN, P., ALLEN, C., PARISH, J., LADHER, R., ALLEN, S., MACPHERSON, S., LUYTEN, F. & ARCHER, C. 1999. Mechanisms of GDF-5 action during skeletal development. *Development*, 126, 1305-1315.
- FRASER, J., LAURENT, T. & LAURENT, U. 1997. Hyaluronan: its nature, distribution, functions and turnover. *Journal of internal medicine*, 242, 27-33.
- FRIEDMAN, R. C., FARH, K. K.-H., BURGE, C. B. & BARTEL, D. P. 2009. Most mammalian mRNAs are conserved targets of microRNAs. *Genome research*, 19, 92-105.
- FRISBIE, D., CROSS, M. & MCILWRAITH, C. 2006. A comparative study of articular cartilage thickness in the stifle of animal species used in human pre-clinical studies compared to articular cartilage thickness in the human knee. *Veterinary and Comparative Orthopaedics and Traumatology (VCOT)*, 19, 142-146.
- FRYE, S. R., YEE, A., ESKIN, S. G., GUERRA, R., CONG, X. & MCINTIRE, L. V. 2005. cDNA microarray analysis of endothelial cells subjected to cyclic mechanical strain: importance of motion control. *Physiological genomics*, 21, 124-30.

- FUJIOKA, R., AOYAMA, T. & TAKAKUWA, T. 2013. The layered structure of the articular surface. *Osteoarthritis and Cartilage*, 21, 1092-1098.
- GABRIELY, G., WURDINGER, T., KESARI, S., ESAU, C. C., BURCHARD, J., LINSLEY, P. S. & KRICHEVSKY, A. M. 2008. MicroRNA 21 promotes glioma invasion by targeting matrix metalloproteinase regulators. *Molecular and cellular biology*, 28, 5369-5380.
- GARDINER, M., VINCENT, T., DRISCOLL, C., BURLEIGH, A., BOU-GHARIOS, G., SAKLATVALA, J., NAGASE, H. & CHANALARIS, A. 2015. Transcriptional analysis of micro-dissected articular cartilage in post-traumatic murine osteoarthritis. *Osteoarthritis and Cartilage*, 23, 616-628.
- GARG, M., KANOJIA, D., OKAMOTO, R., JAIN, S., MADAN, V., CHIEN, W., SAMPATH, A., DING, L. W., XUAN, M., SAID, J. W., DOAN, N. B., LIU, L. Z., YANG, H., GERY, S., BRAUNSTEIN, G. D. & KOEFFLER, H. P. 2014. Laminin-5gamma-2 (LAMC2) is highly expressed in anaplastic thyroid carcinoma and is associated with tumor progression, migration, and invasion by modulating signaling of EGFR. *J Clin Endocrinol Metab*, 99, E62-72.
- GAROFALO, M., DI LEVA, G., ROMANO, G., NUOVO, G., SUH, S.-S., NGANKEU, A., TACCIOLI, C., PICHIORRI, F., ALDER, H. & SECCHIERO, P. 2009. miR-221&222 regulate TRAIL resistance and enhance tumorigenicity through PTEN and TIMP3 downregulation. *Cancer cell*, 16, 498-509.
- GELSE, K., PÖSCHL, E. & AIGNER, T. 2003. Collagens—structure, function, and biosynthesis. *Advanced drug delivery reviews*, 55, 1531-1546.
- GHADIALLY, F. N. 1983. *Fine structure of synovial joints: a text and atlas of the ultrastructure of normal and pathological articular tissues*, Butterworth-Heinemann.
- GIBSON, G. & ASAHARA, H. 2013. microRNAs and cartilage. *Journal of Orthopaedic Research*, 31, 1333-1344.
- GLARE, E., DIVJAK, M., BAILEY, M. & WALTERS, E. 2002.  $\beta$ -Actin and GAPDH housekeeping gene expression in asthmatic airways is variable and not suitable for normalising mRNA levels. *Thorax*, 57, 765-770.
- GLASSON, S., BLANCHET, T. & MORRIS, E. 2007. The surgical destabilization of the medial meniscus (DMM) model of osteoarthritis in the 129/SvEv mouse. *Osteoarthritis and Cartilage*, 15, 1061-1069.
- GLASSON, S. S., ASKEW, R., SHEPPARD, B., CARITO, B., BLANCHET, T., MA, H.-L., FLANNERY, C. R., PELUSO, D., KANKI, K. & YANG, Z. 2005. Deletion of active ADAMTS5 prevents cartilage degradation in a murine model of osteoarthritis. *Nature*, 434, 644-648.
- GLASSON, S. S., ASKEW, R., SHEPPARD, B., CARITO, B. A., BLANCHET, T., MA, H. L., FLANNERY, C. R., KANKI, K., WANG, E. & PELUSO, D. 2004. Characterization of and osteoarthritis susceptibility in ADAMTS-4–knockout mice. *Arthritis & Rheumatism*, 50, 2547-2558.
- GOLDRING, M. B. & MARCU, K. B. 2009. Cartilage homeostasis in health and rheumatic diseases. *Arthritis Res Ther*, 11, 224.
- GOLDRING, M. B. & MARCU, K. B. 2012. Epigenomic and microRNA-mediated regulation in cartilage development, homeostasis, and osteoarthritis. *Trends in molecular medicine*, 18, 109-118.
- GOLJI, J. & MOFRAD, M. R. 2013. The interaction of vinculin with actin. *PLoS Comput Biol*, 9, e1002995.
- GOMES, A. Q., NOLASCO, S. & SOARES, H. 2013. Non-coding RNAs: multi-tasking molecules in the cell. *Int J Mol Sci*, 14, 16010-39.
- GONG, Y., CHIPPADE-VENKATA, U. D. & OH, W. K. 2014. Roles of matrix metalloproteinases and their natural inhibitors in prostate cancer progression. *Cancers*, 6, 1298-1327.
- GORDON, M. K. & HAHN, R. A. 2010. Collagens. *Cell Tissue Res*, 339, 247-57.
- GREGORY, R. I. & SHIEKHATTAR, R. 2005. MicroRNA biogenesis and cancer. *Cancer research*, 65, 3509-12.

- GRIFFIN, T. M. & GUILAK, F. 2005. The role of mechanical loading in the onset and progression of osteoarthritis. *Exercise and sport sciences reviews*, 33, 195-200.
- GRIFFITHS-JONES, S., GROCOCK, R. J., VAN DONGEN, S., BATEMAN, A. & ENRIGHT, A. J. 2006. miRBase: microRNA sequences, targets and gene nomenclature. *Nucleic Acids Res*, 34, D140-4.
- GRIMSON, A., FARH, K. K.-H., JOHNSTON, W. K., GARRETT-ENGELE, P., LIM, L. P. & BARTEL, D. P. 2007. MicroRNA targeting specificity in mammals: determinants beyond seed pairing. *Molecular cell*, 27, 91-105.
- GRODZINSKY, A. J., LEVENSTON, M. E., JIN, M. & FRANK, E. H. 2000. Cartilage tissue remodeling in response to mechanical forces. *Annu Rev Biomed Eng*, 2, 691-713.
- GUAN, J.-L. 1997. Role of focal adhesion kinase in integrin signaling. *The international journal of biochemistry & cell biology*, 29, 1085-1096.
- GUAN, Y., YANG, X. & CHEN, Q. 2014. MicroRNA-146a is a hypertrophic cartilage specific microRNA induced by mechanical loading. *ORS 2014 Annual Meeting*. <http://www.ors.org/Transactions/60/1297.pdf>.
- GUAN, Y. J., YANG, X., WEI, L. & CHEN, Q. 2011. MiR-365: a mechanosensitive microRNA stimulates chondrocyte differentiation through targeting histone deacetylase 4. *FASEB J*, 25, 4457-66.
- GUILAK, F., ZELL, R. A., ERICKSON, G. R., GRANDE, D. A., RUBIN, C. T., MCLEOD, K. J. & DONAHUE, H. J. 1999. Mechanically induced calcium waves in articular chondrocytes are inhibited by gadolinium and amiloride. *Journal of orthopaedic research*, 17, 421-429.
- GUNNING, P. W., GHOSHASTIDER, U., WHITAKER, S., POPP, D. & ROBINSON, R. C. 2015. The evolution of compositionally and functionally distinct actin filaments. *J Cell Sci*, 128, 2009-2019.
- GUO, H., INGOLIA, N. T., WEISSMAN, J. S. & BARTEL, D. P. 2010. Mammalian microRNAs predominantly act to decrease target mRNA levels. *Nature*, 466, 835-840.
- HAAPALA, J., AROKOSKI, J. P., HYTTINEN, M. M., LAMMI, M., TAMMI, M., KOVANEN, V., HELMINEN, H. J. & KIVIRANTA, I. 1999. Remobilization does not fully restore immobilization induced articular cartilage atrophy. *Clinical orthopaedics and related research*, 362, 218-229.
- HAASPER, C., JAGODZINSKI, M., DRESCHER, M., MELLER, R., WEHMEIER, M., KRETTEK, C. & HESSE, E. 2008. Cyclic strain induces FosB and initiates osteogenic differentiation of mesenchymal cells. *Experimental and Toxicologic Pathology*, 59, 355-363.
- HALL, S. L. & PADGETT, R. A. 1996. Requirement of U12 snRNA for in vivo splicing of a minor class of eukaryotic nuclear pre-mRNA introns. *Science*, 271, 1716.
- HAMAMURA, K., ZHANG, P., ZHAO, L., SHIM, J. W., CHEN, A., DODGE, T. R., WAN, Q., SHIH, H., NA, S., LIN, C. C., SUN, H. B. & YOKOTA, H. 2013. Knee loading reduces MMP13 activity in the mouse cartilage. *BMC Musculoskelet Disord*, 14, 312.
- HAN, J., LEE, Y., YEOM, K. H., KIM, Y. K., JIN, H. & KIM, V. N. 2004. The Drosha-DGCR8 complex in primary microRNA processing. *Genes & development*, 18, 3016-27.
- HAQUE, S., GORDON, C., ISENBERG, D., RAHMAN, A., LANYON, P., BELL, A., EMERY, P., MCHUGH, N., TEH, L. S., SCOTT, D. G., AKIL, M., NAZ, S., ANDREWS, J., GRIFFITHS, B., HARRIS, H., YOUSSEF, H., MCLAREN, J., TOESCU, V., DEVAKUMAR, V., TEIR, J. & BRUCE, I. N. 2010. Risk factors for clinical coronary heart disease in systemic lupus erythematosus: the lupus and atherosclerosis evaluation of risk (LASER) study. *J Rheumatol*, 37, 322-9.
- HARADA, Y., YOKOTA, C., HABAS, R., SLUSARSKI, D. C. & HE, X. 2007. Retinoic acid-inducible G protein-coupled receptors bind to frizzled receptors and may activate non-canonical Wnt signaling. *Biochem Biophys Res Commun*, 358, 968-75.

- HAUSSECKER, D., HUANG, Y., LAU, A., PARAMESWARAN, P., FIRE, A. Z. & KAY, M. A. 2010. Human tRNA-derived small RNAs in the global regulation of RNA silencing. *Rna*, 16, 673-695.
- HAUSSER, J., SYED, A. P., BILEN, B. & ZAVOLAN, M. 2013. Analysis of CDS-located miRNA target sites suggests that they can effectively inhibit translation. *Genome Res*, 23, 604-15.
- HECHT, J. T., HAYES, E., HAYNES, R. & COLE, W. G. 2005. COMP mutations, chondrocyte function and cartilage matrix. *Matrix Biology*, 23, 525-533.
- HEDBOM, E. & HEINEGÅRD, D. 1993. Binding of fibromodulin and decorin to separate sites on fibrillar collagens. *Journal of Biological Chemistry*, 268, 27307-27312.
- HEINEGÅRD, D. 2009. Fell-Muir Lecture: Proteoglycans and more—from molecules to biology. *International journal of experimental pathology*, 90, 575-586.
- HEINEGÅRD, D. & SAXNE, T. 2011. The role of the cartilage matrix in osteoarthritis. *Nature Reviews Rheumatology*, 7, 50-56.
- HILDEBRAND, A., ROMARIS, M., RASMUSSEN, L., HEINEGÅRD, D., TWARDZIK, D., BORDER, W. & RUOSLAHTI, E. 1994. Interaction of the small interstitial proteoglycans biglycan, decorin and fibromodulin with transforming growth factor  $\beta$ . *Biochemical Journal*, 302, 527-534.
- HODGE, W., FIJAN, R., CARLSON, K., BURGESS, R., HARRIS, W. & MANN, R. 1986. Contact pressures in the human hip joint measured in vivo. *Proceedings of the National Academy of Sciences*, 83, 2879-2883.
- HOGAN, B. 1996. Bone morphogenetic proteins: multifunctional regulators of vertebrate development. *Genes & development*, 10, 1580-1594.
- HOLMES, D. F. & KADLER, K. E. 2006. The 10+4 microfibril structure of thin cartilage fibrils. *Proceedings of the National Academy of Sciences*, 103, 17249-17254.
- HOMANDBERG, G. A., DAVIS, G., MANIGLIA, C. & SHRIKHANDE, A. 1997. Cartilage chondrolysis by fibronectin fragments causes cleavage of aggrecan at the same site as found in osteoarthritic cartilage. *Osteoarthritis and Cartilage*, 5, 450-453.
- HU, W., ZHANG, W., LI, F., GUO, F. & CHEN, A. 2016. miR-139 is up-regulated in osteoarthritis and inhibits chondrocyte proliferation and migration possibly via suppressing EIF4G2 and IGF1R. *Biochemical and biophysical research communications*, 474, 296-302.
- HUANG, J., BALLOU, L. R. & HASTY, K. A. 2007. Cyclic equibiaxial tensile strain induces both anabolic and catabolic responses in articular chondrocytes. *Gene*, 404, 101-9.
- HUANG, K. & WU, L. D. 2008. Aggrecanase and aggrecan degradation in osteoarthritis: a review. *J Int Med Res*, 36, 1149-60.
- HUANG, W.-H., CHAO, H.-W., TSAI, L.-Y., CHUNG, M.-H. & HUANG, Y.-S. 2014. Elevated activation of CaMKII $\alpha$  in the CPEB3-knockout hippocampus impairs a specific form of NMDAR-dependent synaptic depotentiation. *Frontiers in cellular neuroscience*, 8.
- HUMKE, E. W., DORN, K. V., MILENKOVIC, L., SCOTT, M. P. & ROHATGI, R. 2010. The output of Hedgehog signaling is controlled by the dynamic association between Suppressor of Fused and the Gli proteins. *Genes & development*, 24, 670-682.
- HWANG, S.-G., YU, S.-S., LEE, S.-W. & CHUN, J.-S. 2005. Wnt-3a regulates chondrocyte differentiation via c-Jun/AP-1 pathway. *FEBS letters*, 579, 4837-4842.
- IJIRI, K., ZERBINI, L. F., PENG, H., OTU, H. H., TSUCHIMOCCHI, K., OTERO, M., DRAGOMIR, C., WALSH, N., BIERBAUM, B. E., MATTINGLY, D., VAN FLANDERN, G., KOMIYA, S., AIGNER, T., LIBERMANN, T. A. & GOLDRING, M. B. 2008. Differential expression of GADD45beta in normal and osteoarthritic cartilage: potential role in homeostasis of articular chondrocytes. *Arthritis Rheum*, 58, 2075-87.
- ILIOPOULOS, D., MALIZOS, K. N., OIKONOMOU, P. & TSEZOU, A. 2008. Integrative microRNA and proteomic approaches identify novel osteoarthritis genes and their collaborative metabolic and inflammatory networks. *PLoS one*, 3, e3740.

- INOUE, D., KIDO, S. & MATSUMOTO, T. 2004. Transcriptional induction of FosB/ $\Delta$ FosB gene by mechanical stress in osteoblasts. *Journal of Biological Chemistry*, 279, 49795-49803.
- IOZZO, R. V. 1998. Matrix proteoglycans: from molecular design to cellular function. *Annual review of biochemistry*, 67, 609-652.
- IRIANTO, J., RAMASWAMY, G., SERRA, R. & KNIGHT, M. M. 2014. Depletion of chondrocyte primary cilia reduces the compressive modulus of articular cartilage. *Journal of biomechanics*, 47, 579-582.
- IRIZARRY, R. A., HOBBS, B., COLLIN, F., BEAZER-BARCLAY, Y. D., ANTONELLIS, K. J., SCHERF, U. & SPEED, T. P. 2003. Exploration, normalization, and summaries of high density oligonucleotide array probe level data. *Biostatistics*, 4, 249-264.
- JAY, G. D. & WALLER, K. A. 2014. The biology of Lubricin: Near frictionless joint motion. *Matrix Biology*, 39, 17-24.
- JIN, L., ZHAO, J., JING, W., YAN, S., WANG, X., XIAO, C. & MA, B. 2014. Role of miR-146a in human chondrocyte apoptosis in response to mechanical pressure injury in vitro. *International journal of molecular medicine*, 34, 451-463.
- JOHNSON, J. L., DWIVEDI, A., SOMERVILLE, M., GEORGE, S. J. & NEWBY, A. C. 2011. Matrix metalloproteinase (MMP)-3 activates MMP-9 mediated vascular smooth muscle cell migration and neointima formation in mice. *Arteriosclerosis, thrombosis, and vascular biology*, 31, e35-e44.
- JONES, A. R., GLEGHORN, J. P., HUGHES, C. E., FITZ, L. J., ZOLLNER, R., WAINWRIGHT, S. D., CATERSON, B., MORRIS, E. A., BONASSAR, L. J. & FLANNERY, C. R. 2007. Binding and localization of recombinant lubricin to articular cartilage surfaces. *Journal of orthopaedic research*, 25, 283-292.
- JONES, S., WATKINS, G., LE GOOD, N., ROBERTS, S., MURPHY, C., BROCKBANK, S., NEEDHAM, M., READ, S. & NEWHAM, P. 2009. The identification of differentially expressed microRNA in osteoarthritic tissue that modulate the production of TNF- $\alpha$  and MMP13. *Osteoarthritis and cartilage*, 17, 464-472.
- JORTIKKA, M. O., INKINEN, R. I., TAMMI, M. I., PARKKINEN, J. J., HAAPALA, J., KIVIRANTA, I., HELMINEN, H. J. & LAMMI, M. J. 1997. Immobilisation causes longlasting matrix changes both in the immobilised and contralateral joint cartilage. *Annals of the rheumatic diseases*, 56, 255-260.
- JULOVI, S. M., YASUDA, T., SHIMIZU, M., HIRAMITSU, T. & NAKAMURA, T. 2004. Inhibition of interleukin-1 $\beta$ -stimulated production of matrix metalloproteinases by hyaluronan via CD44 in human articular cartilage. *Arthritis & Rheumatism*, 50, 516-525.
- KADLER, K. E., HILL, A. & CANTY-LAIRD, E. G. 2008. Collagen fibrillogenesis: fibronectin, integrins, and minor collagens as organizers and nucleators. *Current opinion in cell biology*, 20, 495-501.
- KANG, L., YANG, C., SONG, Y., LIU, W., WANG, K., LI, S. & ZHANG, Y. 2016. MicroRNA-23a-3p promotes the development of osteoarthritis by directly targeting SMAD3 in chondrocytes. *Biochemical and Biophysical Research Communications*.
- KARLSEN, T. A., JAKOBSEN, R. B., MIKKELSEN, T. S. & BRINCHMANN, J. E. 2013. microRNA-140 targets RALA and regulates chondrogenic differentiation of human mesenchymal stem cells by translational enhancement of SOX9 and ACAN. *Stem cells and development*, 23, 290-304.
- KAWAKITA, A., YANAMOTO, S., YAMADA, S.-I., NARUSE, T., TAKAHASHI, H., KAWASAKI, G. & UMEDA, M. 2014. MicroRNA-21 promotes oral cancer invasion via the Wnt/ $\beta$ -catenin pathway by targeting DKK2. *Pathology & Oncology Research*, 20, 253-261.
- KEVORKIAN, L., YOUNG, D. A., DARRAH, C., DONELL, S. T., SHEPSTONE, L., PORTER, S., BROCKBANK, S., EDWARDS, D. R., PARKER, A. E. & CLARK, I. M. 2004. Expression profiling of metalloproteinases and their inhibitors in cartilage. *Arthritis & Rheumatism*, 50, 131-141.

- KEY, M. D., ANDRES, D. A., DER, C. J. & REPASKY, G. A. 2006. Characterization of RERG: An Estrogen-Regulated Tumor Suppressor Gene. *Methods in enzymology*, 407, 513-527.
- KHALID, A. B. & KRUM, S. A. 2016. Estrogen receptors alpha and beta in bone. *Bone*, 87, 130-135.
- KIANI, C., CHEN, L., WU, Y. J., YEE, A. J. & YANG, B. B. 2002. Structure and function of aggrecan. *Cell Res*, 12, 19-32.
- KIM, D., SONG, J. & JIN, E. J. 2010. MicroRNA-221 regulates chondrogenic differentiation through promoting proteosomal degradation of slug by targeting Mdm2. *J Biol Chem*, 285, 26900-7.
- KIM, I., OTTO, F., ZABEL, B. & MUNDLOS, S. 1999. Regulation of chondrocyte differentiation by Cbfa1. *Mechanisms of development*, 80, 159-170.
- KIM, Y. J., SAH, R. L., GRODZINSKY, A. J., PLAAS, A. H. & SANDY, J. D. 1994. Mechanical regulation of cartilage biosynthetic behavior: physical stimuli. *Arch Biochem Biophys*, 311, 1-12.
- KIPPENBERGER, S., LOITSCH, S., GUSCHEL, M., MÜLLER, J., KNIES, Y., KAUFMANN, R. & BERND, A. 2005. Mechanical stretch stimulates protein kinase B/Akt phosphorylation in epidermal cells via angiotensin II type 1 receptor and epidermal growth factor receptor. *Journal of Biological Chemistry*, 280, 3060-3067.
- KIRALY, K., HYTTINEN, M., PARKKINEN, J., AROKOSKI, J., LAPVETELÄINEN, T., TÖRRÖNEN, K., KIVIRANTA, I. & HELMINEN, H. 1998. Articular cartilage collagen birefringence is altered concurrent with changes in proteoglycan synthesis during dynamic in vitro loading. *The Anatomical Record*, 251, 28-36.
- KISIDAY, J. D., KURZ, B., DIMICCO, M. A. & GRODZINSKY, A. J. 2005. Evaluation of medium supplemented with insulin-transferrin-selenium for culture of primary bovine calf chondrocytes in three-dimensional hydrogel scaffolds. *Tissue engineering*, 11, 141-51.
- KIVIRANTA, I., JURVELIN, J., TAMMI, M., SÄÄMÄUNEN, A. M. & HELMINEN, H. J. 1987. Weight bearing controls glycosaminoglycan concentration and articular cartilage thickness in the knee joints of young beagle dogs. *Arthritis & Rheumatism*, 30, 801-809.
- KLATT, A. R., BECKER, A.-K. A., NEACSU, C. D., PAULSSON, M. & WAGENER, R. 2011. The matrilins: modulators of extracellular matrix assembly. *The international journal of biochemistry & cell biology*, 43, 320-330.
- KLEIN, T., SCHUMACHER, B., SCHMIDT, T., LI, K., VOEGTLIN, M., MASUDA, K., THONAR, E.-M. & SAH, R. 2003. Tissue engineering of stratified articular cartilage from chondrocyte subpopulations. *Osteoarthritis and cartilage*, 11, 595-602.
- KNIGHT, M., TOYODA, T., LEE, D. & BADER, D. 2006. Mechanical compression and hydrostatic pressure induce reversible changes in actin cytoskeletal organisation in chondrocytes in agarose. *Journal of biomechanics*, 39, 1547-1551.
- KOBAYASHI, T., LU, J., COBB, B. S., RODDA, S. J., MCMAHON, A. P., SCHIPANI, E., MERKENSCHLAGER, M. & KRONENBERG, H. M. 2008. Dicer-dependent pathways regulate chondrocyte proliferation and differentiation. *Proc Natl Acad Sci U S A*, 105, 1949-54.
- KOMORI, T. 2010. Regulation of bone development and extracellular matrix protein genes by RUNX2. *Cell and tissue research*, 339, 189-195.
- KOZERA, B. & RAPACZ, M. 2013. Reference genes in real-time PCR. *Journal of applied genetics*, 54, 391-406.
- KREK, A., GRÜN, D., POY, M. N., WOLF, R., ROSENBERG, L., EPSTEIN, E. J., MACMENAMIN, P., DA PIEDADE, I., GUNSALUS, K. C. & STOFFEL, M. 2005. Combinatorial microRNA target predictions. *Nature genetics*, 37, 495-500.
- KUBOKI, T., KANTAWONG, F., BURCHMORE, R., DALBY, M. J. & KIDOAKI, S. 2012. 2D-DIGE proteomic analysis of mesenchymal stem cell cultured on the elasticity-tunable hydrogels. *Cell structure and function*, 37, 127-139.

- KUHN, D. E., MARTIN, M. M., FELDMAN, D. S., TERRY, A. V., NUOVO, G. J. & ELTON, T. S. 2008. Experimental validation of miRNA targets. *Methods*, 44, 47-54.
- KUMAR, P., ANAYA, J., MUDUNURI, S. B. & DUTTA, A. 2014. Meta-analysis of tRNA derived RNA fragments reveals that they are evolutionarily conserved and associate with AGO proteins to recognize specific RNA targets. *BMC biology*, 12, 1.
- KUNO, K., OKADA, Y., KAWASHIMA, H., NAKAMURA, H., MIYASAKA, M., OHNO, H. & MATSUSHIMA, K. 2000. ADAMTS-1 cleaves a cartilage proteoglycan, aggrecan. *FEBS letters*, 478, 241-245.
- KURZ, B., JIN, M., PATWARI, P., CHENG, D. M., LARK, M. W. & GRODZINSKY, A. J. 2001. Biosynthetic response and mechanical properties of articular cartilage after injurious compression. *Journal of Orthopaedic Research*, 19, 1140-1146.
- LADEWIG, E., OKAMURA, K., FLYNT, A. S., WESTHOLM, J. O. & LAI, E. C. 2012. Discovery of hundreds of mirtrons in mouse and human small RNA data. *Genome research*, 22, 1634-1645.
- LAI, W. M., HOU, J. & MOW, V. C. 1991. A triphasic theory for the swelling and deformation behaviors of articular cartilage. *Journal of biomechanical engineering*, 113, 245-258.
- LAURENT, T. C. & FRASER, J. 1992. Hyaluronan. *The FASEB Journal*, 6, 2397-2404.
- LE, L. T., SWINGLER, T. E. & CLARK, I. M. 2013. Review: the role of microRNAs in osteoarthritis and chondrogenesis. *Arthritis & Rheumatism*, 65, 1963-1974.
- LE, L. T., SWINGLER, T. E., CROWE, N., VINCENT, T. L., BARTER, M. J., DONELL, S. T., DELANY, A. M., DALMAY, T., YOUNG, D. A. & CLARK, I. M. 2016. The microRNA-29 family in cartilage homeostasis and osteoarthritis. *Journal of Molecular Medicine*, 94, 583-596.
- LEE, C., GRAD, S., WIMMER, M. & ALINI, M. 2005a. The influence of mechanical stimuli on articular cartilage tissue engineering. *Topics in tissue engineering*, 2, 1-32.
- LEE, C. R., GRAD, S., MACLEAN, J. J., IATRIDIS, J. C. & ALINI, M. 2005b. Effect of mechanical loading on mRNA levels of common endogenous controls in articular chondrocytes and intervertebral disk. *Analytical biochemistry*, 341, 372-375.
- LEE, D. A. & BADER, D. L. 1997. Compressive strains at physiological frequencies influence the metabolism of chondrocytes seeded in agarose. *Journal of orthopaedic research*, 15, 181-188.
- LEE, D. Y., DENG, Z., WANG, C.-H. & YANG, B. B. 2007. MicroRNA-378 promotes cell survival, tumor growth, and angiogenesis by targeting SuFu and Fus-1 expression. *Proceedings of the National Academy of Sciences*, 104, 20350-20355.
- LEE, I., AJAY, S. S., YOON, J. I., KIM, H. S., HONG, S. H., KIM, N. H., DHANASEKARAN, S. M., CHINNAIYAN, A. M. & ATHEY, B. D. 2009. New class of microRNA targets containing simultaneous 5'-UTR and 3'-UTR interaction sites. *Genome Res*, 19, 1175-83.
- LEE, J. H., FITZGERALD, J. B., DIMICCO, M. A. & GRODZINSKY, A. J. 2005c. Mechanical injury of cartilage explants causes specific time-dependent changes in chondrocyte gene expression. *Arthritis & Rheumatism*, 52, 2386-2395.
- LEE, K. C. & LANYON, L. E. 2004. Mechanical loading influences bone mass through estrogen receptor  $\alpha$ . *Exercise and sport sciences reviews*, 32, 64-68.
- LEE, M. R., MANTEL, C., LEE, S. A., MOON, S.-H. & BROXMEYER, H. E. 2016. MiR-31/SDHA Axis Regulates Reprogramming Efficiency through Mitochondrial Metabolism. *Stem Cell Reports*, 7, 1-10.
- LEIGH, D. R., ABREU, E. L. & DERWIN, K. A. 2008. Changes in gene expression of individual matrix metalloproteinases differ in response to mechanical unloading of tendon fascicles in explant culture. *J Orthop Res*, 26, 1306-12.
- LEONG, D. J., LI, Y. H., GU, X. I., SUN, L., ZHOU, Z., NASSER, P., LAUDIER, D. M., IQBAL, J., MAJESKA, R. J., SCHAFFLER, M. B., GOLDRING, M. B., CARDOSO, L., ZAIDI, M. & SUN, H. B. 2011. Physiological loading of joints prevents cartilage degradation through CITED2.

*FASEB journal : official publication of the Federation of American Societies for Experimental Biology*, 25, 182-91.

- LEWIS, B. P., BURGE, C. B. & BARTEL, D. P. 2005. Conserved seed pairing, often flanked by adenosines, indicates that thousands of human genes are microRNA targets. *cell*, 120, 15-20.
- LEWIS, B. P., SHIH, I.-H., JONES-RHOADES, M. W., BARTEL, D. P. & BURGE, C. B. 2003. Prediction of mammalian microRNA targets. *Cell*, 115, 787-798.
- LI, B. H., ZHOU, J. S., YE, F., CHENG, X. D., ZHOU, C. Y., LU, W. G. & XIE, X. 2011a. Reduced miR-100 expression in cervical cancer and precursors and its carcinogenic effect through targeting PLK1 protein. *European Journal of Cancer*, 47, 2166-2174.
- LI, J., HUANG, J., DAI, L., YU, D., CHEN, Q., ZHANG, X. & DAI, K. 2012. miR-146a, an IL-1 $\beta$  responsive miRNA, induces vascular endothelial growth factor and chondrocyte apoptosis by targeting Smad4. *Arthritis research & therapy*, 14, R75.
- LI, Q., SHEN, K., ZHAO, Y., HE, X., MA, C., WANG, L., WANG, B., LIU, J. & MA, J. 2013. MicroRNA-222 promotes tumorigenesis via targeting DKK2 and activating the Wnt/ $\beta$ -catenin signaling pathway. *FEBS letters*, 587, 1742-1748.
- LI, S., JIA, X., DUANCE, V. C. & BLAIN, E. J. 2011b. The effects of cyclic tensile strain on the organisation and expression of cytoskeletal elements in bovine intervertebral disc cells: an in vitro study. *European cells & materials*, 21, 508-22.
- LI, W., WU, M., JIANG, S., DING, W., LUO, Q. & SHI, J. 2014. Expression of ADAMTs-5 and TIMP-3 in the condylar cartilage of rats induced by experimentally created osteoarthritis. *Archives of oral biology*, 59, 524-529.
- LI, X., GIBSON, G., KIM, J. S., KROIN, J., XU, S., VAN WIJNEN, A. J. & IM, H. J. 2011c. MicroRNA-146a is linked to pain-related pathophysiology of osteoarthritis. *Gene*, 480, 34-41.
- LIANG, P., GUO, Y., ZHOU, X. & GAO, X. 2014. Expression profiling in Bemisia tabaci under insecticide treatment: indicating the necessity for custom reference gene selection.
- LIANG, Z. J., ZHUANG, H., WANG, G. X., LI, Z., ZHANG, H. T., YU, T. Q. & ZHANG, B. D. 2012. MiRNA-140 is a negative feedback regulator of MMP-13 in IL-1 $\beta$ -stimulated human articular chondrocyte C28/I2 cells. *Inflammation research : official journal of the European Histamine Research Society ... [et al.]*, 61, 503-9.
- LIN, A. C., SEETO, B. L., BARTOSZKO, J. M., KHOURY, M. A., WHETSTONE, H., HO, L., HSU, C., ALI, S. A. & ALMAN, B. A. 2009. Modulating hedgehog signaling can attenuate the severity of osteoarthritis. *Nature medicine*, 15, 1421-1425.
- LIPKA, D. & BORATYNSKI, J. 2008. [Metalloproteinases. Structure and function]. *Postepy Hig Med Dosw (Online)*, 62, 328-36.
- LITON, P. B., LIU, X., CHALLA, P., EPSTEIN, D. L. & GONZALEZ, P. 2005. Induction of TGF- $\beta$ 1 in the trabecular meshwork under cyclic mechanical stress. *Journal of cellular physiology*, 205, 364-71.
- LIU, Q., ZHANG, X., DAI, L., HU, X., ZHU, J., LI, L., ZHOU, C. & AO, Y. 2014. Long Noncoding RNA Related to Cartilage Injury Promotes Chondrocyte Extracellular Matrix Degradation in Osteoarthritis. *Arthritis & Rheumatology*, 66, 969-978.
- LIVAK, K. J. & SCHMITTGEN, T. D. 2001. Analysis of relative gene expression data using real-time quantitative PCR and the 2(-Delta Delta C(T)) Method. *Methods*, 25, 402-8.
- LOECHEL, F., FOX, J. W., MURPHY, G., ALBRECHTSEN, R. & WEWER, U. M. 2000. ADAM 12-S cleaves IGFBP-3 and IGFBP-5 and is inhibited by TIMP-3. *Biochemical and biophysical research communications*, 278, 511-515.
- LOESER, R. F. 2002. Integrins and cell signaling in chondrocytes. *Biorheology*, 39, 119-24.
- LOLLI, A., LAMBERTINI, E., PENOLAZZI, L., ANGELOZZI, M., MORGANTI, C., FRANCESCHETTI, T., PELUCCHI, S., GAMBARI, R. & PIVA, R. 2014. Pro-Chondrogenic Effect of miR-221 and Slug Depletion in Human MSCs. *Stem Cell Rev*.

- LOLLI, A., NARCISI, R., LAMBERTINI, E., PENOLAZZI, L., ANGELOZZI, M., KOPS, N., GASPARINI, S., OSCH, G. J. & PIVA, R. 2016. Silencing of Antichondrogenic MicroRNA-221 in Human Mesenchymal Stem Cells Promotes Cartilage Repair In Vivo. *STEM CELLS*.
- LORENZ, H. & RICHTER, W. 2006. Osteoarthritis: cellular and molecular changes in degenerating cartilage. *Progress in histochemistry and cytochemistry*, 40, 135-63.
- LOVE, M. I., HUBER, W. & ANDERS, S. 2014. Moderated estimation of fold change and dispersion for RNA-seq data with DESeq2. *Genome biology*, 15, 1-21.
- LUNA, C., LI, G., QIU, J., EPSTEIN, D. L. & GONZALEZ, P. 2011a. Cross-talk between miR-29 and transforming growth factor-betas in trabecular meshwork cells. *Investigative ophthalmology & visual science*, 52, 3567-72.
- LUNA, C., LI, G., QIU, J., EPSTEIN, D. L. & GONZALEZ, P. 2011b. MicroRNA-24 regulates the processing of latent TGFbeta1 during cyclic mechanical stress in human trabecular meshwork cells through direct targeting of FURIN. *Journal of cellular physiology*, 226, 1407-14.
- MACCONAILL, M. 1951. The movements of bones and joints; the mechanical structure of articulating cartilage. *The Journal of bone and joint surgery. British volume*, 33, 251-257.
- MACCOUX, L. J., CLEMENTS, D. N., SALWAY, F. & DAY, P. J. 2007. Identification of new reference genes for the normalisation of canine osteoarthritic joint tissue transcripts from microarray data. *BMC molecular biology*, 8, 62.
- MACKINTOSH, C. 2004. Dynamic interactions between 14-3-3 proteins and phosphoproteins regulate diverse cellular processes. *Biochemical Journal*, 381, 329-342.
- MADEJ, W., VAN CAAM, A., DAVIDSON, E. B., VAN DER KRAAN, P. & BUMA, P. 2014. Physiological and excessive mechanical compression of articular cartilage activates Smad2/3P signaling. *Osteoarthritis and Cartilage*, 22, 1018-1025.
- MADHAVAN, S., ANGHELINA, M., RATH-DESCHNER, B., WYPASEK, E., JOHN, A., DESCHNER, J., PIESCO, N. & AGARWAL, S. 2006. Biomechanical signals exert sustained attenuation of proinflammatory gene induction in articular chondrocytes. *Osteoarthritis and cartilage*, 14, 1023-1032.
- MALFAIT, A.-M., LIU, R.-Q., IJIRI, K., KOMIYA, S. & TORTORELLA, M. D. 2002. Inhibition of ADAM-TS4 and ADAM-TS5 prevents aggrecan degradation in osteoarthritic cartilage. *Journal of Biological Chemistry*, 277, 22201-22208.
- MANTILA ROOSA, S. M., LIU, Y. & TURNER, C. H. 2011. Gene expression patterns in bone following mechanical loading. *Journal of Bone and Mineral Research*, 26, 100-112.
- MARIANI, E., PULSATELLI, L. & FACCHINI, A. 2014. Signaling pathways in cartilage repair. *International journal of molecular sciences*, 15, 8667-8698.
- MARIN, R. M., SULC, M. & VANICEK, J. 2013. Searching the coding region for microRNA targets. *RNA*, 19, 467-74.
- MARTIN, J. A. & BUCKWALTER, J. A. 1998. Effects of fibronectin on articular cartilage chondrocyte proteoglycan synthesis and response to insulin-like growth factor-I. *Journal of orthopaedic research*, 16, 752-757.
- MARTIN, M. 2011. Cutadapt removes adapter sequences from high-throughput sequencing reads. *EMBnet. journal*, 17, pp. 10-12.
- MARTINEZ-SANCHEZ, A., DUDEK, K. A. & MURPHY, C. L. 2012. Regulation of human chondrocyte function through direct inhibition of cartilage master regulator SOX9 by microRNA-145 (miRNA-145). *Journal of Biological Chemistry*, 287, 916-924.
- MASOTTI, A., MOSSA, G., CAMETTI, C., ORTAGGI, G., BIANCO, A., DEL GROSSO, N., MALIZIA, D. & ESPOSITO, C. 2009. Comparison of different commercially available cationic liposome-DNA lipoplexes: Parameters influencing toxicity and transfection efficiency. *Colloids and Surfaces B: Biointerfaces*, 68, 136-144.

- MATSUKAWA, T., SAKAI, T., YONEZAWA, T., HIRAIWA, H., HAMADA, T., NAKASHIMA, M., ONO, Y., ISHIZUKA, S., NAKAHARA, H. & LOTZ, M. K. 2013. MicroRNA-125b regulates the expression of aggrecanase-1 (ADAMTS-4) in human osteoarthritic chondrocytes. *Arthritis Res Ther*, 15, R28.
- MAUCK, R. L., SOLTZ, M. A., WANG, C. C., WONG, D. D., CHAO, P.-H. G., VALHMU, W. B., HUNG, C. T. & ATESHIAN, G. A. 2000. Functional tissue engineering of articular cartilage through dynamic loading of chondrocyte-seeded agarose gels. *Journal of biomechanical engineering*, 122, 252-260.
- MCALINDEN, A., VARGHESE, N., WIRTHLIN, L. & CHANG, L.-W. 2013. Differentially expressed microRNAs in chondrocytes from distinct regions of developing human cartilage. *PloS one*, 8, e75012.
- MCCULLOCH, E., RAMAGE, G., RAJENDRAN, R., LAPPIN, D. F., JONES, B., WARN, P., SHRIEF, R., KIRKPATRICK, W. R., PATTERSON, T. F. & WILLIAMS, C. 2012. Antifungal treatment affects the laboratory diagnosis of invasive aspergillosis. *J Clin Pathol*, 65, 83-6.
- MCGLASHAN, S. R., KNIGHT, M. M., CHOWDHURY, T. T., JOSHI, P., JENSEN, C. G., KENNEDY, S. & POOLE, C. A. 2010. Mechanical loading modulates chondrocyte primary cilia incidence and length. *Cell biology international*, 34, 441-446.
- MEISTER, G., LANDTHALER, M., DORSETT, Y. & TUSCHL, T. 2004. Sequence-specific inhibition of microRNA-and siRNA-induced RNA silencing. *Rna*, 10, 544-550.
- MENDELL, J. T. 2005. MicroRNAs: critical regulators of development, cellular physiology and malignancy. *Cell cycle*, 4, 1179-84.
- MENDIAS, C. L., GUMUCIO, J. P. & LYNCH, E. B. 2012. Mechanical loading and TGF- $\beta$  change the expression of multiple miRNAs in tendon fibroblasts. *Journal of Applied Physiology*, 113, 56-62.
- MILNER, J. M., ROWAN, A. D., CAWSTON, T. E. & YOUNG, D. A. 2006. Metalloproteinase and inhibitor expression profiling of resorbing cartilage reveals pro-collagenase activation as a critical step for collagenolysis. *Arthritis research & therapy*, 8, R142.
- MIRZAMOHAMMADI, F., PAPAIOANNOU, G. & KOBAYASHI, T. 2014. microRNAs in cartilage development, homeostasis, and disease. *Current osteoporosis reports*, 12, 410-419.
- MITRA, R. & BANDYOPADHYAY, S. 2011. MultiMiTar: a novel multi objective optimization based miRNA-target prediction method. *PloS one*, 6, e24583.
- MIYAKI, S. & ASAHARA, H. 2012. Macro view of microRNA function in osteoarthritis. *Nature Reviews Rheumatology*, 8, 543-552.
- MIYAKI, S., NAKASA, T., OTSUKI, S., GROGAN, S. P., HIGASHIYAMA, R., INOUE, A., KATO, Y., SATO, T., LOTZ, M. K. & ASAHARA, H. 2009. MicroRNA-140 is expressed in differentiated human articular chondrocytes and modulates interleukin-1 responses. *Arthritis & Rheumatism*, 60, 2723-2730.
- MIYAKI, S., SATO, T., INOUE, A., OTSUKI, S., ITO, Y., YOKOYAMA, S., KATO, Y., TAKEMOTO, F., NAKASA, T., YAMASHITA, S., TAKADA, S., LOTZ, M. K., UENO-KUDO, H. & ASAHARA, H. 2010. MicroRNA-140 plays dual roles in both cartilage development and homeostasis. *Genes & development*, 24, 1173-85.
- MIYOSHI, K., MIYOSHI, T. & SIOMI, H. 2010. Many ways to generate microRNA-like small RNAs: non-canonical pathways for microRNA production. *Molecular Genetics and Genomics*, 284, 95-103.
- MOHAMED, J. S., LOPEZ, M. A. & BORIEK, A. M. 2010. Mechanical stretch up-regulates microRNA-26a and induces human airway smooth muscle hypertrophy by suppressing glycogen synthase kinase-3 $\beta$ . *Journal of biological chemistry*, 285, 29336-29347.
- MONFORT, J., GARCIA-GIRALT, N., LÓPEZ-ARMADA, M. J., MONLLAU, J. C., BONILLA, A., BENITO, P. & BLANCO, F. J. 2006. Decreased metalloproteinase production as a response to mechanical pressure in human cartilage: a mechanism for homeostatic regulation. *Arthritis research & therapy*, 8, R149.

- MOQADAM, F. A., PIETERS, R. & DEN BOER, M. 2013. The hunting of targets: challenge in miRNA research. *Leukemia*, 27, 16-23.
- MORGAN, M. 2011. An introduction to Rsamtools. Disponível <http://prs.ism.ac.jp/bioc/2.6/bioc/html/rsamtools.html>. Acessado em outubro de.
- MORGAN, M., ANDERS, S., LAWRENCE, M., ABOYOUN, P., PAGÈS, H. & GENTLEMAN, R. 2009. ShortRead: a bioconductor package for input, quality assessment and exploration of high-throughput sequence data. *Bioinformatics*, 25, 2607-2608.
- MUELLER, O., LIGHTFOOT, S. & SCHROEDER, A. 2004. RNA integrity number (RIN)– Standardization of RNA Quality Control. *Agilent Application Note, Publication*, 1-8.
- MUHAMMAD, H., RAIS, Y., MIOSGE, N. & ORNAN, E. M. 2012. The primary cilium as a dual sensor of mechanochemical signals in chondrocytes. *Cellular and Molecular Life Sciences*, 69, 2101-2107.
- MURAD, S., GROVE, D., LINDBERG, K., REYNOLDS, G., SIVARAJAH, A. & PINNELL, S. 1981. Regulation of collagen synthesis by ascorbic acid. *Proceedings of the National Academy of Sciences*, 78, 2879-2882.
- MURPHY, G. 2011. Tissue inhibitors of metalloproteinases. *Genome Biol*, 12, 233.
- MURPHY, G., KNÄUPER, V., ATKINSON, S., BUTLER, G., ENGLISH, W., HUTTON, M., STRACKE, J. & CLARK, I. 2002. Matrix metalloproteinases in arthritic disease. *Arthritis Research & Therapy*, 4, 1.
- NAGASE, H. & KASHIWAGI, M. 2003. Aggrecanases and cartilage matrix degradation. *Arthritis Res Ther*, 5, 94-103.
- NAGASE, H., VISSÉ, R. & MURPHY, G. 2006. Structure and function of matrix metalloproteinases and TIMPs. *Cardiovasc Res*, 69, 562-73.
- NAITO, S., SHIOMI, T., OKADA, A., KIMURA, T., CHIJIWA, M., FUJITA, Y., YATABE, T., KOMIYA, K., ENOMOTO, H. & FUJIKAWA, K. 2007. Expression of ADAMTS4 (aggrecanase-1) in human osteoarthritic cartilage. *Pathology international*, 57, 703-711.
- NAKAMURA, Y., HE, X., KATO, H., WAKITANI, S., KOBAYASHI, T., WATANABE, S., IIDA, A., TAHARA, H., WARMAN, M. L., WATANAPOKASIN, R. & POSTLETHWAIT, J. H. 2012. Sox9 is upstream of microRNA-140 in cartilage. *Appl Biochem Biotechnol*, 166, 64-71.
- NAKAMURA, Y., INLOES, J. B., KATAGIRI, T. & KOBAYASHI, T. 2011. Chondrocyte-specific microRNA-140 regulates endochondral bone development and targets Dnpep to modulate bone morphogenetic protein signaling. *Molecular and cellular biology*, 31, 3019-3028.
- NAKAYAMA, N., CHUN-YA, E. H., CAM, L., LEE, J. I., PRETORIUS, J., FISHER, S., ROSENFELD, R., SCULLY, S., NISHINAKAMURA, R. & DURYEA, D. 2004. A novel chordin-like BMP inhibitor, CHL2, expressed preferentially in chondrocytes of developing cartilage and osteoarthritic joint cartilage. *Development*, 131, 229-240.
- NELSON, D. L. 2005. Oxidative phosphorylation and photophosphorylation. *Principles of biochemistry*.
- NI, C. W., QIU, H. & JO, H. 2011. MicroRNA-663 upregulated by oscillatory shear stress plays a role in inflammatory response of endothelial cells. *American journal of physiology. Heart and circulatory physiology*, 300, H1762-9.
- NICOT, N., HAUSMAN, J.-F., HOFFMANN, L. & EVERS, D. 2005. Housekeeping gene selection for real-time RT-PCR normalization in potato during biotic and abiotic stress. *Journal of experimental botany*, 56, 2907-2914.
- NOVACK, D. V. 2011. Role of NF-kappaB in the skeleton. *Cell Res*, 21, 169-82.
- O'CONNOR, M., GREGORY, S. T. & DAHLBERG, A. E. 2004. Multiple defects in translation associated with altered ribosomal protein L4. *Nucleic acids research*, 32, 5750-5756.
- O'CONNOR, C. J., RAMALINGAM, S., ZELENSKI, N. A., BENEFIELD, H. C., RIGO, I., LITTLE, D., WU, C.-L., CHEN, D., LIEDTKE, W. & MCNULTY, A. L. 2016. Cartilage-specific knockout of the

- mechanosensory ion channel TRPV4 decreases age-related osteoarthritis. *Scientific Reports*, 6.
- OKADA, A., MOCHIZUKI, S., YATABE, T., KIMURA, T., SHIOMI, T., FUJITA, Y., MATSUMOTO, H., SEHARA-FUJISAWA, A., IWAMOTO, Y. & OKADA, Y. 2008. ADAM-12 (meltrin  $\alpha$ ) is involved in chondrocyte proliferation via cleavage of insulin-like growth factor binding protein 5 in osteoarthritic cartilage. *Arthritis & Rheumatism*, 58, 778-789.
- OKAMURA, K., HAGEN, J. W., DUAN, H., TYLER, D. M. & LAI, E. C. 2007. The mirtron pathway generates microRNA-class regulatory RNAs in *Drosophila*. *Cell*, 130, 89-100.
- OTTERNESS, I. G., ESKRA, J. D., BLIVEN, M. L., SHAY, A. K., PELLETIER, J. P. & MILICI, A. J. 1998. Exercise protects against articular cartilage degeneration in the hamster. *Arthritis Rheum*, 41, 2068-76.
- PALMOSKI, M., PERRICONE, E. & BRANDT, K. D. 1979. Development and reversal of a proteoglycan aggregation defect in normal canine knee cartilage after immobilization. *Arthritis & Rheumatism*, 22, 508-517.
- PALMOSKI, M. J. & BRANDT, K. D. 1981. Running inhibits the reversal of atrophic changes in canine knee cartilage after removal of a leg cast. *Arthritis & Rheumatism*, 24, 1329-1337.
- PALMOSKI, M. J. & BRANDT, K. D. 1984. Effects of static and cyclic compressive loading on articular cartilage plugs in vitro. *Arthritis & Rheumatism*, 27, 675-681.
- PAP, G., EBERHARDT, R., STÜRMER, I., MACHNER, A., SCHWARZBERG, H., ROESSNER, A. & NEUMANN, W. 1998. Development of osteoarthritis in the knee joints of Wistar rats after strenuous running exercise in a running wheel by intracranial self-stimulation. *Pathology-Research and Practice*, 194, 41-47.
- PARKKINEN, J., IKONEN, J., LAMMI, M., LAAKKONEN, J., TAMMI, M. & HELMINEN, H. 1993. Effects of cyclic hydrostatic pressure on proteoglycan synthesis in cultured chondrocytes and articular cartilage explants. *Archives of biochemistry and biophysics*, 300, 458-465.
- PATHI, S., PAGAN-WESTPHAL, S., BAKER, D. P., GARBER, E. A., RAYHORN, P., BUMCROT, D., TABIN, C. J., PEPINSKY, R. B. & WILLIAMS, K. P. 2001. Comparative biological responses to human Sonic, Indian, and Desert hedgehog. *Mechanisms of development*, 106, 107-117.
- PATWARI, P., COOK, M. N., DIMICCO, M. A., BLAKE, S. M., JAMES, I. E., KUMAR, S., COLE, A. A., LARK, M. W. & GRODZINSKY, A. J. 2003. Proteoglycan degradation after injurious compression of bovine and human articular cartilage in vitro: interaction with exogenous cytokines. *Arthritis Rheum*, 48, 1292-301.
- PAULEY, K. M. & CHA, S. 2011. miRNA-146a in rheumatoid arthritis: a new therapeutic strategy. *Immunotherapy*, 3, 829-31.
- PAULSSON, M. & HEINEGÅRD, D. 1979. Matrix proteins bound to associatively prepared proteoglycans from bovine cartilage. *Biochemical Journal*, 183, 539-545.
- PEARLE, A. D., WARREN, R. F. & RODEO, S. A. 2005. Basic science of articular cartilage and osteoarthritis. *Clin Sports Med*, 24, 1-12.
- PENG, S.-C., LAI, Y.-T., HUANG, H.-Y., HUANG, H.-D. & HUANG, Y.-S. 2010. A novel role of CPEB3 in regulating EGFR gene transcription via association with Stat5b in neurons. *Nucleic acids research*, gkq634.
- PERKINS, M. E., JI, T. H. & HYNES, R. O. 1979. Cross-linking of fibronectin to sulfated proteoglycans at the cell surface. *Cell*, 16, 941-952.
- PFAFFL, M. W., TICHOPAD, A., PRGOMET, C. & NEUVIANS, T. P. 2004. Determination of stable housekeeping genes, differentially regulated target genes and sample integrity: BestKeeper–Excel-based tool using pair-wise correlations. *Biotechnology letters*, 26, 509-515.

- PIDGEON, G. P., KANDOUZ, M., MERAM, A. & HONN, K. V. 2002. Mechanisms controlling cell cycle arrest and induction of apoptosis after 12-lipoxygenase inhibition in prostate cancer cells. *Cancer Research*, 62, 2721-2727.
- PILLAI, R. S. 2005. MicroRNA function: multiple mechanisms for a tiny RNA? *RNA*, 11, 1753-61.
- PINKERTON, M. N., WESCOTT, D. C., GAFFEY, B. J., BEGGS, K. T., MILNE, T. J. & MEIKLE, M. C. 2008. Cultured human periodontal ligament cells constitutively express multiple osteotropic cytokines and growth factors, several of which are responsive to mechanical deformation. *Journal of periodontal research*, 43, 343-351.
- POLITZ, J. C. R., ZHANG, F. & PEDERSON, T. 2006. MicroRNA-206 colocalizes with ribosome-rich regions in both the nucleolus and cytoplasm of rat myogenic cells. *Proceedings of the National Academy of Sciences*, 103, 18957-18962.
- POMBO-SUAREZ, M., CALAZA, M., GOMEZ-REINO, J. J. & GONZALEZ, A. 2008. Reference genes for normalization of gene expression studies in human osteoarthritic articular cartilage. *BMC molecular biology*, 9, 17.
- POOLE, A., KOBAYASHI, M., YASUDA, T., LAVERTY, S., MWALE, F., KOJIMA, T., SAKAI, T., WAHL, C., EL-MAADAWY, S. & WEBB, G. 2002. Type II collagen degradation and its regulation in articular cartilage in osteoarthritis. *Annals of the rheumatic diseases*, 61, ii78-ii81.
- POOLE, A. R., KOJIMA, T., YASUDA, T., MWALE, F., KOBAYASHI, M. & LAVERTY, S. 2001. Composition and structure of articular cartilage: a template for tissue repair. *Clin Orthop Relat Res*, S26-33.
- POOLE, C. A., AYAD, S. & SCHOFIELD, J. R. 1988. Chondrons from articular cartilage: I. Immunolocalization of type VI collagen in the pericellular capsule of isolated canine tibial chondrons. *Journal of Cell Science*, 90, 635-643.
- PRYDZ, K. 2015. Determinants of Glycosaminoglycan (GAG) Structure. *Biomolecules*, 5, 2003-2022.
- QI, Y., MA, N., YAN, F., YU, Z., WU, G., QIAO, Y., HAN, D., XIANG, Y., LI, F. & WANG, W. 2013. The expression of intronic miRNAs, miR-483 and miR-483\*, and their host gene, Igf2, in murine osteoarthritis cartilage. *International journal of biological macromolecules*, 61, 43-49.
- QIN, X., WANG, X., WANG, Y., TANG, Z., CUI, Q., XI, J., LI, Y. S., CHIEN, S. & WANG, N. 2010. MicroRNA-19a mediates the suppressive effect of laminar flow on cyclin D1 expression in human umbilical vein endothelial cells. *Proceedings of the National Academy of Sciences of the United States of America*, 107, 3240-4.
- RAABE, C. A., TANG, T.-H., BROSIUS, J. & ROZHDESTVENSKY, T. S. 2014. Biases in small RNA deep sequencing data. *Nucleic acids research*, 42, 1414-1426.
- RAINA, M. & IBBA, M. 2014. tRNAs as regulators of biological processes. *Non-Coding RNA*, 5, 171.
- RAMAGE, L., NUKI, G. & SALTER, D. M. 2009. Signalling cascades in mechanotransduction: cell-matrix interactions and mechanical loading. *Scand J Med Sci Sports*, 19, 457-69.
- RAMOS-DESIMONE, N., HAHN-DANTONA, E., SIPLEY, J., NAGASE, H., FRENCH, D. L. & QUIGLEY, J. P. 1999. Activation of matrix metalloproteinase-9 (MMP-9) via a converging plasmin/stromelysin-1 cascade enhances tumor cell invasion. *Journal of Biological Chemistry*, 274, 13066-13076.
- RAMSHAW, J. A., SHAH, N. K. & BRODSKY, B. 1998. Gly-XY tripeptide frequencies in collagen: a context for host-guest triple-helical peptides. *Journal of structural biology*, 122, 86-91.
- REICHENBERGER, E., AIGNER, T., VON DER MARK, K., STÖSS, H. & BERTLING, W. 1991. In situ hybridization studies on the expression of type X collagen in fetal human cartilage. *Developmental biology*, 148, 562-572.
- RETTING, K. N., SONG, B., YOON, B. S. & LYONS, K. M. 2009. BMP canonical Smad signaling through Smad1 and Smad5 is required for endochondral bone formation. *Development*, 136, 1093-1104.

- REYNARD, L. N. & LOUGHLIN, J. 2012. Genetics and epigenetics of osteoarthritis. *Maturitas*, 71, 200-4.
- RHEE, J., PARK, S.-H., KIM, S.-K., KIM, J.-H., HA, C.-W., CHUN, C.-H. & CHUN, J.-S. 2016. Inhibition of BATF/JUN transcriptional activity protects against osteoarthritic cartilage destruction. *Annals of the rheumatic diseases*, annrheumdis-2015-208953.
- RITCHIE, M. E., PHIPSON, B., WU, D., HU, Y., LAW, C. W., SHI, W. & SMYTH, G. K. 2015. limma powers differential expression analyses for RNA-sequencing and microarray studies. *Nucleic acids research*, gkv007.
- ROBINSON, M. D., MCCARTHY, D. J. & SMYTH, G. K. 2010. edgeR: a Bioconductor package for differential expression analysis of digital gene expression data. *Bioinformatics*, 26, 139-140.
- ROHATGI, R., MILENKOVIC, L. & SCOTT, M. P. 2007. Patched1 regulates hedgehog signaling at the primary cilium. *Science*, 317, 372-376.
- ROUGHLEY, P. 2006. The structure and function of cartilage proteoglycans. *Eur Cell Mater*, 12, 92-101.
- ROUGHLEY, P. J. 2001. Articular cartilage and changes in arthritis: noncollagenous proteins and proteoglycans in the extracellular matrix of cartilage. *Arthritis Res*, 3, 342-7.
- RUIZ-DE-LUZURIAGA, B. C., FERMOR, B., HANNING, C., KUMAR, S., LARK, M. W. & GUILAK, F. P38 MITOGEN ACTIVATED PROTEIN KINASE REGULATES MECHANICALLY-INDUCED NITRIC OXIDE AND PROSTAGLANDIN PRODUCTION IN ARTICULAR CARTILAGE.
- SAH, R. L. Y., KIM, Y. J., DOONG, J. Y. H., GRODZINSKY, A. J., PLASS, A. H. & SANDY, J. D. 1989. Biosynthetic response of cartilage explants to dynamic compression. *Journal of Orthopaedic Research*, 7, 619-636.
- SAHEBJAM, S., KHOKHA, R. & MORT, J. S. 2007. Increased collagen and aggrecan degradation with age in the joints of Timp3<sup>-/-</sup> mice. *Arthritis & Rheumatism*, 56, 905-909.
- SAITO, T. & SÆTROM, P. 2010. MicroRNAs—targeting and target prediction. *New biotechnology*, 27, 243-249.
- SALTER, D., HUGHES, D., SIMPSON, R. & GARDNER, D. 1992. Integrin expression by human articular chondrocytes. *Rheumatology*, 31, 231-234.
- SALTER, D., WRIGHT, M. & MILLWARD-SADLER, S. 2004. NMDA receptor expression and roles in human articular chondrocyte mechanotransduction. *Biorheology*, 41, 273-281.
- SALTER, D. M. & LEE, H.-S. 2010a. Expression and Function of Articular Chondrocyte NMDA Receptors. *J Med Sci*, 30, 231-236.
- SALTER, D. M. & LEE, H.-S. 2010b. Mechanical Signalling in Osteoarticular Tissues. *J Med Sci*, 30, 141-147.
- SCHIEMANN, W. P., GRAVES, L. M., BAUMANN, H., MORELLA, K. K., GEARING, D. P., NIELSEN, M. D., KREBS, E. G. & NATHANSON, N. M. 1995. Phosphorylation of the human leukemia inhibitory factor (LIF) receptor by mitogen-activated protein kinase and the regulation of LIF receptor function by heterologous receptor activation. *Proceedings of the National Academy of Sciences*, 92, 5361-5365.
- SCHÖNHERR, E., SUNDERKÖTTER, C., IOZZO, R. V. & SCHAEFER, L. 2005. Decorin, a novel player in the insulin-like growth factor system. *Journal of Biological Chemistry*, 280, 15767-15772.
- SCHWARZ, D. S., HUTVAGNER, G., DU, T., XU, Z., ARONIN, N. & ZAMORE, P. D. 2003. Asymmetry in the assembly of the RNAi enzyme complex. *Cell*, 115, 199-208.
- SCOTT, M. S., AVOLIO, F., ONO, M., LAMOND, A. I. & BARTON, G. J. 2009. Human miRNA precursors with box H/ACA snoRNA features. *PLoS Comput Biol*, 5, e1000507.
- SELBACH, M., SCHWANHÄUSSER, B., THIERFELDER, N., FANG, Z., KHANIN, R. & RAJEWSKY, N. 2008. Widespread changes in protein synthesis induced by microRNAs. *Nature*, 455, 58-63.

- SETHUPATHY, P., MEGRAW, M. & HATZIGEORGIOU, A. G. 2006. A guide through present computational approaches for the identification of mammalian microRNA targets. *Nature methods*, 3, 881-886.
- SHAULIAN, E. & KARIN, M. 2002. AP-1 as a regulator of cell life and death. *Nature cell biology*, 4, E131-E136.
- SHIEH, A. & ATHANASIOU, K. A. 2007. Dynamic compression of single cells. *Osteoarthritis and cartilage*, 15, 328-334.
- SHIN, C., NAM, J.-W., FARH, K. K.-H., CHIANG, H. R., SHKUMATAVA, A. & BARTEL, D. P. 2010. Expanding the microRNA targeting code: functional sites with centered pairing. *Molecular cell*, 38, 789-802.
- SHOULDERS, M. D. & RAINES, R. T. 2009. Collagen structure and stability. *Annual review of biochemistry*, 78, 929.
- SILVER, N., BEST, S., JIANG, J. & THEIN, S. L. 2006. Selection of housekeeping genes for gene expression studies in human reticulocytes using real-time PCR. *BMC molecular biology*, 7, 33.
- SMALLEY, M. J., SIGNORET, N., ROBERTSON, D., TILLEY, A., HANN, A., EWAN, K., DING, Y., PATERSON, H. & DALE, T. C. 2005. Dishevelled (Dvl-2) activates canonical Wnt signalling in the absence of cytoplasmic puncta. *Journal of cell science*, 118, 5279-5289.
- SMITH, R. L., GOODMAN, S., SCHURMAN, D. & CARTER, D. 2000. Time-dependent effects of intermittent hydrostatic pressure on articular chondrocyte type II collagen and aggrecan mRNA expression. *J. Rehabil. Res. Dev.*, 37, 153-161.
- SPELLING, S., ROUTH, R., DAVIDSON, R., CLARK, I., CARR, A., HULLEY, P. & PRICE, A. 2014. A gene expression study of normal and damaged cartilage in anteromedial gonarthrosis, a phenotype of osteoarthritis. *Osteoarthritis and Cartilage*, 22, 334-343.
- SNOEK-VAN BEURDEN, P. A. & VON DEN HOFF, J. W. 2005. Zymographic techniques for the analysis of matrix metalloproteinases and their inhibitors. *Biotechniques*, 38, 73-83.
- SOIFER, H. S., ROSSI, J. J. & SÆTROM, P. 2007. MicroRNAs in disease and potential therapeutic applications. *Molecular Therapy*, 15, 2070-2079.
- SONG, J., JIN, E.-H., KIM, D., KIM, K. Y., CHUN, C.-H. & JIN, E.-J. 2015. MicroRNA-222 regulates MMP-13 via targeting HDAC-4 during osteoarthritis pathogenesis. *BBA Clinical*, 3, 79-89.
- SONG, R. H., TORTORELLA, M., MALFAIT, A. M., ALSTON, J. T., YANG, Z., ARNER, E. C. & GRIGGS, D. W. 2007. Aggrecan degradation in human articular cartilage explants is mediated by both ADAMTS-4 and ADAMTS-5. *Arthritis & Rheumatism*, 56, 575-585.
- SOREFAN, K., PAIS, H., HALL, A. E., KOZOMARA, A., GRIFFITHS-JONES, S., MOULTON, V. & DALMAY, T. 2012. Reducing ligation bias of small RNAs in libraries for next generation sequencing. *Silence*, 3, 4-4.
- STANTON, H., ROGERSON, F. M., EAST, C. J., GOLUB, S. B., LAWLOR, K. E., MEEKER, C. T., LITTLE, C. B., LAST, K., FARMER, P. J. & CAMPBELL, I. K. 2005. ADAMTS5 is the major aggrecanase in mouse cartilage in vivo and in vitro. *Nature*, 434, 648-652.
- STARKMAN, B. G., CRAVERO, J. D., DELCARLO, M. & LOESER, R. F. 2005. IGF-I stimulation of proteoglycan synthesis by chondrocytes requires activation of the PI 3-kinase pathway but not ERK MAPK. *Biochemical Journal*, 389, 723-729.
- STEFANI, G. & SLACK, F. J. 2008. Small non-coding RNAs in animal development. *Nature reviews. Molecular cell biology*, 9, 219-30.
- SWINGLER, T. E., WHEELER, G., CARMONT, V., ELLIOTT, H. R., BARTER, M. J., ABU-ELMAGD, M., DONELL, S. T., BOOT-HANDFORD, R. P., HAJIHOSEINI, M. K. & MÜNSTERBERG, A. 2012. The expression and function of microRNAs in chondrogenesis and osteoarthritis. *Arthritis & Rheumatism*, 64, 1909-1919.
- TAGANOV, K. D., BOLDIN, M. P., CHANG, K.-J. & BALTIMORE, D. 2006. NF- $\kappa$ B-dependent induction of microRNA miR-146, an inhibitor targeted to signaling proteins of innate

- immune responses. *Proceedings of the National Academy of Sciences*, 103, 12481-12486.
- TANG, R., LI, L., ZHU, D., HOU, D., CAO, T., GU, H., ZHANG, J., CHEN, J., ZHANG, C.-Y. & ZEN, K. 2012. Mouse miRNA-709 directly regulates miRNA-15a/16-1 biogenesis at the posttranscriptional level in the nucleus: evidence for a microRNA hierarchy system. *Cell research*, 22, 504-515.
- TAO SONG, J., HU, B., YAN QU, H., LONG BI, C., ZHEN HUANG, X. & ZHANG, M. 2012. Mechanical stretch modulates microRNA 21 expression, participating in proliferation and apoptosis in cultured human aortic smooth muscle cells.
- TARDIF, G., HUM, D., PELLETIER, J.-P., DUVAL, N. & MARTEL-PELLETIER, J. 2009. Regulation of the IGFBP-5 and MMP-13 genes by the microRNAs miR-140 and miR-27a in human osteoarthritic chondrocytes. *BMC musculoskeletal disorders*, 10, 148.
- TESHIMA, R., OTSUKA, T., TAKASU, N., YAMAGATA, N. & YAMAMOTO, K. 1995. Structure of the most superficial layer of articular cartilage. *Bone & Joint Journal*, 77, 460-464.
- THALI, M., BUKOVSKY, A., KONDO, E., ROSENWIRTH, B., WALSH, C. T., SODROSKI, J. & GÖTTLINGER, H. G. 1994. Functional association of cyclophilin A with HIV-1 virions. *Nature*, 372, 363-365.
- THELLIN, O., ELMOUALIJ, B., HEINEN, E. & ZORZI, W. 2009. A decade of improvements in quantification of gene expression and internal standard selection. *Biotechnology advances*, 27, 323-333.
- THOMA, B., BIRD, T. A., FRIEND, D. J., GEARING, D. P. & DOWER, S. K. 1994. Oncostatin M and leukemia inhibitory factor trigger overlapping and different signals through partially shared receptor complexes. *Journal of Biological Chemistry*, 269, 6215-6222.
- THOMAS, R. S., CLARKE, A. R., DUANCE, V. C. & BLAIN, E. J. 2011. Effects of Wnt3A and mechanical load on cartilage chondrocyte homeostasis. *Arthritis Res Ther*, 13, R203.
- THOMPSON, C., CHAPPLE, J. & KNIGHT, M. 2014. Primary cilia disassembly down-regulates mechanosensitive hedgehog signalling: a feedback mechanism controlling ADAMTS-5 expression in chondrocytes. *Osteoarthritis and Cartilage*, 22, 490-498.
- THOMSON, D. W., BRACKEN, C. P. & GOODALL, G. J. 2011. Experimental strategies for microRNA target identification. *Nucleic acids research*, 39, 6845-6853.
- THORFVE, A., DEHNE, T., LINDAHL, A., BRITTBERG, M., PRUSS, A., RINGE, J., SITTINGER, M. & KARLSSON, C. 2012. Characteristic markers of the WNT signaling pathways are differentially expressed in osteoarthritic cartilage. *Cartilage*, 3, 43-57.
- THYSEN, S., LUYTEN, F. P. & LORIES, R. J. 2015. Targets, models and challenges in osteoarthritis research. *Disease Models and Mechanisms*, 8, 17-30.
- TONG, A. W. & NEMUNAITIS, J. 2008. Modulation of miRNA activity in human cancer: a new paradigm for cancer gene therapy? *Cancer gene therapy*, 15, 341-55.
- TORRES, R. J. & PUIG, J. G. 2007. Hypoxanthine-guanine phosphoribosyltransferase (HPRT) deficiency: Lesch-Nyhan syndrome. *Orphanet journal of rare diseases*, 2, 1.
- TORZILLI, P. A., BHARGAVA, M. & CHEN, C. T. 2011. Mechanical Loading of Articular Cartilage Reduces IL-1-Induced Enzyme Expression. *Cartilage*, 2, 364-373.
- TROEBERG, L. & NAGASE, H. 2012. Proteases involved in cartilage matrix degradation in osteoarthritis. *Biochim Biophys Acta*, 1824, 133-45.
- TSUMAKI, N., NAKASE, T., MIYAJI, T., KAKIUCHI, M., KIMURA, T., OCHI, T. & YOSHIKAWA, H. 2002. Bone morphogenetic protein signals are required for cartilage formation and differently regulate joint development during skeletogenesis. *Journal of Bone and Mineral Research*, 17, 898-906.
- TUDDENHAM, L., WHEELER, G., NTOUNIA-FOUSARA, S., WATERS, J., HAJIHOSSEINI, M. K., CLARK, I. & DALMAY, T. 2006. The cartilage specific microRNA-140 targets histone deacetylase 4 in mouse cells. *FEBS Lett*, 580, 4214-7.

- TYC, K. & STEITZ, J. A. 1989. U3, U8 and U13 comprise a new class of mammalian snRNPs localized in the cell nucleolus. *The EMBO journal*, 8, 3113.
- ULAHANNAN, D., KOVAC, M., MULHOLLAND, P., CAZIER, J. & TOMLINSON, I. 2013. Technical and implementation issues in using next-generation sequencing of cancers in clinical practice. *British journal of cancer*, 109, 827-835.
- URBAN, J. P. 1994. The chondrocyte: a cell under pressure. *Br J Rheumatol*, 33, 901-8.
- URBICH, C., KALUZA, D., FRÖMEL, T., KNAU, A., BENNEWITZ, K., BOON, R. A., BONAUER, A., DOEBELE, C., BOECKEL, J.-N. & HERGENREIDER, E. 2012. MicroRNA-27a/b controls endothelial cell repulsion and angiogenesis by targeting semaphorin 6A. *Blood*, 119, 1607-1616.
- VAN DER KRAAN, P. M., GOUMANS, M.-J., DAVIDSON, E. B. & TEN DIJKE, P. 2012. Age-dependent alteration of TGF- $\beta$  signalling in osteoarthritis. *Cell and tissue research*, 347, 257-265.
- VANDESOMPELE, J., DE PRETER, K., PATTYN, F., POPPE, B., VAN ROY, N., DE PAEPE, A. & SPELEMAN, F. 2002. Accurate normalization of real-time quantitative RT-PCR data by geometric averaging of multiple internal control genes. *Genome biology*, 3, research0034.
- VENKATESAN, N., BARRE, L., BOURHIM, M., MAGDALOU, J., MAINARD, D., NETTER, P., FOURNEL-GIGLEUX, S. & OUZZINE, M. 2012. Xylosyltransferase-I regulates glycosaminoglycan synthesis during the pathogenic process of human osteoarthritis. *PLoS One*, 7, e34020.
- VERMA, R. P. & HANSCH, C. 2007. Matrix metalloproteinases (MMPs): chemical-biological functions and (Q)SARs. *Bioorg Med Chem*, 15, 2223-68.
- VERSCHURE, P., VAN MARLE, J., HELSEN, M., LAFEVER, F. & VAN DEN BERG, W. 1996. Localization of insulin-like growth factor-1 receptor in human normal and osteoarthritic cartilage in relation to proteoglycan synthesis and content. *Rheumatology*, 35, 1044-1055.
- VISSE, R. & NAGASE, H. 2003. Matrix metalloproteinases and tissue inhibitors of metalloproteinases: structure, function, and biochemistry. *Circ Res*, 92, 827-39.
- VONK, L. A., KRAGTEN, A. H., DHERT, W., SARIS, D. B. & CREEMERS, L. B. 2014. Overexpression of hsa-miR-148a promotes cartilage production and inhibits cartilage degradation by osteoarthritic chondrocytes. *Osteoarthritis and cartilage*, 22, 145-153.
- VYNIOS, D. H., PAPAGEORGAKOPOULOU, N., SAZAKLI, H. & TSIGANOS, C. P. 2001. The interactions of cartilage proteoglycans with collagens are determined by their structures. *Biochimie*, 83, 899-906.
- WÄHÄMAA, H., SCHIERBECK, H., HREGGVIDSDOTTIR, H. S., PALMBLAD, K., AVEBERGER, A.-C., ANDERSSON, U. & HARRIS, H. E. 2011. High mobility group box protein 1 in complex with lipopolysaccharide or IL-1 promotes an increased inflammatory phenotype in synovial fibroblasts. *Arthritis research & therapy*, 13, 1.
- WALLER, K. A., ZHANG, L. X., ELSAID, K. A., FLEMING, B. C., WARMAN, M. L. & JAY, G. D. 2013. Role of lubricin and boundary lubrication in the prevention of chondrocyte apoptosis. *Proceedings of the National Academy of Sciences*, 110, 5852-5857.
- WANG, B.-W., WU, G.-J., CHENG, W.-P. & SHYU, K.-G. 2013a. Mechanical stretch via transforming growth factor- $\beta$ 1 activates microRNA-208a to regulate hypertrophy in cultured rat cardiac myocytes. *Journal of the Formosan Medical Association*, 112, 635-643.
- WANG, N., ZHANG, C.-Q., HE, J.-H., DUAN, X.-F., WANG, Y.-Y., JI, X., ZANG, W.-Q., LI, M., MA, Y.-Y. & WANG, T. 2013b. MiR-21 down-regulation suppresses cell growth, invasion and induces cell apoptosis by targeting FASL, TIMP3, and RECK genes in esophageal carcinoma. *Digestive diseases and sciences*, 58, 1863-1870.

- WANG, X., GUO, Y., WANG, C., YU, H., YU, X. & YU, H. 2016a. MicroRNA-142-3p Inhibits Chondrocyte Apoptosis and Inflammation in Osteoarthritis by Targeting HMGB1. *Inflammation*, 1-11.
- WANG, Y., ZHAO, Y., HERBST, A., KALINSKI, T., QIN, J., WANG, X., JIANG, Z., BENEDIX, F., FRANKE, S. & WARTMAN, T. 2016b. miR-221 Mediates Chemoresistance of Esophageal Adenocarcinoma by Direct Targeting of DKK2 Expression. *Annals of Surgery*.
- WANN, A. K., ZUO, N., HAYCRAFT, C. J., JENSEN, C. G., POOLE, C. A., MCGLASHAN, S. R. & KNIGHT, M. M. 2012. Primary cilia mediate mechanotransduction through control of ATP-induced Ca<sup>2+</sup> signaling in compressed chondrocytes. *The FASEB Journal*, 26, 1663-1671.
- WARDALE, R. J. & DUANCE, V. C. 1993. Quantification and immunolocalisation of porcine articular and growth plate cartilage collagens. *J Cell Sci*, 105 ( Pt 4), 975-84.
- WASSARMAN, D. A. & STEITZ, J. A. 1992. Interactions of small nuclear RNA's with precursor messenger RNA during in vitro splicing. *Science*, 257, 1918-1925.
- WEBER, M., BAKER, M. B., MOORE, J. P. & SEARLES, C. D. 2010. MiR-21 is induced in endothelial cells by shear stress and modulates apoptosis and eNOS activity. *Biochemical and biophysical research communications*, 393, 643-648.
- WEHLAND, M., ALESHCHEVA, G., SCHULZ, H., SAAR, K., HÜBNER, N., HEMMERSBACH, R., BRAUN, M., MA, X., FRETT, T. & WARNKE, E. 2015. Differential gene expression of human chondrocytes cultured under short-term altered gravity conditions during parabolic flight maneuvers. *Cell Communication and Signaling*, 13, 1.
- WESTHOLM, J. O. & LAI, E. C. 2011. Mirtrons: microRNA biogenesis via splicing. *Biochimie*, 93, 1897-1904.
- WIBERG, C., KLATT, A. R., WAGENER, R., PAULSSON, M., BATEMAN, J. F., HEINEGÅRD, D. & MÖRGELIN, M. 2003. Complexes of matrilin-1 and biglycan or decorin connect collagen VI microfibrils to both collagen II and aggrecan. *Journal of Biological Chemistry*, 278, 37698-37704.
- WIENHOLDS, E., KLOOSTERMAN, W. P., MISKA, E., ALVAREZ-SAAVEDRA, E., BEREZIKOV, E., DE BRUIJN, E., HORVITZ, H. R., KAUPPINEN, S. & PLASTERK, R. H. 2005. MicroRNA expression in zebrafish embryonic development. *Science*, 309, 310-1.
- WILSON, W., VAN DONKELAAR, C. & HUYGHE, J. M. 2005. A comparison between mechano-electrochemical and biphasic swelling theories for soft hydrated tissues. *Journal of biomechanical engineering*, 127, 158-165.
- WINDAHL, S. H., SAXON, L., BÖRJESSON, A. E., LAGERQUIST, M. K., FRENKEL, B., HENNING, P., LERNER, U. H., GALEA, G. L., MEAKIN, L. B. & ENGDAHL, C. 2013. Estrogen receptor- $\alpha$  is required for the osteogenic response to mechanical loading in a ligand-independent manner involving its activation function 1 but not 2. *Journal of Bone and Mineral Research*, 28, 291-301.
- WONG, M., SIEGRIST, M. & CAO, X. 1999. Cyclic compression of articular cartilage explants is associated with progressive consolidation and altered expression pattern of extracellular matrix proteins. *Matrix Biol*, 18, 391-9.
- WRIGHT, M., NISHIDA, K., BAVINGTON, C., GODOLPHIN, J., DUNNE, E., WALMSLEY, S., JOBANPUTRA, P., NUKI, G. & SALTER, D. M. 1997. Hyperpolarisation of cultured human chondrocytes following cyclical pressure-induced strain: Evidence of a role for  $\alpha 5\beta 1$  integrin as a chondrocyte mechanoreceptor. *Journal of orthopaedic research*, 15, 742-747.
- WU, D., SHI, M. & FAN, X.-D. 2015. Mechanism of miR-21 via Wnt/ $\beta$ -catenin signaling pathway in human A549 lung cancer cells and Lewis lung carcinoma in mice. *Asian Pacific journal of tropical medicine*, 8, 479-484.

- YAMASAKI, K., NAKASA, T., MIYAKI, S., ISHIKAWA, M., DEIE, M., ADACHI, N., YASUNAGA, Y., ASAHARA, H. & OCHI, M. 2009. Expression of MicroRNA-146a in osteoarthritis cartilage. *Arthritis and rheumatism*, 60, 1035-41.
- YAN, C., WANG, Y., SHEN, X.-Y., YANG, G., JIAN, J., WANG, H.-S., CHEN, G.-Q. & WU, Q. 2011. MicroRNA regulation associated chondrogenesis of mouse MSCs grown on polyhydroxyalkanoates. *Biomaterials*, 32, 6435-6444.
- YAN, J., GUO, D., YANG, S., SUN, H., WU, B. & ZHOU, D. 2016. Inhibition of miR-222-3p activity promoted osteogenic differentiation of hBMSCs by regulating Smad5-RUNX2 signal axis. *Biochemical and Biophysical Research Communications*.
- YANG, B., GUO, H., ZHANG, Y., CHEN, L., YING, D. & DONG, S. 2011. MicroRNA-145 regulates chondrogenic differentiation of mesenchymal stem cells by targeting Sox9. *PLoS one*, 6, e21679.
- YANG, J.-S. & LAI, E. C. 2011. Alternative miRNA biogenesis pathways and the interpretation of core miRNA pathway mutants. *Molecular cell*, 43, 892-903.
- YANG, X., GUAN, Y., TIAN, S., WANG, Y., SUN, K. & CHEN, Q. 2016a. Mechanical and IL-1 $\beta$  Responsive miR-365 Contributes to Osteoarthritis Development by Targeting Histone Deacetylase 4. *International journal of molecular sciences*, 17, 436.
- YANG, Y., LIU, Y., HE, J., WANG, J., SCHEMMER, P., MA, C., QIAN, Y., YAO, W., ZHANG, J. & QI, W. 2016b. 14-3-3 $\zeta$  and aPKC- $\iota$  synergistically facilitate epithelial-mesenchymal transition of cholangiocarcinoma via GSK-3 $\beta$ /snail signaling pathway. *Oncotarget*.
- YANG, Z., YUAN, Z., FAN, Y., DENG, X. & ZHENG, Q. 2013. Integrated analyses of microRNA and mRNA expression profiles in aggressive papillary thyroid carcinoma. *Molecular medicine reports*, 8, 1353-1358.
- YATABE, T., MOCHIZUKI, S., TAKIZAWA, M., CHIJIIWA, M., OKADA, A., KIMURA, T., FUJITA, Y., MATSUMOTO, H., TOYAMA, Y. & OKADA, Y. 2009. Hyaluronan inhibits expression of ADAMTS4 (aggrecanase-1) in human osteoarthritic chondrocytes. *Annals of the rheumatic diseases*, 68, 1051-1058.
- YE, F., YUAN, F., LI, X., COOPER, N., TINNEY, J. P. & KELLER, B. B. 2013. Gene expression profiles in engineered cardiac tissues respond to mechanical loading and inhibition of tyrosine kinases. *Physiological reports*, 1, e00078.
- YE, S., ERIKSSON, P., HAMSTEN, A., KURKINEN, M., HUMPHRIES, S. E. & HENNEY, A. M. 1996. Progression of coronary atherosclerosis is associated with a common genetic variant of the human stromelysin-1 promoter which results in reduced gene expression. *Journal of Biological Chemistry*, 271, 13055-13060.
- YU, C., CHEN, W. & WANG, X. 2011. MicroRNA in osteoarthritis. *Journal of International Medical Research*, 39, 1-9.
- ZHAI, Z., YAO, Y. & WANG, Y. 2013. Importance of suitable reference gene selection for quantitative RT-PCR during ATDC5 cells chondrocyte differentiation.
- ZHANG, A., LIU, Y., SHEN, Y., XU, Y. & LI, X. 2011. miR-21 modulates cell apoptosis by targeting multiple genes in renal cell carcinoma. *Urology*, 78, 474. e13-474. e19.
- ZHANG, C., ZHANG, J., HAO, J., SHI, Z., WANG, Y., HAN, L., YU, S., YOU, Y., JIANG, T. & WANG, J. 2012. High level of miR-221/222 confers increased cell invasion and poor prognosis in glioma. *Journal of translational medicine*, 10, 1.
- ZHANG, X., ZHU, J., LIU, F., LI, Y., CHANDRA, A., LEVIN, L. S., BEIER, F., ENOMOTO-IWAMOTO, M. & QIN, L. 2014a. Reduced EGFR signaling enhances cartilage destruction in a mouse osteoarthritis model. *Bone Res*, 2, 14015.
- ZHANG, Y., JIA, J., YANG, S., LIU, X., YE, S. & TIAN, H. 2014b. MicroRNA-21 controls the development of osteoarthritis by targeting GDF-5 in chondrocytes. *Experimental & molecular medicine*, 46, e79.
- ZHENG, C., YINGHAO, S. & LI, J. 2012. MiR-221 expression affects invasion potential of human prostate carcinoma cell lines by targeting DVL2. *Medical oncology*, 29, 815-822.

- ZHOU, J., WANG, K.-C., WU, W., SUBRAMANIAM, S., SHYY, J. Y.-J., CHIU, J.-J., LI, J. Y.-S. & CHIEN, S. 2011. MicroRNA-21 targets peroxisome proliferators-activated receptor- $\alpha$  in an autoregulatory loop to modulate flow-induced endothelial inflammation. *Proceedings of the National Academy of Sciences*, 108, 10355-10360.
- ZHOU, Y., MILLWARD-SADLER, S. J., LIN, H., ROBINSON, H., GOLDRING, M., SALTER, D. M. & NUKI, G. 2007. Evidence for JNK-dependent up-regulation of proteoglycan synthesis and for activation of JNK1 following cyclical mechanical stimulation in a human chondrocyte culture model. *Osteoarthritis Cartilage*, 15, 884-93.

# Appendices

## Appendix 1

Table of the genes present on RT<sup>2</sup> Profiler Wnt PCR array (Qiagen).

PCR Array Catalog #: PABT-043Z				
Position	Unigene	GenBank	Symbol	Description
A01	Bt.9945	NM_001128497	AES	Amino-terminal enhancer of split
A02	Bt.11086	NM_001075986	APC	Adenomatous polyposis coli
A03	Bt.21602	NM_001191398	AXIN1	Axin 1
A04	Bt.4412	NM_001192299	AXIN2	Axin 2
A05	N/A	XM_010803098	BCL9	B-cell CLL/lymphoma 9
A06	Bt.25271	NM_001083475	BTRC	Beta-transducin repeat containing
A07	Bt.88783	NM_001046273	CCND1	Cyclin D1
A08	Bt.4895	NM_001076372	CCND2	Cyclin D2
A09	Bt.65222	NM_174711	CSNK1A1	Casein kinase 1, alpha 1
A10	Bt.64603	NM_174635	CSNK2A1	Casein kinase 2, alpha 1 polypeptide
A11	Bt.1780	XM_010806373	CTBP1	C-terminal binding protein 1
A12	Bt.33687	NM_001076141	CTNNB1	Catenin (cadherin-associated protein), beta 1, 88kDa
B01	Bt.8208	NM_001081588	DAAM1	Dishevelled associated activator of morphogenesis 1
B02	Bt.15382	NM_001193246	DAB2	Disabled homolog 2, mitogen-responsive phosphoprotein (Drosophila)
B03	N/A	XM_002693011	DIXDC1	DIX domain containing 1
B04	Bt.13880	NM_001205544	DKK1	Dickkopf homolog 1 (Xenopus laevis)
B05	Bt.18710	NM_001100306	DKK3	Dickkopf homolog 3 (Xenopus laevis)
B06	Bt.27892	NM_001206601	DVL1	Dishevelled, dsh homolog 1 (Drosophila)
B07	Bt.17972	NM_001191382	DVL2	Dishevelled, dsh homolog 2 (Drosophila)
B08	Bt.30467	XM_002696250	FBXW11	F-box and WD repeat domain containing 11
B09	Bt.26327	NM_001101985	FBXW4	F-box and WD repeat domain containing 4
B10	Bt.62944	NM_001040605	FGF4	Fibroblast growth factor 4
B11	Bt.17885	NM_001205985	FOSL1	FOS-like antigen 1
B12	Bt.88317	NM_001192452	FOXN1	Forkhead box N1
C01	N/A	XM_002698415	FRAT1	Frequently rearranged in advanced T-cell lymphomas
C02	Bt.121	NM_174059	FRZB	Frizzled-related protein
C03	Bt.26635	NM_001101048	FZD1	Frizzled family receptor 1
C04	Bt.79602	NM_001192964	FZD3	Frizzled family receptor 3
C05	Bt.76547	NM_001206269	FZD4	Frizzled family receptor 4
C06	N/A	XM_005197510	FZD5	Frizzled family receptor 5
C07	Bt.104004	XM_863880	FZD6	Frizzled homolog 6 (Drosophila)
C08	Bt.105583	NM_001144091	FZD7	Frizzled family receptor 7
C09	N/A	XM_005214320	FZD8	Frizzled family receptor 8
C10	N/A	XM_002698189	FZD9	Frizzled family receptor 9
C11	Bt.33944	NM_001102192	GSK3A	Glycogen synthase kinase 3 alpha
C12	Bt.48740	NM_001101310	GSK3B	Glycogen synthase kinase 3 beta
D01	Bt.11159	NM_001077827	JUN	Jun proto-oncogene
D02	N/A	XM_010814133	KREMEN1	Kringle containing transmembrane protein 1
D03	Bt.18467	NM_001192856	LEF1	Lymphoid enhancer-binding factor 1
D04	Bt.45360	XM_010821189	LRP5	Low density lipoprotein receptor-related protein 5
D05	Bt.60913	XM_002687783	LRP6	Low density lipoprotein receptor-related protein 6
D06	Bt.14050	NM_001192974	MAPK8	Mitogen-activated protein kinase 8
D07	Bt.13092	NM_001075130	MMP7	Matrix metalloproteinase 7 (matrilysin, uterine)

Table of the genes present on RT<sup>2</sup> Profiler Wnt PCR array (Qiagen) contd.

PCR Array Catalog #: PABT-043Z				
D08	Bt.21164	NM_001046074	MYC	V-myc myelocytomatosis viral oncogene homolog (avian)
D09	Bt.45162	NM_001166615	NFATC1	Nuclear factor of activated T-cells, cytoplasmic, calcineurin-dependent 1
D10	Bt.60075	NM_001105453	NKD1	Naked cuticle homolog 1 (Drosophila)
D11	Bt.43996	NM_001193253	NLK	Nemo-like kinase
D12	Bt.18496	NM_001097991	PITX2	Paired-like homeodomain 2
E01	Bt.38004	NM_001101208	PORCN	Porcupine homolog (Drosophila)
E02	Bt.13264	NM_001083636	PPARD	Peroxisome proliferator-activated receptor delta
E03	Bt.57449	NM_001102534	PRICKLE1	Prickle homolog 1 (Drosophila)
E04	N/A	XM_002690892	PYGO1	Pygopus homolog 1 (Drosophila)
E05	Bt.49678	NM_176645	RHOA	Ras homolog gene family, member A
E06	Bt.2846	NM_001098147	RHOU	Ras homolog gene family, member U
E07	Bt.41723	NM_001101076	RUVBL1	RuvB-like 1 (E. coli)
E08	Bt.5226	NM_174460	SFRP1	Secreted frizzled-related protein 1
E09	Bt.3540	NM_001075764	SFRP4	Secreted frizzled-related protein 4
E10	Bt.112292	NM_001206251	SOX17	SRY (sex determining region Y)-box 17
E11	Bt.44634	NM_001099186	TCF7	Transcription factor 7 (T-cell specific, HMG-box)
E12	N/A	XM_002691408	TCF7L1	Transcription factor 7-like 1 (T-cell specific, HMG-box)
F01	Bt.3589	NM_001098020	TLE1	Transducin-like enhancer of split 1 (E(sp1) homolog, Drosophila)
F02	Bt.87234	NM_001205875	VANGL2	Vang-like 2 (van gogh, Drosophila)
F03	Bt.63013	NM_001075996	WIF1	WNT inhibitory factor 1
F04	N/A	XM_005215320	WISP1	WNT1 inducible signaling pathway protein 1
F05	Bt.101628	NM_001114191	WNT1	Wingless-type MMTV integration site family, member 1
F06	Bt.61102	NM_001099078	WNT10A	Wingless-type MMTV integration site family, member 10A
F07	Bt.21876	NM_001082456	WNT11	Wingless-type MMTV integration site family, member 11
F08	Bt.37171	NM_001014949	WNT16	Wingless-type MMTV integration site family, member 16
F09	Bt.37360	NM_001013001	WNT2	Wingless-type MMTV integration site family member 2
F10	Bt.27254	NM_001099363	WNT2B	Wingless-type MMTV integration site family, member 2B
F11	Bt.112395	NM_001206024	WNT3	Wingless-type MMTV integration site family, member 3
F12	N/A	XM_010806514	WNT3A	Wingless-type MMTV integration site family, member 3A
G01	Bt.88484	NM_001205971	WNT5A	Wingless-type MMTV integration site family, member 5A
G02	Bt.6367	NM_001205628	WNT5B	Wingless-type MMTV integration site family, member 5B
G03	Bt.27385	NM_001205563	WNT6	Wingless-type MMTV integration site family, member 6
G04	Bt.69615	NM_001192788	WNT7A	Wingless-type MMTV integration site family, member 7A
G05	N/A	XM_603482	LOC525135	Wingless-type MMTV integration site family, member 7B
G06	Bt.106446	NM_001192370	WNT8A	Wingless-type MMTV integration site family, member 8A
G07	N/A	XM_002688510	WNT9A	Wingless-type MMTV integration site family, member 9A
G08	Bt.17918	NM_174739	CBY1	Chibby homolog 1 (Drosophila)
G09	Bt.24868	NM_001082615	DKK2	Dickkopf homolog 2 (Xenopus laevis)
G10	N/A	XM_010820369	DKK4	Dickkopf homolog 4 (Xenopus laevis)
G11	Bt.9084	XM_010819270	KREMEN2	Kringle containing transmembrane protein 2
G12	N/A	XM_001254723	MAP2K7	Mitogen-activated protein kinase kinase 7

Table of the genes present on RT<sup>2</sup> Profiler Wnt PCR array (Qiagen) contd.

PCR Array Catalog #: PABT-043Z				
H01	Bt.14186	NM_173979	ACTB	Actin, beta
H02	Bt.87389	NM_001034034	GAPDH	Glyceraldehyde-3-phosphate dehydrogenase
H03	Bt.49238	NM_001034035	HPRT1	Hypoxanthine phosphoribosyltransferase 1
H04	Bt.22662	NM_001075742	TBP	TATA box binding protein
H05	Bt.111451	NM_174814	YWHAZ	Tyrosine 3-monooxygenase/tryptophan 5-monooxygenase activation protein, zeta polypeptide
H06	N/A	SA_00137	BGDC	Cow Genomic DNA Contamination
H07	N/A	SA_00104	RTC	Reverse Transcription Control
H08	N/A	SA_00104	RTC	Reverse Transcription Control
H09	N/A	SA_00104	RTC	Reverse Transcription Control
H10	N/A	SA_00103	PPC	Positive PCR Control
H11	N/A	SA_00103	PPC	Positive PCR Control
H12	N/A	SA_00103	PPC	Positive PCR Control

# Publications